TERPENES IN RADICAL POLYMERISATION: POLYMER SYNTHESIS AND APPLICATIONS

Marina Fuentes Sainz, MSci

Thesis submitted to the University of Nottingham

for the degree of Doctor in Philosophy



The University of Nottingham

UNITED KINGDOM • CHINA • MALAYSIA

Disclaimer

With the exception of work referenced to other sources, all work presented in this thesis is the original work of the author. It has not been submitted, in any form, as part of any other degree or professional qualification.

Signed: Marina Fuentes Sainz

Date……

Acknowledgements

First of all I would like to thank my two supervisors Steve Howdle and Derek Irvine, not only for their continuous guidance and support, but also for all the fun times at REFINE meetings, group building activities and of course, at the pub.

I would also like to thank all the people that at some point have collaborated with this project. Starting with Robert Stockman, Jose Souto and Dominika Regentova, the success of this project would not have been possible without your help. This project was clearly enriched by the secondments at TUE in Eindhoven and DSM Zwolla, where I counted with the help of Chunliang Li and the expertise of Cor Koning, Paul Biunjsen and Gert Dijkstra to prepare and test coating films. Special thanks go to Susana Torron and Mats Johansson from KTH Stockholm, who assisted me during the FTIR-monitoring experiments and helped me with the spectral interpretation. Thanks as well to the Master students Amy Stimpson and Andrew Law for their enthusiasm and their input in the CTA studies, and Chris Seymour for his help with the monomer synthesis.

Thanks also to everyone in B10 for sharing these four years with me. Special thanks to Amy and Silvio, with whom I have shared not only B10 but also amazing trips and experiences. I would also like to thank all members of staff in the School of Chemistry for all their backing and assistance. The smooth running of the School of Chemistry would not be possible without you.

Thank you to all REFINE members with whom I have shared scientific meetings, interesting discussions, fun nights and wonderful experiences. Marie Curie Actions foundation deserves special mention, since thanks to them hundreds of people have incredible opportunities every year to conduct research abroad and experience new countries and cultures. It truly was a life changing experience for me.

Finally, I want to thank Ed and my family for always being there. Thank you.

Funding statement

The research leading to these results has received funding from the People Programme (Marie Curie Actions) of the European Union's Seventh Framework Programme FP7/ 2007–2013/under REA grant agreement no. [289253].

Abstract

This thesis describes novel research into the use of terpenes as monomers and controlling agents in radical polymerisation.

The use of terpenes as controlling agents represents an interesting alternative to the use of synthetic, toxic and expensive additives that are most commonly used in radical polymerisation. However, there is little information in the literature about the mechanism they undergo. In this work, the first systematic study regarding the use of terpinolene and γ-terpinene as controlling agents in radical polymerisation was reported (Chapter 2). The effectiveness of these terpenes at preventing the Trommsdorff effect and regulating molecular weight and dispersity in the polymerisation of methyl methacrylate, methyl acrylate, styrene and vinyl acetate was carefully studied and their mechanism was elucidated.

The development of functional renewable polymers has been gathering growing interest among the scientific community for the last decade. Terpenes are one of the most attractive alternatives to petrol-derived monomers because of their natural abundance and the presence of unsaturated moieties in their chemical structure, which offers, in theory, the possibility for polymerisation. However, a limited range of terpene-based polymers have been synthesised to date. In order to create readily polymerisable monomers, the introduction of (meth)acrylate functionalities into a range of natural terpenes was explored (Chapter 3). Initially, a two-step methodology, consisting of hydrolysis and subsequent esterification, was explored. As an alternative to the two-step protocol, allylic C-H activation catalysed by $Pd(OAc)_2$ was also investigated as a more sustainable route to introduce a (meth)acrylate functionality into β-pinene. These synthetic protocols led to a wide range of new terpene-based monomers.

In the subsequent chapter, the polymerisability of the new terpene-based monomers was evaluated (Chapter 4). The new (meth)acrylate monomers were polymerised for the first time using free radical polymerisation (FRP) techniques. A variety of new polymers showing diverse structures, from linear through to

branched and crosslinked, were obtained. The polymers also exhibited a wide scope of glass transition temperatures, which allows for the tailoring of mechanical properties by changing the starting terpene. A study of the reactivity of the different functionalities in bifunctional monomers was conducted by monitoring the polymerisation *via* FTIR.

Finally, the evaluation of carvone-based polymers as cross-linkable polymers for coating applications was conducted (Chapter 5). The carvone-based polymers were successfully coated by solvent casting or powder coating and then cured *via* thiol-ene chemistry. The properties of the films were carefully studied and compared to commercial acrylic coatings.

List of Abbreviations and Acronyms

9-BBN	9-Borabicyclo(3.3.1)nonane
AIBN	Azobisisobutyronitrile
AN	Acrylonitrile
ASTM	American Standard Test Method
ATRP	Atom Transfer Radical Polymerisation
BDE	Bond Dissociation Energy
BP	Benzophenone
BQ	Benzoquinone
C_{app}	Apparent Chain Transfer Constant
CDI	Carbonyldiimidazole
COMU	(1-Cyano-2-ethoxy-2-oxoethylidenaminooxy) dimethylamino-morpholino-carbenium hexafluorophosphate
CRP	Controlled Radical Polymerisation
CTA	Chain Transfer Agent
C_{tr}	Chain Transfer Constant
Đ	Dispersity
DCC	*N*,*N*'-Dicyclohexylcarbodiimide
DCM	Dichloromethane
DDM	Dodecyl mercaptan
DIC	*N*,*N*′-Diisopropylcarbodiimide
DP	Degree of Polymerisation
DSC	Differential Scanning Calorimetry
FRP	Free Radical Polymerisation
FTIR	Fourier Transformed Infrared Spectroscopy
GPC	Gel Permeation Chromatography
IR	Infrared
k_p	Propagation rate constant
k_{re}	Reinitiation rate constant
k_{tr}	Chain transfer rate constant

MA	Methyl acrylate
MALDI-TOF	Matrix-Assisted Laser Desorption/Ionisation Time Of Flight
MAO	Methylaluminoxane
MeTHF	Methyl-tetrahydrofuran
MMA	Methyl methacrylate
MMA-d8	Deuterated methyl methacrylate
M_n	Number average molecular weight
M_w	Weight average molecular weight
nBA	n-Butyl acrylate
ND	Not determined
NMI	1-Methyl imidazole
NMP	Nitroxide Mediated Polymerisation
NMR	Nuclear Magnetic Resonance
NO	Not observed
PCI	Powder Coating Institute
PE	Petroleum ether
PHU	Poly(hydroxyl urethanes)
PMA	Poly methyl acrylate
PMMA	Poly methyl methacrylate
PSty	Polystyrene
RAFT	Reversible Adittion-Fragmentation Chain Transfer Polymerisation
ROP	Ring Opening Polymerisation
rt	Room temperature
SFRP	Stable Free Radical Polymerisation
Sty	Styrene
T3P	Propylphosphonic anhydride
T_g	Glass transition temperature
TGA	Thermogravimetric Analysis
THF	Tetrahydrofuran
TLC	Thin Layer Chromatography
TMP-SH	Trimethylpropane tris(3-mercaptopropionate)

UV	Ultraviolet
V88	1,1'-azobis(cyclohexane-1-carbonytryle)
VAc	Vinyl acetate

Contents

Chapter 1: Introduction……...1

1.1 Polymerisation techniques……2

1.1.1 Free radical polymerisation (FRP)……...5

1.1.1.1 Molecular Weight, Degree of Polymerisation and Dispersity…….6

1.1.1.2 Controlled radical polymerisation (CRP)……7

1.2 Polymers from renewable sources……9

1.3 Terpenes and their applications……14

1.3.1 Polymers from terpenes……18

1.3.1.1 Radical polymerisation of terpenes……...18

1.3.1.2 Cationic polymerisation of terpenes……..22

1.3.1.3 Application of thiol-ene chemistry to terpene polymerisation……..26

1.3.1.4 Other transformations of terpenes into polymerisable monomers……29

1.4 Summary and thesis aims……...36

1.5 References…… 37

Chapter 2: Terpinolene and γ-terpinene as controlling agents in radical polymerisation……..41

2.1 Introduction……41

2.1.1 Trommsdorff-Norrish Effect……41

2.1.2 Traditional chain transfer methods in radical polymerisation…….....43

2.1.3 Mayo equation and evaluation of chain transfer constants……...44

2.1.4 Other methods of polymerisation control…… 45

2.1.5 Summary and research aims…… 46

2.2 Experimental …….. 47

2.2.1 Materials……... 47

2.2.2 General polymerisation method…… 48

2.2.2.1 Deuterated MMA polymerisation …….....49

2.2.3 Polymer characterisation……..49

2.2.3.1 Gel Permeation Chromatography (GPC)…… 49

2.2.3.2 Nuclear magnetic resonance (NMR)……49

2.2.3.3 Matrix-assisted laser desorption/ionisation time-of-flight mass spectrometry (MALDI-TOF)…….. 49
2.2.4 Monitoring of reaction exotherms…… ……...50
2.3 Results and discussion……50
2.3.1 Terpenes as chain transfer agents…….50
2.3.2 Kinetic profiles of terpinolene and γ -terpinene……..59
2.3.3 Effect of terpene concentration on MMA polymerisation……...62
2.3.4 Mechanistic studies: MMA-d^8 polymerisations and MALDI analysis…….66
2.3.5 Chain transfer constant calculations……..76
2.3.6 Exotherm measurements……...79
2.3.7 Control of other monomers: styrene, methyl acrylate, vinyl acetate……...82
2.3.7.1 Methyl acrylate…….82
2.3.7.2 Styrene……...86
2.3.7.3 Vinyl acetate…….89
2.3.7.4 Comparison of the effects of terpinolene and terpinene on the polymerisation reactions of methyl methacrylate, methyl acrylate, styrene and vinyl acetate……...91
2.4 Conclusions…….. 95
2.5 References……96
Chapter 3: Synthesis of terpene-based (meth)acrylate monomers……..…....99
3.1 Introduction……99
3.1.1 Hydration of alkenes…….99
3.1.2 C-H activation via Pd(II) catalysis……..102
3.1.3 Summary and research aims……104
3.2 Experimental……..105
3.2.1 Materials and analytical techniques……105
3.2.2 Nuclear magnetic resonance (NMR)……...106
3.2.3 Synthesis of hydroxilated terpene derivatives……106
3.2.4 Synthesis of acrylate derivatives *via* esterification……..108
3.2.5 Synthesis of methacrylate derivatives *via* esterification……..109
3.2.6 Catalytic synthesis of β -pinene derived (meth)acrylate monomers…...110

3.2.7 Monomer characterisation……...111
3.3 Results and discussion……...123
3.3.1 Synthesis of terpene-based (metha)crylate monomers via 2-step methodology……123
3.3.1.1 Synthesis of terpene alcohols……...124
3.3.1.2 Esterification of terpene-based alcohols……..128
3.3.1.3 Esterification in the presence of coupling agents……130
3.3.2 1-pot synthesis of terpene-based (meth)acrylate monomers via a Pd(II) catalysis……138
3.4 Conclusions……142
3.5 References……...143
Chapter 4: Synthesis of terpene-based polyacrylates and polymethacrylates……146
4.1 Introduction……146
4.1.1 Infrared (IR) spectroscopy……...147
4.1.1.1 Fourier transform infrared spectroscopy (FTIR)……148
4.1.2 Summary and research aims……149
4.2 Experimental……..149
4.2.1 Materials……..149
4.2.2 General polymerisation method……..150
4.2.3 Real Time Fourier Transform Infrared spectroscopy (RT-FTIR)……...151
4.2.4 Nuclear Magnetic Resonance (NMR)……151
4.2.5 Gel Permeation Chromatography (GPC)……151
4.2.6 Differential scanning calorimetry (DSC)……152
4.2.6 Thermo Gravimetric analysis (TGA)……..152
4.3 Results and discussion……...152
4.3.1 Synthesis of polymers from monofunctional terpene-based acrylate and methacrylate monomers……...152
4.3.2 Synthesis of polymers from bifunctional terpene-based acrylate and methacrylate monomers……...159
4.3.2.1 Polymerisation of carvone acrylate and carvone methacrylate **4b** and **4c**……..159

4.3.2.2 Polymerisation of carvone-derived (meth)acrylates in the presence of a chain transfer agent……..170
4.3.2.3 FTIR-monitored polymerisation of carvone acrylate……..…174
4.3.2.4 FTIR-monitored polymerisation of carvone methacrylate……..181
4.3.2.5 Polymerisation of bifunctional β-pinene (meth)acrylate derivatives…185
4.3.2.6 FTIR-monitored polymerisation of bifunctional β-pinene (meth)acrylate derivatives……193
4.4 Conclusions……..198
4.5 References……..…198
4.6 Appendix: ^{1}H-NMR and TGA spectra ……..201
4.6.1 ^{1}H-NMR spectra (300 MHz, CDCl3) ……201
4.6.2 TGA spectra……205
Chapter 5: Application testing: Carvone-based poly(meth)acrylate coatings……208
5.1 Introduction……208
5.1.1 Curing process: crosslinking……209
5.1.2 Thiol-ene curing……..212
5.1.3 Summary and research aims……216
5.2 Experimental……..216
5.2.1 Materials……216
5.2.2 Solvent casting……216
5.2.3 Powder coating preparation and curing……..216
5.2.4 Measurement of coatings properties……217
5.3 Results and discussion……..218
5.3.1 Solvent casting and curing of carvone-based poly(meth)acrylates using thiol-ene chemistry……218
5.3.2 Powder coating and UV curing of poly (carvone methacrylate)……225
5.3.3 Evaluation of coatings properties……227
5.4 Conclusions……232
5.5 References……..233
Chapter: 6 Conclusions and Future work……..235
6.1 Conclusions……235
6.2 Future work……237

6.3 References……..237

Chapter 1: Introduction

One of the main challenges that our society faces today is the replacement of fossil feedstock for renewable sources in the production of our day-to-day commodities. The great majority of manufactured products that we use are made of or contain polymers, ranging from all kinds of plastic materials to paints and shampoos. Around 300 million tons of plastic are produced worldwide every year with the share of renewable polymers being around 5 %. This small share is mainly due to their high cost and inferior performance compared with synthetic polymers produced from petroleum chemicals.[1-4]

However, although utilisation of renewable monomers and polymers is generally uneconomical when compared to petrol derivatives, it must be noted that petrol-derived polymers have undergone decades of research and processes optimisation, especially during the development "boom" in polymer science and technology that happened after World War II.[5] In that sense, renewable polymers are relatively new. Although natural polymers have been utilised by human kind for thousands of years, the chemical modification of biomacromolecules and the exploitation of renewable monomers is a relatively new field.

Renewable raw materials have the potential to provide a wide range of monomers arguably as comprehensive as those provided by the petrochemical industry.[6] In the last ten years, there has been a growing shift of interest to renewable resources, with a considerable increase in the number of scientific publications, monographs, books, international symposia, patents, and industrial as well as public investments.[5] Bioplastics consumption is predicted to reach 3 million tonnes by 2020 and its global production capacity is projected to increase to 6 million tonnes/year in 2020 in Europe. If considering that biobased plastics could potentially substitute around 85 % of polymers, the potential for bioplastics in Europe could reach, by 2050, up to 50 million tonnes.[7]

Natural polymers such as lignin, cellulose, hemicellulose and chitin have been exploited for hundreds of years without major modifications. However, in order to synthesise a comprehensive range of materials with properties that mimic those of petrol-derived polymers, it is necessary to utilise small molecular biomass, such as vegetable oils and fatty acids. These materials can be directly obtained from forestry and agriculture products and can be precisely engineered at a monomer level into renewable polymers, in the same fashion as petrol-based monomers.[8]

One potential source of renewable monomers is terpenes, the most common of which are derived from citrus and wood waste and are already available on the multi-tonne scale; a scale that is likely to grow dramatically as new industrial biotechnology routes come on stream.[9] Despite the natural abundance of terpenes and the fact that they contain, in theory, readily polymerisable moieties, the number of terpene-based polymers is still very limited.[5, 8, 10-13]

In this thesis, utilisation of terpenes as monomers and controlling agents in radical polymerisation is investigated. Radical polymerisation is probably the most common form of polymerisation in industry and certainly one of the most versatile, since it can be applied to a very wide range of monomers in a broad variety of solvents.[14] In this chapter, an overview of existing terpene-polymers is given, as well as the key concepts of radical polymerisation are described.

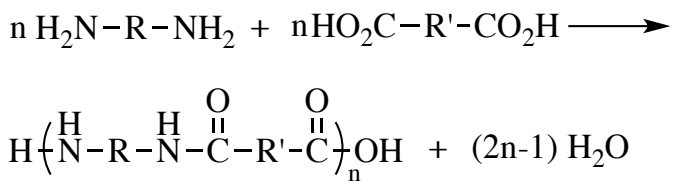
1.1 Polymerisation techniques

Polymerisation reactions are classified into step and chain polymerisations according to the polymerisation mechanism. Chain and step polymerisations differ in several features, but the most important differences are the identities of the species that can react with each other and the manner in which the polymer molecular size depends on the extent of conversion. In step-growth polymerisations, bifunctional or multifunctional monomers react in a stepwise manner leading to dimers, then trimers, tetramers, pentamers and so on until eventually large-sized polymer molecules have been formed. The characteristic of

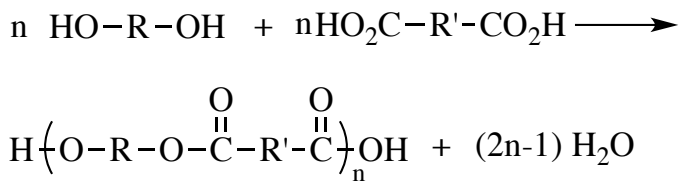
step polymerisation that distinguishes it from chain polymerisation is that the reaction occurs between any of the different-sized species present in the reaction system:

Monomer + monomer ➔ dimer
Dimer + monomer ➔trimer
Trimer + monomer ➔ tetramer
Dimer + dimer ➔ tetramer
Trimer + dimer ➔ pentamer
Trimer + trimer ➔ hexamer
Etc.

Typical examples of step-growth polymerisations include the formation of polyamides (1) and polyesters (2) through polycondensation reactions.



(1)



(2)

Due to the nature of the polymerisation mechanism, molecular weight increases slowly with conversion and high extents of reaction are necessary in order to obtain high chain lengths. The characteristic kinetic profile is represented in Figure 1-1.[15]

If we look at chain polymerisation, the situation is quite different. In chain polymerisation, an initiator is used to catalyse the reaction. The initiator species R*, which can be a radical, a cation or an anion, reacts with a monomer unit.

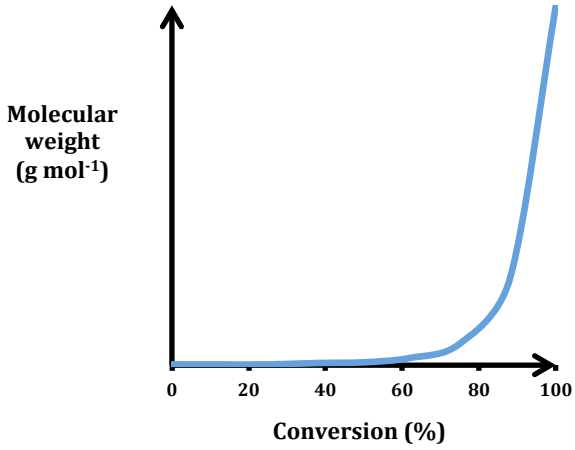


Figure 1-1. Typical kinetic profile of step polymerisations, where molecular weights remain generally low until very high conversions are achieved.

Polymerisation occurs by propagation of the reactive center by the successive additions of monomer units in a chain reaction. The distinguishing characteristic of the mechanism of chain polymerisation is that polymer growth, or chain propagation, takes place by monomer reacting only with the reactive center. As a result, high molecular weight polymer is formed early on in the reaction, to then remain essentially constant (Figure 1-2). The overall percent conversion of monomer to polymer increases with reaction time.[14, 15]

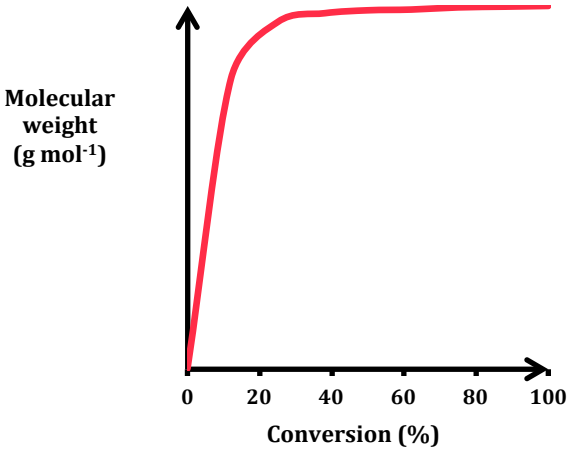


Figure 1-2. Characteristic kinetic profile of chain polymerisation, where molecular increases rapidly at low conversions and then plateaus at mid-high conversions.

Radical polymerisation, a type of chain growth polymerisation will be the focus on this thesis and a detailed introduction is given below. Other types of step-growth and chain-growth polymerisation techniques will only be discussed when relevant on this thesis.

1.1.1 Free radical polymerisation (FRP)

Free radical polymerisation proceeds *via* a chain mechanism, which basically consists of four different types of reactions involving free radicals: preinitiation, initiation, propagation and termination. The general mechanism is shown in Figure 1-3.

The initiation step is considered to involve two reactions. Preinitiation consists of the dissociation of the initiator to yield a pair of radicals (I•), where k_d is the dissociation rate constant. In the decomposition rate equation f represents the initiator efficiency and [I] corresponds to the initiator concentration. Initiation involves the addition of I• to a monomer molecule (M) to produce the chain-initiating radical M_1•. The rate of the generation of radicals that are capable of initiating the polymerisation process (R_i) depends on the initiation rate constant (k_i), the concentration of primary radicals [I] and the concentration of monomer [M].

Preinitiation $I_2 \xrightarrow{k_d} 2\,I^{\cdot}$ $\qquad R_d = 2fk_d[I_2]$

I=Initiator
R•=Radical

Initiation $I^{\cdot} + M \xrightarrow{k_i} M_1^{\cdot}$ $\qquad R_i = k_i[M][I^{\cdot}]$

M=Monomer

Propagation $M_n^{\cdot} + M \xrightarrow{k_p} M_{n+1}^{\cdot}$ $\qquad R_p = k_p[M][M_n^{\cdot}]$

Termination

- Combination $M_x^{\cdot} + M_y^{\cdot} \xrightarrow{k_{tc}} M_{x+y}$ $\qquad R_t = k_t[M_n^{\cdot}]$
- Disproportionation $M_x^{\cdot} + M_y^{\cdot} \xrightarrow{k_{td}} M_x + M_y$ $\qquad k_t = a\,k_{tc} + (1\text{-}a)\,k_{td}$

Figure 1-3. General mechanism of FRP.

The growth of $M_1^{\bullet}$ by the successive additions of monomer molecules, is known as the propagation step, in which each addition creates a new radical that has the same identity as the previous one, except that it is larger by one monomer unit. In the propagation rate expression shown in Figure 1-3, k_p represents the rate constant for propagation while $[M^{\bullet}]$ and $[M_n^{\bullet}]$ correspond to the concentration of monomeric and propagating radical respectively. At some point, the propagating polymer chain terminates. Termination occurs by bimolecular reaction between radicals *via* combination (coupling) by disproportionation (Figure 1-3).

The rate constants for termination by coupling and disproportionation are represented by k_{tc} and k_{td} respectively. In the termination rate equation k_t represents the termination rate constant, which is defined as a function of k_{tc}, k_{td} and a (a and (1-a) are the fractions of termination by coupling and disproportionation, respectively).[11, 14, 15]

1.1.1.1 Molecular Weight, Degree of Polymerisation and Dispersity

The molecular weight of a polymer is important because it determines many physical properties (such as transition temperatures, stiffness, strength, viscosity and so on). The molecular weight distribution in a polymer describes the relationship between the number of moles of each polymer species (N_i) and the molar mass of that species (M_i). Depending on the statistical method that is applied different average values can be defined: number average molecular weight (M_n) and weight average molecular weight (M_w) are the values more commonly used by chemists.

Number average molecular weight is the arithmetic average of the molecular weights of the individual chains:

$$M_n = \frac{\sum_i N_i M_i}{\sum_i N_i}$$

Weight average molecular weight measures the weights of polymer chain by taking bias of the heavier chains, and hence will be more affected by larger chains than M_n:

$$M_w = \frac{\sum_i N_i M_i^2}{\sum_i N_i M_i}$$

The degree of polymerization (DP) is defined as the number of monomeric units in a polymer (M_0 represents the molecular weight of the monomer):

$$DP = \frac{M_n}{M_0}$$

Another important characteristic of polymers is the dispersity (Đ). Dispersity is a measure of the distribution of molecular mass, that is to say, of the heterogeneity of the polymer sample. It is calculated using the following formula:

$$Đ = \frac{M_w}{M_n}$$

The closer the value of Đ is to 1, the more uniform the sample is (Đ≥1).[14, 15]

1.1.1.2 Controlled radical polymerisation (CRP)

FRP, although ideal for certain optimised industrial processes, has the disadvantage of being largely uncontrollable. Controlled radical polymerisation (CRP)[14, 16, 17] is a technique that consists of reducing the radical concentration in the reaction medium. This causes, as a consequence, a reduction in the number of termination reactions and a constant concentration of propagating chains. Therefore, all chains grow at approximately the same rate and molecular weight increases linearly with conversion. This allows for the synthesis of polymers with tailored molecular weights. The three most common forms of CRP are stable free radical polymerisation (SFRP), atom transfer radical polymerisation (ATRP) and reversible addition-fragmentation chain transfer polymerisation (RAFT). In all kinds of CRP, control is provided by an equilibrium between the reactive polymeric radical and dormant species. The fact that the equilibrium is favoured

towards the dormant species causes a decrease in the concentration of polymer radicals.[17, 18]

SFRP employs a stable free radical (e.g. nitroxides in nitroxide mediated polymerisation, NMP) that reversibly react with the growing polymer to form a dormant species (Figure 1-4).[19]

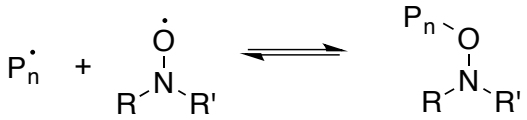


Figure 1-4. In NMP, a type of SRP, the reaction between a nitroxide and the growing polymer chain generates a thermally labile alkoxamine. The fact that the equilibrium favours the formation of the alkoxamine allows for the polymerisation to be controlled.

In ATRP, radical suppression is achieved by reversible ligand exchange with a copper complex (Figure 1-5).

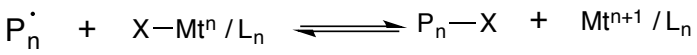


Figure 1-5. Equilibrium between active and dormant species in ATRP, where Mt is the metal, X is the halide (Br or Cl), and L_n are the ligands coordinated with the metal.

A halogenated initiator is activated by halogen exchange with the copper complex and subsequently initiates the polymerisation. The polymeric radical can then reversibly exchange a halogen with the metal complex, forming a reversible termination equilibrium.[20, 21]

RAFT polymerisation exploits reversible chain transfer to a thiocarbonyl chain transfer agent (CTA) (Figure 1-6).

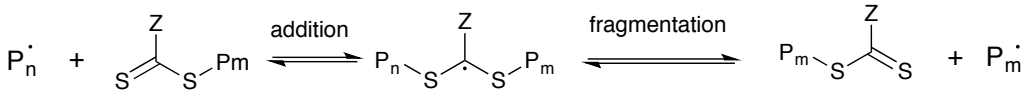


Figure 1-6. Equilibrium between active and dormant species in RAFT polymerisation.

The key step in RAFT mechanism is the equilibrium that is established between growing polymer chains and the intermediate radical species, which fragments to release a polymeric radical. This polymeric radical undergoes further propagation before once again adding to the RAFT agent and releasing another polymeric radical. From this equilibrium, all chains have an equal chance to grow at the same rate and hence Đ remains typically low in RAFT polymerisations.[22]

CRP is not the focus of this thesis and therefore no further details will be discussed in this introduction.

1.2 Polymers from renewable sources

The term 'renewable resource' is defined as "any animal or vegetable species which is exploited without endangering its survival and which is renewed by biological (short term) instead of geochemical (very long term) activities".[11] A brief overview of the utilisation of renewable polymeric materials by mankind is given below.

Biomacromolecules are ubiquitous in nature as a result of enzymatic, bacterial and chemical polymerisation of certain natural molecules. Therefore, natural polymers such as cellulose, hemicellulose, lignin, chitin, and chitosan constitute abundant and low-cost feedstock. Through human history, natural biopolymers have been used for a wide range of applications such as clothing, tools, weapons, utensils and a source of energy.

Cellulose (Figure 1-7), for example, constitutes around 40 % of wood composition and it is also found in plant fibers such as cotton, hemp, flax and jute. Cellulose has been used to make paper since the Chinese first invented the process around 100 A.D. Cellulose and hemicellulose (Figure 1-7) constitute a key component in human and other animals diet, despite the fact that we cannot digest them, since they act as bulk or roughage that helps the movements through our intestines.[11]

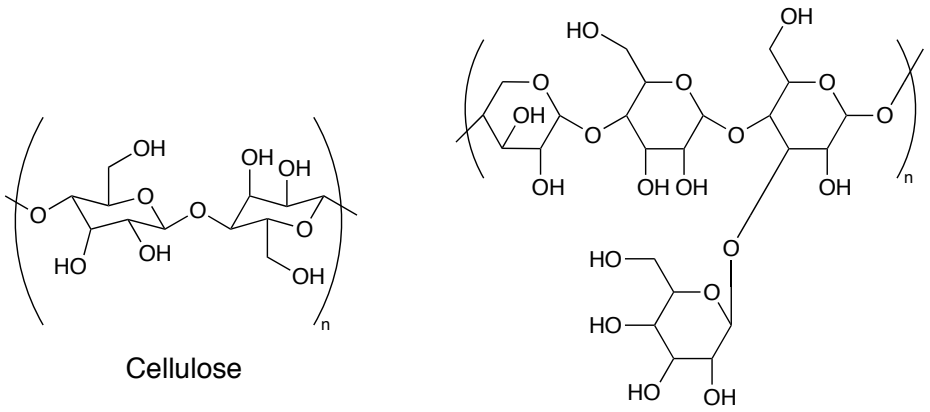


Figure 1-7. Typical structures of cellulose and hemicellulose. Cellulose is a linear polymer made of repeated units of glucose while hemicellulose is a branched polymer formed by different monomeric sugars. Cellulose and hemicellulose are present in almost all plant cell walls. Hydrogen bonding gives them their characteristic hardness.

Another interesting biomacromolecule is chitin (Figure 1-8), the most abundant animal polysaccharide on earth. It constitutes the basic element of the *exo*-skeleton of insects and crustaceans, but it is also found in the outer skin of *fungi*. Chitosan (Figure 1-8) is a linear polysaccharide obtained by extensive deacetylation of chitin.[11]

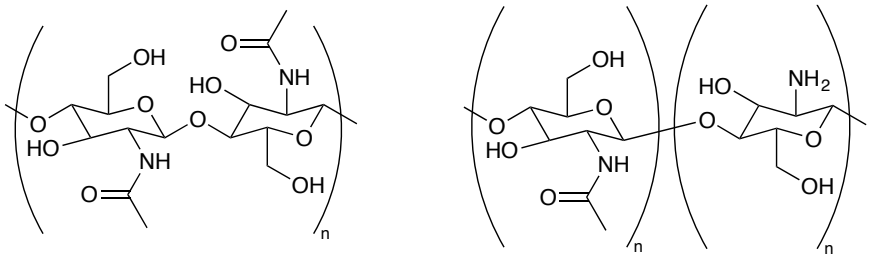


Figure 1-8. Chemical structures of chitin and chitosan. Chitin is a long-chain polymer of an N-acetylglucosamine composed of randomly distributed β--linked D-glucosamine and N-acetyl-D-glucosamine.

Chitin and chitosan have traditional uses in different national food products. Chitin is found in foods containing unpeeled shrimp and edible fungi such as *Aspergillus niger* and *Agaricus campestris*. Chitosan is also found in food products, such as the Norwegian old cheese *gamalost* where the yeast *Muco mucedo*, which contains chitosan in the cell walls, is used in the fermentation process.[23] They also have pharmaceutical applications in traditional Chinese medicine.[24]

One of the traditional applications of biopolymers is leather tanning. Tannins (Figure 1-9) are a group of polyphenols that are found in the tree barks in high concentrations.

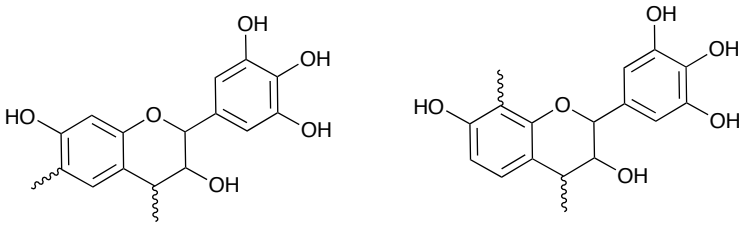


Figure 1-9. Typical flavonoid monomer units found in the chemical structure of tannins.

Tannins receive their name from their ability to tan leather, which is, to crosslink and precipitate the proteins present in animals hide, turning it into leather (Figure 1-10). Tannins can also react with iron salts to form coloured insoluble

precipitates with colours ranging from dark blues and greens through to blacks. This property has made tannins useful for applications such dyes and inks.[25]

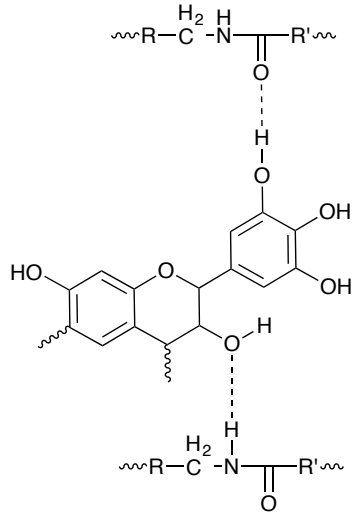


Figure 1-10. Crosslinking between peptide chains occurs via hydrogen bonding between the polar groups in the protein and the hydroxy groups present in tannins.

Another natural polymer traditionally used for tanning applications is lignin (Figure 1-11).

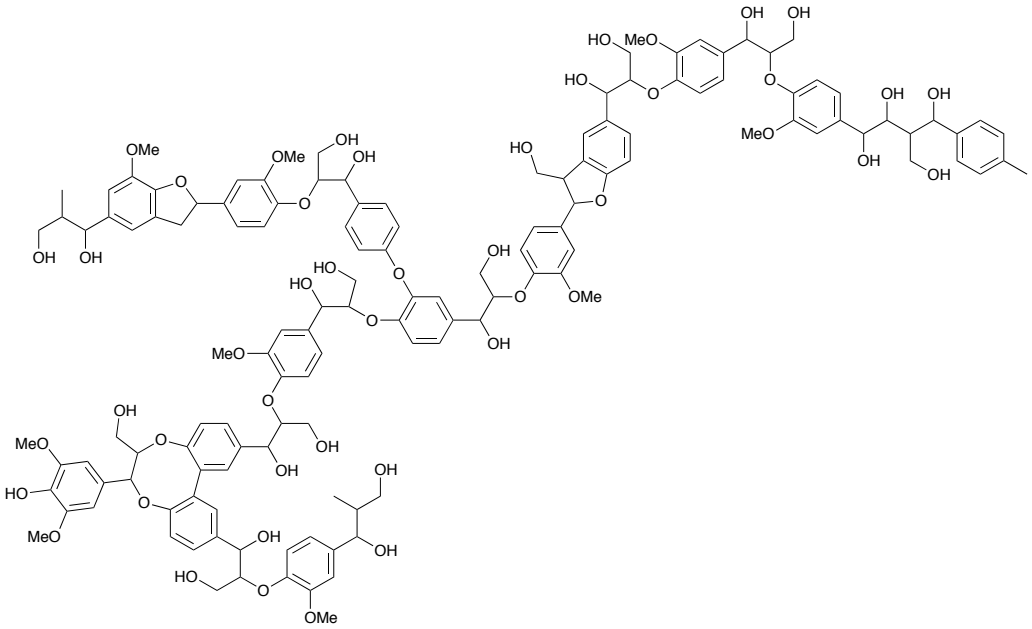


Figure 1-11. Example of a typical structure of lignin with its most characteristic building blocks.

Lignin is the amorphous matrix of wood and is characterised by a highly irregular structure compared with that of cellulose (Figure 1-7). Aditionally, lignin structure is a function of the wood family and of the isolation process. The pulping technology calls upon a delignification mechanism, which is based on the use of sulfites, hence it yields lignin fragments bearing sulfonate moieties. In tanning applications, lignin sulfonates are generally used in combination with chrome tanning agents.[26]

These are only a few examples. The progressive development of improved technologies led to, by the end of the 19th century, a sophisticated exploitation of natural polymers including applications such as dying of natural fibres, vulcanisation of natural rubber, formulation of inks, paints and lacquers, photograph printing, starch and resins-based adhesives and cellulose-based thermoplastic polymers.[5, 10, 11, 27-29]

However, the flourishment of petrol-based chemistry during the 20th century and the petrochemical boom revolutionised the field of macromolecular materials, causing a setback on the further development of renewable-based polymers. The success of the new petrol-derived materials resided on the low-cost of the starting materials and the wide diversity of monomer structures that were made available, which led to a wide array of products and technological advances. Such exponential development of polymeric materials, especially during the last 40 years, is the reason why our era is often referred to as the "Plastic Age".[5, 11, 30-32]

Nowadays, the scarcity of fossil resources and a sense of urgency related to sustainability has caused a growing interest in renewable materials, with the number of scientific publications and investment rising considerably in the last decade.[5] Advanced polymerisation techniques are being used to manipulate biomacromolecular structures to further improve their performance. However, the synthesis of renewable polymeric materials from a monomer approach offers a wider window of possibilities. Natural resources like vegetable oils, fatty acids, hydroxyalkanoates, lactic acids, terpenes and rosins among others are a class of natural molecular biomass, which can be used as they exist in nature or

derivatised through simple procedures into renewable monomers, and polymerised with controlled architectures and desirable properties, potentially to a level comparable to that of their petroleum-based counterparts.[5, 10, 11, 13, 33-36]

This thesis is focused on the exploitation of a particular group of natural monomers, terpenes. Other natural sources of renewable monomers will not be further discussed unless they are relevant.

1.3 Terpenes and their applications

Terpenes are a family natural hydrocarbons, which are synthesised mainly by plants, but also by a limited number of insects, microorganisms and fungi. Most terpenes share isoprene (Figure 1-12) as a common building block.

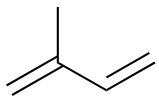


Figure 1-12. Chemical structure of isoprene. The chemical structure of any terpene can be divided into isoprene units.

This structural relationship was identified by Wallach in 1887, who observed that most terpenic structures result from the 'head-to-tail' condensation of isoprene units. Based on this generic rule, terpenes can be classified according to the number of isoprene units (Table 1-1) ranging from hemiterpenes, containing one isoprene unit, to tetraterpenes containing eight units. Molecules with a higher number of isoprene units are generally denominated polyterpenes.[11]

Table 1-1. Classification of terpenes according to the number of isoprene units present in their chemical structure.

Classification	Isoprene units	Carbon atoms
Hemiterpenes	1	5
Monoterpenes	2	10
Sesquiterpenes	3	15
Diterpenes	4	20
Sesterpenes	5	25
Triterpenes	6	30
Tetraterpenes	8	40
Polyterpenes	n	n

The most representative source of terpenes is turpentine, the volatile fraction of pine resin, whose chemical composition depends on the tree species, geographical location and the overall procedure to isolate it. However, the major components are a few monoterpenes ($C_{10}H_{16}$) whose chemical structures are shown in Figure 1-13.

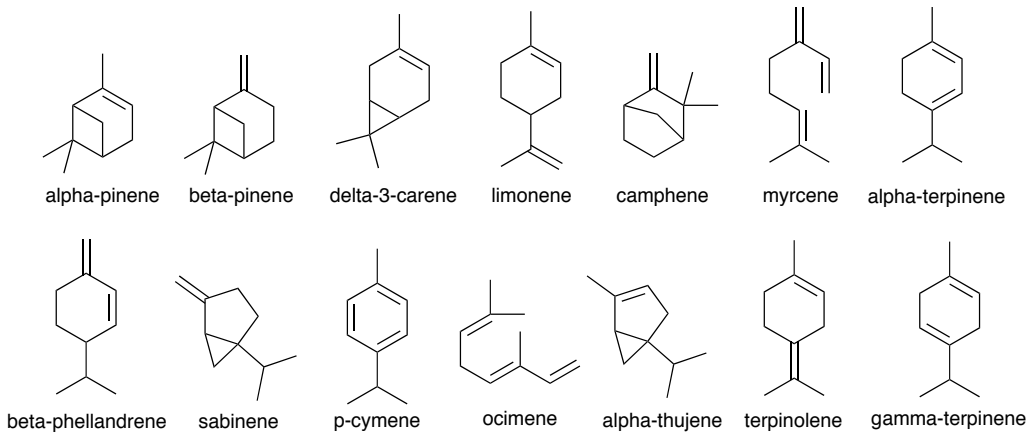


Figure 1-13. Chemical structures of some of the most abundant monoterpenes.

Natural monoterpenes containing oxygen atoms are denominated terpenoids and although they do not meet the isoprenic rule their structures are similar enough to be generally considered as part of the terpene family. Some of the most common terpenoids are depicted in Figure 1-14.

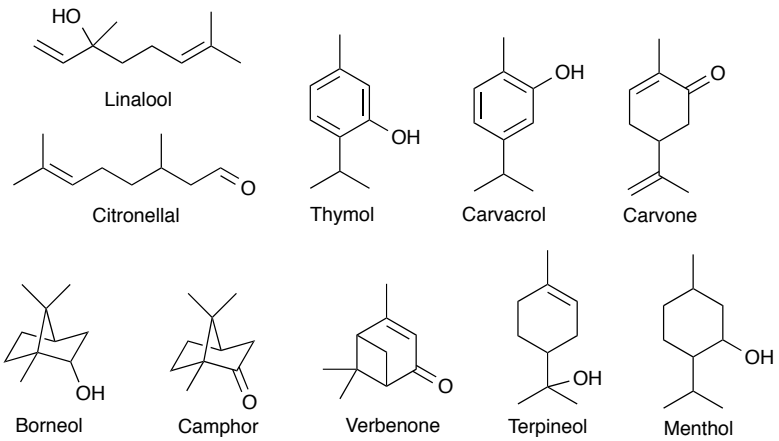


Figure 1-14. Chemical structures of some of the most naturally abundant terpenoids.

An important feature of terpenes is the ease with which the basic skeletons can interconvert to give rise to any monoterpene.[37] Numerous catalytic chemical processes have been developed for the production of valuable products from terpenes through hydrogenation, oxidation, isomerisation/rearrangement, hydration, hydroformylation, condensation, cyclization, ring contraction, etc, providing a considerable number of renewable and potentially polymerisable building blocks (Figure 1-15).[38]

The systematic study of monoterpene chemistry started in the late 19th century, although their use as naturally occurring oils, known as 'essential oils', is a millenary activity. Turpentine is by far the most widely produced essential oil in the world and consequently the source for applications requiring large-scale supplies, its yearly production amounts for 350,000 tonnes. Historically, the most relevant use of turpentine components as reagents include insecticides (although this application was progressively banned from the 1970s), pine oil production, flavours, fragrances and other fine chemicals as well as polyterpene resins.[10, 11]

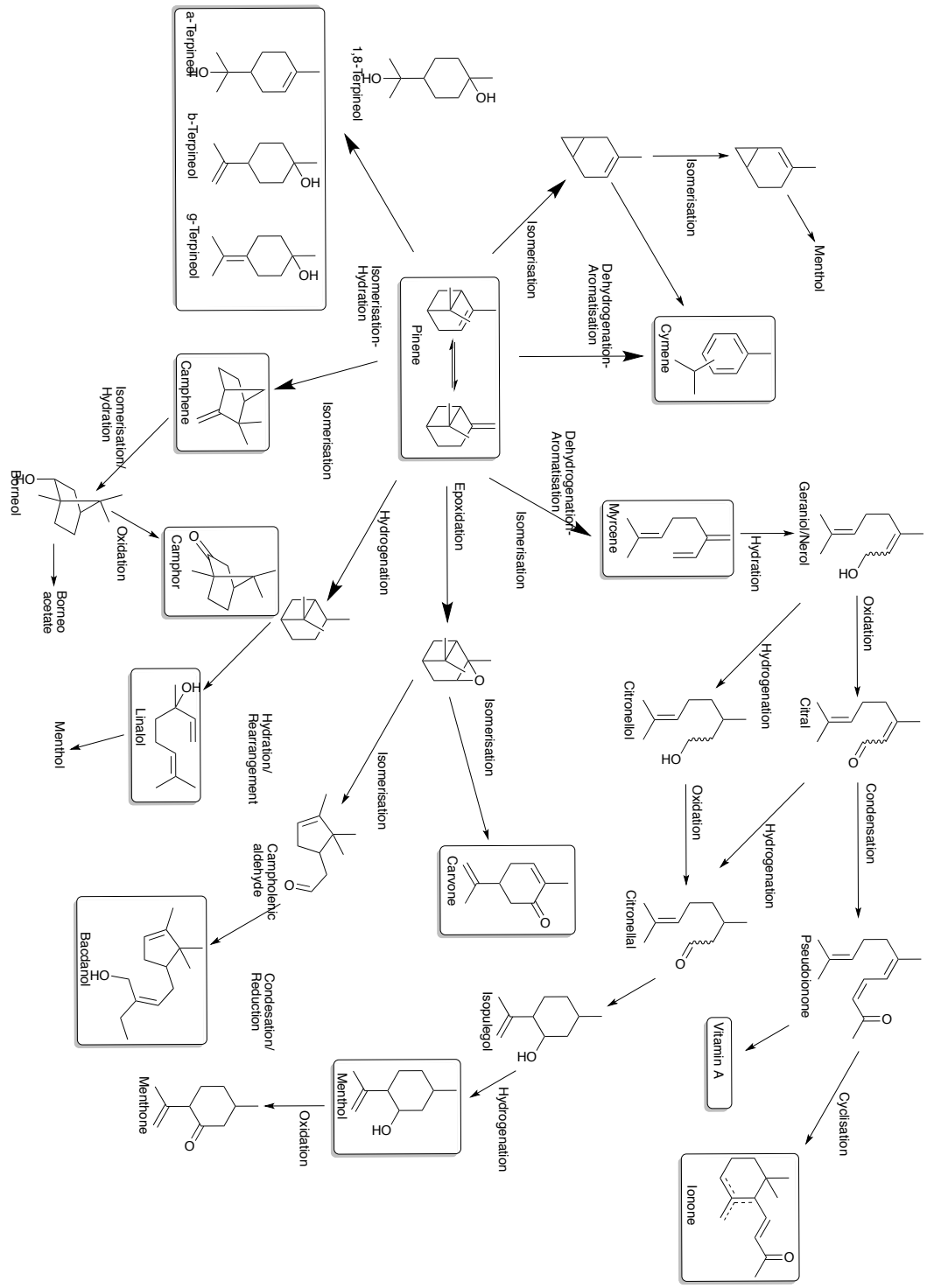


Figure 1-15. Example of some valuable building blocks that can be obtained from pinenes.[38]

1.3.1 Polymers from terpenes

Despite the vast range of terpenes available, only the most abundant ones, such as α-pinene, β-pinene, limonene, myrcene and carvone (Figure 1-16), have been the subject of polymerisation studies reported in the literature.

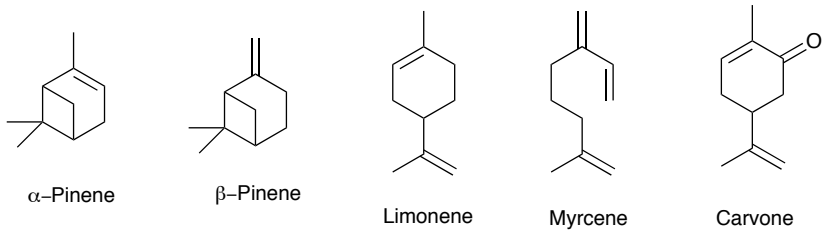


Figure 1-16. Chemical structures of some of the terpenes that have gathered more interest the polymer field.

The polymerisation techniques that have attracted most attention regarding terpenes polymerisation are cationic and radical polymerisation. However, the utilisation of cationic and radical methods have afforded to date a very limited number of terpene-based polymeric materials. Studies regarding other polymerisation techniques such as thiol-ene functionalisation or oxidation and subsequent polymerisation have also been reported.[5, 8, 10, 11, 13] An overview is detailed below.

1.3.1.1 Radical polymerisation of terpenes

There have been significant efforts to create polymers *via* the radical polymerisation of terpenes because their structures contain alkene moieties that appear to offer the opportunity for facile polymerisation. However, extensive research has shown that the terpenes do not easily homopolymerise radically, and even in the presence of a co-monomer (such as styrene or an acrylate) the level of incorporation of the terpene is minimal and the polymers produced thus far have only very low molecular weights.[5, 10-12]

α-Pinene and β-pinene are the most abundant components of turpentine, the volatile fraction of pine resin. They are the two most abundant terpenes and therefore, they have attracted considerable interest regarding their polymerisation.

Turpentine composition varies depending on the type of tree and the geographical area. α- and β-pinene account for 45-90 % and 1-30 % of the total composition respectively. Studies from the late 90's regarding radical homopolymerisation of α- and β-pinene revealed that although they do participate in radical processes, only oligomers were obtained with a maximum M_w of around 850 g mol^{-1}.[39]

Attempts of copolymerising terpenes with synthetic monomers have been reported. Conventional free radical copolymerisation of β-pinene and methyl methacrylate (MMA) or styrene (St), initiated by AIBN, yielded copolymers with M_w of around 11,600 and 25,400 g mol^{-1} respectively.[39] However analysis of the unreacted monomer mixtures revealed that most of the pinene remained unreacted in all cases. Copolymerisation of β-pinene with acrylonitrile (AN),[40] methyl acrylate (MA)[41] or *n*-butyl acrylate (nBA)[42] as comonomers yielded polymers with M_n of up to 7,000 g mol^{-1} with a structure characterised by the presence of AN, MA or *n*BA blocks alternated with single β-pinene units, due to the low reactivity ratio of β-pinene.

Similarly, attempts of homopolymerisation of limonene showed that limonene does not react with itself.[43] Limonene is obtained as a by-product of the citrus industry and is present in more than 300 plants.[44] Limonene is a chiral molecule and its (*R*)-enantiomer is produced on a scale of over 70,000 tonnes per year.[45]

However, when limonene was copolymerised with N-phenylmaleimide by FRP or RAFT[43] in the presence of a fluorinated solvent polymers with a M_n of 9,200 g mol^{-1} and 8,400 g mol^{-1} were obtained respectively. Fluorinated solvents had been successfully utilised in the radical copolymerisation of polar monomers with nonpolar monomers in the past, since they seem to alternate the monomers reactivity ratios, enhancing copolymerisation.[46] The fluorinated solvent interacts with the carbonyl groups in N-phenylmaleimide *via* hydrogen bonding (Figure 1-17), withdrawing electron density and therefore facilitating the addition of the electron-rich limonene monomer.

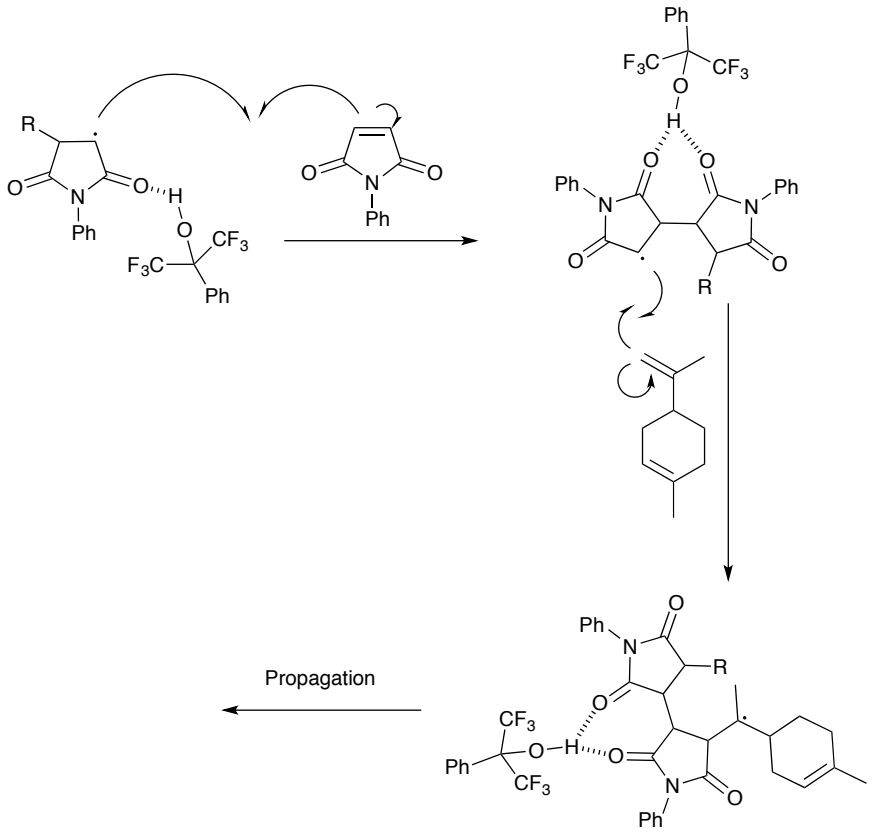


Figure 1-17. Radical polymerisation of N-Phenylmaleimide and limonene in a 2:1 fashion. Copolymerisation between both monomers is enhanced by the effect of the coordination of the fluorinated alcohol with the carbonyl groups at the end of the polymer chain.

A recent study reported the successful radical homopolymerisation of limonene using benzyol peroxide as an initiator at 85 ^{o}C in xylene.[47] The weight-average molecular weight of resultant polylimonene was 43,000 g mol^{-1}. However, these results are significantly contradictory to previous studies. Hence further investigation should be conducted regarding radical copolymerization of limonene.

Another example of high molecular weight polyterpene synthesised by radical polymerisation was recently published by Sarkar *et al* (Figure 1-18).[48] Myrcene is an acyclic monoterpene and a component of bayberry wax and oils of bay and verbena,[49] but it can also be obtained from the pyrolysis of pinene.[50] Myrcene was transformed into polymers with M_n as high as 96,000 g mol^{-1} when using emulsion polymerisation techniques.

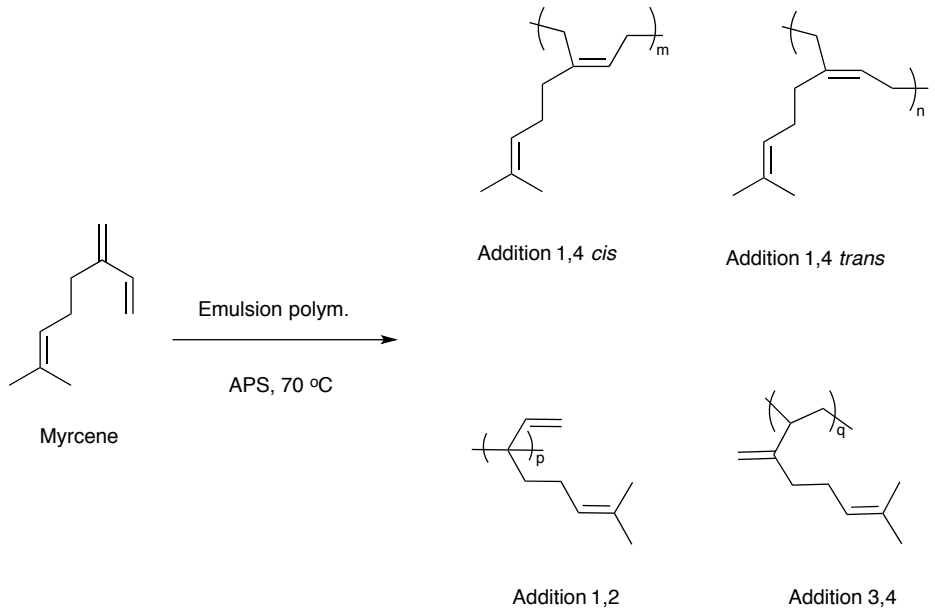


Figure 1-18. Radical emulsion polymerisation of myrcene led to high molecular weight polymyrcene containing 1,2 vinyl and 3,4 defects along with 1,4 cis and 1,4 trans motifs.

A typical emulsion polymerisation formulation comprises monomer, water, surfactant and a water-soluble initiator. The reaction system is characterised by emulsified monomer droplets dispersed in the continuous aqueous phase with the aid of an oil-in-water surfactant. A very small fraction of monomer is dissolved in the water. The reaction starts when the initiator reacts with the monomer present in the aqueous phase, forming oligomers with increasing hydrophobic character as they propagate. Once they reach a critical chain length these oligomers enter the monomer-containing micelles where they continue propagating, forming a polymer particle. The segregation of free radicals among the discrete micelles considerably reduces the probability of bimolecular termination and, thereby, leads to higher molecular weights than those obtained by bulk or solution polymerisation.[51]

High molecular weight polymers obtained from terpenes by emulsion polymerisation is very interesting. However, it has only been applied to myrcene so far, and further investigation is needed to test whether high molecular weight polymers could also be obtained from other terpenes.

1.3.1.2 Cationic polymerisation of terpenes

Attempts to polymerise α-pinene, the most abundant terpene, using cationic polymerisation techniques have been reported.[52-58] However this studies showed little success, obtaining mostly oligomers with generally low yields. This lower reactivity of α-pinene is thought to be caused by the steric hindrance around the endocyclic double bond.[11, 59] On the other hand, β-pinene contains an exocyclic double bond, more reactive towards cationic polymerisation. Therefore, β-pinene has attracted more attention regarding cationic polymerisation, despite being second in abundance.

The cationic polymerisation of β-pinene was first studied using several Lewis acid metal halides like $AlCl_3$, $AlBr_3$ and $ZrCl_4$, as initiators.[59] The polymerisation of β-pinene using $AlCl_3$ as a catalyst was found to be fast and very exothermic, and yielded a solid polymer with a molecular weight of approximately 2,000 g mol^{-1}. The strain release resulting from the opening of the cyclobutane ring and the formation of a relatively stable tertiary carbenium ion are the driving forces of this reaction (Figure 1-17). The polymerisation mechanism involves the formation of a strong proton donor by the reaction of the Lewis acid with water, followed by the protonation of β-pinene molecule and formation of a carbenium ion.

The carbenium ion then rearranges to form a *p*-menthane type carbocation responsible for the propagation reaction. Conventional cationic polymerisation of β-pinene generally results in low molecular weight polyterpene ($M_n \leq 4{,}000$ g mol^{-1}) together with a variety of byproducts.[55, 59, 60]

A common characteristic of cationic polymerisation is their high exothermicity and rapidity of the reaction, which typically leads to unwanted side reactions. Thus, in order to obtain polymers with M_n of at least few thousand and avoid byproducts, the reaction temperature must be kept particularly low.[11, 12, 59] In particular, polymerisation of β-pinene must be kept between -40 and -80 ^oC in order to reach high conversions[61] and high molecular weights of around 40,000 g mol^{-1}.[62]

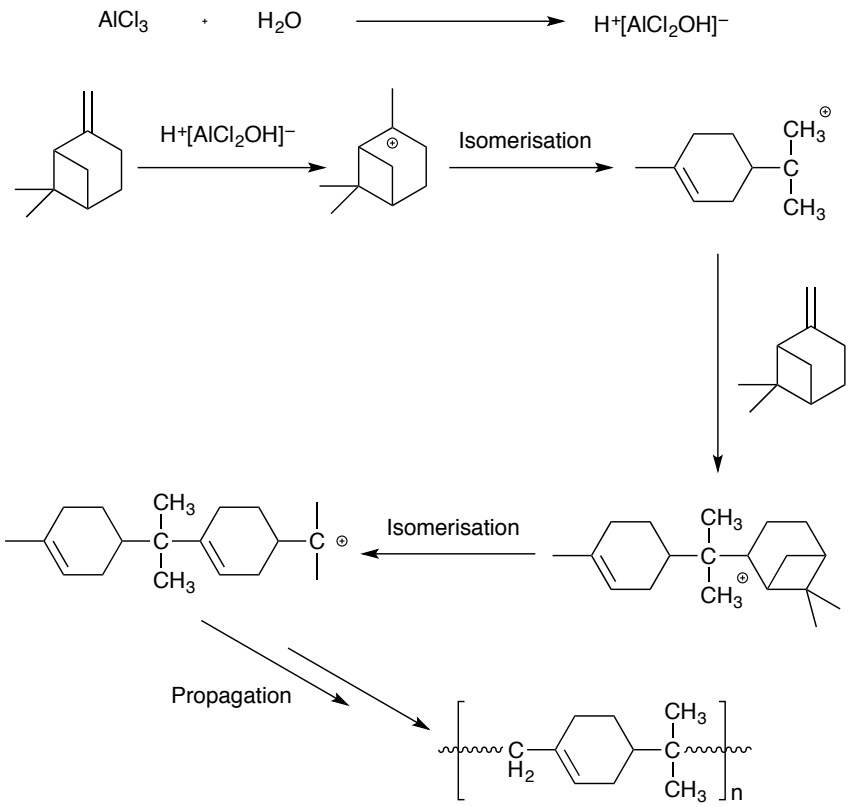


Figure 1-19. Mechanism of cationic polymerisation of β-pinene.

Hillmyer showed that two pinene-derived monomers, α-methyl- p-methylstyrene and myrcene, can be incorporated into ABA tri-block copolymers.[63] This is a significant step forward, but the processes rely upon anionic polymerisation at −78 °C and require scrupulously anaerobic and anhydrous conditions to make useful materials. Unfortunately, the use of such extreme conditions would make a potential industrial process far too expensive and therefore unpractical.

In order to avoid the use of extremely low temperatures during the conventional cationic polymerisations described above, different catalysts were investigated and reported.[64, 65] Lu *et al*.[65] synthesised a Schiff-based nickel complex catalyst (Figure 1-20) to produce poly(β-pinene) by cationic polymerisation. A Schiff-based is a compound with the general structure $R_2C{=}NR'$.

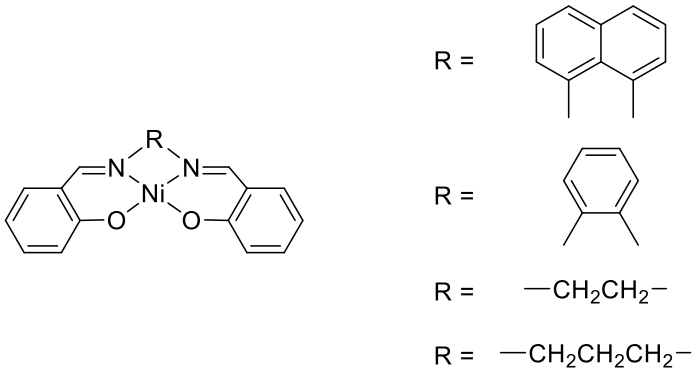


Figure 1-20. Schiff-based Nickel complex used by Lu et al. for the cationic synthesis of poly(β-pinene).

However, this catalyst alone did not produce any polymers. It was necessary to use methylaluminoxane (MAO) as cocatalyst. Under these conditions, they were able to synthesise poly β-pinene with a molecular weight of 11 000 g mol^{-1} at 40 ^{o}C. However, a high ratio of ratio of [MAO]:[Complex] = 500:1 was necessary in order to achieve high conversions. This presents a major drawback since the above-mentioned catalysts (Figure 1-20) are not commercially available, require multi-steps synthesis and MAO is a rather expensive chemical. The polymerisation is initiated by a Ni cation formed by the reaction of the Ni complex and MAO. Then, propagation proceeds in a manner typical for conventional cationic polymerisation of β-pinene.

To overcome these obstacles, Kukhta *et al*. used a $H_2O/AlCl_3{\bullet}OPh_2$ (OPh_2:diphenyl ether) coinitiator system at 20 ^{o}C.[64] Under this conditions they obtained the corresponding poly(β-pinene) with M_n between 9,000 and 14,000 g mol^{-1}. The proposed mechanism for this polymerisation is shown in Figure 1-21.

The reaction starts with the dissociation of the $AlCl_3{.}OPh_2$ complex and the protonation of β-pinene by water, the cocatalyst, which then isomerises into a *p*-menthane-type cation. Transfer of a proton from cationic β-pinene to the $AlCl_3(OH)^-$ counterion would terminate the reaction. This process is denominated termination by chain transfer.

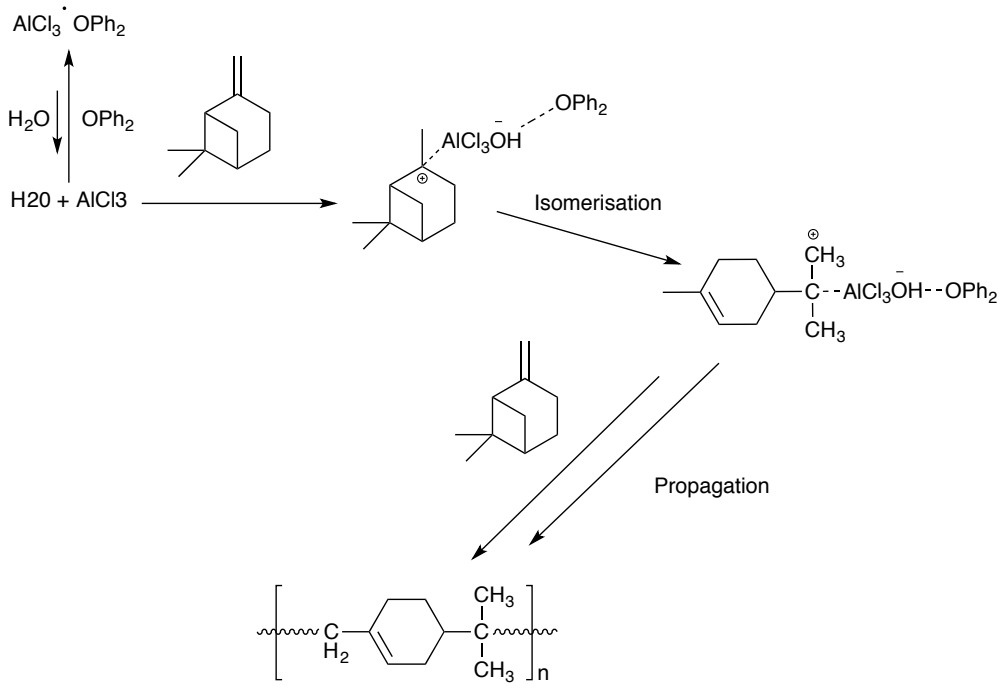


Figure 1-21. Mechanism of cationic polymerisation of beta-pinene catalysed by $AlCl_3.OPh_2$

However, the interaction of $AlCl_3OH^-$ with diphenyl ether generates a weaker counterion, with a lower tendency to abstract hydrogens. As a consequence, there is a decrease in chain transfer reactions, and therefore polymers with higher molecular weights are obtained. Another reason for the production of higher molecular weight polymers is the basicity of the diphenyl ether electron-donating group. The use of a stronger base like dibutyl ether would lead to hydrogen abstraction. With a weaker base like diphenyl ether, this side reaction is no longer present.[64] The mild reaction conditions applied in this study make this cationic polymerisation method very attractive for industrial utilisation. However, molecular weights achieved are still relatively low and further research needs to be conducted in order to apply these conditions to other terpenes.

Copolymers of β-pinene with synthetic monomers have been produced using similar conditions to the ones described above.[66-69] However, very low temperatures were required (-40 ^oC) and polymers with rather low M_n were obtained. Therefore, cationic polymerisation of β-pinene copolymers will not be discussed further in this PhD thesis.

1.3.1.3 Application of thiol-ene chemistry to terpene polymerisation

As detailed above, cationic polymerisation has been utilised to produce mainly β-pinene-based homopolymers. The limited number of monomers that undergo cationic polymerisation has guided researchers to investigate other polymerisation methods for the production of terpene-based homopolymers. One of these methods consists on functionalising terpenes *via* thiol-ene chemistry prior to their polymerisation. Thiol-ene coupling is a radical process that produces a sulfur-carbon bond (Figure 1-22).

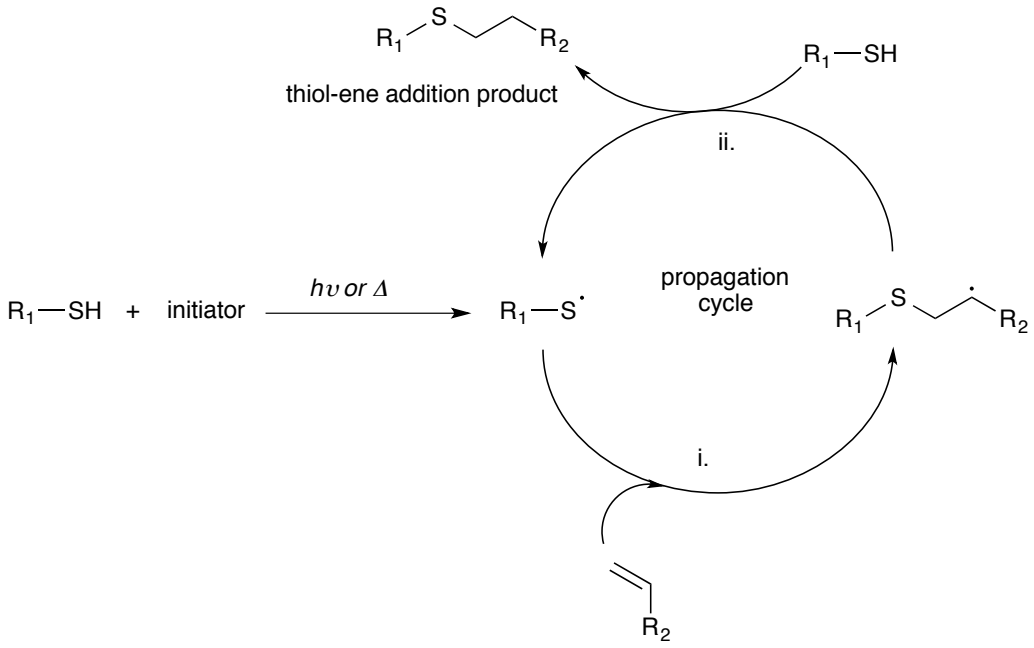


Figure 1-22. Mechanism of free-radical thiol-ene coupling. The propagating cycle revolves around radical addition of the thiol to the alkene (i) and chain-transfer between the thiol and the carbon-centered radical (ii).

In the presence of a radical initiator, a thiol undergoes a homolytic cleavage of the S-H bond, leading to a thiyl radical. Radical addition of the thiyl radical to a double bond functionality (i) is followed by hydrogen abstraction from a new thiol group by the carbon-centered radical (ii), regenerating the thiyl radical and yielding the corresponding thiol-ene product.[70]

Meier *et al.* utilised thiol-ene chemistry to produce limonene based homopolymers.[45] Limonene was reacted with both hydroxyl and methyl ester functionalised thiols (Figure 1-23) to produce bifunctional monomers that could then be polymerised through polycondensation.

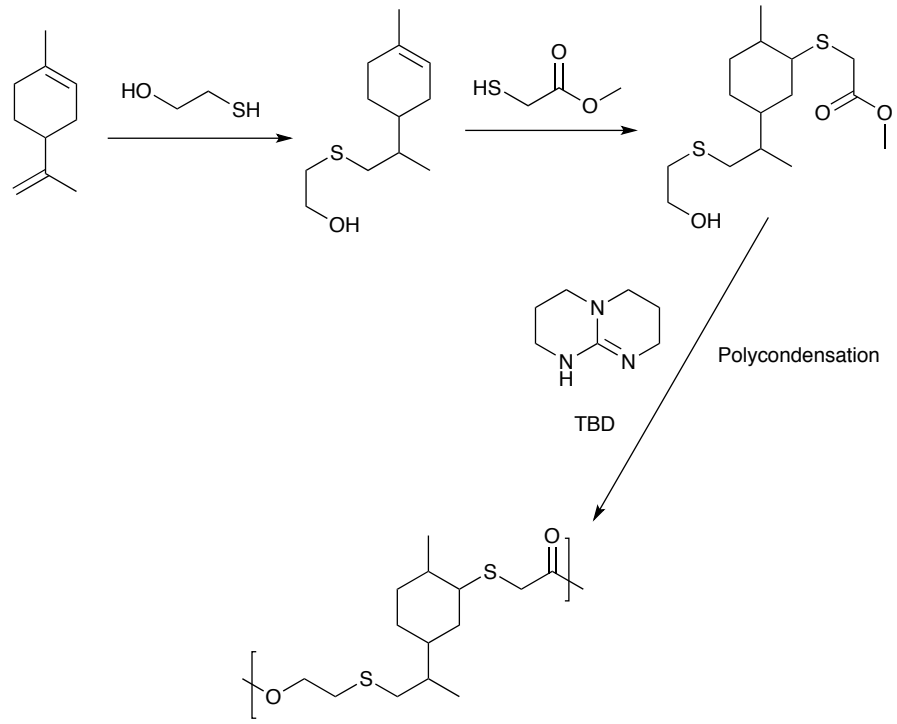


Figure 1-23. Functionalisation of limonene via thiol-ene chemistry followed by polycondensation led to limonene-based homopolymers.

Polycondensation reactions were conducted at room temperature, in the presence of 1,5,7-tri-azabicyclo[4.4.0]dec-5-ene (TBD), an organic base catalyst. Polymers with molecular weights between 8,000 and 10,000 g mol^{-1} were obtained. However, Meier *et al*. discovered that higher molecular weights of 25,000 g mol^{-1} were achieved when the bifunctional limonene-based monomers were copolymerised with long fatty acid-based diols and diesters. The reason for this increase in M_n was believed to be a decrease in the steric hindrance between the limonene units.

More recently, Meier applied a similar strategy to synthesise limonene-based diamines and dicarbamates monomers *via* thiol-ene chemistry (Figure 1-24, Figure 1-25).[71]

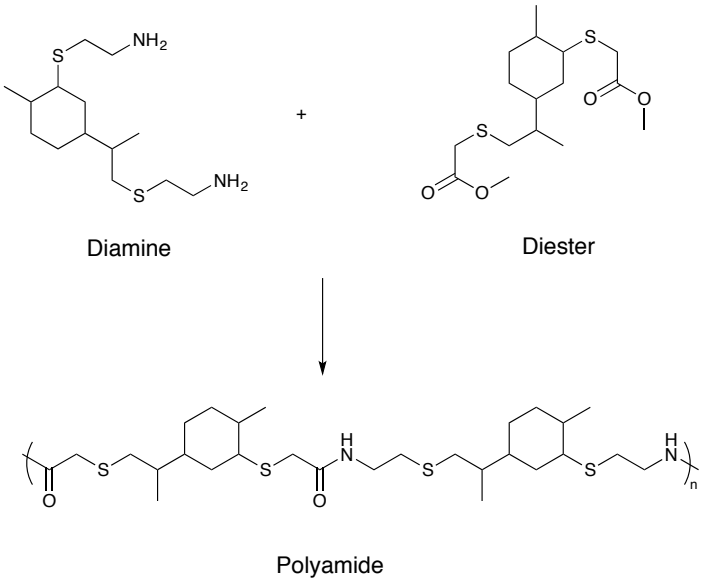


Figure 1-24. Limonene-based diamine and diester synthesised by Meier and workers via thiol-ene chemistry were copolymerised through condensation polymerisation, yielding limonene-based polyamides.

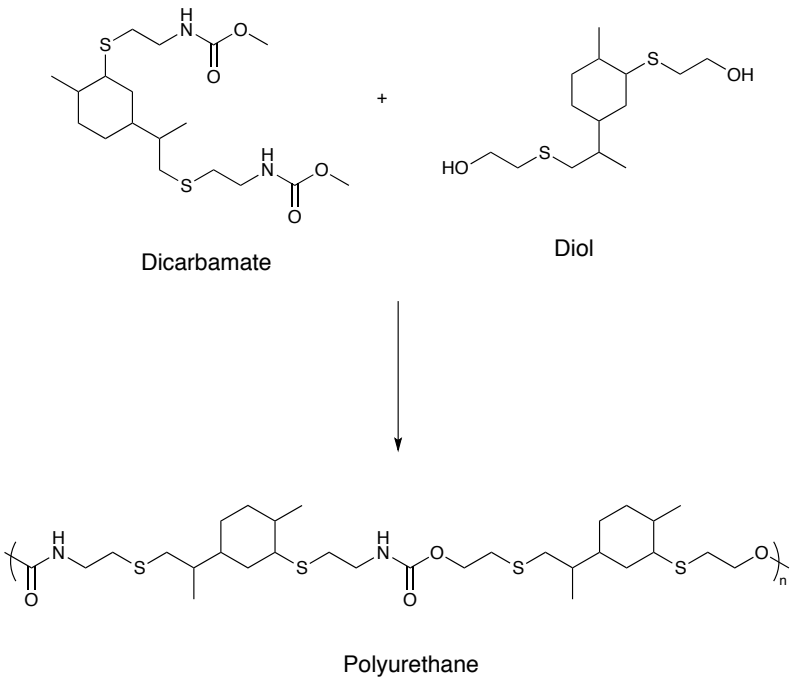


Figure 1-25. Meier et al. prepared limonene-based dicarbamates and diols that were copolymerised to synthesise polyurethanes.

The condensation copolymerisation of limonene-based diamines with diesters (Figure 1-24) allowed for the synthesis of polyamide with a M_n of up to 12,000 g mol^{-1} and a good dispersity of 1.46. Meier also synthesised polyurethanes by copolymerising limonene-based dicarbamates with a series of diols, including limonene-based diols shown in Figure 1-25. Polyurethanes showed a M_n of up to 12,600 g mol-1 with dispersities between 1.79 and 2.15.

These studies conducted in the Meier group demonstrated the potential of thiol-ene chemistry for the transformation of terpenes into polymerisable monomers. The advantages of thiol-ene chemistry are that it can be carried out at room temperature and in absence of solvents. However, challenges still exist, such as preparation of high molecular weight polymers. Additionally, the use of thiols in polymers can lead to discolouration and bad odours, which is disadvantageous when developing polymers for commercial applications.

1.3.1.4 Other transformations of terpenes into polymerisable monomers

As was discussed above, limonene has been the subject of a few thiol-ene functionalisation studies.[45, 71] Another common transformation of limonene is the epoxidation of its double bonds to produce limonene oxide or dioxide (Figure 1-26).[72-75]

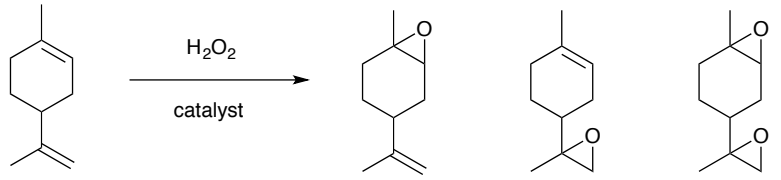


Figure 1-26. The epoxidation of limonene leads to limonene oxide and/or limonene dioxide.

The commercial availability of limonene oxides has encouraged research regarding their polymerisation. Limonene oxide has been tested as monomer using different polymerisation techniques.

Cationic homopolymerisation of limonene oxide was investigated by Crivello *et al*.,[76] revealing a high occurrence of side reactions and therefore suggesting that it is not practical to homopolymerise this monomer *via* cationic polymerisation.

Coates *et al*. copolymerised limonene oxide with carbon dioxide to produce linear polycarbonates[77] (Figure 1-27) based upon prior success of petroleum-based cyclohexane oxide and carbon dioxide copolymerisation.[78]

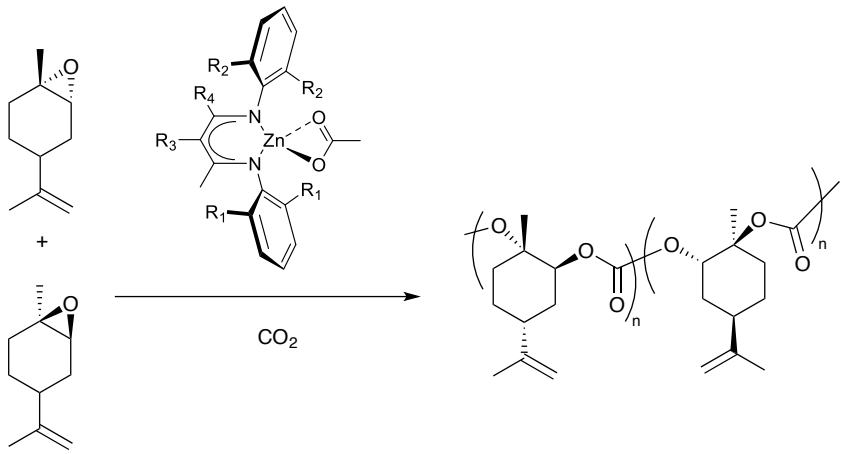


Figure 1-27. Synthesis of polycarbonates from limonene oxide and carbon dioxide in the presence of a β-diiminate zinc catalyst.

Coates utilised β-diiminate zinc acetate complexes as polymerisation catalysts and a commercial mix of *trans*- and *cis*-limonene oxide stereoisomers as starting materials (Figure 1-27). The corresponding polycarbonates were obtained with a M_n of up to 25,000 g mol^{-1} and a narrow dispersity of 1.16. However, mainly the *trans* stereoisomer reacted, with practically all the *cis* stereoisomer remaining unreacted, which means that this was a very uneconomic process.

Later, Kleij *et al*. showed that the use of an Al(III) catalyst incorporated both isomers into the polymer chain,[79] although M_n were still lower than 11,000 g mol^{-1} and the maximum monomer conversion achieved was 75 %.

Very recently, Greiner *et al*. synthesised polycarbonates from limonene dioxide and carbon dioxide using a different β-diiminate Zn catalyst[80] (Figure 1-28). The utilisation of a starting limonene oxide rich in the *trans* isomer and the

purification of the monomer previous to the polymerisation allowed them to obtain polymers with M_n as high as 100,000 g mol^{-1}. Monomer conversion was 90 % and the reaction was scaled up to the kilogram scale, which indicates a very promising process with industrial applicability.

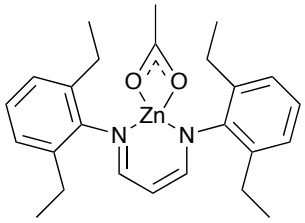


Figure 1-28. Zn catalyst employed by Greiner et al. for the polymerisation of limonene oxide into high molecular weigh polycarbonate.

Another interesting application of limonene epoxides is the synthesis of isocyanate-free polyurethanes, which constitute a green alternative to traditional isocyanate polyurethanes (Figure 1-29) due to the absence of toxic monomers and phosgene.[81]

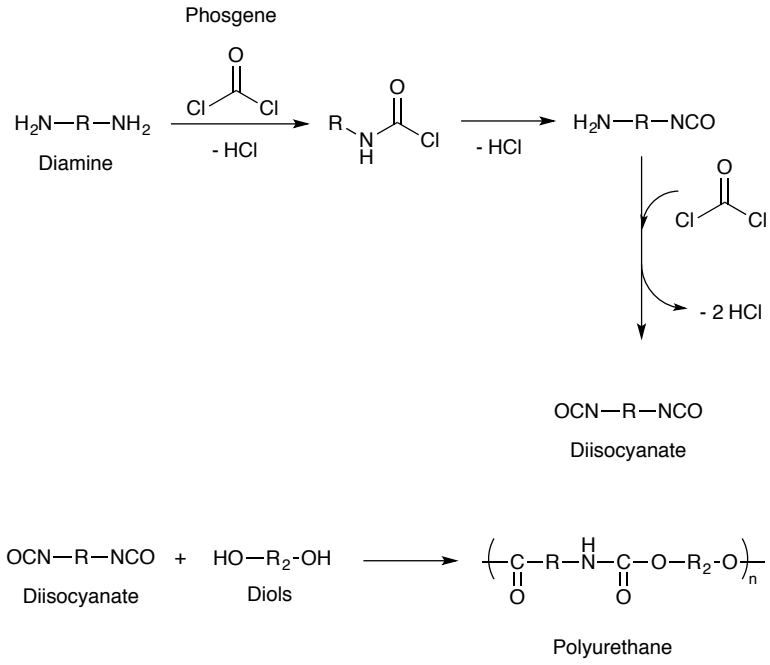


Figure 1-29. Classical synthesis of diisocyanates from diamines and phosgene. The reaction of diols with diisocyanates is one of the most common synthetic routes to polyurethanes.

Mülhaupt and coworkers[44] made limonene dioxide react with CO_2 to produce non-isocyanate polyurethanes (Figure 1-30). Tetrabutylammonium bromide was the catalyst employed for the synthesis of limonene dicarbonate from limonene dioxide. Limonene dicarbonate was then reacted with a series of amines, leading to the corresponding poly(hydroxyl urethanes) (PHUs). PHUs are a type of polyurethanes with hydroxyl groups located at the β-carbon atom of the urethane moiety.[81] Mülhaupt *et al*. prepared linear poly(hydroxyurethanes) with a maximum M_n of 1,800 g mol^{-1}. When limonene dicarbonate was made to react with tri- or polyfunctional amines, crosslinked polyurethanes were obtained instead.

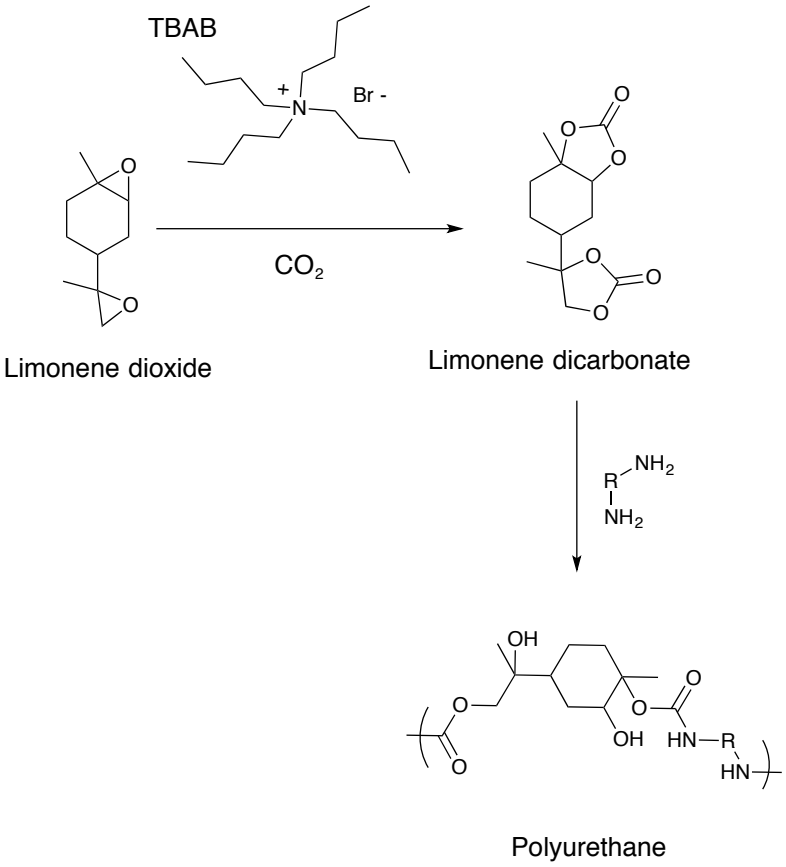


Figure 1-30. Synthetic route towards poly(hydroxiurethanes) utilising limonene dioxide as starting material.

Another interesting work is the transformation of myrcene into a polymerisable cyclopentene conducted by Hillmyer *et al.*[50] Hillmyer prepared high molecular weight polymer from myrcene using a combination of ring-closing metathesis and

cationic polymerisation (Figure 1-31). For the first step, a Grubbs second generation catalyst (G-2) was used, which yielded 3-methylenecyclopentene in a 45 % yield. Subsequent cationic polymerisation led to a polymer with a M_n of 22,000 g mol^{-1} and a narrow dispersity of 1.12.

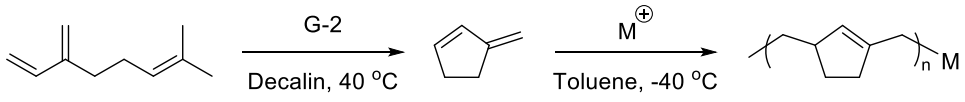


Figure 1-31. Ring-closing metathesis of myrcene led to 3-methylenecyclopentene, which was subsequently polymerised via cationic polymerisation.

Functionalisation of carbonyl-containing terpenoids such as carvone into polymerisable lactones has also been conducted. Carvone is a natural terpenoid found in both *Mentha spicata* (spearmint) and *Carum carvi* (caraway) oils. Spearmint oil yearly production is 10,000 metric tonnes.[82]

Hillmyer and co-workers successfully derived carvone and carvomenthone into lactones (Figure 1-32), which were then polymerised by ring-opening polymerisation (ROP).[83]

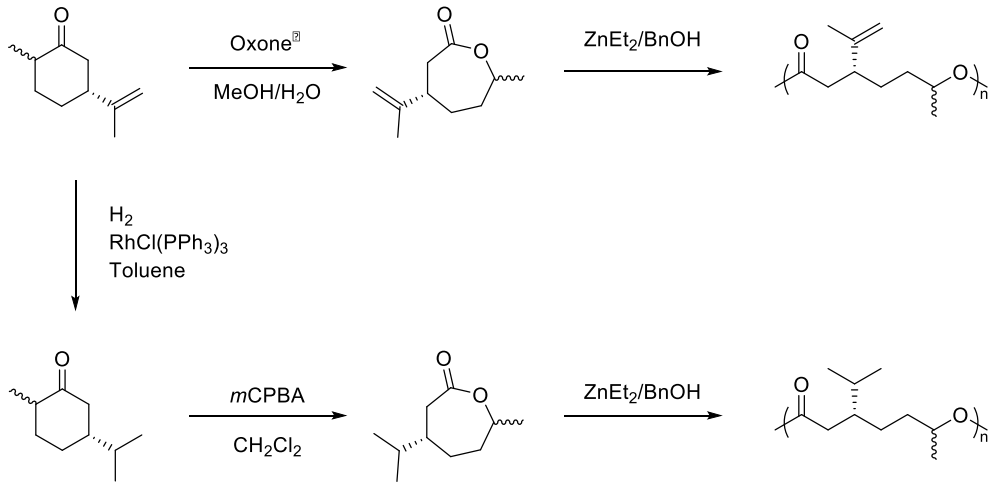


Figure 1-32. Functionalisation of carvone and hydrogenated carvone into lactones that were then polymerised by ROP.

Carvomenthone was synthesised by hydrogenating carvone, for which Wilkinson's catalyst ($RhCl(PPh_3)_3$) was employed. Further modification of both structures by Baeyer-Villiger oxidation afforded the corresponding lactones. To avoid epoxidation of the terminal alkene Oxone® (potassium monopersulfate) was chosen as the oxidant for the Baeyer-Villiger reaction. The polymerisation was carried out in bulk at 100 °C using diethyl zinc as a catalyst and benzyl alcohol as the initiator. The ROP yielded carvomenthone-based polyesters with high molecular weights of 62,000 g mol^{-1}, and a dispersity of 1.16; and dihydrocarvone-based polymers with a molecular weight of 10,500 g mol^{-1}, and a dispersity of 1.24.

In a similar fashion, Hillmyer synthesised polyesters using menthone as precursor (Figure 1-33).[84] Menthone is a constituent of the essential oils of pennyroyal, peppermint, *Mentha arvensis* and *Pelargonium geraniums* among others.

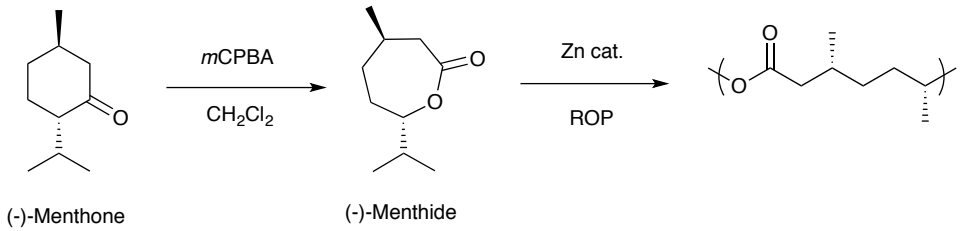


Figure 1-33. Oxidation of (-)-menthone via Bayer-Villiger oxidation yielded (-)-menthide, which was then transformed into a polyester by ROP in the presence of a Zn catalyst.

Menthone was readily converted to a lactone monomer, menthide, by the Baeyer-Villiger oxidation using meta-chloroperoxybenzoic acid as an oxidising agent (Figure 1-33). Polymers with molecular weights ranging from 3,300 to 91,000 g mol^{-1} and dispersities below 1.6 were prepared.

Another interesting work is the acrylation of rosin monomers conducted by Tang *et al*.[85] Rosin monomers have a similar structure to diterpenes, with the difference that they contain carboxylic acid functionalities (Figure 1-34). Rosin is the non-volatile residue obtained after the distillation of the resin exuded by many conifer

trees as a faintly aromatic, semi-transparent brittle solid. Regardless of its origin (gum, wood or tall oil), rosin is mainly composed (90–95 %) of diterpenic monocarboxylic acids, commonly known as resin acids with the generic formula $C_{19}H_{29}COOH$; and around 10 % of neutral compounds, the nature of which depends on the specific origin of the rosin.

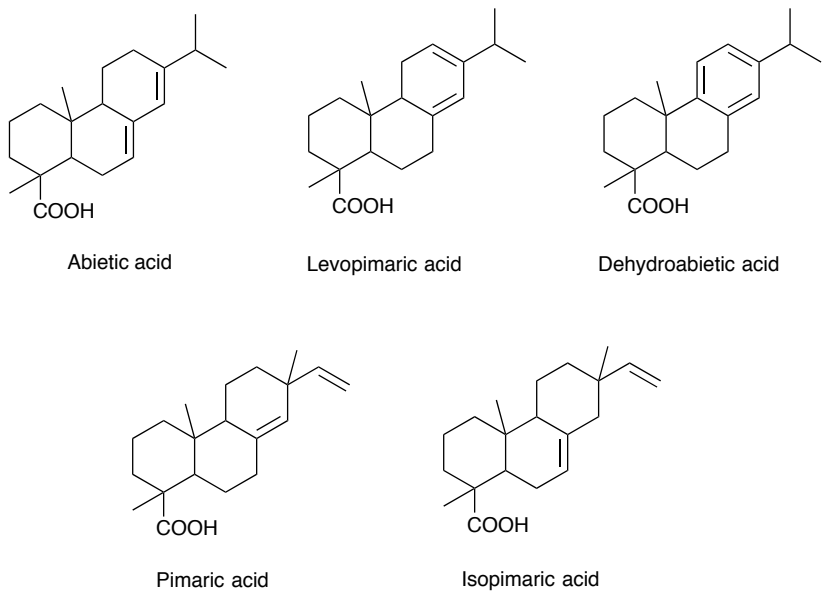


Figure 1-34. Structures of a few representative components of rosin.

Tang and co-workers developed a series of well-defined rosin-containing polymers by polymerising the prefunctionalised (meth)acrylate monomers (Figure 1-35).

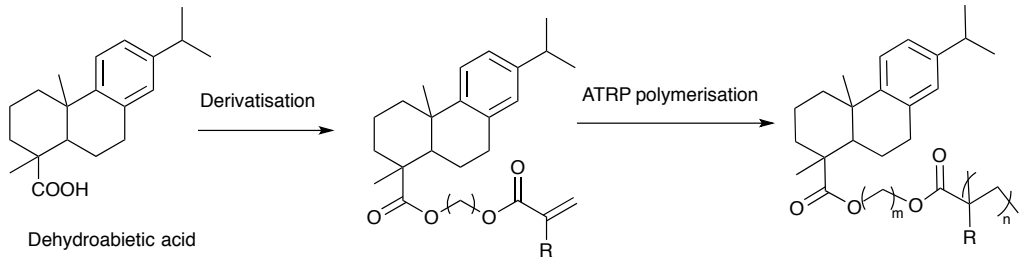


Figure 1-35. (Meth)acrylation of a rosin monomer followed by controlled polymerisation via ATRP.

Atom transfer radical polymerisation (ATRP) was used to polymerise the (meth)acrylate monomers. The molecular weight of the polymers ranged from 10,000 to 100,000 $gmol^{-1}$ and exhibited good Đ below 1.3. Other related approaches can be found in the literature,[86-89] but all are limited to those few terpene structures that have an available –COOH or –OH functionality for esterification; eliminating the potential to use most of the terpene and terpenoid structures that are commercially available.

1.4 Summary and thesis aims

The use of terpenes to produce 'green plastics' has been the subject of a large amount of research in the past decade, however many of the polymers produced using terpenes as monomers have not been able to compete with the current petroleum analogues. Many of the polymerisation processes lack control over molecular weight and structure, or require undesirable conditions such as high temperatures, toxic solvents or precious metal catalysts. Although some methodologies such as thiol-ene chemistry and emulsion polymerisation have afforded polymers with high molecular weights from limonene and myrcene, the number of polymers that have been synthesised from terpenes to date is still extremely limited. In this thesis, the utilisation of terpenes as monomers and controlling agents in radical polymerisation is investigated.

In Chapter 2, two naturally occurring terpenes, terpinolene and γ-terpinene, are evaluated as controlling agents in the radical polymerisation of methyl methacrylate, methyl acrylate, styrene and vinyl acetate separately. Mechanistic studies are conducted in order to elucidate the mechanism by which both terpenes control molecular weight and dispersity of the corresponding polymer. Differences between the control over different monomers are carefully assessed for both terpenes.

In Chapter 3, functionalisation of a range of natural terpenes into readily polymerisable monomers is conducted. A two-step methodology and a catalytic one-pot synthetic route are investigated in order to insert acrylate and

methacrylate functionalities into several terpenic structures. The polymerisability of the corresponding terpene-based (meth)acrylate monomers is studied in Chapter 4. FTIR studies are conducted to study and compare the reactivity between different unsaturations in bifunctional monomers.

Finally, in Chapter 5, crosslinking of some of terpene-based polymers is conducted for coating applications. The properties of the corresponding terpene-based coating films are carefully assessed and compare with commercial petrol-derived coatings.

1.5 References

1. Worldwatch, http://www.worldwatch.org/global-plastic-production-rises-recycling-lags-0, (accessed 8th of July, 2016).
2. G. Lligadas, J. C. Ronda, M. Galià and V. Cádiz, *Materials Today*, 2013, **16**, 337-343.
3. SPOTCHEMI, https://blog.spotchemi.com/the-market-for-biodegradable-and-biobased-polymers-and-plastics, (accessed 8th of July, 2016).
4. http://www.plasticsindustry.org/files/about/BPC/Industry Overview Guide Executive Summary - 0912 - Final.pdf, (accessed 11th July, 2016).
5. A. Gandini, *Macromolecules (Washington, DC, U. S.)*, 2008, **41**, 9491-9504.
6. C. Vilela, A. F. Sousa, A. C. Fonseca, A. C. Serra, J. F. J. Coelho, C. S. R. Freire and A. J. D. Silvestre, *Polym. Chem.*, 2014, **5**, 3119-3141.
7. N. Scarlat, J.-F. Dallemand, F. Monforti-Ferrario and V. Nita, *Environ. Dev.*, 2015, **15**, 3-34.
8. M. Winnacker and B. Rieger, *ChemSusChem*, 2015, **8**, 2455-2471.
9. P. P. Peralta-Yahya, F. Zhang, S. B. del Cardayre and J. D. Keasling, *Nature*, 2012, **488**, 320-328.
10. A. Gandini, in *Biocatalysis in Polymer Chemistry*, Wiley-VCH Verlag GmbH & Co. KGaA, 2010, pp. 1-33.
11. A. J. D. Silvestre and A. Gandini, in *Monomers, Polymers and Composites from Renewable Resources*, eds. M. N. Belgacem and A. Gandini, Elsevier, Oxford, 2008.
12. P. A. Wilbon, F. Chu and C. Tang, *Macromol. Rapid Commun.*, 2013, **34**, 8-37.
13. K. Yao and C. Tang, *Macromolecules*, 2013, **46**, 1689-1712.
14. K. Matyjaszewski and T. P. Davis, *Handbook of Radical Polymerization*, Wiley-Interscience, 2002.
15. G. Odian, *Principles of Polymerization*, John Wiley and Sons, Inc., New Jersey, 2004.

16. M. D. Green, M. H. Allen, Jr., J. M. Dennis, D. Salas-de la Cruz, R. Gao, K. I. Winey and T. E. Long, *Eur. Polym. J.*, 2011, **47**, 486-496.
17. W. A. Braunecker and K. Matyjaszewski, *Prog. Polym. Sci.*, 2007, **32**, 93-146.
18. K. Matyjaszewski and A. H. E. Müller, *Controlled and Living Polymerizations: From Mechanisms to Applications*, Wiley, 2009.
19. C. J. Hawker, A. W. Bosman and E. Harth, *Chem. Rev.*, 2001, **101**, 3661-3688.
20. J.-S. Wang and K. Matyjaszewski, *Macromolecules*, 1995, **28**, 7901-7910.
21. K. Min, H. Gao and K. Matyjaszewski, *J. Am. Chem. Soc.*, 2005, **127**, 3825-3830.
22. C. Barner-Kowollik and S. Perrier, *J. Polym. Sci., Part A: Polym. Chem.*, 2008, **46**, 5715-5723.
23. A. M. Stephen and G. O. Phillips, *Food Polysaccharides and Their Applications*, CRC Press, 2016.
24. B. Zhou, W. Gao, T. Zhang and H. Chen, *Zhongguo Zhongyao Zazhi*, 2005, **30**, 1313-1316.
25. O. Smidsrød, *Biopolymer Chemistry*, Tapir Academic Press, Trondheim, 2008.
26. D. Fengel and G. Wegener, *Wood: Chemistry, Ultrastructure, Reactions*, W. de Gruyter, 1989.
27. S. Thomas, W. John and Sons, *Handbook of biopolymer-based materials : from blends and composites to gels and complex networks. Vol. 1 Vol. 1*, Wiley-VCH Verlag, Weinheim, 2013.
28. S. Ebnesajjad, *Handbook of biopolymers and biodegradable plastics : properties, processing and applications*, William Andrew ; Elsevier Health Sciences, Norwich, N.Y.; London, 2012.
29. A. K. Mohanty, M. Misra and L. T. Drzal, *Natural Fibers, Biopolymers, and Biocomposites*, CRC Press, 2005.
30. A. L. Andrady and M. A. Neal, *Philos. Trans. R. Soc., B*, 2009, **364**, 1977-1984.
31. J. Buffington, *Frictionless Markets: The 21st Century Supply Chain*, Springer International Publishing, 2015.
32. L. Galambos, T. Hikino and V. Zamagni, *The Global Chemical Industry in the Age of the Petrochemical Revolution*, Cambridge University Press, 2007.
33. A. J. Ragauskas, C. K. Williams, B. H. Davison, G. Britovsek, J. Cairney, C. A. Eckert, W. J. Frederick, Jr., J. P. Hallett, D. J. Leak, C. L. Liotta, J. R. Mielenz, R. Murphy, R. Templer and T. Tschaplinski, *Science*, 2006, **311**, 484-489.
34. C. K. Williams and M. A. Hillmyer, *Polym. Rev.*, 2008, **48**, 1-10.
35. R. T. Mathers, *J. Polym. Sci., Part A: Polym. Chem.*, 2012, **50**, 1-15.
36. S. Mecking, *Angew. Chem., Int. Ed.*, 2004, **43**, 1078-1085.
37. L. Ruzicka, *Experientia*, 1953, **9**, 357-367.
38. A. Corma, S. Iborra and A. Velty, *Chem Rev*, 2007, **107**, 2411-2502.
39. A. M. Ramos, L. S. Lobo and J. M. Bordado, *Macromol. Symp.*, 1998, **127**, 43-50.
40. A.-L. Li, Y. Wang, H. Liang and J. Lu, *J. Polym. Sci., Part A: Polym. Chem.*, 2006, **44**, 2376-2387.

41. Y. Wang, A.-L. Li, H. Liang and J. Lu, *Eur. Polym. J.*, 2006, **42**, 2695-2702.
42. A.-L. Li, X.-Y. Wang, H. Liang and J. Lu, *React. Funct. Polym.*, 2007, **67**, 481-488.
43. K. Satoh, M. Matsuda, K. Nagai and M. Kamigaito, *J. Am. Chem. Soc.*, 2010, **132**, 10003-10005.
44. M. Baehr, A. Bitto and R. Muelhaupt, *Green Chem.*, 2012, **14**, 1447-1454.
45. M. Firdaus, L. Montero de Espinosa and M. A. R. Meier, *Macromolecules*, 2011, **44**, 7253-7262.
46. K. Koumura, K. Satoh and M. Kamigaito, *Macromolecules*, 2009, **42**, 2497-2504.
47. A. Singh and M. Kamal, *J. Appl. Polym. Sci.*, 2012, **125**, 1456-1459.
48. P. Sarkar and A. K. Bhowmick, *RSC Adv.*, 2014, **4**, 61343-61354.
49. W. H. Brown, B. L. Iverson, E. V. Anslyn and C. S. Foote, *Organic chemistry*, Wadsworth Cengage Learning, 2014.
50. S. Kobayashi, C. Lu, T. R. Hoye and M. A. Hillmyer, *J. Am. Chem. Soc.*, 2009, **131**, 7960-7961.
51. C. S. Chern, *Prog. Polym. Sci.*, 2006, **31**, 443-486.
52. T. Higashimura, J. Lu, M. Kamigaito, M. Sawamoto and Y.-X. Deng, *Makromol. Chem.*, 1993, **194**, 3441-3453.
53. T. Higashimura, J. Lu, M. Kamigaito, M. Sawamoto and Y. X. Deng, *Makromol. Chem.*, 1993, **194**, 3455-3465.
54. T. Higashimura, J. Lu, M. Kamigaito, M. Sawamoto and Y.-X. Deng, *Makromol. Chem.*, 1992, **193**, 2311-2321.
55. J. Lu, M. Kamigaito, M. Sawamoto, T. Higashimura and Y.-X. Deng, *J. Appl. Polym. Sci.*, 1996, **61**, 1011-1016.
56. A. B. Radbil, T. A. Zhurinova, E. B. Starostina and B. A. Radbil, *Russ. J. Appl. Chem.*, 2005, **78**, 1126-1130.
57. J. Lu, H. Liang, R.-J. Zhang and Y.-X. Deng, *Chem. J. Chin. Univ.*, 1996, **17**, 1314-1318.
58. L. Li, S. Yu, F. Liu, J. Yang and S. Zhaug, *Catal. Lett.*, 2005, **100**, 227-233.
59. W. J. Roberts and A. R. Day, *J. Am. Chem. Soc.*, 1950, **72**, 1226-1230.
60. R. P. F. Guiné and J. A. A. M. Castro, *J. Appl. Polym. Sci.*, 2001, **82**, 2558-2565.
61. J. Lu, M. Kamigaito, M. Sawamoto and T. Higashimura, *Macromolecules*, 1997, **30**, 27-31.
62. K. Satoh, H. Sugiyama and M. Kamigaito, *Green Chem.*, 2006, **8**, 878-882.
63. J. M. Bolton, M. A. Hillmyer and T. R. Hoye, *ACS Macro Lett.*, 2014, **3**, 717-720.
64. N. A. Kukhta, I. V. Vasilenko and S. V. Kostjuk, *Green Chem.*, 2011, **13**, 2362-2364.
65. P. Yu, A.-L. Li, H. Liang and J. Lu, *J. Polym. Sci., Part A: Polym. Chem.*, 2007, **45**, 3739-3746.
66. H. Sheffer, G. Greco and G. Paik, *J. Appl. Polym. Sci.*, 1983, **28**, 1701-1705.
67. C. Snyder, W. McIver and H. Sheffer, *J. Appl. Polym. Sci.*, 1977, **21**, 131-139.

68. H. Pietila, A. Sivola and H. Sheffer, *J. Polym. Sci., Part A-1: Polym. Chem.*, 1970, **8**, 727-737.
69. A.-L. Li, W. Zhang, H. Liang and J. Lu, *Polymer*, 2004, **45**, 6533-6537.
70. C. E. Hoyle, T. Y. Lee and T. Roper, *J. Polym. Sci., Part A: Polym. Chem.*, 2004, **42**, 5301-5338.
71. M. Firdaus and M. A. R. Meier, *Green Chem.*, 2013, **15**, 370-380.
72. A. J. Bonon, Y. N. Kozlov, J. O. Bahu, R. M. Filho, D. Mandelli and G. B. Shul'pin, *J. Catal.*, 2014, **319**, 71-86.
73. M. G. Egusquiza, C. I. Cabello, I. L. Botto, H. J. Thomas, S. Casuscelli, E. Herrero and D. Gazzoli, *Catal. Commun.*, 2012, **26**, 117-121.
74. A. L. Villa de P, F. Taborda A and C. Montes de Correa, *J. Mol. Catal. A: Chem.*, 2002, **185**, 269-277.
75. A. Wroblewska, *Molecules*, 2014, **19**, 19907-19922.
76. H. J. Park, C. Y. Ryu and J. V. Crivello, *J. Polym. Sci., Part A: Polym. Chem.*, 2013, **51**, 109-117.
77. C. M. Byrne, S. D. Allen, E. B. Lobkovsky and G. W. Coates, *J. Am. Chem. Soc.*, 2004, **126**, 11404-11405.
78. D. J. Darensbourg, *Chem. Rev.*, 2007, **107**, 2388-2410.
79. L. Pena Carrodeguas, J. Gonzalez-Fabra, F. Castro-Gomez, C. Bo and A. W. Kleij, *Chem. - Eur. J.*, 2015, **21**, 6115-6122.
80. O. Hauenstein, M. Reiter, S. Agarwal, B. Rieger and A. Greiner, *Green Chem.*, 2016, **18**, 760-770.
81. L. Maisonneuve, O. Lamarzelle, E. Rix, E. Grau and H. Cramail, *Chem. Rev.* , 2015, **115**, 12407-12439.
82. C. C. C. R. de Carvalho and M. M. R. da Fonseca, *Food Chemistry*, 2006, **95**, 413-422.
83. J. R. Lowe, M. T. Martello, W. B. Tolman and M. A. Hillmyer, *Polym. Chem.*, 2011, **2**, 702-708.
84. D. Zhang, M. A. Hillmyer and W. B. Tolman, *Biomacromolecules*, 2005, **6**, 2091-2095.
85. Y. Zheng, K. Yao, J. Lee, D. Chandler, J. Wang, C. Wang, F. Chu and C. Tang, *Macromolecules*, 2010, **43**, 5922-5924.
86. N. Shida, T. Ushirogouchi, T. Naito, M, Nakase, *Light-sensitive material useful as photoresist with short wavelength light*, DE19525221A1, 1996.
87. Hercules Inc., *Coating Polyolefins*, GB1109746, 1968.
88. G. D. Friends, M. F. Vanburen, *Contact lens made from polymers of polysiloxane and polycyclic esters of acrylic acid or methacrylic acid,* US4254248A, 1981.
89. C. E. Rehberg, C. H. Fisher, *Acrylates of olefinic alcohols and polymers thereof,* US2456647, 1948.

Chapter 2: Terpinolene and γ-terpinene as controlling agents in radical polymerisation.

2.1 Introduction

2.1.1 Trommsdorff-Norrish Effect

Bulk radical polymerisations (bulk meaning in the absence of solvent) are characterised by the potential for an auto-acceleration of the polymerisation rate as the reaction proceeds. As the polymer chains grow during the polymerisation, the viscosity of the reaction medium increases. Since termination is a diffusion-controlled step, this can result in a significant drop in the termination rate, resulting in an increase of the concentration of radicals and acceleration in propagation (Figure 2-1). Furthermore, because the overall polymerisation process is exothermic, this increase in propagation rate means that the temperature increases, further enhancing initiation and propagation rates, creating a positive feedback loop. Ultimately, this may result in an uncontrolled process and sometimes, even in an explosion. This is known as the Trommsdorff-Norrish effect or gel effect.[1]

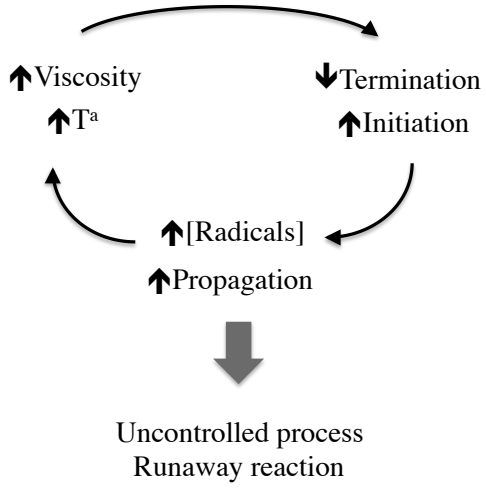
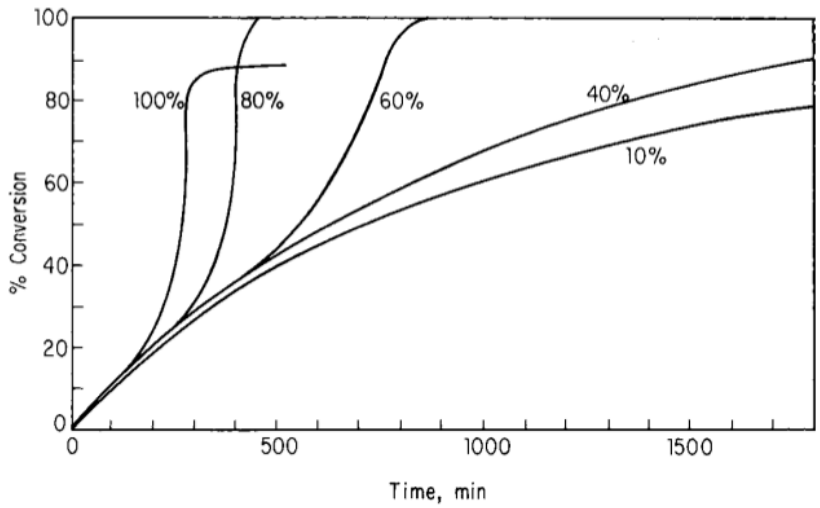


Figure 2-1. Auto-acceleration cycle that characterises the Trommsdorff-Norrish effect.

The problem of the Trommsdorff effect is usually avoided by performing the free radical polymerisation (FRP) in the presence of solvent. In this way the increase of the viscosity is limited (Figure 2-2). However, the use of considerable amounts of solvents usually requires an extra separation step to remove them from the product. Moreover the solvents are usually hazardous chemicals and their use is subjected to increasing limitation.



Graph extracted from "Principles of Polymerisation", by G. Odian.[2, 3]

Figure 2-2. Effect of solvent in the polymerisation of MMA in benzene at 50°C. Monomer concentrations are shown in % volume next to the conversion curves. When monomer concentration is below 40 % the viscosity is considerably decreased, leading to lower monomer conversions, an indicative of the absence of an auto-acceleration in the reaction.

An alternative way to prevent the Trommsdorff effect involves the addition of substances that react with radicals yielding either low reactivity radicals (often termed persistent), dormant species or terminated, low molecular weight polymer. The resultant reduction of the concentration of propagating radicals slows down the propagation rate and therefore prevents the Trommsdorff effect from happening. Substances added to polymerisation reactions for such a purpose can be chain transfer agents, retarders or inhibitors. The mechanism of action of these substances is discussed below.

2.1.2 Traditional chain transfer methods in radical polymerisation

The process of chain transfer in free-radical polymerisation is used to control the molecular weight and dispersity of polymers and in some cases to introduce functionality at the ends of polymer chains. The chain transfer process is mediated by the use of a chain transfer agent (CTA) and typically follows the mechanism represented in Figure 2-3.

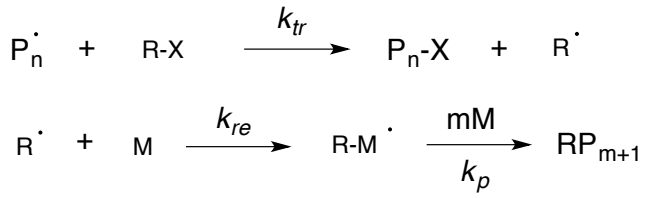


Figure 2-3. General mechanism for traditional Chain Transfer Agents, where R-X can be a thiol, halomethane or other compound with a readily abstractable proton.

A growing polymer chain, or propagating radical $P_n^{\bullet}$ reacts with a chain transfer agent R–X terminating the propagating chain and forming a terminated polymer chain P_n–X and a new radical $R^{\bullet}$. The radical $R^{\bullet}$ then reacts with monomer (M) to form a new propagating chain.

The effect of a chain transfer agent on polymerisation rate R_p varies depending on the relative rate constants of chain transfer k_{tr}, reinitiation k_{re} and propagation k_p. Depending on the net effects on molecular weight and polymerisation rate several chain transfer scenarios are possible:

1) *Conventional chain transfer*: In this scenario, the radical formed by the chain transfer reaction $R^{\bullet}$ is reactive enough to reinitiate polymerisation at approximately the same rate as a propagating radical. Therefore reinitiation and propagation rate constants are of the same order $k_{re} \approx k_p$ and the polymerisation rate R_p is not affected. In this scenario the rate constant of propagation rate is considerably higher than that of chain transfer $k_{p>>}k_{tr}$, hence molecular weight will be decreased compared to a FRP in the absence of CTA, but the product will still be macromolecular.
2) *Telomerisation*: If chain transfer is more rapid than propagation $k_{p<<}k_{tr}$,

then the decrease in molecular weight will be considerable and only low molecular weight polymers, or telomers, will be obtained. However, the polymerisation rate will not be affected as long as reinitiation and propagation rate constants remain similar $k_{re} \approx k_p$.

3) *Retardation*: When the radical formed by the chain transfer reaction R$^{\bullet}$ is not as reactive as a propagating chain then $k_{re} < k_p$, and the polymerisation rate decreases. If $k_{p>>}k_{tr}$ molecular weight decreases along with the propagation rate.
4) *Degradative chain transfer / Inhibition*: This scenario is similar to retardation in the sense that reinitiation rate is lower than propagation $k_{re} < k_p$. However, if propagation is slower than chain transfer ($k_{p<<}k_{tr}$) molecular weight is dramatically decreased. When polymerisation rate and molecular weight are so severely decreased that polymerisation is prevented, the process is called *inhibition*.[4] Retarders and inhibitors are commonly used to prevent the Trommsdorff effect. They are also called "peak suppressants", since their addition to the polymerisation reaction prevents a temperature or pressure maxima from taking place.

Some of the more widely used CTA include halomethanes, disulfides, thiols, and other compounds that have a readily abstractable H-atom. The effectivity of a CTA at moderating molecular weight is measured by the chain transfer constant C_{tr}, defined as the ratio of the chain transfer rate constant to the propagation rate constant $C_{tr} = k_{tr}/k_p$. The higher the value of C_{tr} the lower the concentration of CTA is required to achieve a determined decrease in molecular weight.[1, 4]

2.1.3 Mayo equation and evaluation of chain transfer constants.

The effect of CTA on molecular weight is quantitatively described by the Mayo equation expressed below,

$$\frac{1}{DP} = \frac{1}{DP_0} + C_{tr}\frac{[CTA]}{[Monomer]}$$

where DP is the degree of polymerisation in the presence of the corresponding CTA, DP_0 is the degree of polymerisation with no CTA, [CTA] is the concentration of the CTA present in the reaction medium and [Monomer] is the concentration of the monomer. The procedure for measuring the chain transfer constant consists of determining the number average degree of polymerisation DP for a range of different CTA concentrations, and expressing this data in the form of a Mayo plot. The Mayo plot is obtained by plotting 1/DP versus [CTA]/[Monomer]. The slope of the trend line obtained corresponds to the C_{tr} value.

However, the conditions used the experiments must be carefully chosen so that transfer to initiator, monomer and solvent are essentially avoided and that chain transfer to CTA is the dominating chain-terminating event. These conditions are typically met when the radical flux is kept low and the polymerisation is stopped at low conversions.[5,6]

2.1.4 Other methods of polymerisation control.

Chain transfer methods other than traditional CTAs such as RAFT, NMP and ATRP have been developed. These methods were briefly described in Chapter 1. They provide efficient control over molecular weight, dispersity and end-group functionality. However, these polymerisation control methods are not objects of study in this thesis and therefore no more details will be discussed. It is important to note however, that depending on the mechanism of control, all control methods are classified into conventional FRP or controlled radical polymerisation (CRP).

CRP methods are characterised by a reversible deactivation of a growing radical chain (Figure 2-4), and this feature is what distinguishes them from conventional FRP. In CRP, an active polymer chain $P^{\bullet}$ propagates until it is deactivated by reacting with X and forming an end-capped dormant species P-X. The chain length of P–X generally becomes larger after an activation-deactivation cycle. If the reversible activation occurs frequently enough, every dormant chain will have a nearly equal chance to grow, thus yielding a low-dispersity polymer.[1]

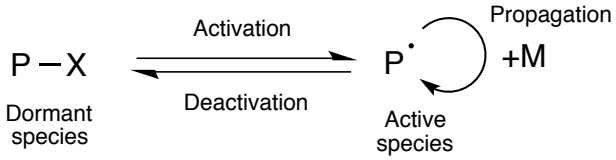


Figure 2-4. General scheme of reversible activation during living polymerisation. The fact that the equilibrium favours the formation of the dormant species allows for the polymerisation to be controlled.

This gradual increase of molecular weight translates into a linear kinetic profile, characteristic of CRP methods, where molecular weight increases with conversion (Figure 2-5), which allows for the synthesis of polymers with accurate tailored molecular weight.

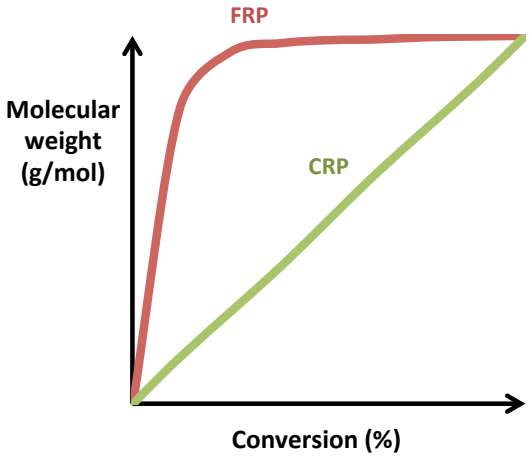


Figure 2-5. Kinetic profiles of conventional FRP and CRP. Kinetic profiles are built by plotting molecular weight versus conversion.

Conventional FRP, such as CTA-controlled polymerisations present a different kinetic profile, where molecular weight increases fast at low conversions, to then plateau at low-mid conversions (Figure 2-5).

2.1.5 Summary and research aims

Today, a wide range of renewable sources are being explored as monomers for radical polymerisation. However, when it comes to polymerisation control,

mainly synthetic and expensive additives are used. The drawbacks of the most popular controlling agents are listed in Table 2-1.

Table 2-1. Common controlling agents in radical polymerisation and their disadvantages.

Controlling Agents	Disadvantages
RAFT Agents	Multistep synthesis, unwanted colour, expensive
Nitroxides	Flammable, corrosive, expensive
Mercaptans	Toxic, flammable, irritating, odour
ATRP: Cu catalysts	Toxic, Cu contaminants difficult to remove
Cobalt complexes	Irritant, expensive

By comparison, terpenes represent a renewable alternative to synthetic additives. However, there is little information in the literature about their mechanism of action. Rather, terpenes are mainly mentioned as peak suppressors or molecular weight regulators in patents and no systematic study has been reported to date. In this work, several terpenes were tested in order to define their ability to act as CTAs and peak suppressors. As part of this study, the differences between them were carefully studied. The effect of terpinolene and γ-terpinene on the polymerisation of methyl methacrylate, methyl acrylate, styrene and vinyl acetate was investigated and mechanistic studies were conducted.

2.2 Experimental

2.2.1 Materials

Unless otherwise stated, reagents were purchased from commercial sources and used without further purification. Methyl methacrylate (MMA, 99 %), methyl acrylate (MA, 99 %), 2,2-Azobis(2-methylpropionitrile) (AIBN, 98%), terpinolene (≥85 %), γ-terpinene (97 %), deuterated methyl methacrylate (MMA-

d^8, ≥99 atom % D, ≥99 %) and dichloromethane (DCM, 99.5 %) were purchased from Sigma Aldrich. Styrene (Sty, 99 %) and vinyl acetate (VAc, 99 %) were obtained from Alfa Aesar. Toluene (99.5 %) was supplied by Fisher Scientific and methanol (99.8 %) was provided by VWR. MMA, MA, Sty, VAc and γ-terpinene were passed through a column of basic alumina to remove inhibitors prior to use.

2.2.2 General polymerisation method

The liquid reagents (monomer, terpene and solvent if applicable) were degassed using a flow of argon for 30 minutes. The solid reagents (such as initiator) were introduced directly into the reaction vessel along with a magnetic stirrer bar and were degassed by flushing argon through the flask for 30 minutes. Then, the required amounts of degassed monomer, terpene and solvent were transferred into the reaction vessel under an argon atmosphere. The reaction vessel was then immersed in a pre-heated oil bath, which was thermostatically controlled to remain at the set reaction temperature and the reaction was allowed to proceed for the allotted reaction time. To quench the reaction, the reaction vessel was removed from the oil bath and submerged into an ice bath for 10 minutes. When pure polymers were required for analysis, the reaction crude was dissolved in the minimum amount of DCM and precipitated in methanol (DCM:Methanol ratio of 1:20). The obtained powder was filtered and dried in a vacuum oven at 50 ^{o}C for 72 hr.

A typical experiment, in which 1 mol% of terpinolene was added to MMA polymerisation (Table 2-6, entry 1), was conducted by introducing 2 weight % (wt%) of AIBN (374 mg, 2.2 mmol) with respect to monomer to a sealed 100 mL vessel containing a magnetic stirrer. After 30 min of degassing, 20 mL of MMA (18.7 mol), and 0.34 mL of terpinolene (187 mmol), which had been pre-degassed using the methodology described above, were transferred into the reaction vessel *via* a previously pre-purged syringe. After 24 h of reaction at 65 ^{o}C, the reaction vessel was place into an ice bath for 10 minutes, after which 20 mL of DCM were added to the reaction mixture. After complete dissolution the reaction mixed was precipitated drop wise into 400 mL of cold methanol.

2.2.2.1 Deuterated MMA polymerisation

250 mg of MMA-d^8, 10 mol% of terpinolene or γ-terpinene, and 2 wt% of AIBN were placed into a 10 mL flask and a septum was fitted. After sealing the reaction, oxygen was removed by 3 cycles of freeze-pump-thaw, after which the mixture was submerged into a preheated oil bath at 65 ^oC. After 1 week of reaction, a sample was taken and dissolved in $CDCl_3$ for ^1H-NMR analysis.

2.2.3 Polymer characterisation

2.2.3.1 Gel Permeation Chromatography (GPC)

Gel Permeation Chromatography (GPC) was performed on a Polymer Labs GPC-120 instrument at 40 ^oC equipped with a PLgel 5 μm guard column and two 30 cm PolarGel-M Columns in series coupled with a refractive index detector using HPLC grade THF as the mobile phase at a flow of 1.0 $cm^3.min^{-1}$. The GPC was calibrated with poly(methyl methacrylate) narrow D standards ranging from 690–1,944,000 g mol^{-1}. All GPC equipment and standards were supplied by Polymer Laboratories (Varian) GPC data and were analysed using the Cirrus GPC Offline software package.

2.2.3.2 Nuclear magnetic resonance (NMR)

^1H NMR spectra were recorded at 25 ^oC using a Bruker DPX-300 spectrometer (300 MHz). Chemical shifts were recorded in δ_H (ppm). Samples are prepared as solutions in $CDCl_3$ to which chemical shifts are referenced (residual chloroform at 7.28 ppm). Analysis of the spectra was conducted using MestreNova software.

2.2.3.3 Matrix-assisted laser desorption/ionisation time-of-flight mass spectrometry (MALDI-TOF)

Samples were prepared by dissolving 15 mg of polymer in 2 mL of acetonitrile. 10 μL of this polymer solution were then mixed with 20 μL of a solution of 2-[(2E)-3-(4-tert-Butylphenyl)-2-methylprop-2-enylidene]malononitrile (DCTB) in acetonitrile in a 10 mg/mL concentration and 0.5 μL of a solution of silver trifluoroacetate on a 5mg/mL concentration. After mixing, 1 μL of the solution was placed on a MALDI plate and analysed in a Bruker Ultraflex III spectrometer

using a positive reflection method. The results were processed with a MultiFlex Analysis software.

2.2.4 Monitoring of reaction exotherms

The reactions were set up as described before in the "General polymerisation method" section. A thermocouple attached to a Picolog was placed into the reaction vessel through the septum to measure the internal bulk temperature of the reaction. The software measured the temperature of the reaction mixture every second for 24 h.

2.3 Results and discussion

2.3.1 Terpenes as chain transfer agents.

As discussed in the introduction, terpenes generally do not undergo radical homopolymerisation.[7-9] However it had been previously reported in the literature that they do copolymerise with other non-terpene monomers, although with modest levels of terpene incorporation.[7, 9-11] These copolymerisation studies have been conducted mainly with α- and β-pinene[12-17] and limonene[18-28] (Figure 2-6).

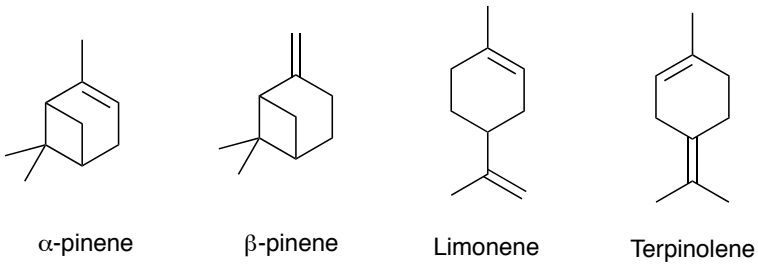


Figure 2-6. Chemical structures of some of the most abundant and inexpensive terpenes.

During the first stages of this PhD research, radical copolymerisation of natural terpenes with methyl methacrylate (MMA) was attempted. Initially two terpenes were tested: α-pinene and terpinolene (Figure 2-6). Interestingly, these copolymerisation reactions of α-pinene and terpinolene with MMA revealed not

only a lack of polymerisation of the terpene in both cases but a total inhibition of MMA polymerisation in the terpinolene reaction (Table 2-2).

Table 2-2. Copolymerisation between α-pinene and terpinolene with methyl methacrylate.[*]



MMA

50 : 50

Entry	M_1[a]	M_2[a]	M_n[b] (g/mol)	MMA Conversion[c]	Terpene conversion
1	α-Pinene	MMA	21000	75%	<5%[d]
2	Terpinolene	MMA	-[e]	-[e]	-[e]

*All reactions were conducted at 65 °C for 24 hr in the presence of 2 wt% of AIBN. Terpene and MMA were made to react in a 50:50 ratio. [a] M: Monomer [b] Calculated by GPC-SEC using PMMA standards. [c] Calculated by ^{1}H-NMR. [d] No pinene was detected by 1H-NMR. 5% corresponds to the NMR equipment detection limit. [e] No polymer detected.

Copolymerisation reactions were conducted by mixing the corresponding terpene and MMA in a 50:50 ratio, and then subjecting them to a 24 h reaction at 65 °C in the presence of AIBN as initiator. These reactions were quenched by placing in an ice bath for 10 min. The reaction mixture containing α-pinene had the appearance of a white solid. This reaction mixture was then dissolved in DCM, precipitated in methanol and subsequently dried in a vacuum oven at 50 °C for 72 h. GPC analysis revealed a polymer with a molecular weight of 21,000 g mol^{-1}. ^{1}H-NMR analysis of the precipitated product showed a PMMA homopolymer with no α-pinene incorporated into the polymer. This result was not a surprise since previous publications had reported a very modest α-pinene incorporation into MMA-pinene copolymers.[12] Ramos *et al.* quantified α-pinene incorporation by analysis of the composition of the residual monomer. However, α-pinene can undergo radical reactions leading to structural isomerisation (Figure 2-7),[12] which

would lead to a decrease in α-pinene concentration but does not imply α-pinene incorporation into the polymer.

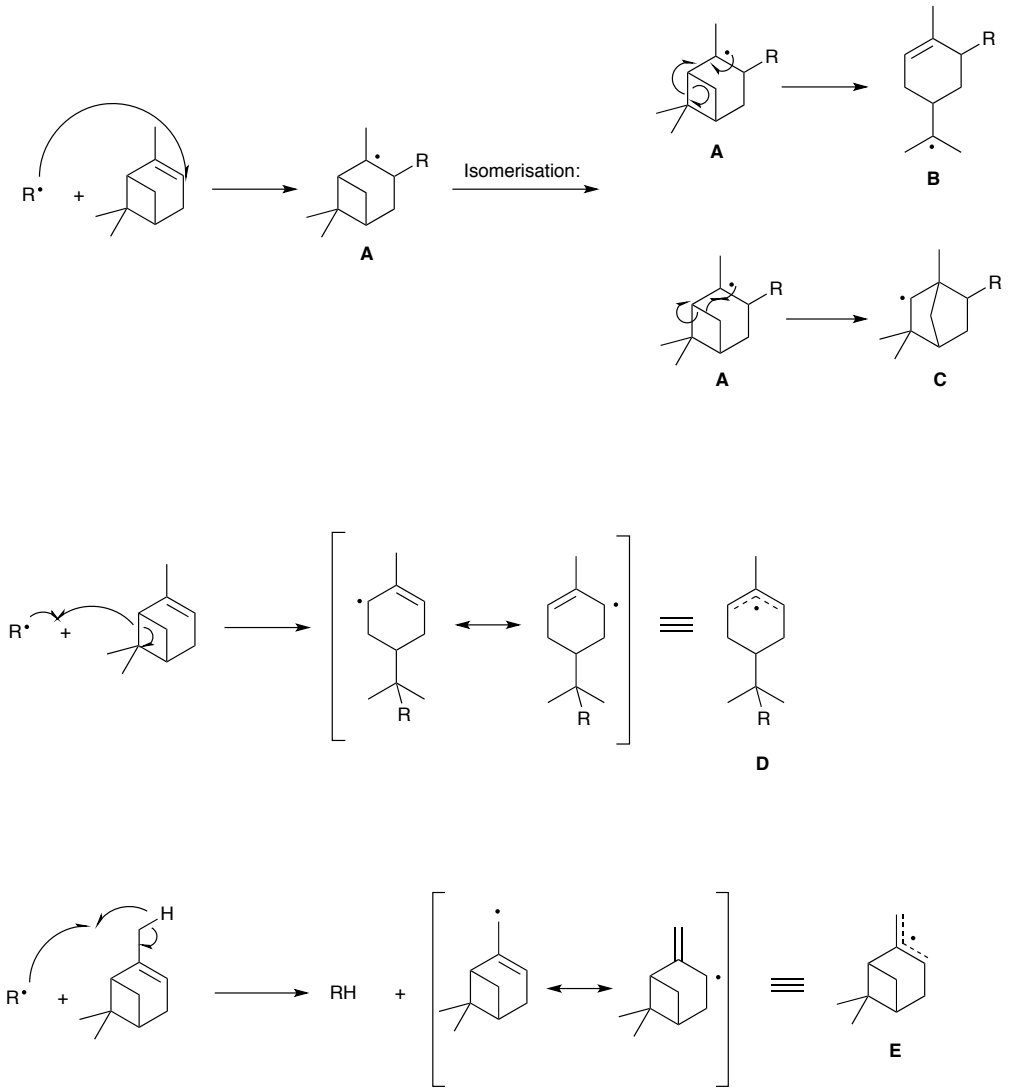


Figure 2-7. Possible structures formed upon radical attack to α-pinene.[12]

By comparison, in the terpinolene copolymerisation, after 24 h of reaction no polymer was detected. The reaction mixture had a liquid appearance, and both the GPC traces and ^{1}H-NMR spectrum were equivalent to those of the monomer mixture. These data indicated that terpinolene inhibited MMA polymerisation. A literature search confirmed that terpinolene had been used before as controlling agent in radical polymerisation. There are several patents in the literature claiming the use of terpinolene as chain transfer agent or as peak suppressor,

which is to say, as a substance that delays or completely supresses the exotherm characteristic of polymerisation reactions.[29-40]

The use of terpinolene as a peak suppressor is indeed well known in the polymer industry. However, the mechanism through which terpinolene controls radical polymerisation is not clear. While in most publications terpinolene is referred to as a chain transfer agent (Figure 2-8), some authors proposed that terpinolene actually copolymerises with MMA at a low rate, which causes a delay in the polymerisation and an attenuation of the gel effect.[41, 42]

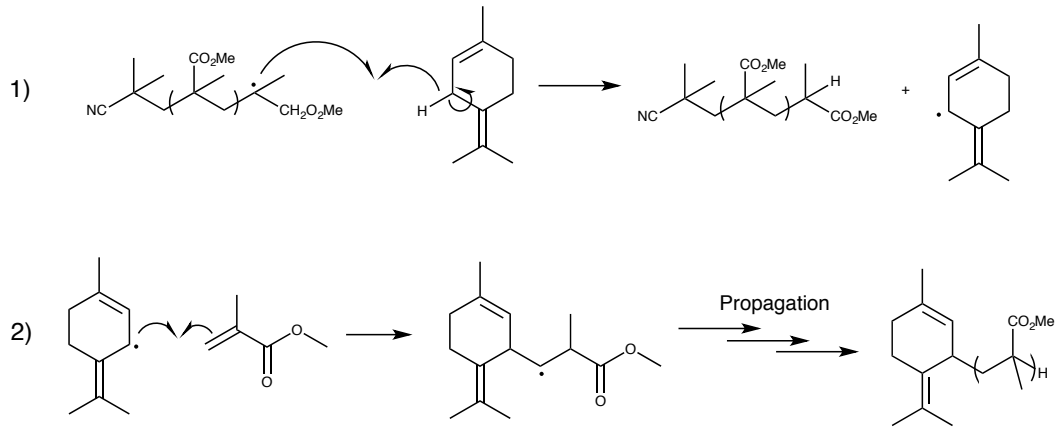


Figure 2-8. Proposed mechanism that terpinolene would follow as a conventional chain transfer agent. In the first step of the reaction, a growing polymer chain would abstract a hydrogen from terpinolene. During the second step, chain transfer agents react with a monomer unit generating propagation.

Buergle *et al*.[41] studied the kinetics of the reaction between terpinolene and MMA and proposed that the decrease in the polymerisation rate with increasing terpinolene concentration was caused by the stability of the terpinolene-terminated macroradicals (Figure 2-9).

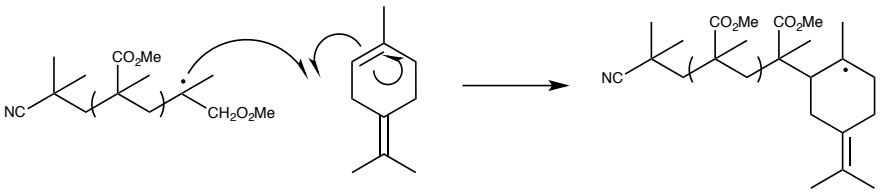


Figure 2-9. Proposed mechanism of copolymerisation between MMA and terpinolene. Buergle et al.[41] suggested that when terpinolene is added to MMA polymerisation in low concentrations, it copolymerises with MMA, generating a terpinolene-terminated macroradical with low reactivity.

However, to our knowledge, there is no published evidence supporting either theory, and no systematic study of the effect of terpinolene on radical polymerisation has been conducted to date. The use of terpenes as polymerisation control agents is very attractive since they are renewable, and do not have the unpleasant odour exhibited by mercaptans. For these reasons, in this chapter we look into the use of terpenes as chain transfer agents and the mechanism they follow.

Terpinolene is not the only terpene that has been used as controlling agent in radical polymerisation. Other terpenes such as α-pinene, limonene, myrcene, α-terpinene and γ-terpinene (Figure 2-6 and Figure 2-10) have been used to control radical polymerisation.[29, 31, 35]

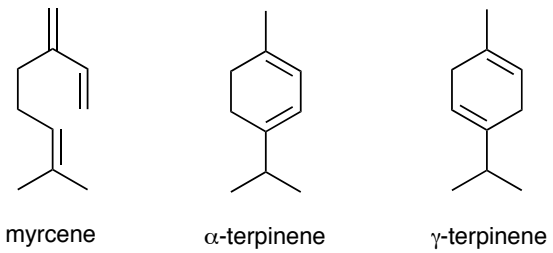


Figure 2-10. Chemical structures of myrcene, α-terpinene and gamma-terpinene. These terpenes contain easily abstractable allylic hydrogens, which makes them useful as polymerisation control agents.

All these terpenes are unsaturated compounds containing allylic hydrogens that are easily abstractable. Bond dissociation energies (BDE) are a direct measure of

the stability of free radicals. Allylic radicals are stabilised by resonance (Figure 2-11), hence allylic hydrogens have lower dissociation energies than non-allylic C-H bonds.[43]

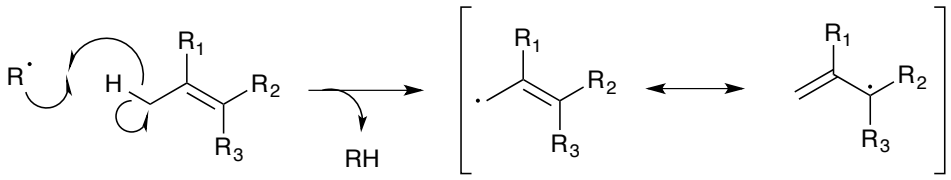


Figure 2-11. Abstraction of an allylic hydrogen leads to a resonance-stabilised structure.

For example, C-H bond dissociation energies at the allylic position in propene and at a terminal carbon in propane differ in 58 kJ/mol (Figure 2-12).

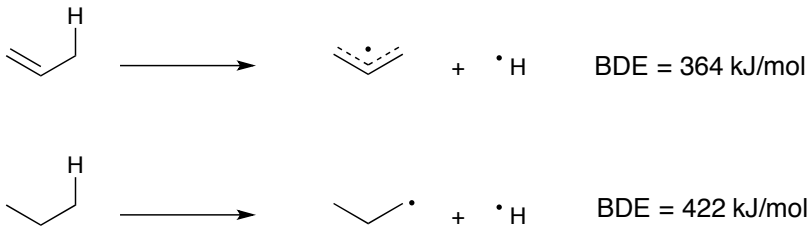


Figure 2-12. Bond dissociation energies for propene and propane. The difference in BDE between the two compounds represents the difference in energy between the allylic and the non-allylic radical.[43]

Copolymerisation experiments in this PhD thesis (Table 2-2) had shown that 50 mol% of terpinolene inhibited MMA polymerisation completely, while α-pinene did not copolymerise (α-pinene was not incorporated into the polymer) but did not inhibit MMA polymerisation either. These observations revealed significant differences in reactivity between the two terpenes. It is proposed that this difference in reactivity is caused by the presence of bis-allylic hydrogens in terpinolene as opposed to just monoallylic hydrogens, as it is the case for α-pinene (Figure 2-13). Bis-allylic hydrogens are hydrogen atoms that are in allylic positions with respect to two different C=C.

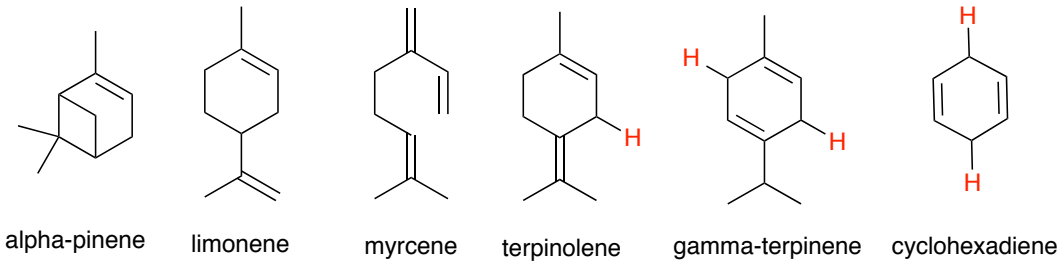


Figure 2-13. Structures of α-pinene, limonene and myrcene, terpinolene, gamma-terpinene and cyclohexadiene. Bis-allylic hydrogens are marked in red. These hydrogens are specially labile and those compounds containing them in their chemical structure are effective as polymerisation control agents.

Cardoso *et al.* calculated the C-H bond dissociation enthalpies for several terpenes and showed that the values for bis-allylic hydrogens was considerably lower than for allylic C-H bonds. For example, the bond dissociation energy for the bis-allylic hydrogen in terpinolene was at least 33 kJ mol^{-1} lower than the allylic hydrogens in limonene and 42 kJ mol^{-1} lower than those ones of α-pinene.[44]

In order to look at the effect of low terpene concentrations in MMA polymerisation a series of reactions were conducted by making MMA polymerise in bulk at 65 ^{o}C in the presence of 2 wt% of AIBN and 1 mol% of different terpenes (Table 2-3).

*Table 2-3. Comparison of the effect of several terpenes on MMA polymerisation when used in 1 mol% concentration in MMA polymerisation.**

Entry	Additive (1 mol%)	T-N Effect[a]	Conv. (%)[b]	M_n (g/mol)[c]	Đ[c,d]
1	None	Yes	- [b]	22,000	3.2
2	α-Pinene	Yes	- [b]	27,000	4.2
3	Myrcene	Yes	- [b]	25,000	3.5
4	Limonene	Yes	- [b]	25,500	3.7
5	Terpinolene	No	86	17,100	1.8
6	γ-Terpinene	No	95	17,200	2.0
7	1,4-cyclohexadiene	No	96	7,800	1.6

*All reactions were conducted by mixing 20 mL of MMA with 1 mol% of the corresponding terpene. The mixture was stirred and heated at 65 ^{o}C for 24 h in the presence of 2 wt% of AIBN. Runaway reactions were stopped after the gel effect took place. 1 mol% of the corresponding terpene was added to MMA [a] Trommsdorff-Norrish effect. [b] Not possible to calculate conversions because of gel effect. [c]Calculated by GPC-SEC using PMMA standards. [d]Dispersity.

A high radical concentration of 2 wt% was chosen in order to evaluate the ability of each terpene to control the polymerisation in the presence of high concentration of radicals. Several terpenes with monoallylic hydrogens such as α-pinene, limonene and myrcene were tested. Terpenes containg bis-allylic hydrogens include terpinolene, β-terpinene, γ-terpinene and β-phellandrene. However β-terpinene and β-phellandrene are not commercially available and therefore could not be studied. Terpinolene and γ-terpinene were the only terpenes with bis-allylic hydrogens tested. A non-terpene compound containing bis-allylic hydrogens, cyclohexadiene, was also tested for comparison. All of these results were compared to a blank reaction containing no control additives.

In reactions containing α-pinene, myrcene, limonene or no additive (entries 1 to 4), a Trommsdorff runaway of the reaction was observed after 40 minutes at 65 ^{o}C. By contrast, those reactions that had been conducted in the presence of 1 mol% of terpinolene, γ-terpinene or 1,4-cyclohexadiene (entries 5 to 7) continued to react without exhibiting a Trommsdorff and were stopped after 24 h (Figure 2-14).

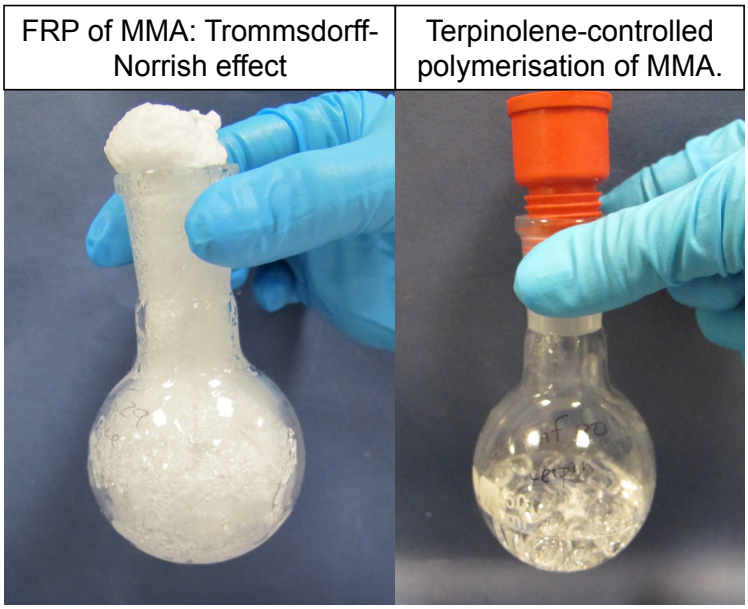


Figure 2-14. Pictures of MMA polymerisation reaction in the presence of 1 mol% of α-pinene (left) and 1 mol% of terpinolene (right) as additive. When MMA is polymerised in bulk, without a chain transfer agent, the reaction experiences an autoacceleration that causes high increases in pressure and temperature. When doubly allylic compounds, such as terpinolene, were added the Trommsdorff-Norrish effect was supressed.

The control over the polymerisation provided by these compounds is also reflected in the dispersities exhibited by the polymers obtained: reactions in the presence of terpinolene, γ-terpinene and cyclohexadiene yielded polymers with dispersities between 1.6 and 2.0 (Table 2-3, entries 5 to 7). However, the runaway reactions (Table 2-3, entries 1 to 4) yielded polymers with dispersities higher than 3, characteristic of an FRP where no controlling agent has been added. As for polymer molecular weight, reactions in the presence of pinene, myrcene, limonene or no additive yielded polymers with molecular weights of between 22,000 and 27,000 g mol^{-1}. The molecular weights obtained with terpinolene and γ-terpinene were 17,100 g mol^{-1} and 17,200 g mol^{-1} respectively, whereas cyclohexadiene reduced further the molecular weight to 7,000 g mol^{-1}, revealing an even more dramatic effect on chain length.

These experiments clearly confirmed the difference between allylic and bis-allylic hydrogens. The presence of bis-allylic hydrogens in terpinolene, γ-terpinene and

cyclohexadiene led to these compounds acting as effective peak suppressors in MMA radical polymerisation. As discussed in the introduction, the Trommsdroff effect is a consequence of the lack of termination reactions. Bis-allylic hydrogens on these terpenes are easily abstracted by growing polymer chains, which then become terminated chains. As a result, the autoacceleration cycle is prevented.

2.3.2 Kinetic profiles of terpinolene and γ-terpinene.

Having confirmed the higher effectiveness of terpinolene and γ-terpinene compared to the mono-allylic terpenes tested, kinetic studies were conducted to investigate the characteristics of the mechanism they follow. Kinetic profiles of controlling agents give information about the mechanism they follow. Kinetic profiles of MMA polymerisation in the presence of 5 % terpinolene and γ-terpinene respectively were built by plotting average molecular weight (M_n) against conversion for samples taken at different reaction times during MMA polymerisation. Reactions were undertaken in the presence of 2 wt% of AIBN as initiator at 80 ^oC. AIBN half-life at 80 ^oC is 1 hour. The mixture was left to react for 20 h, after which full radical consumption was ensured. Samples were taken at regular periods of time.

When 5 % of terpinolene was employed in MMA polymerisation (Table 2-4), after 1 hour of reaction conversion was 43 % and a GPC analysis revealed a molecular weight of 7,700 g mol^{-1}.

*Table 2-4. Average molecular weight and conversion values for MMA polymerisation in the presence of 5 mol% of terpinolene at different reaction times.**

Entry	Time	MMA conversion[a]	M_n (g/mol)[b]
1	1 h	43%	7700
2	2.5 h	58%	7500
3	3.5 h	75%	7200
4	20 h	82%	7200

*20 mL of MMA were mixed with 5 mol% of terpinolene. Reaction was conducted at 80 ^oC for 24 h. Samples were taken at regular intervals of time. [a] Conversion calculated by ^{1}H-NMR. [b]Calculated by GPC-SEC against PMMA standards.

At longer reaction times, the conversion was observed to increase progressively until it reached 82 % after 20 h. Meanwhile, the molecular weight remained essentially unchanged with GPC analysis showing molecular weights of 7,500, 7,200 and 7,200 g mol^{-1} at 58 %, 75 % and 82 % conversions respectively.

When MMA polymerisation was conducted using γ-terpinene as the controlling agent (Table 2-5), similar results were obtained.

Table 2-5. Average molecular weight and conversion values of samples taken at different reaction times during the polymerisation of MMA in the presence of 5 mol% terpinene. [*]

Entry	Time	MMA conversion[a]	M_n (g/mol)[b]
1	1 h	32 %	7,700
2	1.5 h	43 %	8,700
3	2 h	51 %	8,400
4	2.5 h	79 %	8,700
5	20 h	84 %	7,300

* 20 mL of MMA were mixed with 5 mol% of γ-terpinene. Reaction was conducted at 80 ^{o}C for 24 h. Samples were taken at regular intervals of time. [a] Conversion calculated by ^{1}H-NMR. [b]Calculated by GPC-SEC against PMMA standards.

The molecular weight reached a value of 7,700 g mol^{-1} at a low conversion of 32 %. At conversions between 43 % and 79 %, The molecular weight remained very similar at approximately 8,700 g mol^{-1}. After 2.5 h of reaction the reaction became too viscous to take samples, hence the reaction was left overnight and stopped after 20 h, after which conversion had reached 84 % and average molecular weight was 7,300 g mol^{-1}.

The graphic representation of the data obtained for both terpinolene (Figure 2-15) and γ-terpinene-controlled reactions (Figure 2-16), showed kinetic profiles that agree with that of a conventional CTA controlled polymerisation (green dashed lines), where molecular weight increases rapidly at low conversions to then plateau at medium and high conversions.

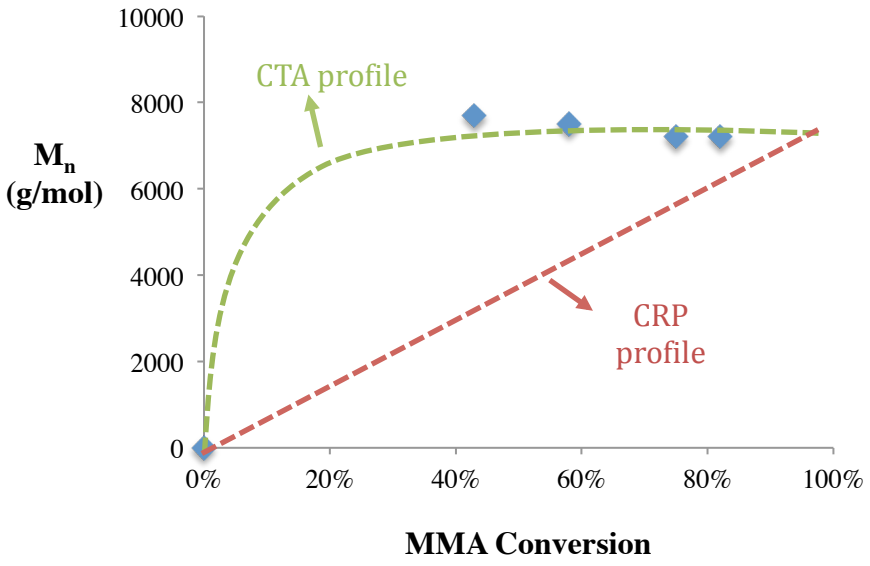


Figure 2-15. Kinetic profile of terpinolene-controlled polymerisation of MMA (blue). Dashed red line represents a characteristic "living" polymerisation profile whereas green dashed line shows a typical FRP or traditional CTA kinetic profile.

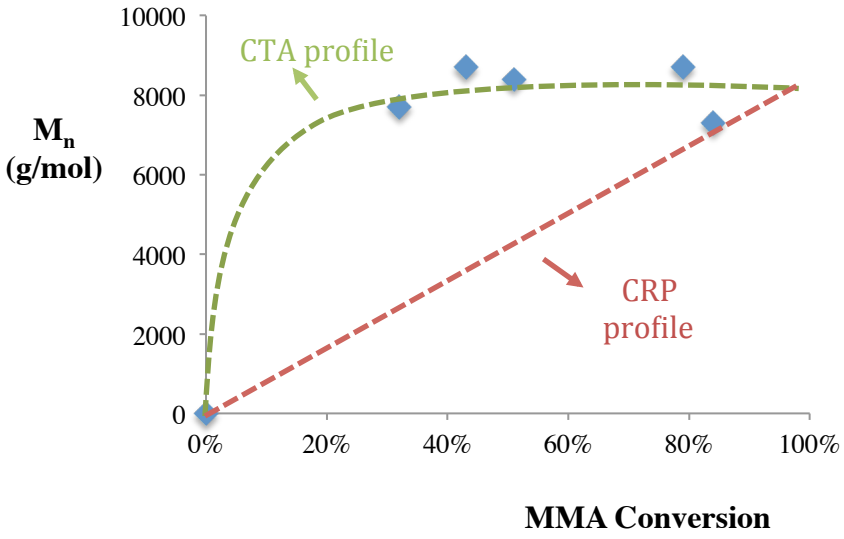


Figure 2-16. Kinetic profile of terpinene-controlled polymerisation of MMA (blue). Green and red dashed line represent traditional CTAs and "living" polymerisation profiles respectively.

Slight deviations in molecular weight from the ideal CTA profile (green dashed line) observed in both kinetic profiles might be caused by the high viscosity that is reached in the early stages of the reaction. This increase in viscosity at early conversions is typical of radical polymerisations, and leads to diffusion issues and heterogeneities in the reaction medium. Therefore samples taken from different regions would differ slightly from each other.

By comparison, in a CRP mechanism, there is an equilibrium between dormant and active growing chains that causes a gradual, linear increase in molecular weight with conversion (red dashed lines in Figure 2-15 and Figure 2-16). Terpinolene and γ-terpinene kinetic profile clearly did not exhibit this type of kinetic profile, indicating that they do not follow a CRP mechanism.

2.3.3 Effect of terpene concentration on MMA polymerisation

In order to study the effect of terpene concentration on radical polymerisation, MMA was polymerised in the presence of different concentrations of terpinolene and γ-terpinene, ranging from 1 to 10 mol% with respect to monomer. It was observed that, with decreasing concentrations of terpinolene (Table 2-6) the molecular weight increased from 7,500 to 17,100 g mol^{-1} and dispersity values rose from 1.84 to 1.51. This would be expected for a standard FRP reaction where the level of control exercised is being reduced.

*Table 2-6. Effect of terpinolene concentration on the polymerisation reaction of methyl methacrylate at 65 ^{o}C.**

Entry	% Terpinolene	Conversion (%)[a]	M_n (g/mol)[b]	Đ[b,c]
1	10	29	5,500	1.51
2	5	44	8,600	1.55
3	2	80	12,500	1.69
4	1	86	17,100	1.84

*20 mL of MMA were mixed with with the corresponding percentage mol of terpinolene. Reaction was conducted at 65 ^{o}C for 24 h. Samples were taken at regular intervals of time. [a]Conversion calculated by ^{1}H-NMR. [b]Calculated by GPC-SEC against PMMA standards. [c]Dispersity.

The same effect was observed with varying concentrations of γ-terpinene (Table 2-7). The average molecular weight increased with decreasing γ-terpinene concentration, ranging from 7,500 g mol^{-1} at 10 mol% concentration of γ-terpinene to 17,200 g mol^{-1} at 1 mol% of γ-terpinene.

*Table 2-7. Effect of γ-terpinene concentration on the polymerisation reaction of methyl methacrylate at 65 °C.**

Entry	% γ-Terpinene	Conversion (%)[a]	M_n (g/mol)[b]	Đ [b,c]
1	10	67	7,500	1.59
2	5	82	9,700	1.71
3	2	96	17,000	1.87
4	1	95	17,200	2.01

*20 mL of MMA were mixed with with the corresponding percentage mol of γ-terpinene. Reaction was conducted at 65 °C for 24 h. Samples were taken at regular intervals of time. [a]Conversion calculated by ^{1}H-NMR. [b]Calculated by GPC-SEC against PMMA standards. [c]Dispersity.

Dispersity values also increased as γ-terpinene concentration was reduced, from 1.59 to 2.01. In radical polymerisation, when termination is dominated by chain transfer events, dispersity values are normally close to 2.[1] The decrease in dispersity with chain transfer agent concentration is caused by a drop on the average molecular weight. The shorter the polymer chains are, the closer the dispersity value is to 1.[45]

With respect to the conversions achieved, the values were noted to decrease with increasing terpene concentration in both cases (Table 2-6, Table 2-7) from 86 % to 29 % with terpinolene and from 95 to 69 % with γ-terpinene. This data reveals that polymerisations were retarded in the presence of either terpene, as would be expected from a CTA-controlled polymerisation. The decrease in conversion is caused by a reduction in the number of reactive radicals. In a chain transfer reaction, a growing polymer chain is terminated by abstracting a leaving group from the chain transfer agent. The chain transfer agent then becomes a radical and depending on its capability to attack a monomer unit and reinitiate polymerisation, the reaction will be retarded to a certain degree. This is because

the overall rate of chain transfer and reinitiation is generally slower than the propagation rate.

When MMA is polymerised in the presence of terpinolene or γ-terpinene, the first step in the chain transfer mechanism consists of a growing PMMA chain abstracting a bis-allylic hydrogen from the terpene. This releases a terpene radical which is stabilised by resonance (Figure 2-17, 1a and 1b).

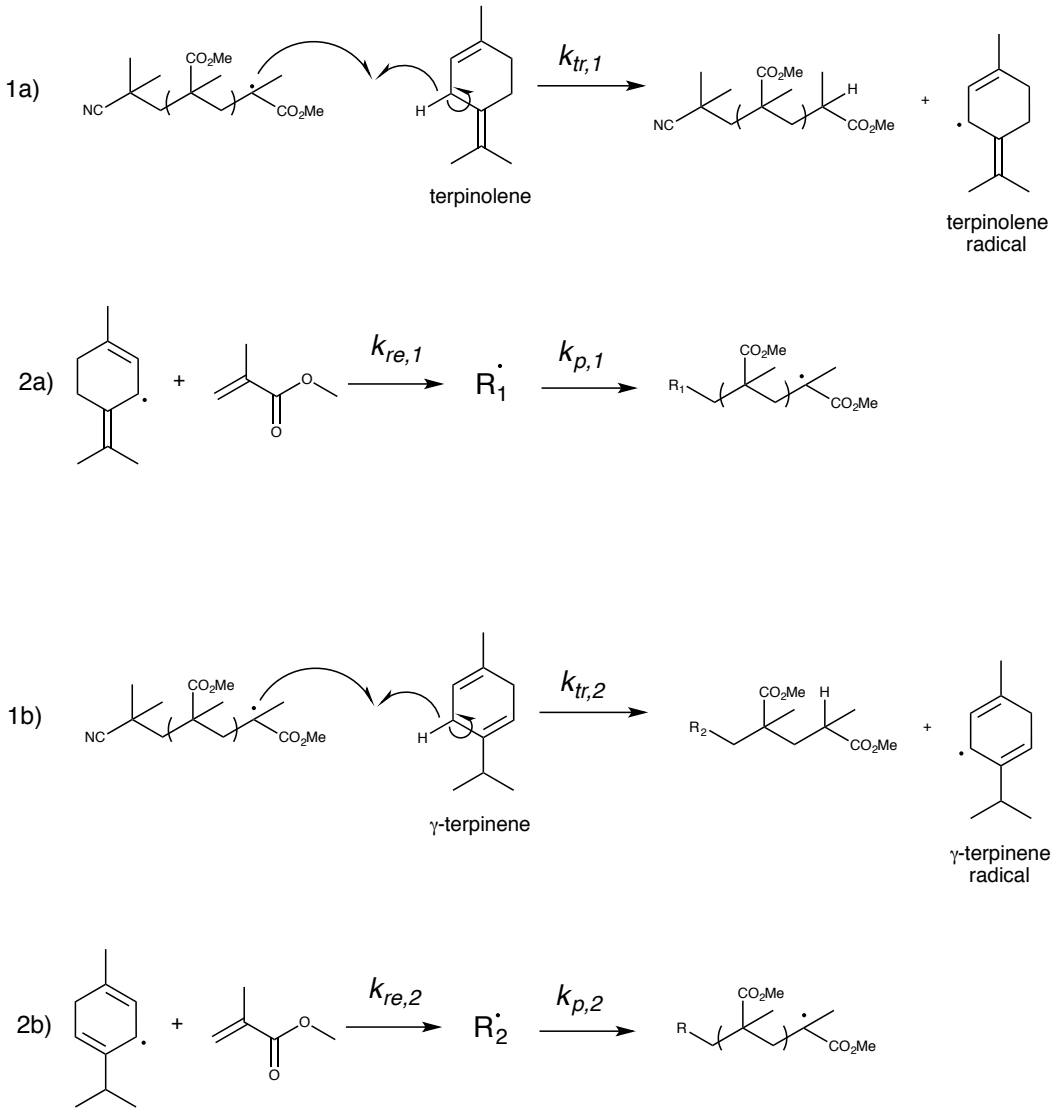


Figure 2-17. Proposed mechanisms for the chain transfer reaction from polymer to terpinolene (1a) and γ-terpinene (1b). The reaction rate will depend on the ability of the terpene radical to reinitiate a polymer chain (2a, 2b). The reinitiation reaction would lead to a new radical $R_1^{\bullet}$ or $R_2^{\bullet}$ able to propagate.

However, one question that remains unanswered is whether these terpinolene and γ-terpinene radicals are able to react reinitiating polymerisation (1b and 2b in Figure 2-17) or not, and what mechanism they achieve this by.

When looking at conversions achieved in the presence of 10% terpene as controlling agents, it can be seen that the reaction containing 10% terpinolene was retarded to a much higher degree than that one in the presence of 10% γ-terpinene, with the conversions being 33 % and 62 % respectively after 24 h. These results suggest that terpinene is able to reinitiate polymerisation much faster than terpinolene. In order to confirm or refute reinitiation by the two terpenes, MMA polymerisations in the presence of 10% of terpene were repeated and were left to react for 7 days (Table 2-8).

*Table 2-8. Conversions of MMA polymerisation in the presence of 10 mol% terpene at different reaction reaction times.**

	Conversion (%)[a]	
t (h)	**Terpinolene**	**γ-Terpinene**
24	33	62
72	46	81
168	53	91

*20 mL of MMA were mixed with 10 mol% of the corresponding terpene. Reaction was conducted at 65 ^{o}C for 1 week. Samples were taken at 24 h, 72 h and 168 h. [a]Conversion calculated by ^{1}H-NMR.

The half-life time of AIBN at 65 ^{o}C is 10 h. Thus after 40 h, the initiator is considered to be essentially consumed. Therefore, if conversion increases after that time, it is most likely caused by a reinitiation mechanism. This would suggest that terpene radicals are still present and can react with either monomer units or polymer chains, releasing a reactive molecule able to propagate.

When the polymerisations were left for longer reaction times conversions kept increasing in both cases. However, this increase was much more modest in the terpinolene reaction, from 33 % after 24 h to 53 % after a week; while in the presence of γ-terpinene conversions increased from 63 % to 91 %. These results

indicate that γ-terpinene reinitiates the reaction at a higher rate than terpinolene. However, the increase of conversion in terpinolene is so modest that it is not clear whether it was caused by terpinolene reinitiation or by residual initiator fragments.

2.3.4 Mechanistic studies: MMA-d^8 polymerisations and MALDI analysis.

In order to investigate further the potential reinitiation mechanism, polymerisation reactions of deuterated MMA (MMA-d^8) in the presence of terpinolene and γ-terpinene were undertaken. Deuterium atoms, ^2D, are paramagnetic and therefore cannot be detected by NMR. Thus, after MMA-d^8 polymerisation, only molecules containing hydrogen atoms would be detected by ^{1}H-NMR, which means that a hydrogen exchange between terpene and monomer/polymer should be clearly observed.

10 mol% was chosen as the initial terpene concentration in order to provide sufficient termination and ensuring the presence of enough chains initiated by the terpene. In these conditions, it would be possible to detect terpene-derived species by ^{1}H-NMR. After 7 days of reaction, a sample was taken, dissolved in deuterated chloroform ($CDCl_3$) and analysed by ^{1}H-NMR (Figure 2-18).

The spectrum revealed a decrease in the integral value of terpinolene bis-allylic hydrogen (labelled as “b” in Figure 2-18). When compared to ^{1}H-NMR spectrum of terpinolene (Figure 2-18, top), it can be seen that the integral value has decreased from 2.00 to 1.40, while the rest of the integrals remain unchanged. This translates into around 60% of terpinolene molecules having a bis-allylic hydrogen abstracted. When the same reaction was undertaken using non-deuterated MMA instead, no decrease in the integral value was observed. Thus it was concluded that the change in the integral value observed in Figure 2-18 is caused by the bis-allylic hydrogen in terpinolene being replaced by a deuterium atom.

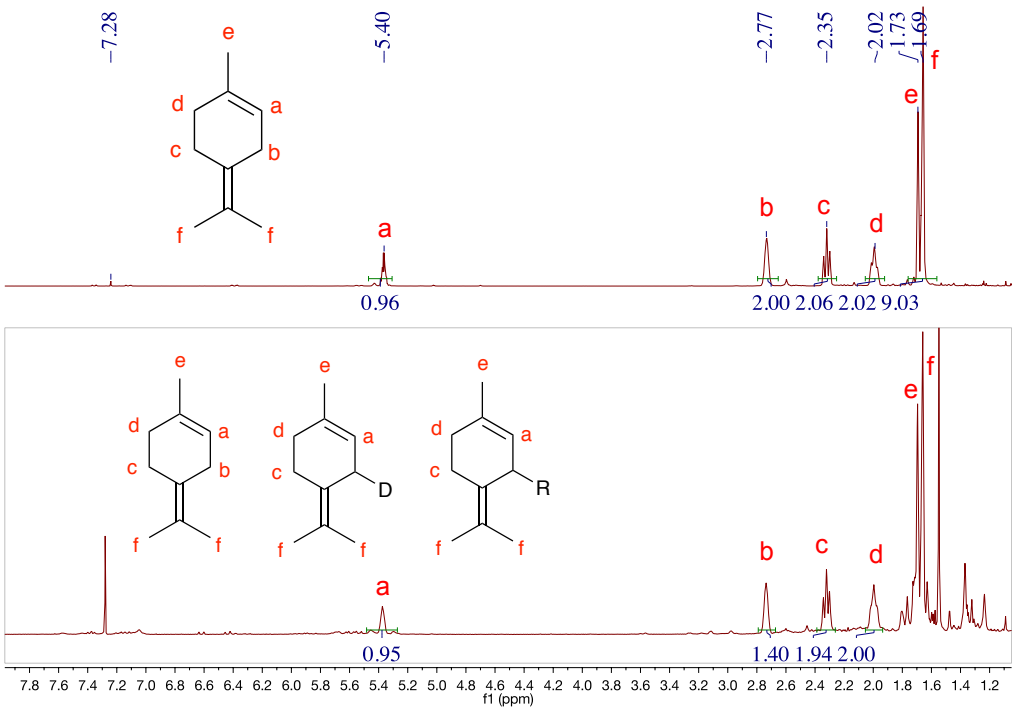


Figure 2-18. ^{1}H-NMR spectra of terpinolene before (top) and after (bottom) MMA-d^{8} polymerisation.

To further investigate this question, MALDI-TOF analysis was conducted on PMMA obtained in the presence of 10% terpinolene. In order to conduct the MALDI analysis, silver trifluoroacetate (AgTFA, Figure 2-19) was added to the polymer sample to ionise the polymer fragments.

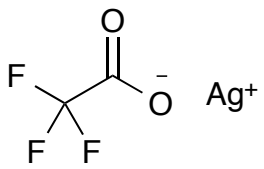


Figure 2-19. Chemical structure of silver trifluoroacetate. Trifluoroacetate salts are commonly used as additives in MALDI-TOF spectrometry to promote ionisation. MALDI-TOF analysis of polymers in the absence of ionisation agent generally yield poor spectra with no or few ions detected.

Hence the m/z of the ions detected correspond to an adduct of polymer chain plus a silver moiety. This means that the atomic mass of silver, 106.91 g mol^{-1}, must be added to the polymer mass to define the peaks in the spectrum.

In the MALDI spectrum of PMMA four main series peaks could be differentiated (Figure 2-20). In each of the series there is a difference of 100 m/z between the peaks, which corresponds to the molecular weight of an MMA repeating unit.

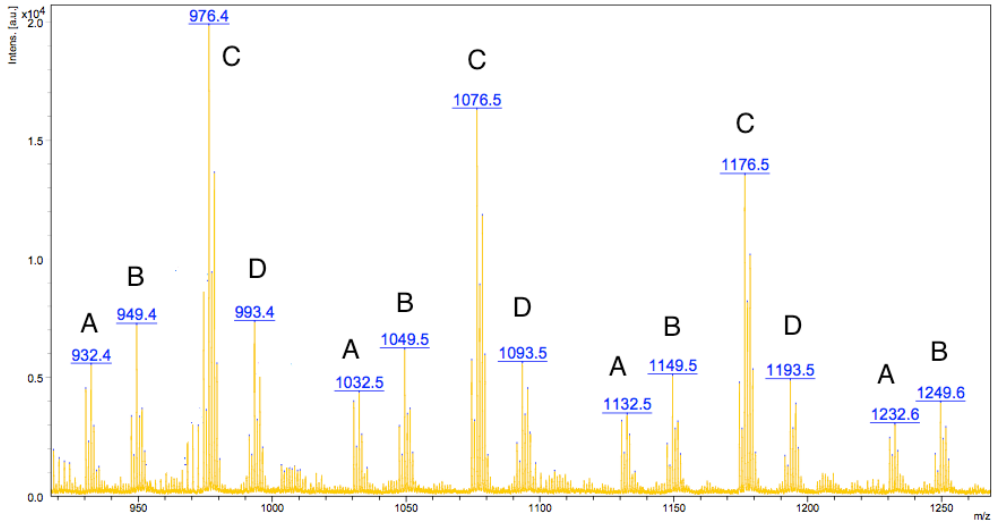


Figure 2-20. Section of MALDI-TOF spectrum of PMMA synthesised in the presence of 10% terpinolene, showing four series of different PMMA chains labelled as A, B, C and D.

The proposed structures for each one of the series are shown in Figure 2-21. The most intense series, m/z 376 + 100 n, corresponds to PMMA chains containing initiator and a hydrogen as end groups, and it is labelled as series "C". The other three series are all much less intense. These were concluded to correspond to PMMA fragments formed in the MALDI chamber as a result of the high-energy laser. These fragmentations of the polymer chain during MALDI analysis are common and have been described before for PMMA.[46-49] The impact of the laser causes homolytic cleavages releasing CO_2, CO_2Me, or splitting the polymer backbone. Series A, with m/z 332 +100 n, matches the molecular weight of a PMMA chain after CO_2 loss (Figure 2-22).

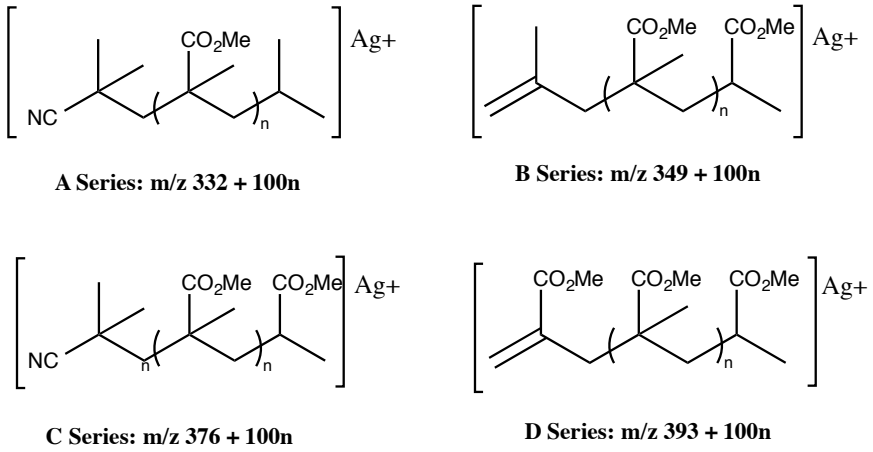


Figure 2-21. Proposed structures for the four series of PMMA fragments detected by MALDI-TOF.

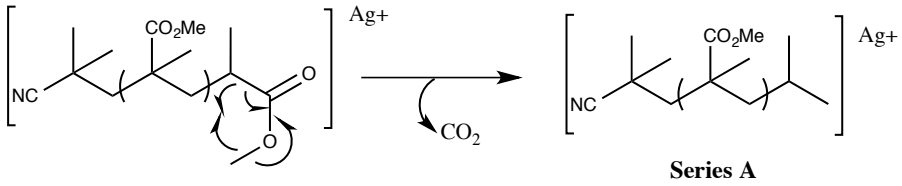


Figure 2-22. Scheme showing a radical rearrangement leading to the loss of CO_2 and giving rise to a structure matching series A.

Series B and D would form by homolytic cleavage of the polymer backbone and subsequent rearrangement. Homolytic cleavage can take place at two different points in the polymer backbone (a) and b) in Figure 2-23).

From the MALDI analysis, it can be concluded that polymer chains synthesised using terpinolene have the structure shown for series C. This suggests that the polymerisation control is indeed caused by hydrogen transfer, the most likely source of which is terpinolene. More importantly, the possible structures that would indicate terpinolene reinitiation (Figure 2-24) were not detected.

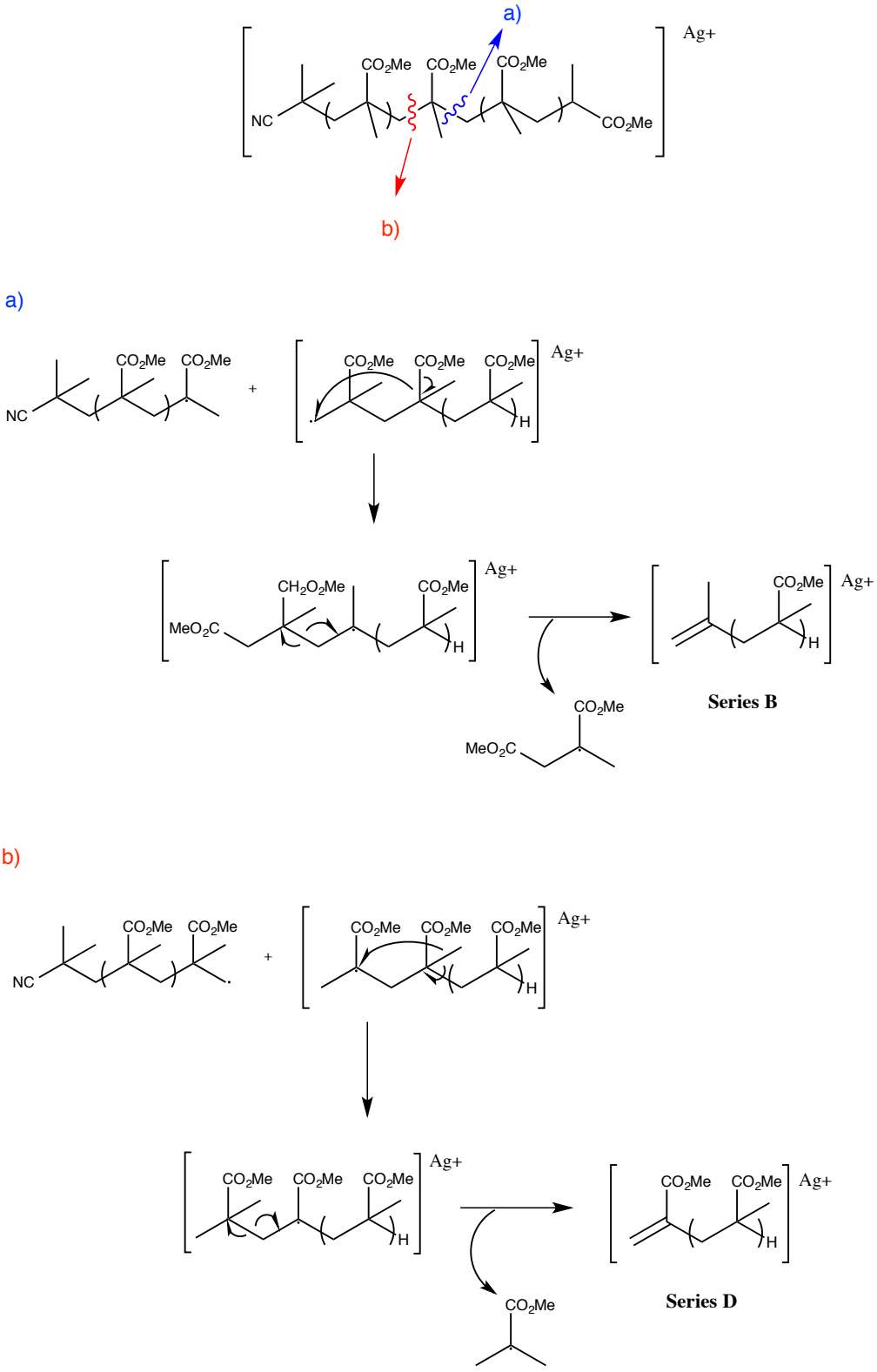


Figure 2-23. Fragmentation of PMMA during MALDI-TOF analysis. Homolytic cleavage can take place at two different points in the polymer backbone. Subsequently, a radical rearrangement would lead to structures matching series B and series D respectively.

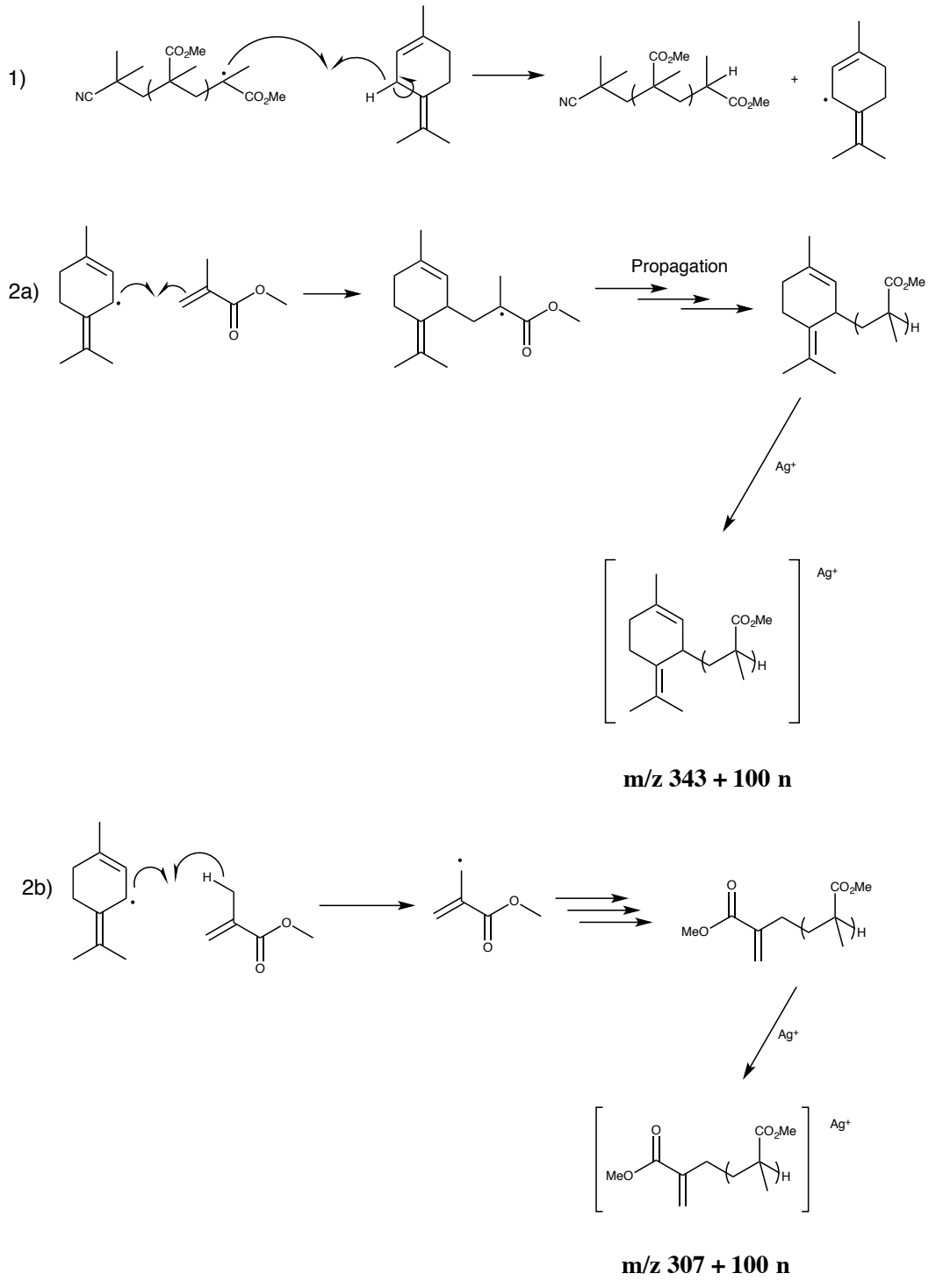


Figure 2-24. Possible PMMA structures formed upon chain transfer reaction from terpinolene to monomer. Figure shows two possible mechanisms giving rise to PMMA chains with m/z 307 + 100n and m/z 343 + 100n respectively. None of these structures were detected by MALDI-TOF.

Therefore, these experiments revealed that terpinolene does not either copolymerise or follow the mechanism of a conventional chain transfer, at least not to a degree that can be detected by NMR or MALDI. In fact, the MALDI-spectrum of terpinolene-controlled PMMA is identical to that of PMMA synthesised by FRP (Figure 2-25).

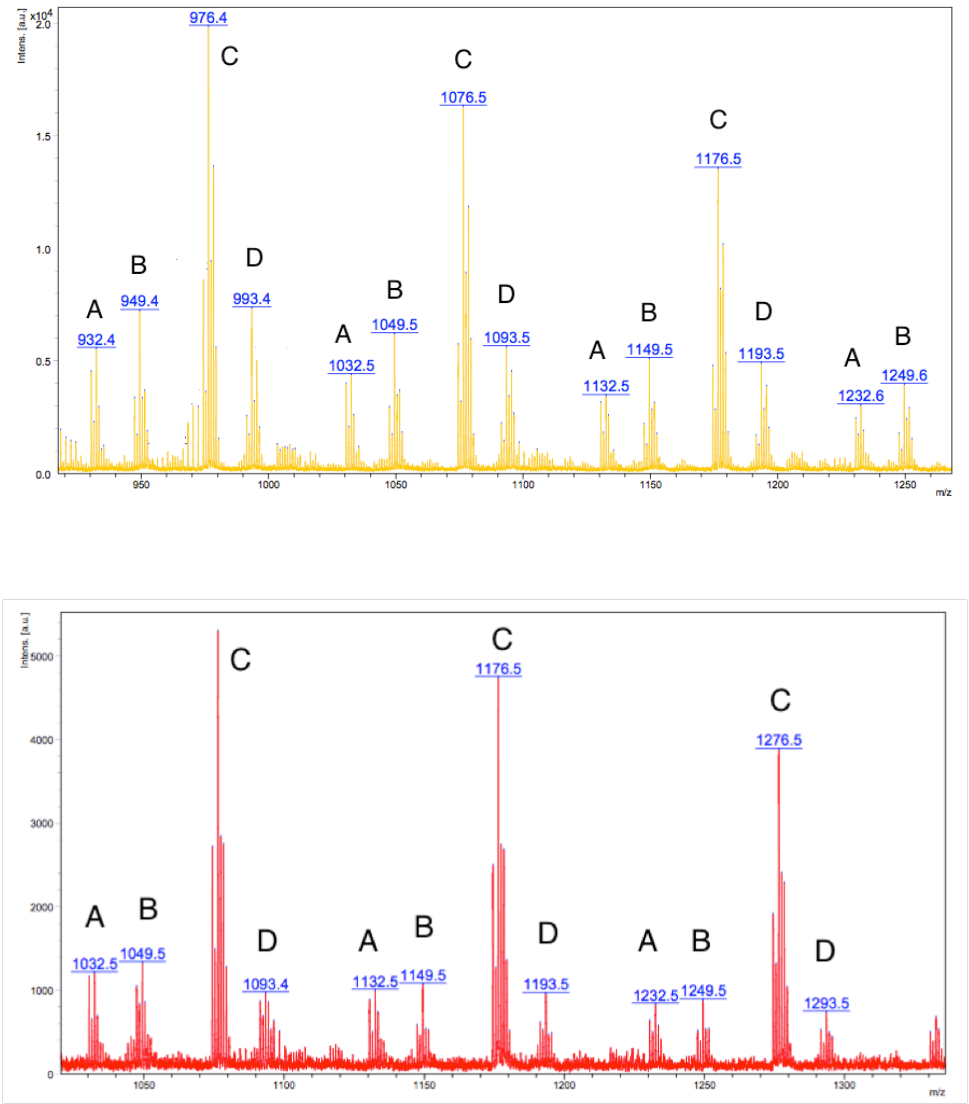


Figure 2-25. MALDI-TOF spectra of PMMA synthesised via terpinolene-controlled polymerisation (top) and via conventional FRP (bottom).

However, it had been confirmed by ^{1}H-NMR that there is a hydrogen exchange between the polymer or monomer and terpinolene. If terpinolene reinitiated the polymerisation by abstracting a hydrogen from the monomer or the polymer, then unsaturated-monomer as end group or a branched polymer should be detected respectively. The fact that none of these structures have been detected suggests that reinitiation by terpinolene radical is negligible. It is possible that the terpinolene radical remains as an unreacted radical during the polymerisation reaction and that it only abstracts a hydrogen back from a polymer chain when the reaction is quenched and all radicals are terminated.

MMA-d^{8} polymerisation reaction was also conducted in the presence of 10 mol% of γ-terpinene, under the same conditions stated for the terpinolene reaction. After 7 days of reaction, a sample was taken for ^{1}H-NMR analysis (Figure 2-26).

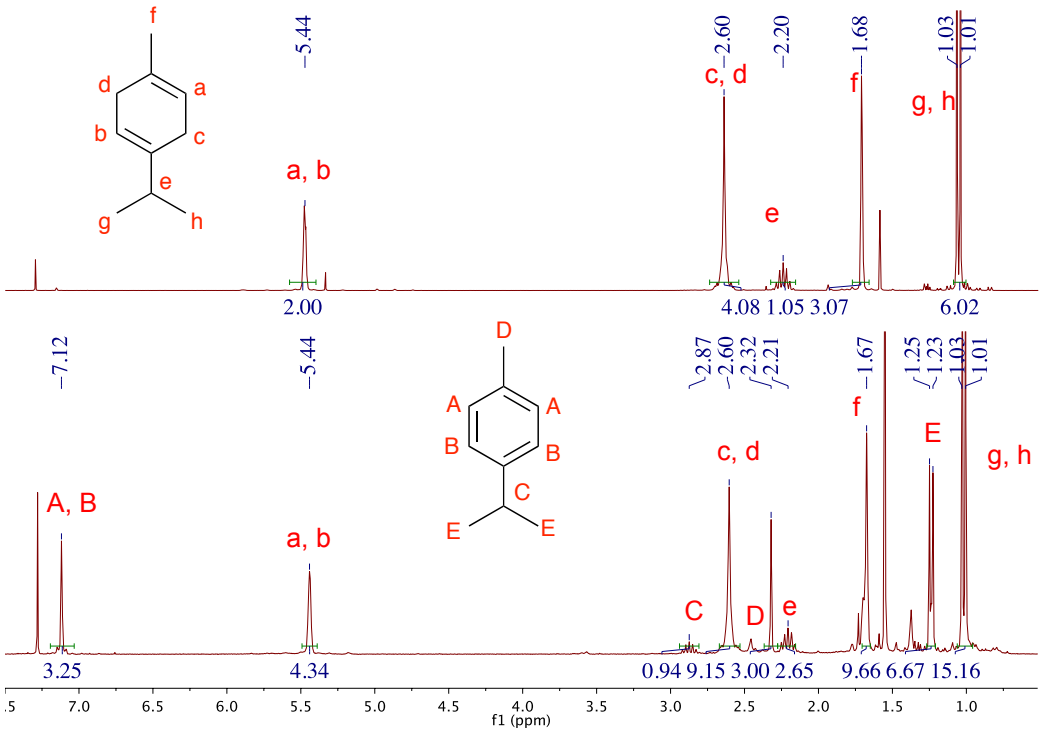


Figure 2-26. ^{1}H-NMR spectra of gamma-terpinene before (top) and after (bottom) being added to MMA-d^{8} polymerisation as controlling agent.

The NMR spectrum revealed intact γ-terpinene with no decrease in the any of the integrals values. This suggested that γ-terpinene does not exchange hydrogen atoms as was observed for terpinolene. It also indicated that there is no γ-terpinene attached to the polymer molecule. However, a set of new signals corresponding to the aromatic compound *p*-cymene were detected.

In fact, the aromatisation of γ-terpinene into *p*-cymene in the presence of radicals had been reported previously in the literature.[50-53] Foti and Ingold[52, 53] proposed an aromatisation mechanism (Figure 2-27) in which, after bis-allylic hydrogen abstraction by a HOO• radical, γ-terpinene radical reacts with oxygen, O_2. The new oxygen-containing radical rearranges, losing HOO• to form an aromatic ring.

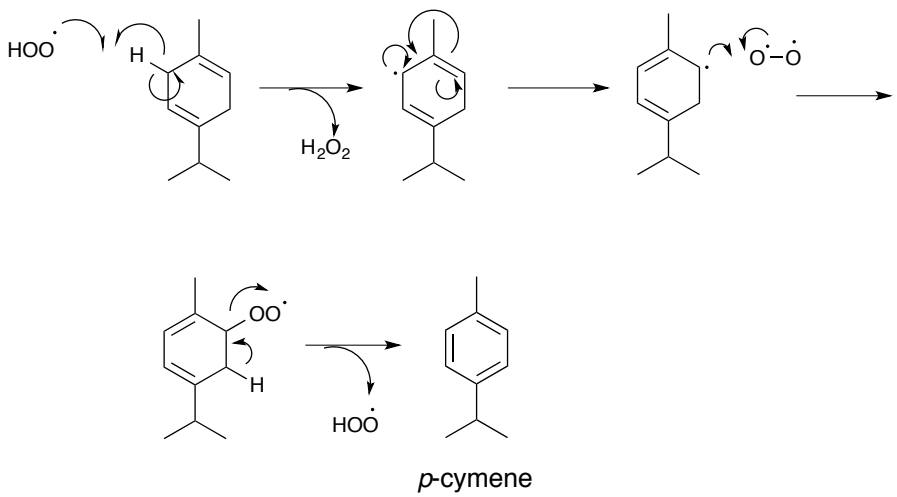


Figure 2-27. Aromatisation of terpinene in the presence of HOO radicals and O_2. The mechanism consists on bis-allylic hydrogen abstraction followed by oxygen addition and radical rearrangement leading to p-cymene.

This aromatisation mechanism would explain the formation of *p*-cymene during MMA polymerisation (Figure 2-28). One of the bis-allylic hydrogens would be abstracted by a growing PMMA chain, leading to a γ-terpinene radical and a terminated polymer chain. The abstraction of a second bis-allylic hydrogen from the γ-terpinene radical would lead to an aromatic ring. A MALDI-TOF analysis of the polymer obtained showed two different PMMA series (Figure 2-29).

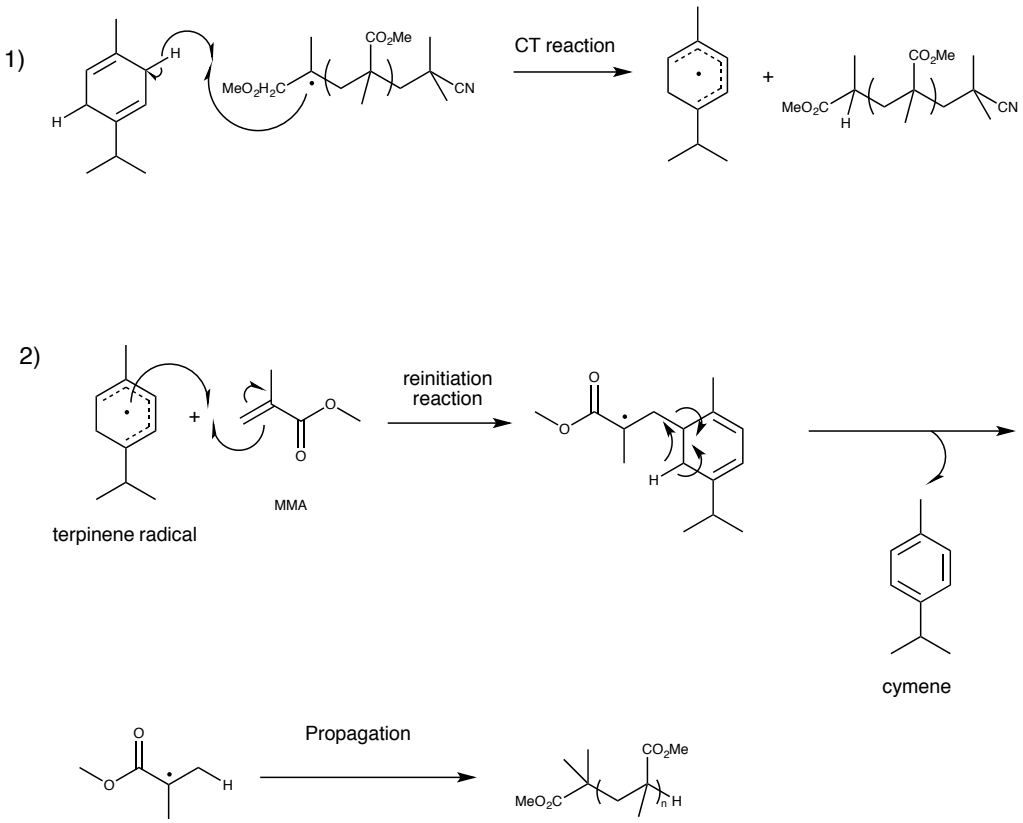


Figure 2-28. Mechanism of action of γ-terpinene as chain transfer agent. After hydrogen abstraction in step 1), γ-terpinene radical attacks a monomer unit and aromatises through a rearrangement, releasing a saturated monomer radical unit able to propagate.

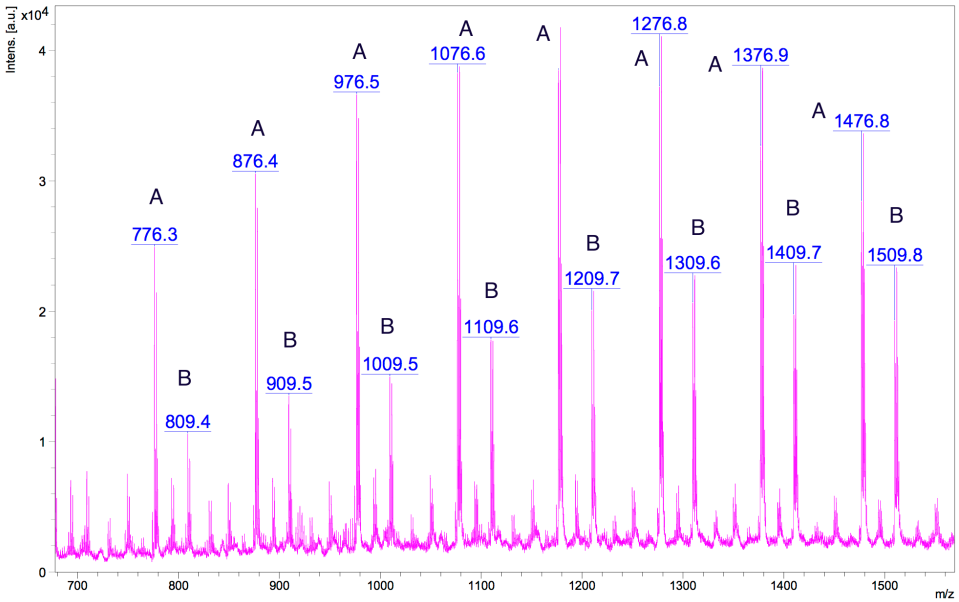
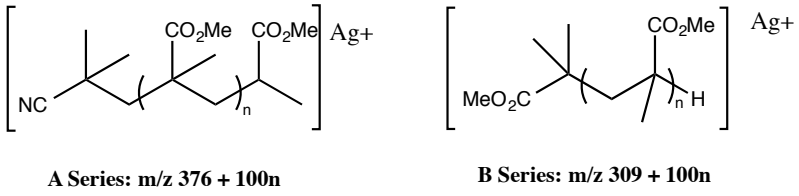


Figure 2-29. MALDI-TOF spectrum of PMMA synthesised in the presence of 10% of γ-terpinene.

One of the peaks, 1176 m/z, was also observed for the terpinolene-controlled reaction and corresponds to a hydrogen-terminated PMMA (Figure 2-30). The second series, appearing at 309 m/z, was not present in the MALDI spectrum of terpinolene-controlled PMMA. This new series matches the molecular weight of saturated MMA-initiated chains that would be formed under attack of γ-terpinene to a monomer unit (Figure 2-30). Therefore, it can be concluded that γ-terpinene controls the molecular weight and reinitiates MMA polymerisation releasing a *p*-cymene molecule.



A Series: m/z 376 + 100n **B Series: m/z 309 + 100n**

Figure 2-30. Molecular structures proposed for the two PMMA series detected by MALDI-TOF.

2.3.5 Chain transfer constant calculations.

After confirming by ^{1}H-NMR that hydrogen chain transfer does occur in the presence of either terpinolene or γ-terpinene during MMA polymerisation, their chain transfer constants were calculated. C_{tr} for terpinolene and γ-terpinene were obtained by plotting $1/DP_0$ against [CTA]/[Monomer] at terpene concentrations of 0, 1, 2, 3, and 5 mol% with respect to monomer. In order to keep the volume and monomer concentration constant, toluene was added to reach a final volume of 25 mL for all reactions. In order to keep radical concentration and conversions low, reactions were conducted at 60 ^{o}C in the presence of 0.5% AIBN for 15 minutes.

The values of DP, [CTA] and [Monomer] necessary to build the Mayo plot are shown in Table 2-9 and Table 2-10 for terpinolene and γ-terpinene-controlled polymerisation respectively.

*Table 2-9. Values of mayo equation parameters for terpinolene-controlled MMA polymerisation.**

Entry	[Terpinolene] (mol%)	[Terpinolene] (mol L^{-1})	[MMA] (mol L^{-1})	M_n (g mol^{-1})[a]	DP[a]
1	0	0	7.51	196,500	1963
2	1	0.077	7.51	49.300	491
3	2	0.154	7.51	38,900	388
4	3	0.232	7.51	24.100	241
5	5	0.386	7.51	15,000	150

*Reactions were conducted by mixing previously degassed MMA (20 mL, 188 mmol), AIBN (0.094 g, 0.5 wt%, 0.6 mmol) and the corresponding mol percentage of terpene. Toluene was added to reach 25 mL of volume in all cases. The mixture was stirred at 60 °C for 15 minutes, after which the reaction was quenched by placing in an ice bath for 10 minutes. [a]Calculated by GPC-SEC against PMMA standards.

Table 2-10. Values of mayo equation parameters for γ-terpinene-controlled MMA polymerisation.*

Entry	[γ-Terpinene] (mol%)	[γ-Terpinene] (mol L^{-1})	[MMA] (mol L^{-1})	M_n (g mol^{-1})[a]	DP[a]
1	0	0	7.51	168,300	1680
2	1	0.077	7.51	57,600	575
3	2	0.154	7.51	33,200	331
4	3	0.232	7.51	25,100	251
5	5	0.386	7.51	16,200	161

*Reactions were conducted by mixing previously degassed MMA (20 mL, 188 mmol), AIBN (0.094 g, 0.5 wt%, 0.6 mmol) and the corresponding mol percentage of terpene. Toluene was added to reach 25 mL of volume in all cases. The mixture was stirred at 60 °C for 15 minutes, after which the reaction was quenched by placing in an ice bath for 10 minutes. [a]Calculated by GPC-SEC against PMMA standards.

The mayo plots are depicted in Figure 2-31 and Figure 2-32. The chain transfer constant values obtained were very similar for the two terpenes: 0.117 for terpinolene and 0.093 for γ-terpinene.

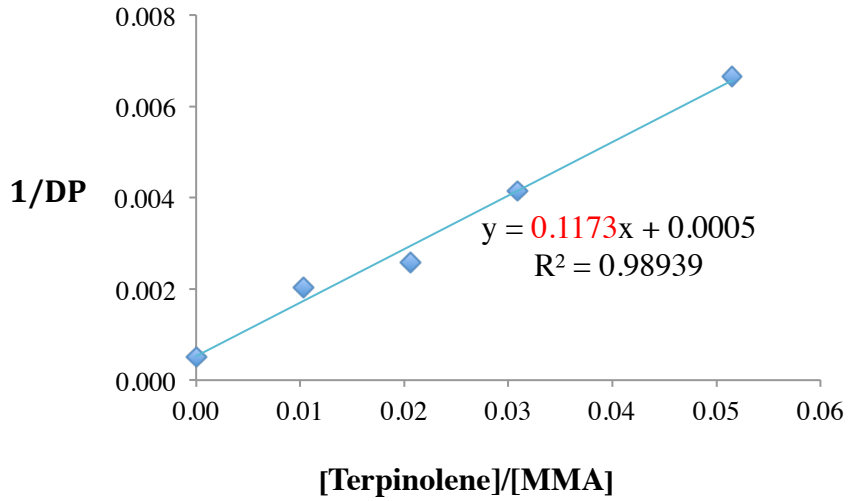


Figure 2-31. Mayo plot for terpinolene in MMA polymerisation, The slope value, highlighted in red, corresponds to terpinolene chain transfer constant.

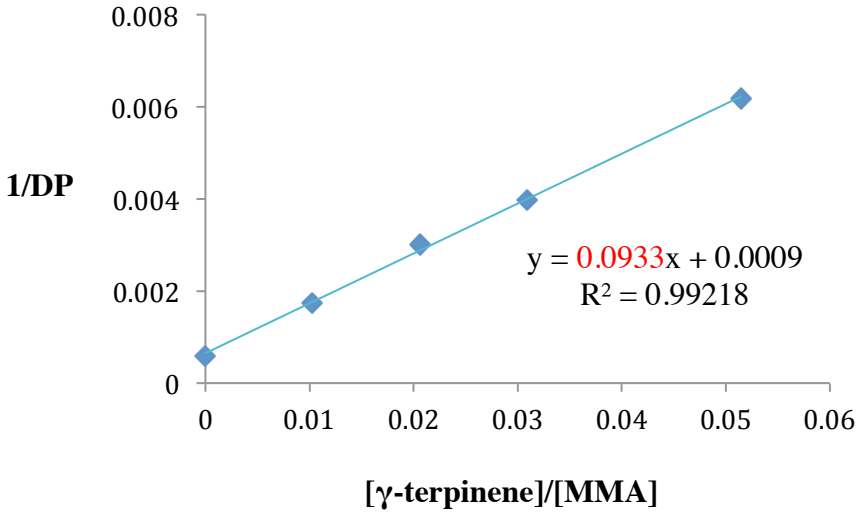


Figure 2-32. Mayo plot for γ-terpinene in MMA polymerisation, The slope value, highlighted in red, corresponds to γ-terpinene chain transfer constant.

When the C_{tr} values obtained for terpinolene and γ-terpinene are compared with the C_{tr} of some of the most commonly used thiols (Table 2-11) it is clear that they are of the same order of magnitude than those of thiols but somewhat lower.

*Table 2-11. Chain transfer constants (C_{tr}) of commonly used thiols (R-SH) for MMA.**

CTA R	C_{tr}
n-C_4H_9	0.67
MeO_2CCH_2	0.30
$H_3N^+CH_2CH_2$	0.11
$HOCH_2CH_2$	0.45

*Data extracted from "Handbook of Radical Polymerization" by Matyjaszewsky.[1]

However, this is not necessarily a disadvantage, since terpinolene and γ-terpinene are renewable and inexpensive compounds. Additionally, the fact that higher concentrations of terpene are necessary to obtain lower molecular weights means that the molecular weight can be controlled more accurately in a commercial process, as addition errors would be reduced.

2.3.6 Exotherm measurements.

A study of the effect that the addition of γ-terpinene and terpinolene has on reaction temperature was conducted. MMA was polymerised in bulk at 65 ^oC in the presence of 2 wt% AIBN and varying terpene concentrations ranging from 0 to 10 mol%. The reaction temperature was monitored by a thermocouple attached to a Picolog. The thermocouple was placed into the reaction vessel through the septum to measure the internal bulk temperature of the reaction. The software was set to constantly measure the temperature of the reaction mixture for 24 h.

In the absence of terpene, a Trommsdorff effect was observed (Figure 2-33). After approximately 2000 seconds of reaction there was a sudden and sharp increase in temperature to over 110 ^oC. This temperature rise was accompanied by a pressure increase that caused the runaway reaction, at which point the heating was stopped.

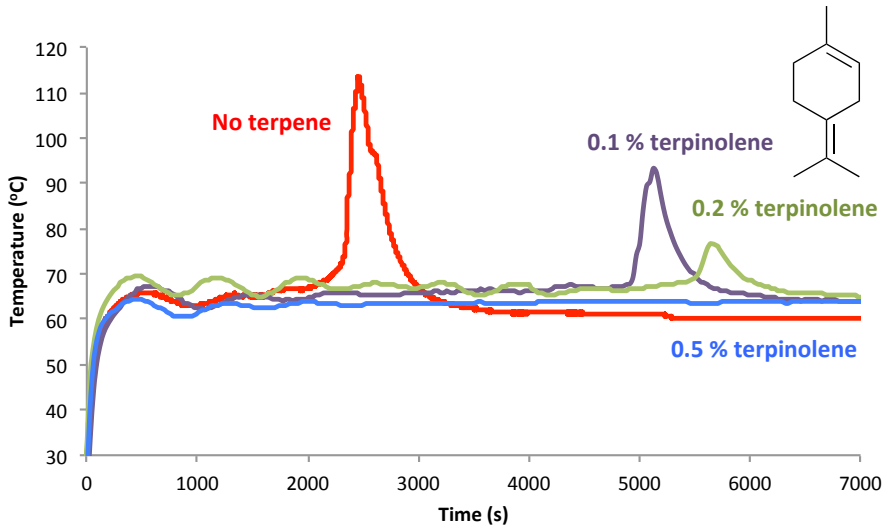


Figure 2-33. Exotherms measured during MMA polymerisation in bulk, at 65 °C, in the presence of 2 wt% AIBN and different terpinolene concentrations between 0 and 0.5 mol%.

At increasing terpinolene concentrations, from 0.1 to 0.5 mol%, the temperature peak was delayed and its magnitude was considerably reduced. At 0.1 mol% of terpinolene, the temperature peak appears at around 5000 seconds, and the temperature increase was of 30 °C. At 0.2 mol% of terpinolene the temperature peak occurred after around 5500 seconds, and exhibited a more modest temperature increase of 10 °C. At the next terpinolene concentration tested, 0.5 mol%, there was no temperature peak observed for the 24 h that the experiment lasted.

When γ-terpinene was added instead, higher concentrations were necessary in order to completely supress the temperature peak (Figure 2-34).

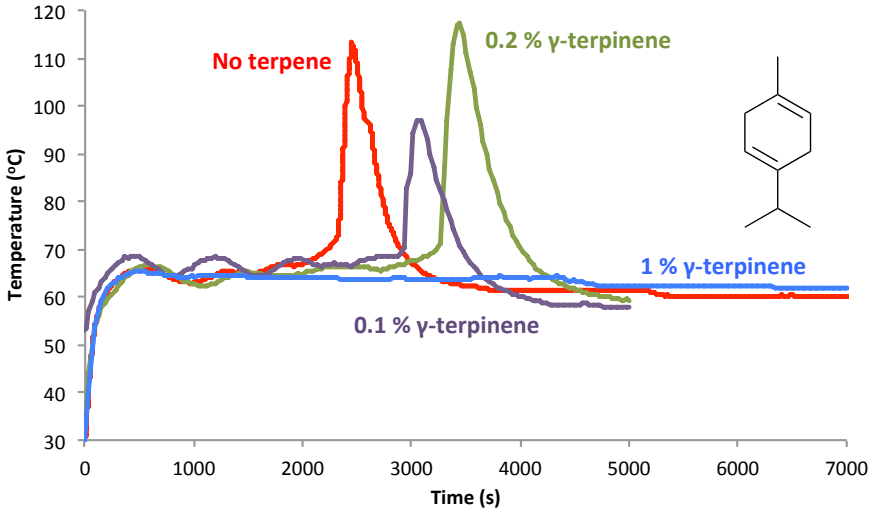


Figure 2-34. Exotherms measured during MMA polymerisation in bulk, at 65 ºC, in the presence of 2 wt% AIBN and different concentrations of γ-terpinene between 0 and 1 mol%.

Concentrations of γ-terpinene of 0.1 and 0.2 mol% did not delay the temperature peak as much as terpinolene did at the same concentrations (Figure 2-33), and at both concentrations the temperature increased at least 35 ºC. At a concentration of 0.2 mol%, the temperature peak was more intense than at 0.1 mol%. This might be caused by the thermocouple being placed in a "hot spot". During MMA bulk polymerisation a high viscosity was reached at the early stages of the reaction, which caused the stirrer to stop working. This provoked heterogeneity in the reaction media, where some areas contained a higher concentration of radicals than others, and therefore experienced further increases in temperature. This means that the measured reaction temperature depends on where the thermocouple is placed. However, it is clear that the temperature peak was delayed further than at 0.1 mol% of γ-terpinene. Since γ-terpinene did not seem as effective as terpinolene, the next concentration tested was 1 mol%. At this concentration, the exotherm was completely supressed.

The fact that a higher concentration of γ-terpinene was needed to supress the temperature peak might be explained by the reinitiation of the polymerisation by γ-terpinene. As discussed above in section 2.3.4, once γ-terpinene radical is formed, it is likely to react with a monomer unit, reinitiating polymerisation and

releasing a *p*-cymene unit (Figure 2-28). This means that γ-terpinene provides both termination and reinitiation. It had been previously observed that terpinolene retards MMA polymerisation to a greater extent that γ-terpinene (Table 2-8), and that is probably caused by a much slower reinitiation step initiated by terpinolene. Therefore, terpinolene was expected to be more effective at preventing the Trommsdorff-Norrish effect, since it provides termination but it does not tend to reinitiate the polymerisation. This means that there is a lower number of active polymer chains, and therefore a break in the autoacceleration of the reaction.

2.3.7 Control of other monomers: styrene, methyl acrylate, vinyl acetate.

The effectivity of terpinolene and γ-terpinene at controlling molecular weight was tested with monomers other than MMA. The ability of terpinolene and γ-terpinene to act as CTAs in the radical polymerisation of methyl acrylate (MA), styrene (Sty) and vinyl acetate (VAc) (Figure 2-35) was tested.

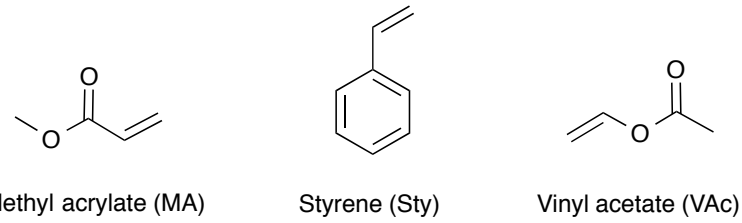


Figure 2-35. Chemical structures of monomers methyl acrylate, styrene and vinyl acetate.

2.3.7.1 Methyl acrylate

Initially, MA was polymerised in the presence of 2 wt% of AIBN and different concentrations of terpinolene between 10 mol% and 0.5 mol% (Table 2-12). Polymer molecular weight increased with decreasing terpinolene concentration, ranging from 3,000 to 24,700 g mol^{-1}. Dispersity values showed the same trend, increasing from 1.55 to 1.79, revealing relatively uniform polymer chain distributions.

*Table 2-12. Bulk polymerisation of MA at 65 °C for 24 h using terpinolene as CTA and 2 wt% AIBN.**

Entry	mol% of terpinolene	Conversion (%)[a]	M_n (g mol^{-1})[b]	Đ[b,c]
1	10	15	3,000	1.55
2	5	39	4,900	1.60
3	2	48	8,900	1.55
4	1	78	14,600	1.56
5	0.5	89	24,700	1.79
7	0	Trommsdorff-Norrish effect		

*10 mL of MA were mixed with the corresponding percentage mol of terpinolene and 2 wt% of AIBN. Reactions were conducted at 65 °C for 24 h. [a]Conversions calculated by ^{1}H-NMR. [b]Calculated by GPC-SEC against PMMA standards. [c] Dispersity

Very similar results were obtained when γ-terpinene was tested (Table 2-13).

*Table 2-13 Bulk polymerisation of MA at 65 °C for 24 h using γ -terpinene as CTA and 2 wt% AIBN.**

Entry	% γ-terpinene	Conversion (%)[b]	M_n (g mol^{-1})[c]	Đ[c,d]
1	10	22	3,100	1.58
2	5	51	4,600	1.60
3	2	75	9,300	1.54
4	1	91	12,400	1.65
5	0.5	96	18,300	1.99
7	0	Trommsdorff-Norrish effect		

*10 mL of MA were mixed with the corresponding percentage mol of γ-terpinene and 2 wt% of AIBN. Reactions were conducted at 65 °C for 24 h. [a] Conversions calculated by ^{1}H-NMR. [b]Calculated by GPC-SEC against PMMA standards. [c] Dispersity.

Molecular weights between 3,100 and 18,100 g mol^{-1} were obtained with dispersity values ranging from 1.54 to 1.99. In all reactions in the presence of γ-terpinene, ^{1}H-NMR analysis revealed the presence of *p*-cymene after they were quenched, suggesting the same reinitiation mechanism for MA as for MMA. As

with MMA, conversions were found to decrease with increasing terpene concentration, being as low as 15 % and 22 % when 10 mol% of terpinolene and γ-terpinene were used respectively.

As for the magnitude of the exotherm exhibited by the reaction, when MA was polymerised in the absence of terpene, a violent runaway reaction took place as a consequence of the Trommsdorff effect. Concentrations as low as 0.5 mol% of terpene were sufficient to prevent the Trommsdorff effect whilst allowing essentially full conversions.

If the results obtained from MA polymerisations (Table 2-12, Table 2-13) are compared with those of MMA (Table 2-6, Table 2-7), it can be observed that the molecular weights of poly(methyl acrylate) (PMA) are considerably lower than those of PMMA. For example, in the presence of 10 mol% terpinolene, polymers with molecular weights of 3,000 and 5,500 g mol^{-1} were obtained for PMA and PMMA respectively. When a concentration of γ-terpinene of 5 mol% was added, PMA and PMMA were formed with molecular weights of 4,600 and 9,700 g mol^{-1}.

As discussed in the introduction to this chapter (section 2.1.2), when a CTA is added to a reaction, the polymerisation rate will depend on the relative rate constants of propagation (k_p) and reinitiation (k_{re}) whilst polymer molecular weight will vary depending on the ratio between the rate constants of propagation (k_p) and chain transfer (k_{tr}).[1, 54] The fact that the molecular weights of PMA were lower than those of PMMA indicated a higher chain transfer rate of the terpenes with MA $k_{tr,MA}$ than with MMA $k_{tr,MA}$. This might be explained by a more reactive MA radical. After radical attack to a MA unit, a very reactive secondary radical is formed (Figure 2-36). Acrylate radicals are more reactive than methacrylate radicals, therefore they are more likely to undergo chain transfer reactions, hence they generally exhibit higher chain transfer rates than methacrylates.[1]

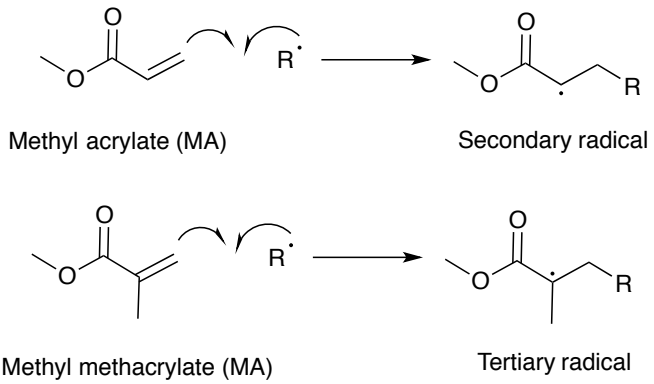


Figure 2-36. Scheme showing radical attack to MA (top) and MMA (bottom) leading to secondary and tertiary radicals respectively. Alkyl groups are electrodonating and therefore radical stability increases with alkyl substitution.

As for MA and MMA conversions, they were very similar for the same concentrations of terpinolene (Figure 2-37, left). However, γ-terpinene seemed to retard MA polymerisation further than it did for MMA (Figure 2-37, right).

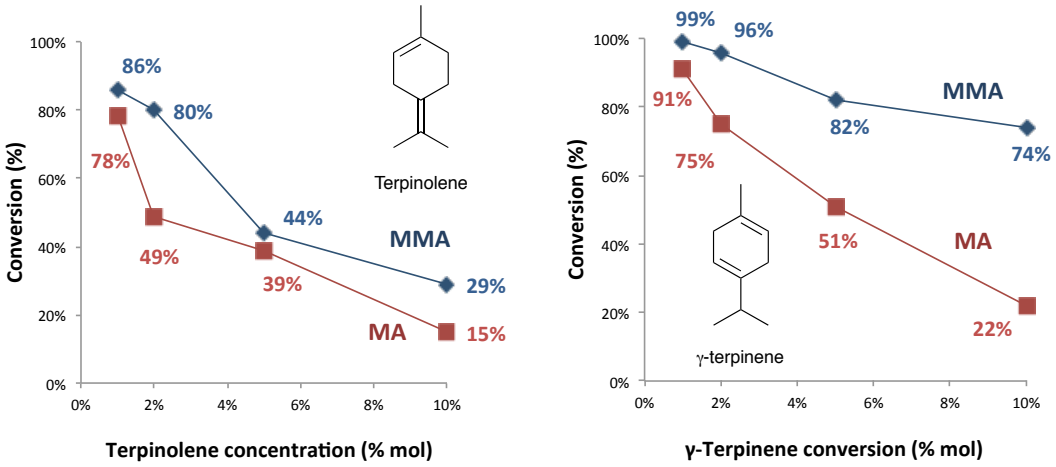


Figure 2-37. MA and MMA conversions after polymerisation in the presence of different concentrations of terpinolene (left) and γ-terpinene (right).

The retardation during MA polymerisation in the presence of γ-terpinene is proposed to be caused by the higher propagation rate of MA than of MMA $k_{p,MA} > k_{p,MA}$, and a lower reinitiation rate of MA $k_{re,MA} < k_{p,MA}$. This means that the difference between the relative rates of propagation and reinitiation is much more

acute in the case of MA, which translates into a lower polymerisation rate and lower conversions.

The reason for the slower reinitation of MA is the lower reactivity of the MA monomer. It is well known that less reactive monomers generate more reactive radicals. MA monomer is less reactive towards radical attack than MMA because it generates a less stable, and therefore more reactive, radical[55-57] (Figure 2-37). As a result, the γ-terpinene radical is more reactive towards MMA than MA reinitiation. In the presence of terpinolene, there was not a significant difference in conversions between MA and MMA because of the negligible reinitiation rates in both cases.

2.3.7.2 Styrene

In order to study terpinolene and γ-terpinene as CTAs for styrene polymerisation, several terpene concentrations were tested. The chosen reaction conditions were the same as those applied to MMA and MA bulk polymerisation, namely 65 ^{o}C, 2 wt% of AIBN and 24 h of reaction time. The expected dependence of polymer molecular weight on terpene concentration was observed for both terpinolene (Table 2-14) and γ-terpinene (Table 2-15).

When decreasing terpinolene concentrations from 10 to 0.5 mol% were added (Table 2-14), polymers with average molecular weights ranging 8,800 to 31,700 g mol^{-1} and good dispersity values between 1.55 and 1.87 were obtained. Similar results were obtained when the same concentrations of γ-terpinene were studied (Table 2-15), yielding polymers with average molecular weights in the range between 7,000 and 28,300 g mol^{-1} and dispersity values between 1.62 and 1.91, as expected from a conventional chain transfer agent. The presence of *p*-cymene in the γ-terpinene-controlled reactions indicated that γ-terpinene is able to reinitiate styrene polymerisation as well as MA and MMA.

*Table 2-14 Bulk polymerisation of Sty at 65 °C for 24 h using terpinolene as CTA and 2 wt% AIBN**

Entry	% terpinolene	Conversion (%)[a]	M_n (g mol^{-1})[b]	Đ[b,c]
1	10	68	8,800	1.69
2	5	78	11,200	1.61
3	2	85	18,200	1.55
4	1	89	21,600	1.58
5	0.5	95	31,700	1.87
7	0	Trommsdorff-Norrish effect		

*10 mL of Sty were mixed with the corresponding percentage mol of terpinolene and 2 wt% of AIBN. Reactions were conducted at 65 °C for 24 h. [b] Conversions calculated by ^{1}H-NMR. [c]Calculated by GPC-SEC against PMMA standards. [d] Dispersity

*Table 2-15 Bulk polymerisation of Sty at 65 °C for 24 h using γ-terpinene as CTA and 2 wt% AIBN.**

Entry	% γ-terpinene	Conversion (%)[a]	M_n (g mol^{-1})[b]	Đ[b,c]
1	10	70	7,000	1.75
2	5	81	11,000	1.61
3	2	86	16,900	1.62
4	1	96	20,000	1.65
5	0.5	99	28,300	1.91
7	0	Trommsdorff-Norrish effect		

*10 mL of Sty were mixed with the corresponding percentage mol of γ-terpinene and 2 wt% of AIBN. Reactions were conducted at 65 °C for 24 h. [a] Conversions calculated by ^{1}H-NMR. [b]Calculated by GPC-SEC against PMMA standards. [c] Dispersity.

With regard to control of the Trommsdorff effect, the lowest terpene concentration tested was 0.5 mol%. At this concentration, this effect was prevented with both terpenes.

The molecular weights of polystyrene (PSty) obtained in the presence of terpene concentrations between 1 to 10 mol% ranged from 7,000 to 20,000 g mol^{-1}. These

values are quite close to the molecular weights of PMMA achieved at the same terpene concentrations, which were between 5,500 and 17,200 g mol^{-1}. This data suggests a similar chain transfer constant value C_{tr} of terpinolene and γ-terpinene with Sty and MMA.

As discussed above, the chain transfer constant is defined by the ratio between chain transfer and propagation rate constants, $C_{tr} = k_{tr}/k_p$. Upon radical attack, styrene forms a styrene radical that is stabilised by resonance (Figure 2-38).

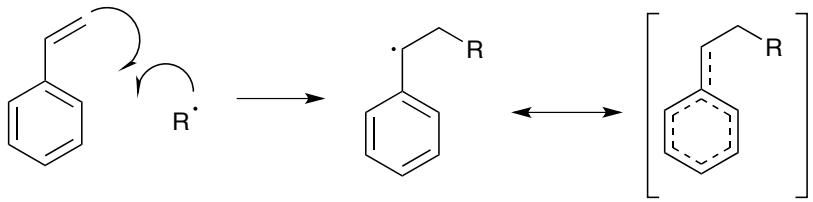


Figure 2-38. Upon radical attack to a styrene monomer unit a radical stabilised by resonance is formed.

This relatively stable radical is not as reactive towards chain transfer as MMA and MA radicals. Although Sty seems to present a lower chain transfer rate constant, $k_{tr,STY}$, its propagation rate is also lower than that of MA and MMA. As a result, the molecular weights obtained for PSty are similar to those of PMMA.

Interestingly, there was a considerable rise in Sty conversion with respect to MMA and MA polymerisations. Even when 10 mol% of terpene was added to Sty polymerisation (Table 2-14, Table 2-15) high conversions of 70 % were reached in both cases. The proposed explanation for these differences is related to the stabilities and reactivities of the Sty radical and the Sty monomer. Sty monomer is relatively reactive because of the highly stabilised radical that is formed after radical attack. Therefore the reinitiation rate will be higher than that of MMA and MA. As for propagation, Sty has a lower propagation rate than MA and MMA, which leads to a propagation rate constant, $k_{p,STY}$, closer in value to the reinitiation rate constant, $k_{re,STY}$, and therefore to a higher polymerisation rate.

2.3.7.3 Vinyl acetate

Finally, vinyl acetate was polymerised in the presence of concentrations of terpinolene and γ-terpinene ranging between 10 and 0.1 mol% (Table 2-16, Table 2-17). In this case, the effect of terpene concentration on polymerisation rate was much more acute than it had been observed for the previous monomers.

*Table 2-16. Bulk polymerisation of VAc at 65 °C for 24 h using terpinolene as CTA and 2 wt% AIBN.**

Entry	% terpinolene	Conversion (%)[a]	M_n (g mol^{-1})[b]	Đ[b,c]
1	10	< 5	ND[e]	ND
2	5	< 5	ND	ND
3	2	5	ND	ND
4	1	42	6400	1.54
5	0.5	52	12900	1.47
6	0.2	88	23700	1.74
7	0.1	85	30500	2.87
8	0	Trommsdorff-Norrish effect		

*10 mL of VAc were mixed with the corresponding percentage mol of terpinolene and 2 wt% of AIBN. Reactions were conducted at 65 °C for 24 h. [a] Conversions calculated by ^{1}H-NMR. [b]Calculated by GPC-SEC against PMMA standards. [c] Dispersity.

*Table 2-17. Bulk polymerisation of VAc at 65 °C for 24 h using γ-terpinene as CTA and 2 wt% AIBN.**

Entry	% γ-terpinene	Conversion (%)[a]	M_n (g mol^{-1})[b]	Đ[b,c]
1	10	< 5	ND[e]	ND
2	5	8	ND	ND
3	2	26	5200	1.55
4	1	44	8300	1.57
5	0.5	47	13000	1.49
6	0.2	88	28500	1.77
7	0.1	87	29400	2.53
8	0	Trommsdorff-Norrish effect		

*10 mL of VAc were mixed with the corresponding percentage mol of γ-terpinene and 2 wt% of AIBN. Reactions were conducted at 65 °C for 24 h. [a] Conversions calculated by ^{1}H-NMR. [b]Calculated by GPC-SEC against PMMA standards. [c] Dispersity.

When 10 mol% of either terpene was added to the reaction, no polymer was detected after 24 h. It was necessary to reduce terpene concentration to 1 mol% in order to reach 42 % and 44 % conversion in the presence of terpinolene and γ-terpinene respectively, and to reduce it further to 0.2 mol% so as to obtain high conversions of 88 % and 82 %. Vinyl acetate is an extremely reactive monomer with a very high propagation rate and it forms a very reactive and unstable radical after initiator attack (Figure 2-39).

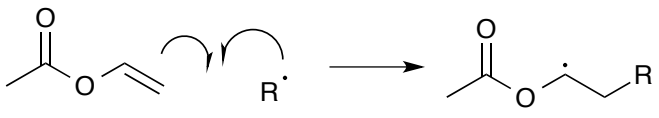


Figure 2-39. After radical attack, vinyl acetate forms a very reactive radical. Unlike styrene, vinyl acetate radical is not stabilised by resonance.

This makes vinyl acetate radical especially prone to abstract a bis-allylic hydrogen from γ-terpinene or terpinolene. Therefore, low molecular weights and the high degree of retardation observed for vinyl acetate polymerisation are

proposed to be caused by a much higher chain transfer rate than that of the other monomers, together with a lower reinitiation rate. Retardation in vinyl acetate polymerisation caused by a hydrogen-donor compound had been observed before.[58-61] It was believed to be a result of the formation of a slow-reacting radical, leading to a very slow reinitiation step to VAc monomer. As a consequence the concentration of propagating radicals was reduced, and retardation was observed.

2.3.7.4 Comparison of the effects of terpinolene and terpinene on the polymerisation reactions of methyl methacrylate, methyl acrylate, styrene and vinyl acetate.

When comparing the conversions reached with the four monomers tested (MMA, MA, Sty and VAc) it is clear that there is a dependency of polymerisation rate on the stability of the monomer radicals. The terpinolene-controlled polymerisation data suggested a negligible reinitiation rate. Thus, conversions increased with increasing radical stability VAc < MA < MMA < Sty (Figure 2-40), since a higher degree of chain transfer would lead to higher number of dead chains.

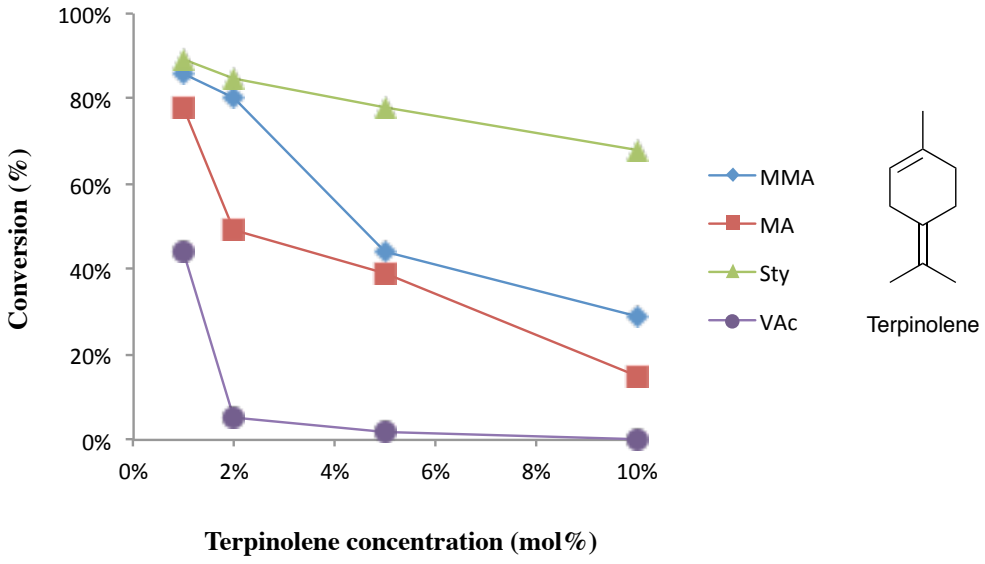


Figure 2-40. Conversions of terpinolene-controlled radical polymerisation of Sty, MMA, MA and VAc.

Conversions reached during γ-terpinene-controlled polymerisations (Figure 2-41) showed a similar trend, increasing in the order VAc < MA < Sty ≤ MMA. In this case, conversions reached during Sty and MMA polymerisations were high and very similar, although slightly higher for MMA reactions. This might be explained by the reinitiation rate in MMA polymerisation. During terpinolene-controlled polymerisations, the lack of reinitiation meant retardation depended only on chain transfer rate. In the case of γ-terpinene, higher reinitiation rates meant higher conversions.

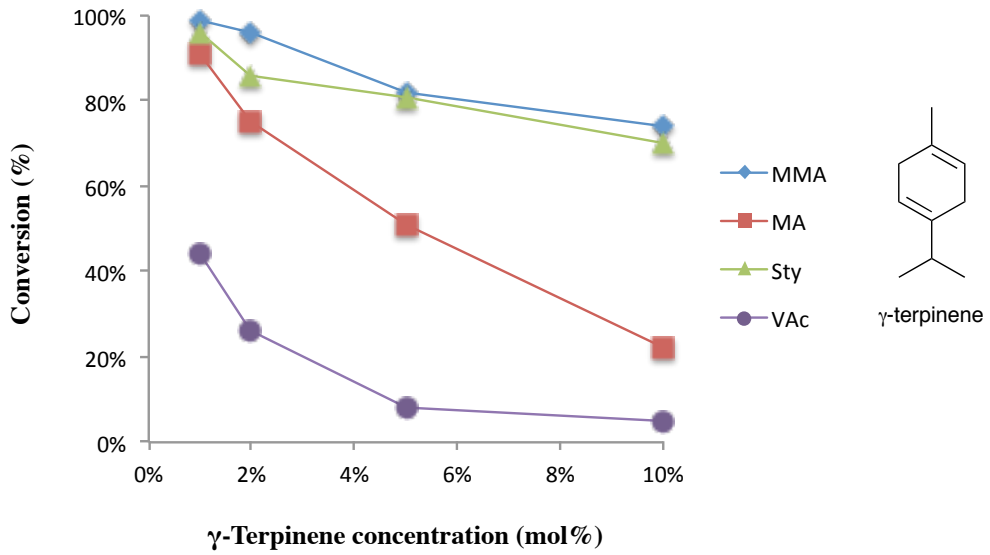


Figure 2-41. Conversions of γ-terpinene-controlled polymerisation of Sty, MMA, MA and VAc.

The same trend is observed when looking at the effectivity of terpinolene and γ-terpinene as chain transfer agents. The representation of 1/DP vs [terpene]/[monomer] using the data discussed in this section gives an idea of how effective terpinolene and terpinene are as CTAs for each monomer. However, this data cannot be used to calculate the chain transfer constants C_{tr} because the necessary conditions where a low flux of radicals is ensured (section 2.1.3) were not met. Therefore an apparent chain transfer constant C_{app} would be obtained instead.

When 1/DP vs [terpinolene]/[monomer] is represented for MMA, MA, Sty and VAc (Figure 2-42), the slope of the trend line increases in the order Sty < MMA < MA < VAc, following the same order than the corresponding radical reactivities.

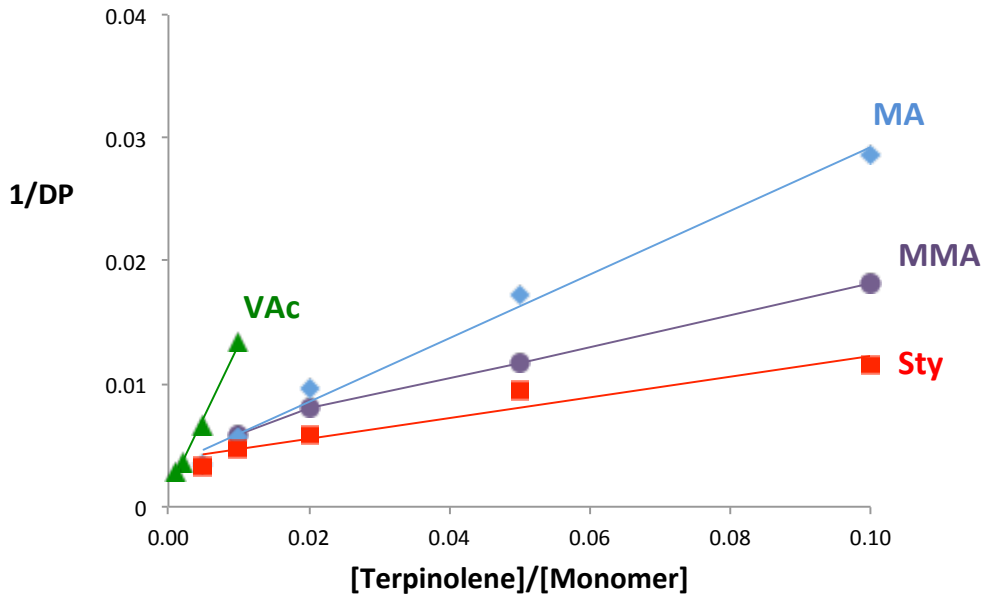


Figure 2-42. Graphical representation of 1/DP vs [Terpinolene]/[Monomer]for VAc, MA, MMA and styrene polymerisations. The steeper the slope of the trendline, the more effective terpinolene is as CTA for the corresponding monomer.

During terpinolene-controlled polymerisations of all four monomers, no *p*-cymene or any structure other than terpinolene and monomer was detected by ^{1}H-NMR. Therefore, it is assumed that little or no reinitiation took place and therefore, polymerisation rate decreased with increasing chain transfer rate. It can be concluded that terpinolene provokes retardation and does not seem to reinitiate polymerisation. However, at low concentrations of terpinolene retardation was not observed and there was no significant decrease in molecular weight, whereas the exotherm was effectively supressed. Hence, terpinolene showed to be an effective Trommssdorff effect inhibitor.

The representation of 1/DP vs [γ-terpinene]/[monomer] (Figure 2-43) shows a trendline for styrene slightly steeper than that of MMA.

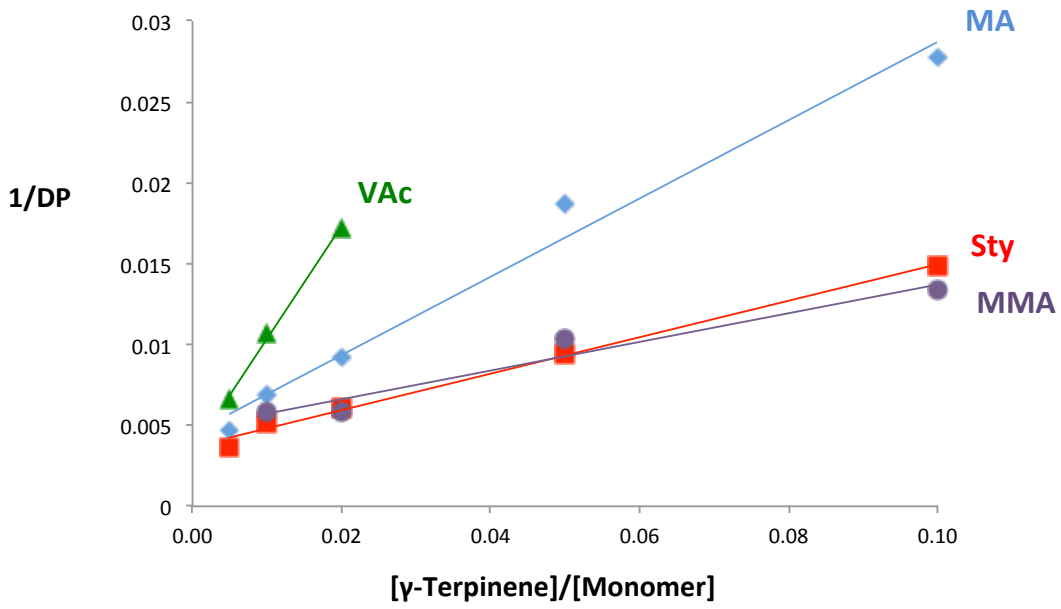


Figure 2-43. Graphical representation of 1/DP vs [γ-Terpinene]/[Monomer] for VAc, MA, MMA and styrene polymerisations.

However, these experiments are not accurate enough to differentiate between similar C_{tr} values since reactions were taken to high conversions. The graph does reveal that γ-terpinene presents similar effectiveness as CTA with MMA and styrene. Generally, traditional CTAs such as thiols, disulfides and halomethanes, react faster with nucleoplilic radicals such as Sty and VAc and therefore show a higher C_{tr} with these monomers[1] (Table 2-18). However, during terpinolene and γ-terpinene-controlled polymerisations, radical stability seems to play a major role and therefore C_{app} increases in the order Sty ≈ MMA < MA < VAc.

*Table 2-18. Chain transfer constants of some traditional CTAs with MMA, MA, Sty and VAc.**

	C_{tr}			
CTA	**MMA**	**MA**	**Sty**	**VAc**
n-C_4H_9	0.67	-	22	48
EtO_2CH_2	0.00065	-	0.015	1.5
CBr_4	0.19	0.41	8.8	739
CCl_4	18.5	1.0	92	>800

*Data extracted from "Handbook of Polymer Chemistry" by K. Matyjaszewski.[1]

Conversions were high for MMA and Sty monomers in all reactions, including those containing 10 mol% of γ-terpinene (Figure 2-41). This means that γ-terpinene is a promising renewable CTA for these two monomers. Regarding MA and VAc polymerisations, conversions were much lower (Figure 2-41), revealing a higher chain transfer rate and probably a lower level of reinitiation. γ-Terpinene inhibited the exotherm in all reactions tested and proved to be an effectibe gel-effect inhibitor for the four monomers.

2.4 Conclusions

Terpinolene and γ-terpinene were proved to be the most effective CTAs among terpenes because of the presence of bis-allylic hydrogens. Mechanistic studies were conducted for the first time and showed that both terpenes control molecular weight through a chain transfer mechanism. Terpinolene does not seem to reinitiate polymerisation to a significant level, leading to high levels of retardation. However, it has shown to be a very efficient peak suppressor for the polymerisation of MMA, MA, Sty and Vac at very low conversions below 1 mol%. As for γ-terpinene, this research suggested that it is able to reinitiate polymerisation upon the formation of a *p*-cymene molecule. It is an effective CTA for the four monomers tested with lower levels of retardation than terpinolene. Terpinolene and γ-terpinene are therefore renewable and suitable peak suppressors and CTAs for the polymerisation of a range of commercial monomers. They offer significant advantages over the use of other common

controlling agents because they are renewable, cheap, colourless. Additionally, they exhibit low toxicities and, in fact, they have been approved by the World Health Organisation as food additives.[62, 63] This work represents the first systematic study of the effect of terpinolene and γ-terpinene over the polymerisation of the four most popular monomers for radical polymerisation.

2.5 References

1. K. Matyjaszewski and T. P. Davis, *Handbook of Radical Polymerization*, Wiley-Interscience, 2002.
2. G. Odian, *Principles of Polymerization*, John Wiley and Sons, Inc., New Jersey, 2004.
3. G. V. Schulz and G. Harborth, *Makromol. Chem.*, 1947, **1**, 106-139.
4. J. F. Kennedy and C. J. Knill, *Carbohydr. Polym.*, 2000, **43**, 89-90.
5. G. Moad and D. H. Solomon, *The Chemistry of Radical Polymerisation*, Elsevier, Boston, 2006.
6. K. G. Suddaby, D. R. Maloney and D. M. Haddleton, *Macromolecules*, 1997, **30**, 702-713.
7. A. J. D. Silvestre and A. Gandini, in *Monomers, Polymers and Composites from Renewable Resources*, eds. M. N. Belgacem and A. Gandini, Elsevier, Oxford, 2008.
8. A. Gandini, *Macromolecules (Washington, DC, U. S.)*, 2008, **41**, 9491-9504.
9. A. Gandini, in *Biocatalysis in Polymer Chemistry*, Wiley-VCH Verlag GmbH & Co. KGaA, 2010, pp. 1-33.
10. K. Yao and C. Tang, *Macromolecules*, 2013, **46**, 1689-1712.
11. P. A. Wilbon, F. Chu and C. Tang, *Macromolecular Rapid Communications*, 2013, **34**, 8-37.
12. A. M. Ramos, L. S. Lobo and J. M. Bordado, *Macromol. Symp.*, 1998, **127**, 43-50.
13. M. Paz-Pazos and C. Pugh, *J. Polym. Sci., Part A: Polym. Chem.*, 2006, **44**, 3114-3124.
14. M. T. Barros, K. T. Petrova and A. M. Ramos, *Eur. J. Org. Chem.*, 2007, 1357-1363.
15. A.-L. Li, X.-Y. Wang, H. Liang and J. Lu, *React. Funct. Polym.*, 2007, **67**, 481-488.
16. A.-L. Li, Y. Wang, H. Liang and J. Lu, *J. Polym. Sci., Part A: Polym. Chem.*, 2006, **44**, 2376-2387.
17. Y. Wang, A.-L. Li, H. Liang and J. Lu, *Eur. Polym. J.*, 2006, **42**, 2695-2702.
18. S. Sharma and A. K. Srivastava, *J. Macromol. Sci., Pure Appl. Chem.*, 2003, **A40**, 593-603.
19. S. Sharma and A. K. Srivastava, *Des. Monomers Polym.*, 2006, **9**, 503-516.

20. S. Sharma and A. K. Srivastava, *Indian J. Chem. Technol.*, 2005, **12**, 62-67.
21. S. Sharma and A. K. Srivastava, *Eur. Polym. J.*, 2004, **40**, 2235-2240.
22. S. Sharma and A. K. Srivastava, *Polym.-Plast. Technol. Eng.*, 2003, **42**, 485-502.
23. G. Mishra and A. K. Srivastava, *J. Appl. Polym. Sci.*, 2006, **102**, 4595-4600.
24. J. Maslinska-Solich, T. Kupka, M. Kluczka and A. Solich, *Macromol. Chem. Phys.*, 1994, **195**, 1843-1850.
25. S. Sharma and A. K. Srivastava, *J. Appl. Polym. Sci.*, 2004, **91**, 2343-2347.
26. S. Ren, E. Trevino and M. A. Dube, *Macromol. React. Eng.*, 2015, **9**, 339-349.
27. Y. Zhang and M. A. Dube, *Polym.-Plast. Technol. Eng.*, 2015, **54**, 499-505.
28. Y. Zhang and M. A. Dube, *Macromol. React. Eng.*, 2014, **8**, 805-812.
29. A. F. Harris, M. S. Azevedo, *1,4-Cyclohexadiene compounds used as chain transfer agents in nitrile polymerization*, US4088811A, 1978.
30. B. E. Giddins, G. E. Coffey, W. M. Giffen, H. Mazeke, *Polymerizing acrylonitrile copolymers employing terpinolene or gamma terpinene as a chain modifier,* US4081592A, 1978.
31. E. Nield, *Copolymerization of acrylonitrile and aromatic olefins*, DE2224113, 1972.
32. A. Song, H. Kern, P. Arnold, *Production of finely particulated starch-containing polymer dispersions for use as sizing agent in paper manufacturing*, WO2011039185A2, 2011.
33. F. M. S. Peng, W. O. Dalton, *Graft polymerization of styrene- and acrylonitrile-type monomers to a latex-form rubber substrate*, DE2628370A1, 1977.
34. Y. Harada, M Inagaki, K. Shimizu, N. Tajiri, *Epoxy-bearing acrylic resins for pinhole-free powder coatings with good gloss and smoothness and manufacture thereof with no dusting or odor problems*, WO9725381A1, 1997.
35. Y. C. Lee, Q. A. Trementozzi, *Rubber-modified terpolymer with improved molding characteristics*, US4223096A, 1980.
36. Y. Ikeda, C. Takamatsu, K. Matsuyama, *Diphenylmethylpentene and terpinolene polymer pregels for moldings*, EP376662A2, 1990.
37. F. Chen, *Liquid casting compositions, production processes and photochromic optical elements*, WO2010105289A1, 2010.
38. S. Fukumoto, H. Iida, *Toluene-, halogen- and formaldehyde-free pressure-sensitive adhesive compositions with good adhesion and pot life and their sheets*, US20050101720A1, 2005.
39. V. Schaedler, L. Manders, R. Ettl, T. Wirth, *Procedure for preparation of aqueous styrene-butadiene polymer dispersions suitable for paper coatings with high dry and wet surface bonding strength,* EP1191044A2, 2002.
40. BASF AG., *Radical polymerization in presence of cyclohexa-2,5-dienecarboxylates as polymerization regulators*, DE10256617A1, 2004.
41. P. Buergle, M. Munzer, P. Quis and A. Wohnhas, *Angew. Makromol. Chem.*, 1970, **11**, 27-40.

42. K. Kabs, F. Schaefer, K.-H. Jakob, B. Klossek, *Production of colorless, transparent or dyed Plexiglass blocks from residual initiator-free prepolymers by thermal polymerization*, DE10349544A1, 2005.
43. R. J. Ouellette and J. D. Rawn, *Organic Chemistry: Structure, Mechanism, and Synthesis*, Elsevier Science, 2014.
44. N. E. C. de Almeida, I. de Aguiar and D. R. Cardoso, *J. Braz. Chem. Soc.*, 2015, **26**, 2362-2368.
45. D. Passey, *New Methods of Polymer Synthesis*, Springer Netherlands, 2012.
46. M. W. F. Nielen, *Mass Spectrom. Rev.*, 1999, **18**, 309-344.
47. A. Baumgaertel, C. R. Becer, M. Gottschaldt and U. S. Schubert, *Macromol. Rapid Commun.*, 2008, **29**, 1309-1315.
48. A. T. Jackson, K. R. Jennings and J. H. Scrivens, *J. Am. Soc. Mass Spectrom.*, 1997, **8**, 76-85.
49. J. H. Scrivens, A. T. Jackson, H. T. Yates, M. R. Green, G. Critchley, J. Brown, R. H. Bateman, M. T. Bowers and J. Gidden, *Int. J. Mass Spectrom. Ion Processes*, 1997, **165/166**, 363-375.
50. S. M. Aschmann, J. Arey and R. Atkinson, *Atmospheric Environment*, 2011, **45**, 4408-4411.
51. M. Asikainen, O. Jauhiainen, O. Aaltonen and A. Harlin, *Green Chemistry*, 2013, **15**, 3230-3235.
52. M. C. Foti and K. U. Ingold, *Journal of Agricultural and Food Chemistry*, 2003, **51**, 2758-2765.
53. M. C. Foti, S. Sortino and K. U. Ingold, *Chemistry – A European Journal*, 2005, **11**, 1942-1948.
54. A. Rudin, *The elements of polymer science and engineering : an introductory text and reference for engineers and chemists*, Academic Press, 1999.
55. P. J. Flory, *Principles of Polymer Chemistry*, Cornell University Press, 1953.
56. R. Schwalm, *UV coatings basics, recent developments and new applications*, Elsevier, 2007.
57. K. Matyjaszewski and A. H. E. Müller, *Controlled and Living Polymerizations: From Mechanisms to Applications*, Wiley, 2009.
58. D. E. Lonsdale, G. Johnston-Hall, A. Fawcett, C. A. Bell, C. N. Urbani, M. R. Whittaker and M. J. Monteiro, *J. Polym. Sci., Part A: Polym. Chem.*, 2007, **45**, 3620-3625.
59. G. F. Meijs, E. Rizzardo and T. P. T. Le, *Polym. Int.*, 1991, **26**, 239-244.
60. J. Rieumont and N. Davidenko, *Acta Polym.*, 1986, **37**, 297-299.
61. R. D. Parnell and K. E. Russell, *J. Polym. Sci., Polym. Chem. Ed.*, 1974, **12**, 347-356.
62. Evaluations of the Joint FAO/WHO Expert Committee on Food Additives, Terpinolene, http://apps.who.int/food-additives-contaminants-jecfa-database/chemical.aspx?chemID=5384, (accessed 18th of July, 2016).
63. Evaluations of the Joint FAO/WHO Expert Committee on Food Additives, p-mentha-1,4-diene, http://apps.who.int/food-additives-contaminants-jecfa-database/chemical.aspx?chemID=3563, (accessed 18th of July, 2016).

Chapter 3: Synthesis of terpene-based (meth)acrylate monomers.

3.1 Introduction

As discussed in Chapter 1, there have been significant efforts to synthesise polymers directly from natural terpenes.[1-3] However, besides a few successes, homopolymerisation of terpenes generally leads to polymers with low molecular weights and/or poor yields.[4, 5] An alternative to polymerising natural terpenes is utilising their functionalisation by combining with readily polymerisable groups to create new monomers. This strategy has been applied in the past to the synthesis of lactones from carvone and menthol,[6] and epoxides from limonene,[7] which then were polymerised to form polyesters and polycarbonates respectively. However, the range of terpene-based polymers available is still very limited. In this chapter, synthetic routes to prepare readily polymerisable (meth)acrylate monomers from the four most abundant terpenes were explored. In order to insert the (meth)acrylate functionality into terpenes two different synthetic routes were investigated: a two-step synthesis consisting on hydroxylation followed by esterification; and a one-pot methodology using Pd-catalysed C-H activation procedures.

3.1.1 Hydration of alkenes.

There are several routes to synthesise alcohols from alkenes: acid catalysed hydration of alkenes, oxymercuration-demercuration and hydroboration-oxidation are the most common and efficient routes. These three routes are described and compared below. The advantages that the hydroboration-oxidation protocol offers over the other two are the reason why this was the protocol chosen to synthesise terpene alcohols in this PhD thesis.

Acid catalysed hydration of alkenes is one of the earliest and most widely studied methods to synthesise alcohols from alkenes. Such reactions proceed *via* the so-called Markovnikov pathway, where the hydrogen atom adds to the less substituted carbon (Figure 3-1). In the presence of an acid catalyst, most commonly concentrated sulfuric acid, water adds to the carbon-carbon bonds of an alkene to give an alcohol. Although this reaction had great commercial importance in the past, it has several disadvantages that caused it to be superseded by mercuration and hydroboration reactions. The main disadvantages are the use of harsh acidic conditions and the production of complex mixtures of isomers due to the lack of regioselectivity and the tendency of the carbenium to rearrange.[8]

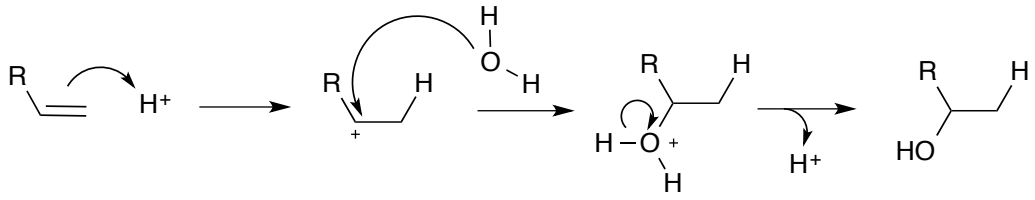


Figure 3-1. Mechanism of acid-catalysed reaction of a generic alkene. This type of hydration follows the Markovnikov rule, giving an alcohol with the hydroxyl functionality placed in the most substituted carbon.

The oxymercuration-demercuration protocol is a two-step sequence that leads to Markovnikov alcohols in a stereospecific fashion (Figure 3-2). In the first step, a mercuric cation, normally $Hg(OAc)^+$ formed by dissociation of $Hg(OAc)_2$, adds to the alkene forming a mercuronium ion. Subsequent hydration leads to a hydroxyalkylmercury species that is then demercurated by a reductive work up in the second step. Although oxymercuration-demercuration has the advantage of leading to products with high selectivity and the possibility of using very mild conditions, the mercury salts used are extremely toxic.[9]

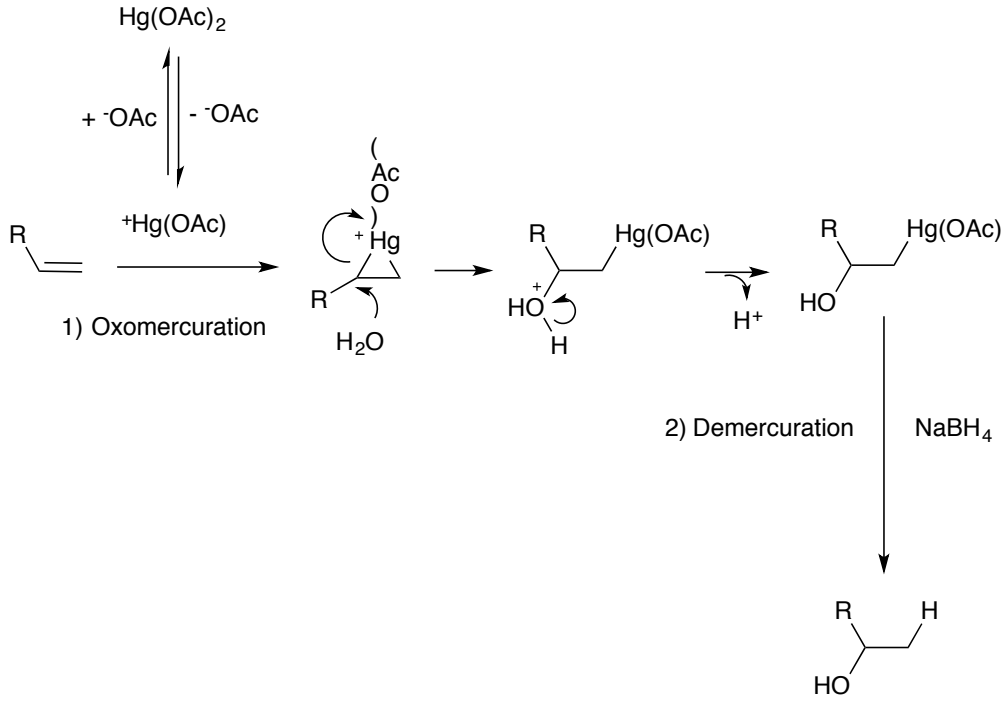


Figure 3-2. Mechanism of oxymercuration/demercuriation.

The acid and metal-catalysed hydration of alkenes is complemented by addition of boranes and their derivatives, the so-called hydroboration-oxidation protocol (Figure 3-3). The addition of diborane to an alkene proceeds through a concerted transition state, leading to *syn* addition of boron and hydrogen on the same side of the alkene, and producing a monoalkyl borane. The boron atom attaches to the less substituted carbon and therefore this is an *anti*-Markovnikov reaction. In the second step of the reaction, the alkyl borane is made to react with hydrogen peroxide (H_2O_2) and sodium hydroxide (NaOH). When the alkyl borane reacts with H_2O_2, it undergoes an oxidative rearrangement that leads to the corresponding alkyl borate. Subsequent nucleophilic attack from the hydroxide to the boron displaces the alkoxide.

Other than borane, a wide variety of alkyl borates are available for use in hydroboration reactions. An increase in the steric hindrance because of the alkyl groups present in the alkyl borate generally leads to an increase in the corresponding regioselectivity of the reaction.

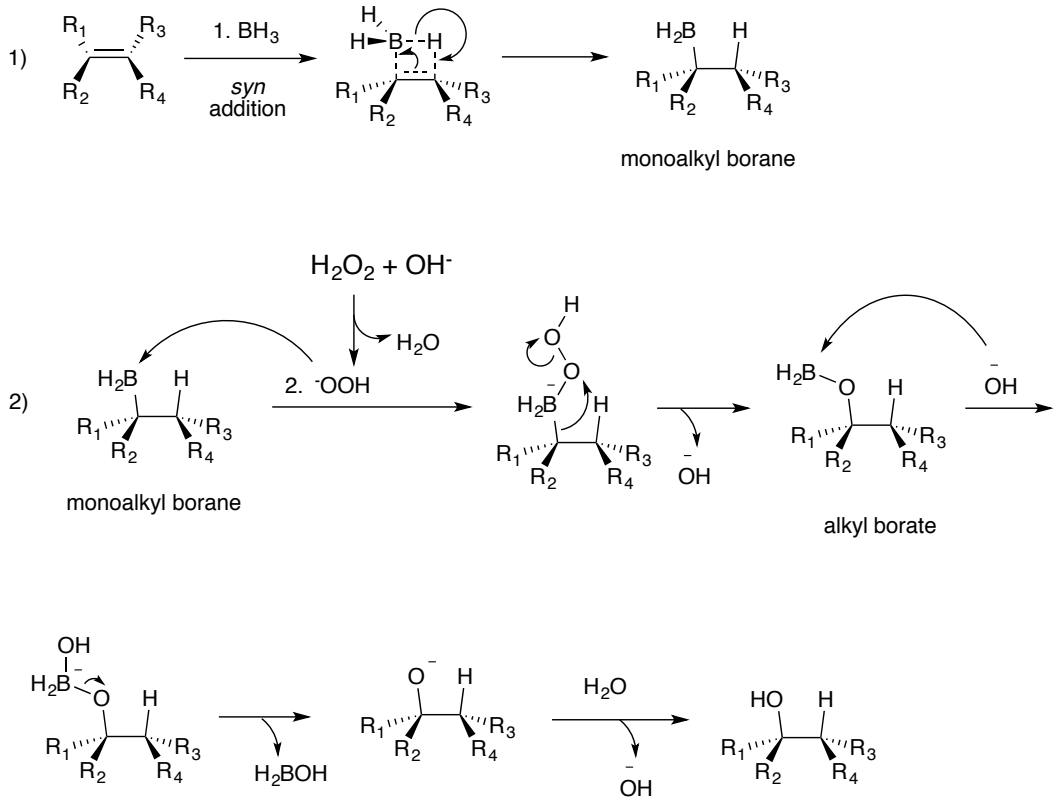


Figure 3-3. General mechanism of hydroboration/oxidation reaction.

The yields of this reaction are generally good and it is one of the most widely used techniques in organic synthesis. When compared with acid catalysed hydration and oxymercuration-demercuration, hydroboration-oxidation has the advantage of being regioselective and stereoselective, while the reagents used are safer and more sustainable than the very toxic mercury salts.[8-10]

3.1.2 C-H activation *via* Pd(II) catalysis

Carbon-hydrogen (C-H) bond activation is a metal-catalysed reaction in which a C-H bond is cleaved and the hydrogen is replaced by a different atom, normally carbon, oxygen or nitrogen. C-H activation is a very useful tool in organic synthesis that allows for the incorporation of a range of functional groups into a variety of substrates. Although C–H bonds possess high kinetic barriers to reactivity, those in allylic positions are more labile and therefore they can be activated more easily. Consequently, a special interest in the functionalisation of allylic C–H bonds has arisen in the past years. Various transition metals such as

palladium (Pd), rhodium (Rh), iridium (Ir) and ruthenium (Ru) are able to promote C-H activation. Among these, Pd is one of the most attractive ones for several reasons: higher abundance; versatility, it is able to install many different types of bonds, including carbon-oxygen, carbon-halogen, carbon- nitrogen, carbon-sulfur, and carbon-carbon linkages; and the fact that most Pd-catalysed C-H activation reactions can be conducted in the presence of ambient air and moisture, which makes it specially practical for applications in organic synthesis.[11-14]

One of the transformations that has attracted most attention is acetoxylation catalysed by palladium acetate ($Pd(OAc)_2$). Allylic acetates have always gathered interest since they are very useful intermediates in organic synthesis, with $Pd(OAc)_2$ being a popular catalyst because of a broad tolerance of substrate and reliable reactivity patterns.[15, 16]

$Pd(OAc)_2$ catalysed allylic acetoxylation was first conducted by Rappoport *et al.* in 1966 (Figure 3-4).[17]

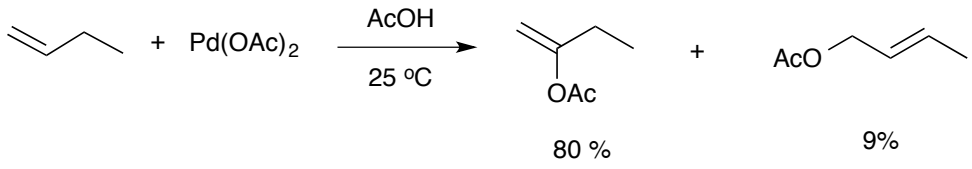


Figure 3-4. Palladium catalysed allylic oxidation was first conducted by Rappoport in 1966 when making to react equimolar amounts of olefin and palladium acetate.

Rappoport conditions consisted of mixing $Pd(OAc)_2$ with 1-butene in stoichiometric quantities, using acetic acetate as reagent and solvent. The outcome of the reaction was the corresponding vinylic acetate as the major product with a small amount of linear allylic acetate. Since then, extensive studies have been conducted to investigate the allylic functionalisation of olefins under a range of different conditions.[15, 16, 18-24]

The $Pd(OAc)_2$-catalysed acetoxylation mechanism is thought to occur through a π-allyl intermediate generated through allylic C-H cleavage (Figure 3-5).[23, 25, 26] The first step of the catalytic cycle (**I**) is the cleavage of the allylic C-H bond. The acetate group abstracts the allylic proton, releasing acetic acid, while the olefin coordinates to the catalyst, forming a π-allyl complex. Next, benzoquinone coordinates to palladium (**II**), activating the π-allyl complex. Subsequently, the π-allyl complex undergoes nucleophilic attack by an acetate group (**III**), releasing the product and reducing Pd^{II} to Pd^0. Finally, Pd^0 is reoxidised to Pd^{II} by benzoquinone (**IV**) through reductive elimination, regenerating the active catalytic species and closing the catalytic cycle (Figure 3-5). Other oxidants such as O_2, Cu^{II} or Ag^I salts and iodine compounds can be used as well.[14, 27]

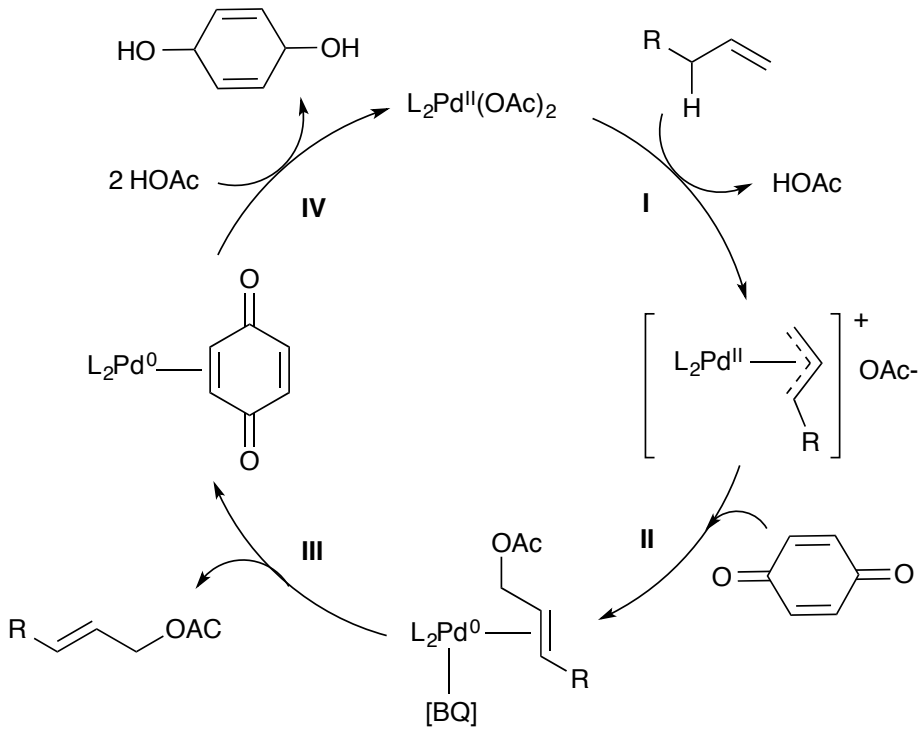


Figure 3-5. General mechanism of Pd-catalysed acetoxylation of olefins with benzoquinone as the oxidising agent.

3.1.3 Summary and research aims

Terpenes are an attractive alternative to petrol-derived monomers in polymer synthesis. However, a limited range of terpene-based polymers have been

synthesised so far. In order to create readily polymerisable monomers, the introduction of (meth)acrylate functionalities into a range of natural terpenes was investigated. Initially, a two-step methodology consisting of hydration and subsequent esterification was explored. As an alternative to the two-step protocol, allylic C-H activation catalysed by $Pd(OAc)_2$ was also investigated as a more sustainable route to introduce a (meth)acrylate functionality into β-pinene.

3.2 Experimental

3.2.1 Materials and analytical techniques

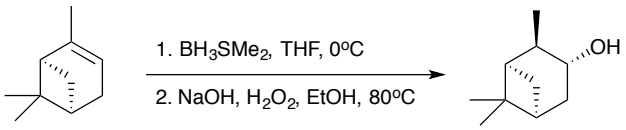
Unless otherwise stated, reagents were purchased from commercial sources and used without further purification. All reactions were carried out in flame-dried glassware under Ar atmosphere. Tetrahydrofuran (THF, 99.9 %) was purchased from Sigma Aldrich and distilled from Na/benzophenone immediately prior to use. DCM (99.5 %) was supplied by Sigma Aldrich and dried over 4Å molecular sieves prior to use. Methyl-tetrahydrofuran (MeTHF) was purchased from Aldrich over 4Å molecular sieves. Borane dimethyl sulfide ($BH_3.SMe_2$, 2M in THF), triethylamine (Et_3N, 99 %), propyl phosphonic anhydride (T3P®, 50 wt% in ethyl acetate), palladium(II) acetate ($Pd(OAc)_2$, 98 %) were provided by Sigma Aldrich. 9-Borabicyclo(3.3.1)nonane (9-BBN, 97 %, 0.5 M in THF), acryloyl chloride (96 %), methacryloyl chloride (97 %), and (1S)-(-)-β-pinene (99 %) were obtained from ALFA AESAR (VWR Intl. Ltd.). (1R)-(+)-α-pinene (99 %, 80 % ee), acrylic acid (98 %), methacrylic acid (99.5 %), R-(+)-limonene (96 %), L-(-)-carvone (99 %) and 1,4-benzoquinone (99 %) were supplied by Acros Organics (Fisher Scientific UK Ltd.) Infrared spectroscopic data were recorded using a Bruker® Tensor27 FTIR spectrometer. Mass spectral data (and HRMS) were obtained using a Bruker® MicroTOF spectrometer. Optical rotations were measured on an ADP440 Polarimeter. Melting points were measured on a Gallenkamp® apparatus. Column chromatography was carried out either manually on silica gel Fluka 60 or on a Biotage® SP4 using Biotage® SNAP KP-Sil cartridges and petroleum ether (40-60°C)/ethyl acetate as eluent, whilst monitoring by UV (254 nm) and thin layer chromatography (PMA stain).

3.2.2 Nuclear magnetic resonance (NMR).

All NMR spectra were obtained in $CDCl_3$ at room temperature using Bruker® DPX300, Bruker® AV400 spectrometers for which chemical shifts are expressed in ppm relative to the solvent and coupling constants are expressed in Hz.

3.2.3 Synthesis of hydroxylated terpene derivatives

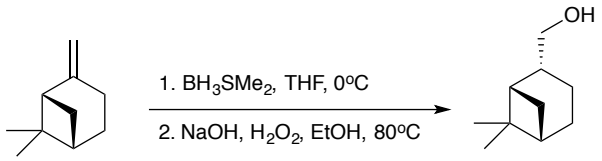
(1*R*,2*R*,3*R*,5*S*)-2,6,6-Trimethylbicyclo[3.1.1]heptan-3-ol (1a)



1a

To a cold solution (0ºC) of α-pinene (24 mL, 148 mmol) in THF (56 mL), $BH_3.SMe_2$ (74 mL, 148 mmol, 2M in THF) was added dropwise and the mixture was stirred at 0ºC for 1 hour. After that time, keeping the solution at 0ºC, EtOH (72 mL), NaOH (80 mL, 1M in H_2O) and H_2O_2 (36 mL, 30% v/v in H_2O) were added subsequently in a drop wise manner. The resulting mixture was stirred for 1 hour warming to room temperature and additionally 2 h at 80ºC. The reaction was then allowed to cool before quenching by addition of a saturated aqueous solution of NH_4Cl. Aqueous layer was extracted with Et_2O (3x). Combined organic layers were washed with brine, dried and solvent was evaporated to yield 21.1 g (84 % yield) of (1*R*,2*R*,3*R*,5*S*)-2,6,6-trimethylbicyclo[3.1.1]heptan-3-ol as a colourless oil that becomes solid after storing at low temperature. Stereochemical assignment based on literature precedent.[28]

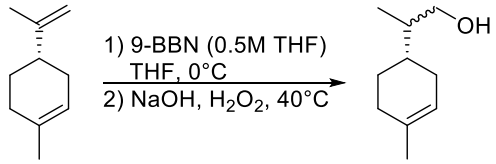
((1*S*,2*R*,5*S*)-6,6-Dimethylbicyclo[3.1.1]heptan-2-yl)methanol (2a)



2a

The synthetic protocol is analogous to that of **1a**. For 24 mL of 1S-(-)-β-pinene (148 mmol), 23.5 g (99 % yield) of ((1*R*,2*S*,5*R*)-6,6-dimethylbicyclo[3.1.1]heptan-2-yl)methanol **1b** were obtained. The product had the appearance of a colourless oil that becomes solid after storing at low temperature. Stereochemical assignment is based on literature precedent.[29]

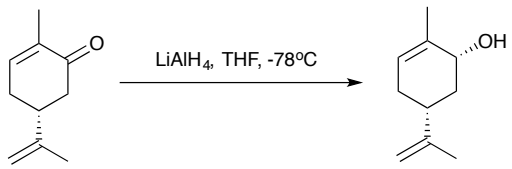
(*R*)-2-((*S*)-4-Methylcyclohex-3-en-1-yl)propan-1-ol & (*S*)-2-((*S*)-4-methylcyclohex-3-en-1-yl)propan-1-ol (3a)



3a

Freshly distilled *R*-(+)- limonene (73.4 mmol, 11.9 mL) was dissolved in anhydrous THF (500 mL) and the solution was cooled to 0 °C. 9-BBN (0.5 M in THF, 84 mmol, 166 mL) was added dropwise and the resulting solution was stirred for 2 h keeping the temperature at 0 °C and then for 2 h at rt. The resulting solution was then re-cooled to 0 °C and NaOH (3 M aq., 120 mL) and H_2O_2 (30 % w/w, 120 mL) were added dropwise sequentially. The solution was stirred at rt for 1 h and then heated at 40 °C for 4 h, before being allowed to cool to rt, the excess of peroxides was quenched with sat. aq. $Na_2S_2O_3$ and the volatiles were removed *in vacuo*. The residue was extracted with EtOAc (3 × 330 mL) and the combined organics were washed with 1 M HCl (aq., 330 mL) and brine (330 mL). The organic layer was dried over $MgSO_4$ and the solvent was removed *in vacuo*. The residue was purified on silica gel chromatography (PE/EtOAc 5 %) to obtain the title compounds as a colourless oil (mixture of 2 diastereoisomers 1:1, (7.9 g, 80% yield).[30]

(1*R*,5*R*)-2-Methyl-5-(prop-1-en-2-yl)cyclohex-2-enol (4a)



4a

To a cold solution (-78ºC) of carvone (13.0 mL, 83.3 mmol) in THF (250 mL), $LiAlH_4$ (100 mL, 100 mmol, 1M in THF) was added dropwise and the mixture was stirred for 3 h as it warmed to room temperature. The reaction was quenched by slowly addition of water (25 mL), aqueous solution of NaOH (50 mL, 1M in H_2O) and water (75 mL). The aqueous layer was extracted with Et_2O (3x). Combined organic layers were washed with brine, dried and solvent was evaporated to yield 12.6 g (99 % yield) of (1*R*,5*S*)-2-methyl-5-(prop-1-en-2-yl)cyclohex-2-enol as a colourless oil that becomes solid after storing at low temperature. Stereochemical assignment based on literature precedent.[31]

3.2.4 Synthesis of acrylate derivatives *via* esterification

Esterification with acryloyl chloride

To a cold solution (0ºC) of terpene alcohol (64.8 mmol) in DCM (500 mL) was added subsequently Et_3N (20 mL, 123 mmol) and acryloyl chloride (9.5 mL, 97.2 mmol) and the mixture was stirred during 24 h warming to room temperature. The reaction was quenched by addition of a saturated aqueous solution of $NaHCO_3$ (1x200 mL). The aqueous phase was extracted with DCM (3x200 mL). Combined organic layers were washed with brine (1x200 mL), dried with $MgSO_4$ and solvent was evaporated in *vacuo*. The resulting residue was purified by chromatography on a Biotage SP4 eluting with 0-5 % petroleum ether/ethyl acetate over 10 column volumes.

Esterification with acrylic acid

To a solution of terpene alcohol (6.48 mmol) in MeTHF (40 mL) was added acrylic acid (0.5 mL, 7.13 mmol), Et_3N (2.7 mL, 19.4 mmol) and T3P (4.95 g, 7.78 mmol) (50 wt% in ethyl acetate). The mixture was stirred for 48 h at room

temperature. The reaction was monitored by TLC. After completion of the reaction, water was added (30 mL) and the aqueous phase extracted with diethyl ether (3x20 mL). Combined organic layers were washed with 1M HCl aq. (1x20 mL), saturated aqueous solution of $NaHCO_3$ (1x20 mL) and brine (1x20 mL), dried with $MgSO_4$, and solvent was evaporated in *vacuo*. The resulting residue was purified by chromatography on a Biotage SP4 eluting with 0-5 % petroleum ether/ethyl acetate over 10 column volumes.

3.2.5 Synthesis of methacrylate derivatives *via* esterification

Esterification with methacryloyl chloride

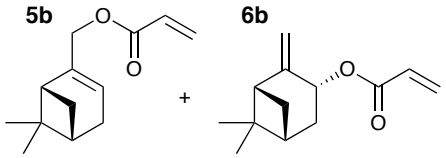
To a cold solution (0°C) of terpene alcohol (64.8 mmol) in DCM (500 mL) was added subsequently Et_3N (20 mL, 123 mmol) and methacryloyl chloride (9.5 mL, 97.2 mmol) and the mixture was stirred during 24 h warming to room temperature. After the reaction was complete the reaction was quenched by addition of saturated aqueous solution of $NaHCO_3$ (1x200 mL). The aqueous phase was extracted with DCM (3x200 mL). Combined organic layers were washed with brine (1x200 mL), dried with $MgSO_4$ and solvent was evaporated. The resulting residue was purified by chromatography on a Biotage SP4 eluting with 0-5 % petroleum ether/ethyl acetate over 10 column volumes.

Esterification with methacrylic acid

To a solution of terpene alcohol (6.48 mmol) in MeTHF (40 mL) was added methacrylic acid (0.6 mL, 7.13 mmol), Et_3N (2.7 mL, 19.4 mmol) and T3P (4.95 g, 7.78 mmol) (50 wt% in ethyl acetate). The mixture was stirred for 48 h at room temperature. The reaction was monitored by TLC. After completion of the reaction, water (30 mL) was added and the aqueous phase extracted with diethyl ether (3x20 mL). Combined organic layers were washed with 1M HCl aq. (1x20 mL), saturated aqueous solution of $NaHCO_3$ (1x20 mL) and brine (1x20 mL), dried with $MgSO_4$, and solvent was evaporated in *vacuo*. The resulting residue was purified by chromatography on a Biotage SP4 eluting with 0-5 % petroleum ether/ethyl acetate over 10 column volumes.

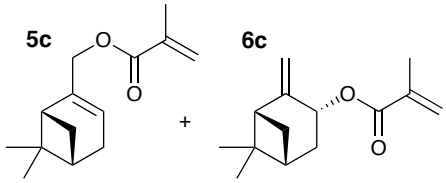
3.2.6 Catalytic synthesis of β-pinene derived (meth)acrylate monomers.

((1*R*,5*S*)-6,6-dimethylbicyclo[3.1.1]hept-2-en-2-yl)methyl acrylate (5b) and (1*R*,3*R*,5*R*)-6,6-dimethyl-2-methylenebicyclo[3.1.1]heptan-3-yl acrylate (6b)



β-Pinene (10.00 g, 11.6 mL, 73.3 mmol) was dissolved in acrylic acid (14 mL, 0.22 mol, 3 eq.). Benzoquinone (16 g, 0.15 mmol, 2 eq.) was added followed by $Pd(OAc)_2$ (400 mg, 2 mol%). The reaction mixture was stirred for 72 h at 50°C after which it was allowed to cool down before flushing through Celite. The residue was diluted with toluene (50 mL) and the solvents were removed in vacuo. The crude product was purified on silica gel chromatography using petroleum ether as solvent system to give a 1:2 mixture of ((1R,5S)-6,6-dimethylbicyclo[3.1.1]hept-2-en-2-yl)methyl acrylate (**5b**) and (1R,3R,5R)-6,6-dimethyl-2-methylenebicyclo[3.1.1]heptan-3-yl acrylate (**6b**) as a yellow oil (3.39 g, 24 % yield).

((1*R*,5*S*)-6,6-dimethylbicyclo[3.1.1]hept-2-en-2-yl)methyl methacrylate (5c) and (1*R*,3*R*,5*R*)-6,6-dimethyl-2-methylenebicyclo[3.1.1]heptan-3-yl methacrylate (6c)

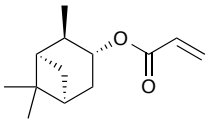


β-Pinene (2.00 g, 2.32 mL, 14.8 mmol) was dissolved in methacrylic acid (10mL, 0.11 mol, 8 eq.). Benzoquinone (3.20 g, 29.6 mmol, 2 eq.) was added followed by $Pd(OAc)_2$ (80.0mg, 2 mol%). The reaction mixture was stirred for 72 h at 50°C after which it was allowed to cool down before flushing through Celite. The residue was diluted with toluene (10 mL) and the solvents were removed in vacuo. The crude product was purified on silica gel chromatography using

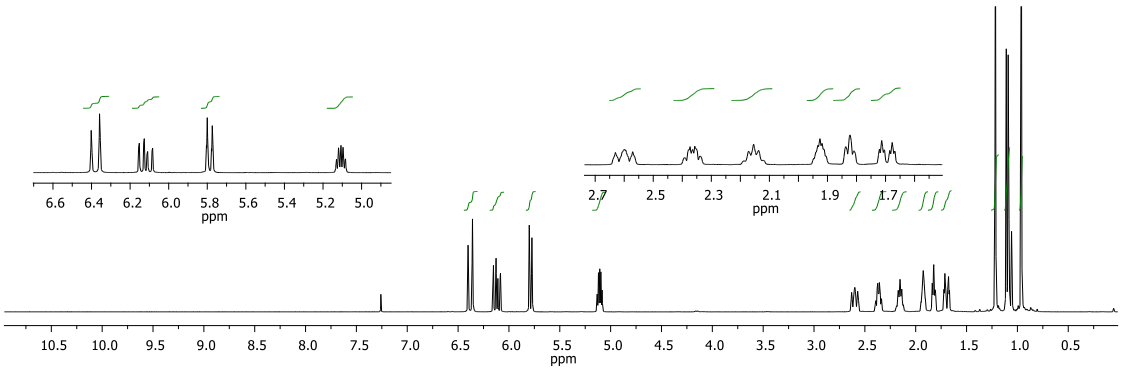
petroleum ether as solvent system to give 1:10 mixture of ((1R,5S)-6,6-dimethylbicyclo[3.1.1]hept-2-en-2-yl)methyl methacrylate (**5c**) and (1*R*,3*R*,5*R*)-6,6-dimethyl-2-methylenebicyclo[3.1.1]heptan-3-yl acrylate (**6c**) as a yellow oil (2.67g, 82% yield).

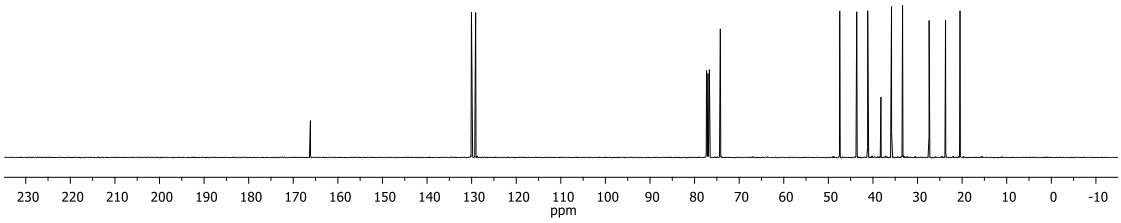
3.2.7 Monomer characterisation

(1*R*,2*R*,3*R*,5*S*)-2,6,6-Trimethylbicyclo[3.1.1]heptan-3-yl acrylate (1b)

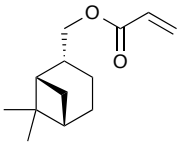


$[\alpha]_D^{21}$ -36 (c 2.2, $CHCl_3$). **^{1}H-NMR (400 MHz, $CDCl_3$):** δ = 6.38 (dt, *J* = 17.3, 1.4 Hz, 1H), 6.12 (ddd, *J* = 17.3, 10.4, 1.3 Hz, 1H), 5.79 (dt, *J* = 10.4, 1.5 Hz, 1H), 5.11 (dt, *J* = 9.4, 4.6 Hz, 1H), 2.6-2.5 (m, 1H), 2.4-2.3 (m, 1H), 2.2-2.1 (m, 1H), 2.0-1.9 (m, 1H), 1.82 (t, *J* = 5.8 Hz, 1H), 1.69 (dt, *J* = 14.4, 3.4 Hz, 1H), 1.22 (s, 3H), 1.10 (dd, *J* = 7.4, 1.1 Hz, 3H), 1.07 (d, *J* = 9.9 Hz, 1H), 0.96 (s, 3H), . **^{13}C-NMR (100 MHz, $CDCl_3$):** δ = 166.2 (s), 130.0 (t), 129.1 (d), 74.2 (d), 47.4 (d), 43.6 (d), 41.2 (d), 38.2 (s), 35.8 (t), 33.4 (t), 27.4 (q), 23.7 (q), 20.5 (q). **IR** ν(cm^{-1}): 3016, 2927, 1731, 1636, 1602, 1439, 1242. **HRMS (ESI-MS)**: calcd. for $C_{13}H_{20}NaO_2$: 231.1356, found: 231.1350.

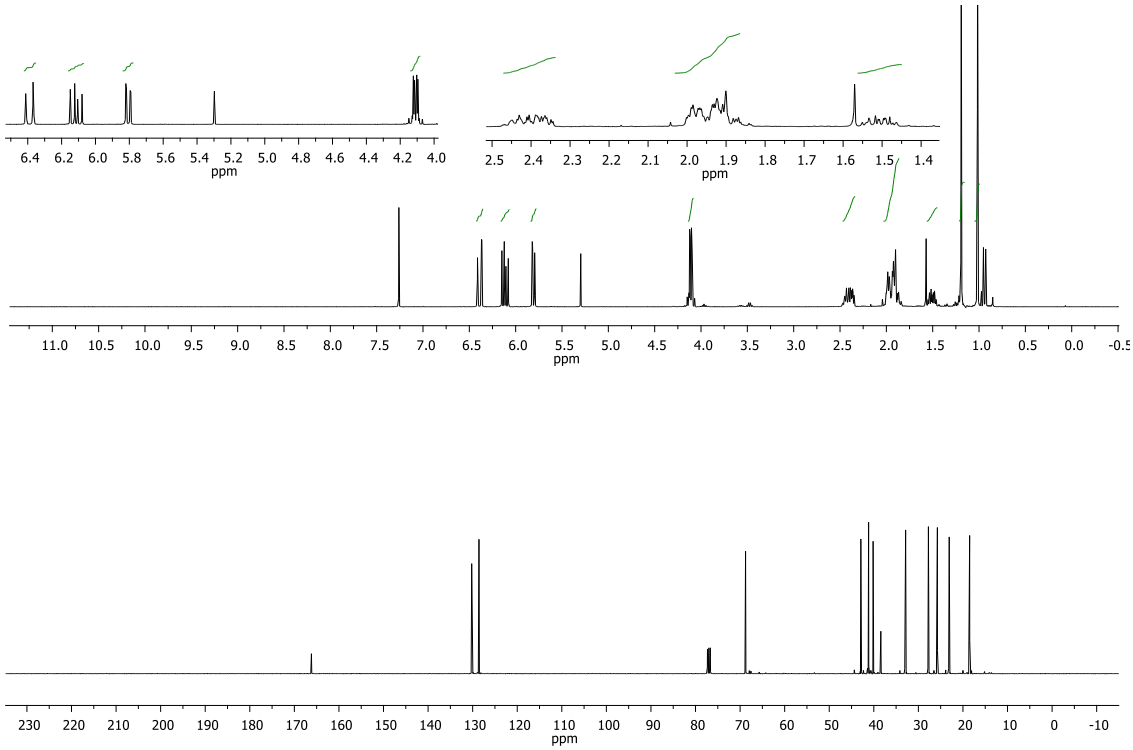




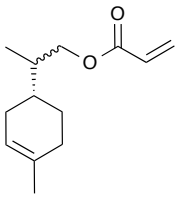
((1*S*,2*R*,5*S*)-6,6-Dimethylbicyclo[3.1.1]heptan-2-yl)methyl acrylate (2b)



$[\alpha]_D^{22}$ -10 (c 13.9, $CHCl_3$). **^{1}H-NMR (400 MHz, $CDCl_3$):** δ = 6.39 (dd, *J* = 17.3, 1.5 Hz, 1H), 6.11 (dd, *J* = 17.3, 10.4 Hz, 1H), 5.81 (dd, *J* = 10.4, 1.5 Hz, 1H), 4.11 (dd, *J* = 7.9, 2.8 Hz, 2H), 2.4-2.3 (m, 2H), 2.0-1.8 (m, 5H), 1.6-1.5 (m, 1H), 1.19 (s, 3H), 1.02 (s, 3H), 0.94 (d, *J* = 9.6 Hz, 1H). **^{13}C-NMR (100 MHz, $CDCl_3$):** δ = 166.2 (s), 130.2 (t), 128.6 (d), 68.8 (t), 42.9 (d), 41.2 (d), 40.2 (d), 38.4 (s), 32.9 (t), 27.8 (q), 25.7 (t), 23.1 (q), 18.5 (t). **IR** ν(cm^{-1}): 3011, 2923, 1717, 1636, 1619, 1470, 1409, 1385, 1367, 1396, 1192, 1059, 985. **HRMS (ESI-MS)**: calcd. for $C_{13}H_{20}NaO_2$: 231.1356, found: 231.1345.

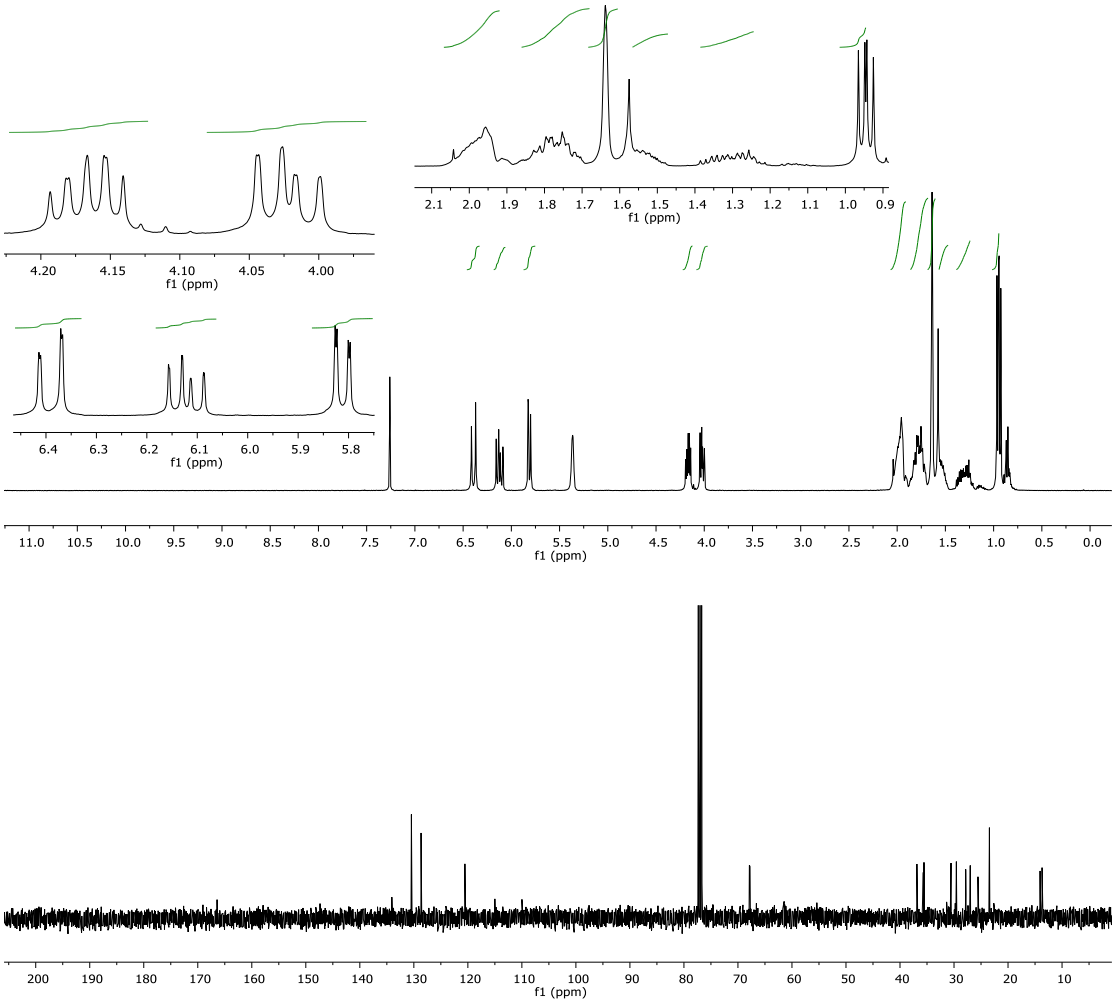


(*R*)-2-((*S*)-4-Methylcyclohex-3-enyl)propyl acrylate & (*S*)-2-((*S*)-4-Methylcyclohex-3-enyl)propyl acrylate (3b)

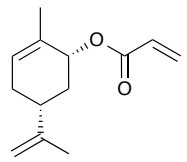


$[\alpha]_D^{22}$ -44 (c 4.9, $CHCl_3$). **^{1}H-NMR (400 MHz, $CDCl_3$):** δ = 6.39 (dd, *J* = 17.4, 1.5 Hz, 1H), 6.12 (ddd, *J* = 17.4, 10.4, 1.0 Hz, 1H), 5.81 (dd, *J* = 10.4, 1.5 Hz, 1H), 5.39 – 5.34 (bs, 1H), 4.17 (ddd, *J* = 10.9, 5.6, 4.5 Hz, 1H), 4.02 (ddd, *J* = 10.9, 6.9, 0.9 Hz, 1H), 2.06 – 1.92 (m, 3H), 1.87 – 1.69 (m, 2H), 1.68 – 1.62 (bs, 3H), 1.55 – 1.47 (m, 1H), 1.41 – 1.23 (m, 1H), 0.96 (d, *J* = 6.9 Hz, 1H). For the other diastereoisomer, the following peaks are discernible, the others overlap with the major product. **^{1}H-NMR (400 MHz, $CDCl_3$):** δ = 0.93 (d, *J* = 7.0 Hz, 1H). **^{13}C-NMR (100 MHz, $CDCl_3$):** δ = ^{13}C NMR (100 MHz, $CDCl_3$) δ 166.42 (2 × C), 134.07 (2 × C), 130.45 (CH_2), 128.66 (CH_2), 120.55 (CH), 120.48 (CH),

115.00 (CH), 109.98 (CH), 67.89 (CH_2), 67.77 (CH_2), 36.87 (CH), 36.80 (CH), 35.69 (CH), 35.56 (CH), 30.64 (CH_2), 30.55 (CH_2), 29.56 (CH_2), 27.83 (CH_2), 27.00 (CH_2), 25.57 (CH_2), 23.45 (2 × CH_3), 14.07 (CH_3), 13.70 (CH_3). **IR** ν(cm^{-1}): 3011, 2973, 2922, 1714, 1637, 1618, 1453, 1437, 1407, 1295, 1276, 1192, 1048, 985, 970. **HRMS (ESI-MS)**: calcd. for $C_{13}H_{18}NaO_2$: 229.1199, found: 229.1196.

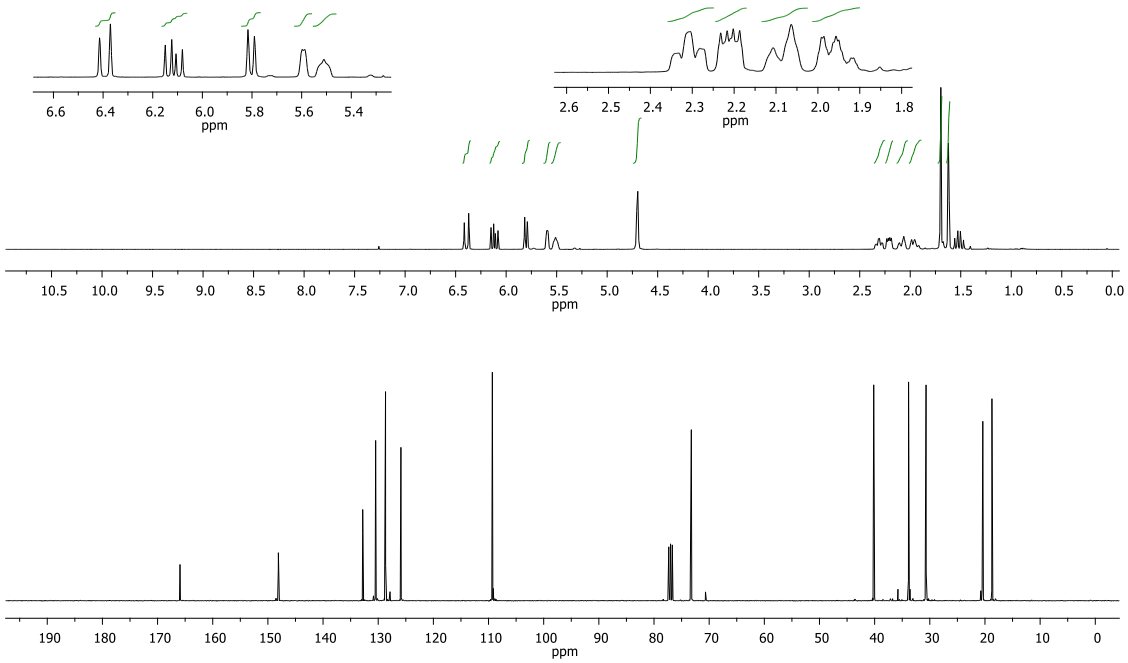


(1*R*,5*R*)-2-Methyl-5-(prop-1-en-2-yl)cyclohex-2-enyl acrylate (4b)

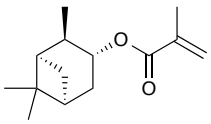


$[\alpha]_D^{22}$ -44 (c 4.9, $CHCl_3$). **^{1}H-NMR (400 MHz, $CDCl_3$):** δ = 6.39 (d, *J* = 17.3 Hz, 1H), 6.11 (dd, *J* = 17.3, 10.4 Hz, 1H), 5.80 (d, *J* = 10.4 Hz, 1H), 5.59 (d, *J* = 4.2 Hz, 1H), 5.51 (bs, 1H), 4.70 (s, 2H), 2.4-2.3 (m, 1H), 2.3-2.2 (m, 1H), 2.1-2.0 (m,

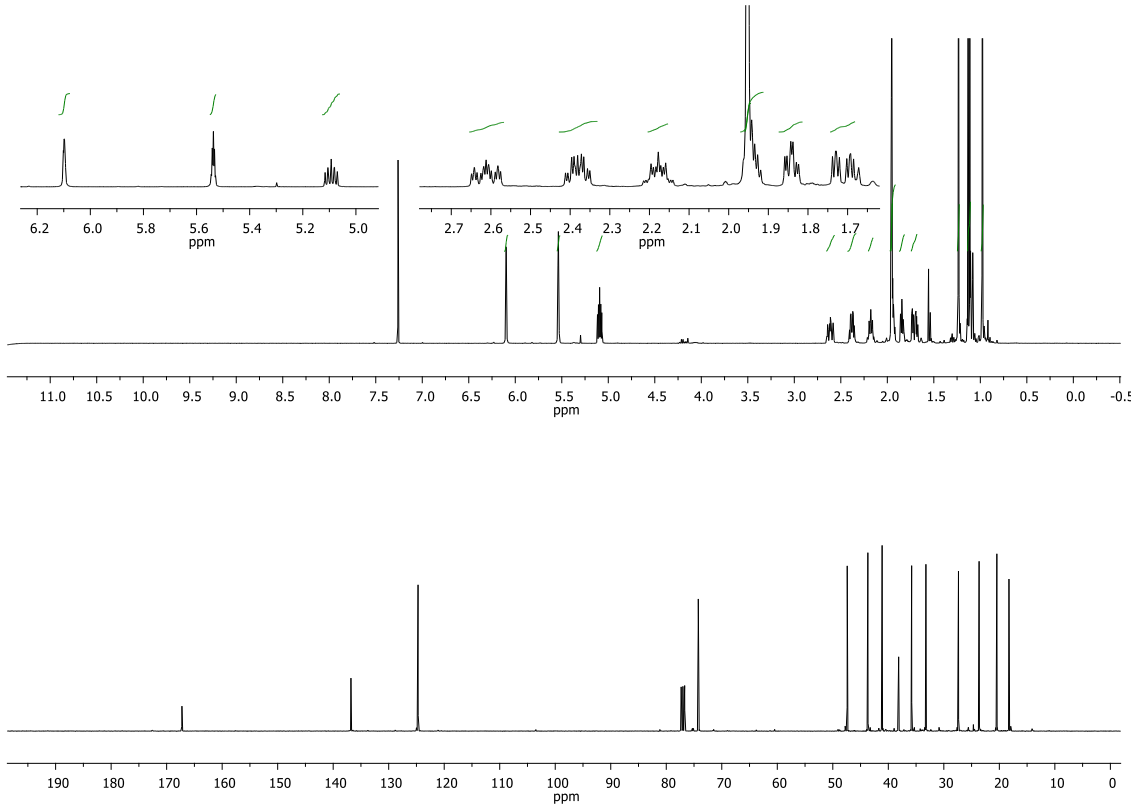
1H), 2.0-1.9 (m, 1H), 1.69 (s, 3H), 1.62 (s, 3H). **^{13}C-NMR (100 MHz, $CDCl_3$):** δ = 165.9 (s), 148.1 (s), 132.8 (s), 130.5 (t), 128.7 (d), 125.9 (d), 109.3 (t), 73.2 (d), 40.2 (d), 33.9 (t), 30.7 (t), 20.4 (q), 18.7 (q). **IR** ν(cm^{-1}): 3011, 2973, 2922, 1714, 1637, 1618, 1453, 1437, 1407, 1295, 1276, 1192, 1048, 985, 970. **HRMS (ESI-MS)**: calcd. for $C_{13}H_{18}NaO_2$: 229.1199, found: 229.1196.



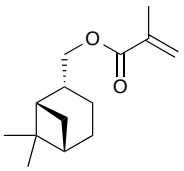
(1*R*,2*R*,3*R*,5*S*)-2,6,6-Trimethylbicyclo[3.1.1]heptan-3-yl methacrylate (1c)



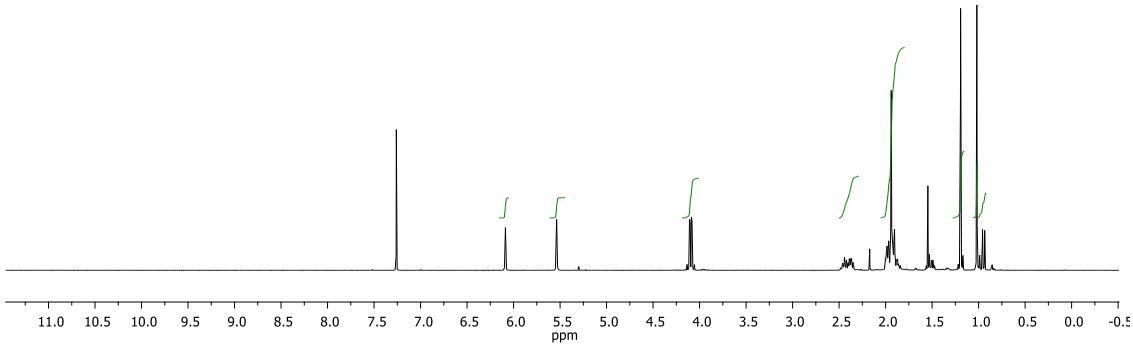
$[\alpha]_D^{22}$ -24 (c 16.8, $CHCl_3$). **^{1}H-NMR (400 MHz, $CDCl_3$):** δ = 6.10 (dd, *J* = 1.7, 0.9 Hz, 1H), 5.54 (p, *J* = 1.6 Hz, 1H), 5.09 (ddd, *J* = 9.2, 4.8, 4.2 Hz, 1H), 2.7-2.6 (m, 1H), 2.4-2.3 (m, 1H), 2.18 (qdd, *J* 7.4, 5.1, 2.3 Hz, 1H), 2.0-1.9 (m, 4H), 1.84 (td, *J* = 5.9, 2.2 Hz, 1H), 1.71 (ddd, *J* = 14.4, 3.9, 3.1 Hz, 1H), 1.23 (s, 3H), 1.12 (d, *J* = 1.1 Hz, 3H), 1.09 (d, *J* = 9.9 Hz, 1H), 0.98 (s, 3H). **^{13}C-NMR (100 MHz, $CDCl_3$):** δ = 167.3 (s), 136.8 (s), 124.7 (t), 74.2 (d), 47.4 (d), 43.7 (d), 41.1 (d), 38.1 (s), 35.8 (t), 33.2 (t), 27.4 (q), 23.7 (q), 20.5 (q), 18.3 (q). **IR** ν(cm^{-1}): 2957, 2919, 1706, 1636, 1452, 1299, 1175, 1154. **HRMS (ESI-MS)**: calcd. for $C_{14}H_{22}NaO_2$: 245.1512, found: 245.1513.

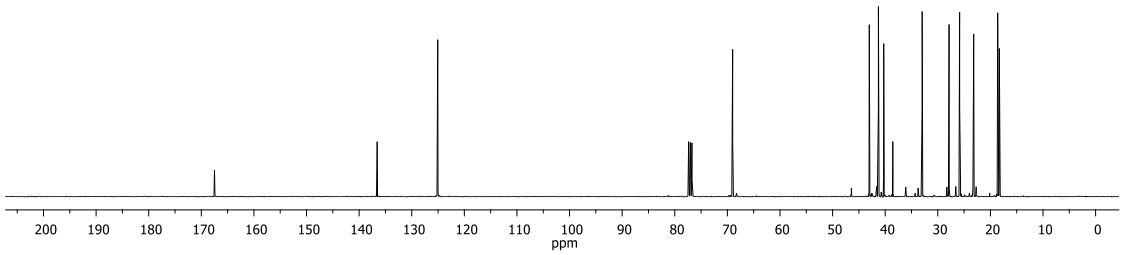


((1*S*,2*R*,5*S*)-6,6-Dimethylbicyclo[3.1.1]heptan-2-yl)methyl methacrylate (2c)

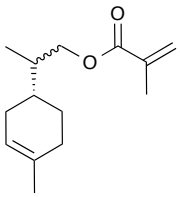


$[\alpha]_D^{22}$ -9.1 (c 3.8, $CHCl_3$). **^{1}H-NMR (400 MHz, $CDCl_3$):** δ =6.09 (dd, *J* = 1.7, 0.9 Hz, 1H), 5.54 (p, *J* = 1.6 Hz, 1H), 4.09 (dd, *J* = 8.0, 2.6 Hz, 2H), 2.5-2.4 (m, 2H), 2.0-1.8 (m, 5H), 1.94 (s, 3H), 1.19 (s, 3H), 1.02 (s, 3H), 1.0-0.9 (m, 2H). **^{13}C-NMR (100 MHz, $CDCl_3$):** δ = 167.5 (s), 136.5 (s), 125.0 (t), 69.0 (t), 43.0 (d), 41.2 (d), 40.2 (d), 38.5 (s), 32.9 (t), 27.8 (q), 25.8 (t), 23.1 (q), 18.6 (t), 18.3 (q). **IR** ν(cm^{-1}): 2988, 2945, 2921, 1708, 1637, 1470, 1453, 1326, 1299, 1175. **HRMS (ESI-MS)**: calcd. for $C_{14}H_{22}NaO_2$: 245.1512, found: 245.1510.



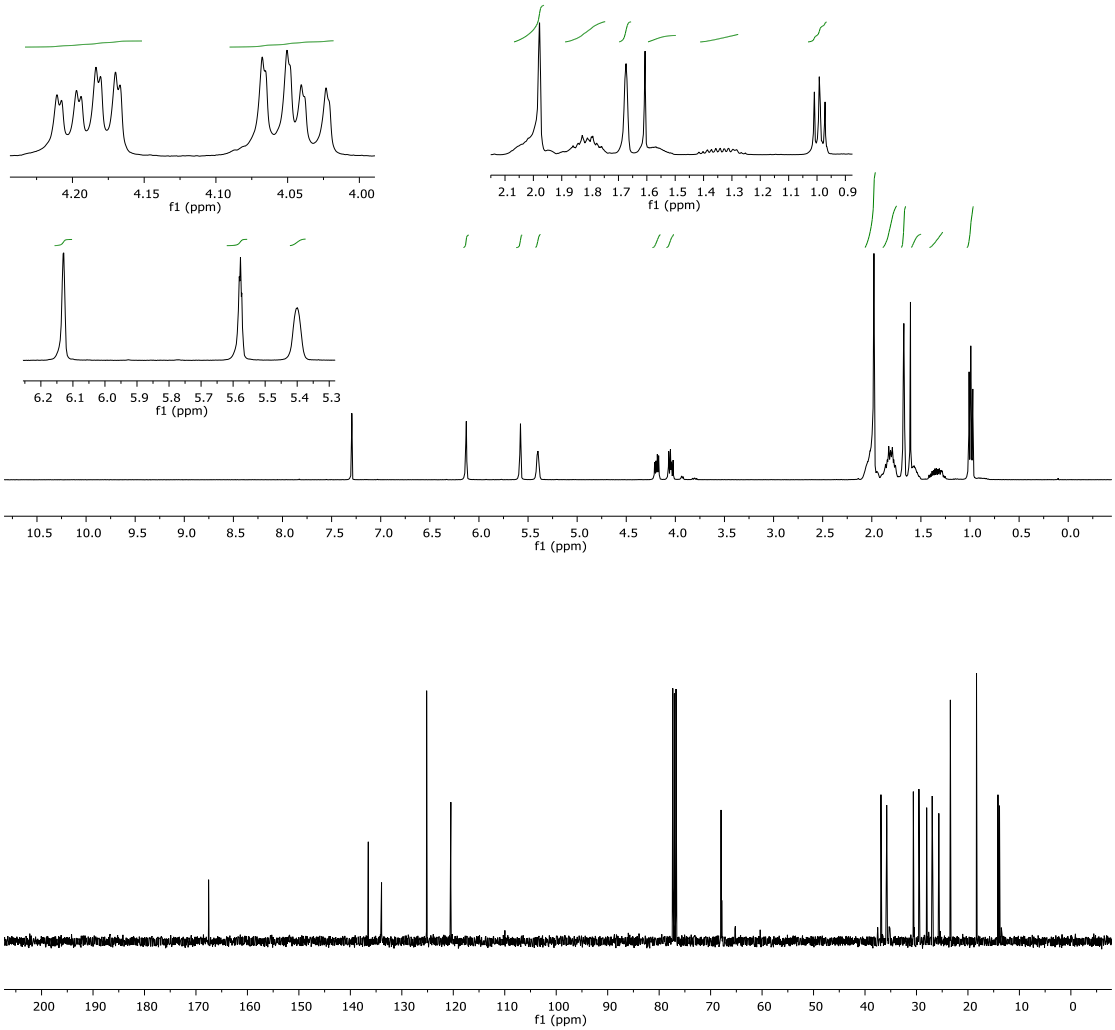


(*R*)-2-((*S*)-4-methylcyclohex-3-en-1-yl)propyl methacrylate & (*S*)-2-((*S*)-4-methylcyclohex -3-en-1-yl)propyl methacrylate (3c)

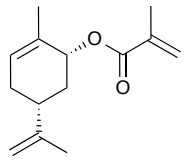


^{1}H-NMR (400 MHz, $CDCl_3$): δ 6.13 (dq, *J* = 1.8, 0.9 Hz, 1H), 5.61 – 5.54 (m, 1H), 5.42 – 5.38 (bs, 1H), 4.18 (ddd, *J* = 11.0, 5.5, 1.6 Hz, 1H), 4.06 (ddd, *J* = 11.0, 6.9, 1.1 Hz, 1H), 2.07 – 1.99 (m, 3H), 1.98 (s, 3H), 1.81 (m, 3H), 1.70 – 1.64 (m, 3H), 1.58 – 1.52 (m, 1H), 1.34 (m, 1H), 1.00 (d, *J* = 6.9 Hz, 3H). For the other diastereoisomer, the following peaks are discernible. The others overlap with the major product. **^{1}H-NMR (400 MHz, $CDCl_3$):** δ 0.98 (d, *J* = 6.9 Hz, 3H). **^{13}C-NMR (100 MHz, $CDCl_3$):** δ 167.55 (2 × C), 136.52 (2 × C), 134.05 (C), 133.99 (C), 125.21 (2 × CH_2), 120.56 (CH), 120.50 (CH), 68.01 (CH_2), 67.89 (CH_2), 36.90 (CH), 36.82 (CH), 35.79 (CH), 35.70 (CH), 30.61 (CH_2), 30.53 (CH_2), 29.53 (CH_2), 28.02 (CH_2), 26.94 (CH_2), 25.66 (CH_2), 23.42 (CH_3), 23.41 (CH_3), 18.33 (2 × CH_3), 14.17 (CH_3), 13.87 (CH_3). **IR** ν(cm^{-1}): 3008, 2965, 2917,

2857, 1711, 1637, 1452, 1438, 1404, 1378, 1325, 1299, 1243, 1178, 1012, 981, 943. **HRMS (ESI-MS)**: calcd. for $C_{14}H_{22}NaO_2$: 245.1512, found: 245.1510.

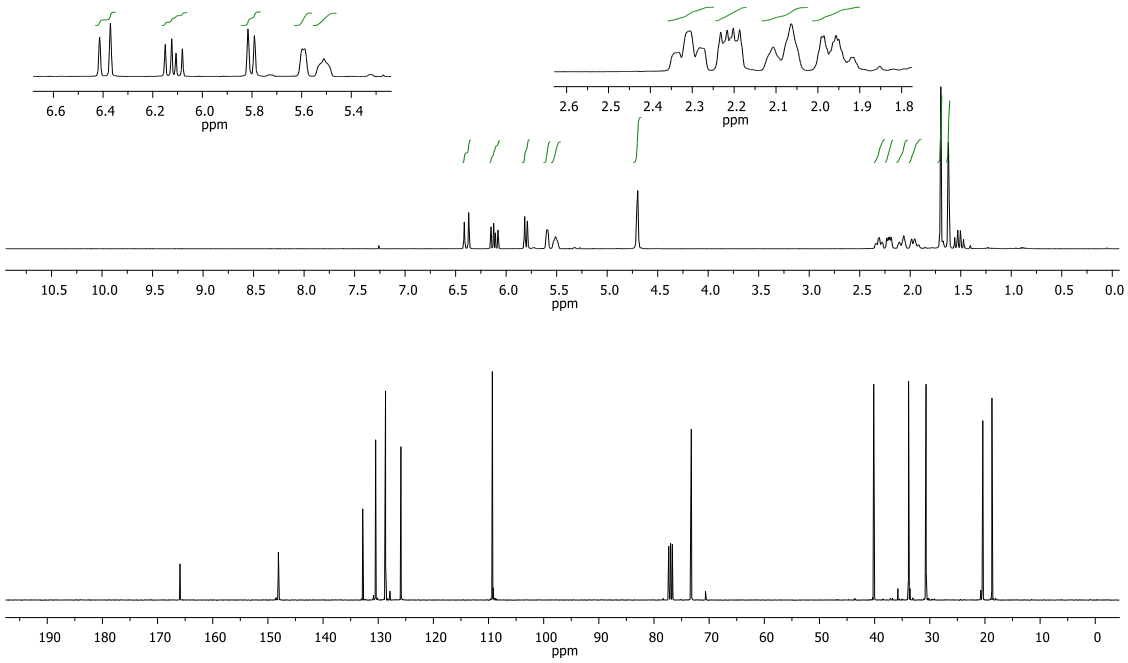


(1*R*,5*R*)-2-Methyl-5-(prop-1-en-2-yl)cyclohex-2-enyl acrylate (4c)

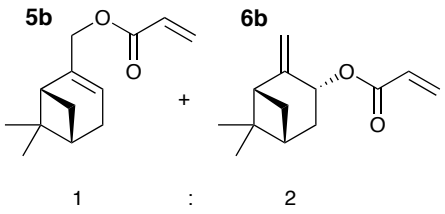


$[\alpha]_D^{22}$ -44 (c 4.9, $CHCl_3$). **^{1}H-NMR (400 MHz, $CDCl_3$):** δ = 6.39 (d, *J* = 17.3 Hz, 1H), 6.11 (dd, *J* = 17.3, 10.4 Hz, 1H), 5.80 (d, *J* = 10.4 Hz, 1H), 5.59 (d, *J* = 4.2 Hz, 1H), 5.51 (bs, 1H), 4.70 (s, 2H), 2.4-2.3 (m, 1H), 2.3-2.2 (m, 1H), 2.1-2.0 (m, 1H), 2.0-1.9 (m, 1H), 1.69 (s, 3H), 1.62 (s, 3H). **^{13}C-NMR (100 MHz, $CDCl_3$):** δ = 165.9 (s), 148.1 (s), 132.8 (s), 130.5 (t), 128.7 (d), 125.9 (d), 109.3 (t), 73.2 (d), 40.2 (d), 33.9 (t), 30.7 (t), 20.4 (q), 18.7 (q). **IR** ν(cm^{-1}): 3011, 2973, 2922, 1714,

1637, 1618, 1453, 1437, 1407, 1295, 1276, 1192, 1048, 985, 970. **HRMS (ESI-MS)**: calcd. for $C_{13}H_{18}NaO_2$: 229.1199, found: 229.1196.

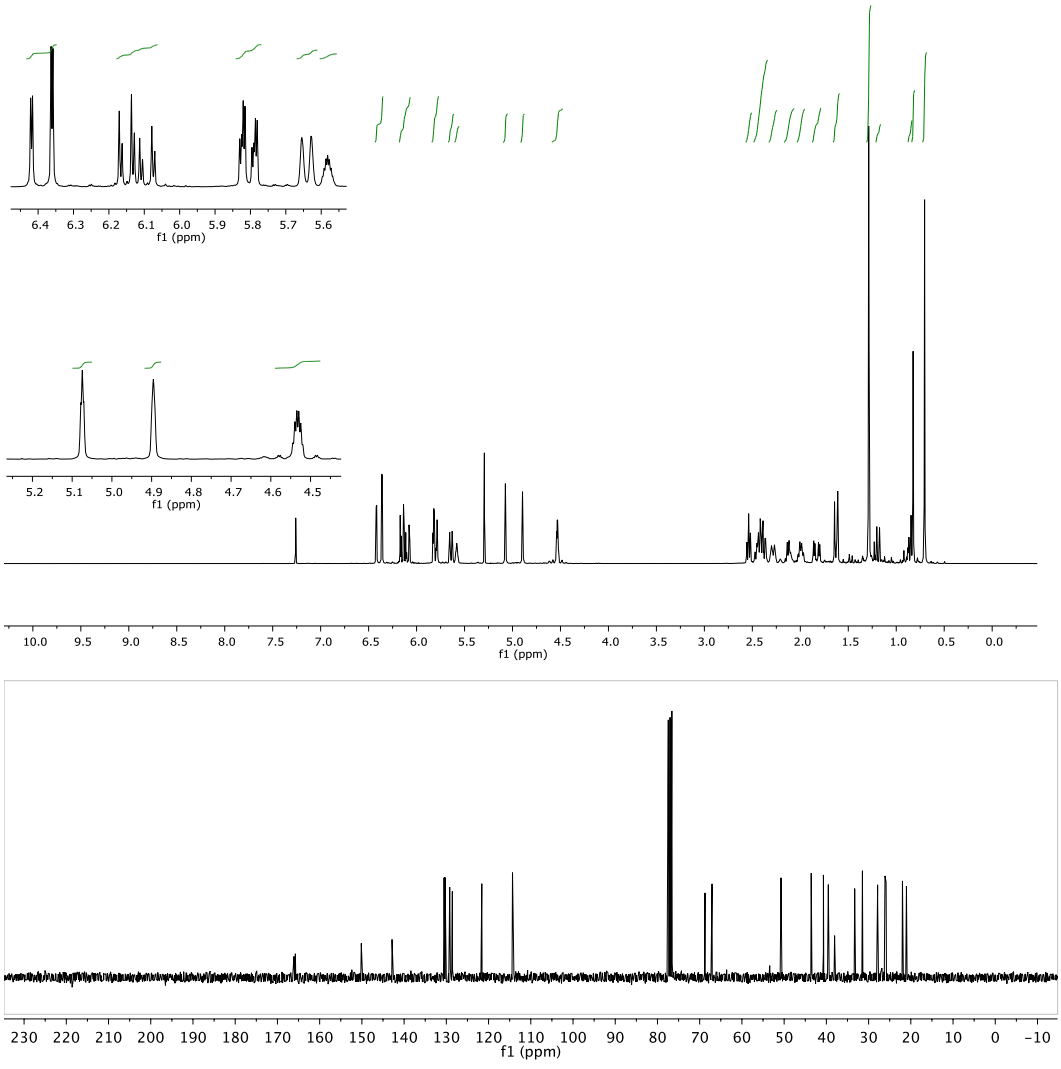


((1*R*,5*S*)-6,6-dimethylbicyclo[3.1.1]hept-2-en-2-yl)methyl acrylate (5b) and (1*R*,3*R*,5*R*)-6,6-dimethyl-2-methylenebicyclo[3.1.1]heptan-3-yl acrylate (6b)

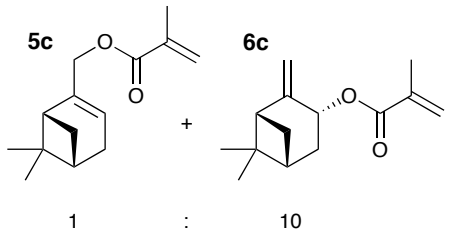


Major compound **6b: ^{1}H-NMR (400 MHz, $CDCl_3$):** δ = 6.40 (1H, dd, J 1.60, 17.33 Hz), 6.13 (1H, ddd, J 2.45, 10.36, 17.33 Hz), 5.81 (1H, ddd, J 1.60, 2.92, 10.36 Hz), 5.65 (1H, d, J 7.91 Hz), 5.08 (1H, t, J 1.13 Hz), 4.90 (1H, br. s), 2.55 (1H, t, J 5.37 Hz), 2.48-2.35 (2H, m), 2.04-1.96 (1H, m), 1.83 (1H, ddd, J 0.94, 4.24, 14.98 Hz), 1.63 (1H, d, J 9.98 Hz), 1.29 (3H, s), 0.71 (3H, s). **^{13}C-NMR (100 MHz, $CDCl_3$):** δ = (100 MHz, $CDCl_3$): 166.3 (q), 150.4 (q) , 130.8 (CH2), 128.8 (CH), 114.6 (CH2), 69.0 (CH), 51.0 (CH), 40.8 (q), 39.8 (CH), 33.5 (CH2), 28.1 (CH2), 26.1 (CH3), 22.2 (CH3).

For minor compound **5b** the following peaks are discernible. The remaining peaks overlap with major compound. **^{1}H-NMR (400 MHz, $CDCl_3$):** δ = (300 MHz, $CDCl_3$): 6.40 (1H, dd, J 1.60, 17.33 Hz), 6.13 (1H, ddd, J 2.45, 10.36, 17.33 Hz), 5.81 (1H, ddd, J 1.60, 2.92, 10.36 Hz), 5.59 (1H, ddd, J 1.41, 2.92, 4.33 Hz), 4.54 (2H, ddd, J 1.41, 2.92, 3.01 Hz), 2.48-2.35 (1H, m), 2.34-2.24 (2H, m), 2.17-2.07 (2H, m), 1.29 (3H, s), 1.20 (1H, d, J 8.67 Hz), 0.83 (3H, s). **^{13}C-NMR (100 MHz, $CDCl_3$):** δ = (100 MHz, $CDCl_3$): 166.0 (q), 143.1 (q), 130.6 (CH2), 129.5 (CH), 121.9 (CH), 67.3 (CH2), 43.8(CH), 40.9 (CH), 38.3 (q), 31.7 (CH2), 31.5 (CH2), 26.4 (CH3), 21.3 (CH3). **HRMS (ESI-MS)**: Calcd. for $C_{13}H_{18}O_2$ ($M+Na^+$): 229.1199, found: 229.1187

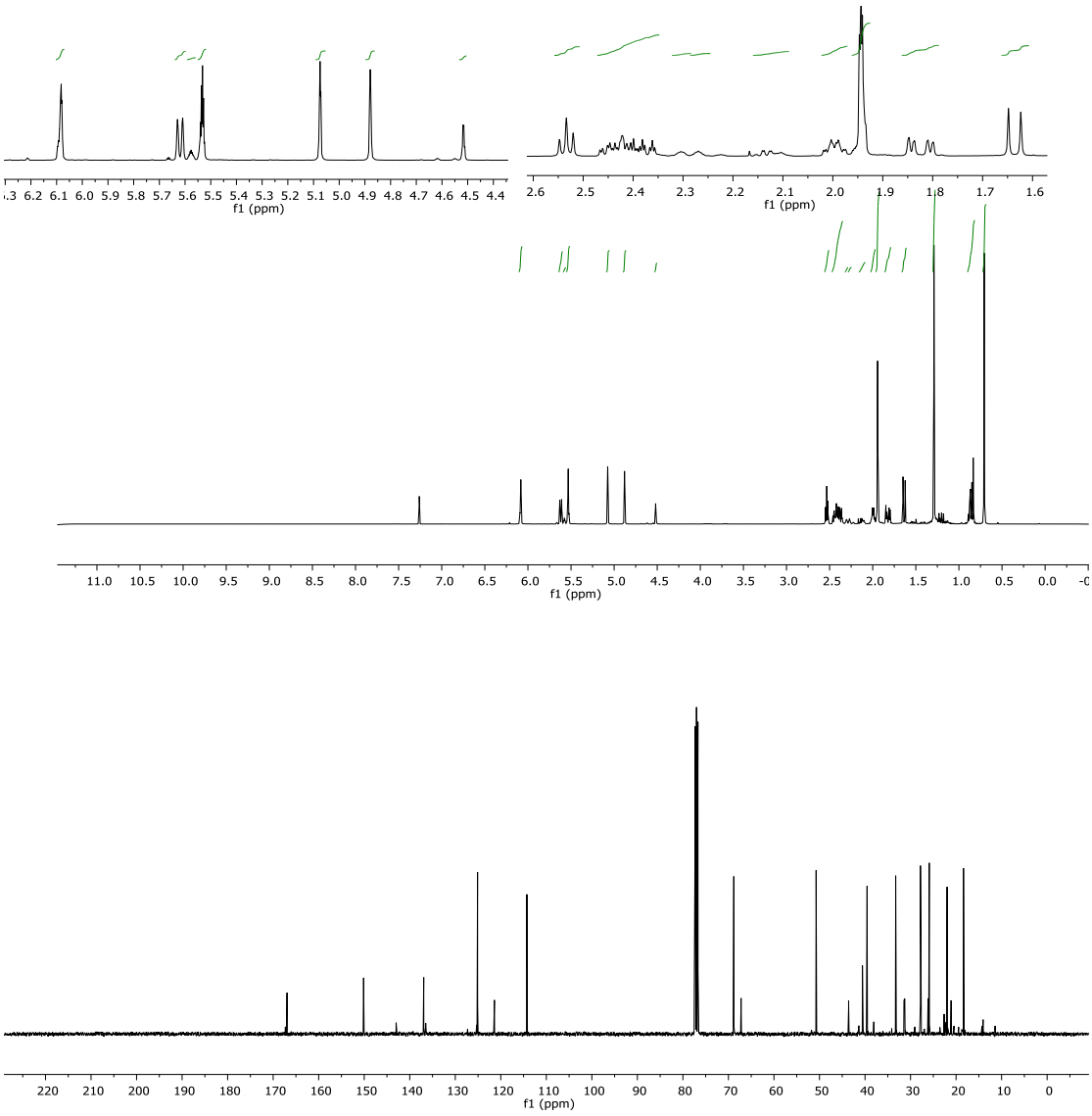


((1*R*,5*S*)-6,6-dimethylbicyclo[3.1.1]hept-2-en-2-yl)methyl methacrylate (5c) and (1*R*,3*R*,5*R*)-6,6-dimethyl-2-methylenebicyclo[3.1.1]heptan-3-yl methacrylate (6c)



Major compound: **6c: ^{1}H-NMR (400 MHz, $CDCl_3$):** δ = 6.11 (dd, *J* = 1.72, 0.88 Hz, 1H), 5.64 (d, *J* = 8.04 Hz, 1H), 5.56 (dt, *J* = 4.82, 1.61 Hz, 1H), 5.10 (t, *J* = 1.17 Hz, 1H), 4.90 (br. s, 1H), 2.56 (t, *J* = 5.55 Hz, 1H), 2.02 (dddd, *J* = 11.55, 5.99, 4.09, 1.75 Hz, 1H), 1.97 (dd, *J* = 1.40, 1.0 Hz, 3H), 1.85 (ddd, *J* = 15.05, 4.24, 0.88 Hz, 1H), 1.66 (d, *J* = 9.94 Hz, 1H), 1.31 (br. s, 3H), 0.92-0.84 (m, 2H), 0.73 (s, 3H). **δ_C** (100 MHz, $CDCl_3$): 166.6 (q), 149.8 (q) , 136.5 (q), 124.7 (CH2), 113.9 (CH2), 68.4 (CH), 50.4 (CH), 40.2 (q), 39.2 (CH), 32.9 (CH2), 27.4 (CH2), 25.5 (CH3), 21.6 (CH3), 18.0 (CH3).

For the minor product (**5c**), the following peaks are discernible. The remaining peaks overlap with the major product. **^{1}H-NMR (400 MHz, $CDCl_3$):** δ = 6.13-6.11 (m, 1H), 5.62 -5.58 (m, 1H), 4.54 (d, *J* = 1.46 Hz, 2H), 2.34-2.28 (m, 2H), 2.18-2.12 (m, 2H), 1.60-1.40 (m, 2H). **^{13}C-NMR (100 MHz, $CDCl_3$):** δ = 166.9 (q), 142.6 (q), 136.1 (q), 124.9 (CH2), 121.0 (CH), 66.8 (CH2), 43.2(CH), 40.3 (CH), 37.7 (q), 31.1 (CH2), 30.9 (CH2), 25.8 (CH3), 22.8 (CH3), 20.7 (CH3). **HRMS (ESI-MS)**: calcd. for $C_{14}H_{20}O_2$ ($M+Na^+$): 243.1356, found: 243.1363


f1 (ppm)
f1 (ppm)
f1 (ppm)

f1 (ppm)

3.3 Results and discussion

As discussed in the introductory chapter of this PhD thesis (Chapter 1), reports of previous attempts of polymerising natural terpenes showed little success. Terpene functionalisations and further polymerisation have been limited to one specific terpene in each case, which makes the number of materials available from natural terpenes still very limited. In this chapter, the application of a synthetic strategy to convert a range of natural terpenes into reactive monomers is discussed. This work is focused on the introduction of acrylate and methacrylate moieties into the chemical structure of the four most commercially available terpenes, thus creating a whole variety of new terpene-based monomers. A two-step methodology and a catalytic one-pot route to new terpene-derived monomers are discussed below.

3.3.1 Synthesis of terpene-based (metha)crylate monomers *via* 2-step methodology

The first synthetic approach towards (meth)acrylate derivatives from terpenes consisted on the hydroxylation of terpenes as the first step, followed by an esterification reaction with a (meth)acrylic acid derivative (Figure 3-6).

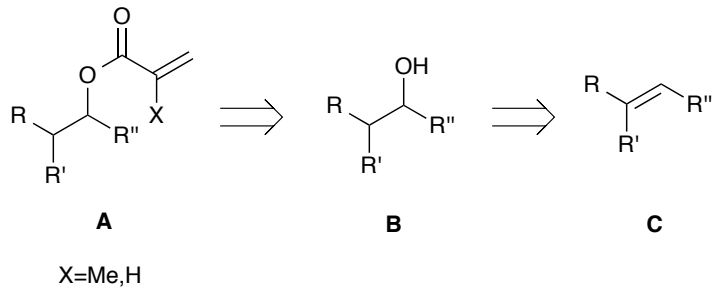


Figure 3-6. Retrosynthetic analysis, showing the formation of terpene acrylate coupled monomers from terpenes with either alkene or ketone functionality.

The four most commercially available terpenes were chosen as starting materials: (+)-α-pinene **1**, (-)-β-pinene **2**, (R)-(+)-limonene **3** and (R)-(-)-carvone **4** (Figure 3-7).

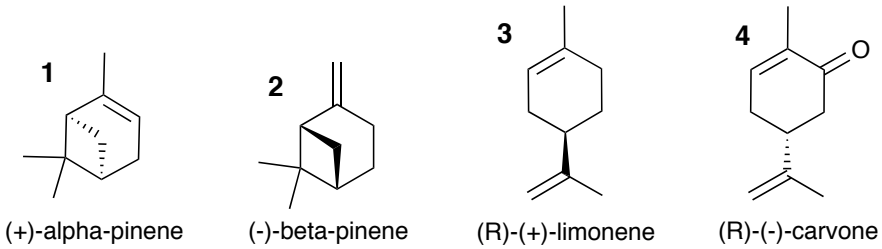


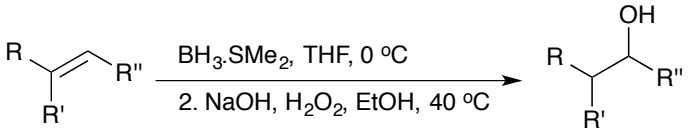
Figure 3-7. Chemical structures of the four most commercially available terpenes.

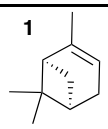
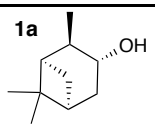
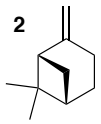
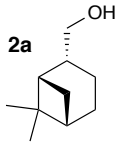
3.3.1.1 Synthesis of terpene alcohols

In order to install hydroxyl functionalities into (+)-α-pinene **1**, (-)-β-pinene **2** and (R)-(+)-limonene **3**, a hydroboration/oxidation tandem protocol[28, 30] was conducted. By contrast, for (R)-(-)-carvone **4**, a reduction of the enone *via* a hydroalumination reaction afforded the corresponding alcohol. The use of a hydroboration protocol allowed for the synthesis of regio- and stereo-pure alcohols from alkenes in an *anti*-Markovnikov fashion, as opposed to the use of an acid-catalysed hydration method, which generally leads to mixtures of regioisomers with no stereoselectivity. In polymer synthesis, the stereochemistry of the monomers can significantly affect the properties of the polymer. Therefore, being able to control the stereochemistry of the polymer means control over the mechanical properties of the polymer.[32, 33]

(+)-α-Pinene and (-)-β-pinene were hydrolysed using $BH_3.SMe_2$ as the boron agent in the hydroboration step. The oxidation step was conducted by adding sodium hydroxide and H_2O_2 to the reaction mixture. These reactions led to enantiopure alcohol derivatives **1a** and **2a** with excellent yields (Table 3-1). The main byproducts of the reaction were boric acid and boron salts that precipitated during the reaction. These alcohols had been previously described by Zweifel and Brown.[28]

Table 3-1. Hydroboration/oxidation of alpha- and beta-pinene.



Entry	Alkene	Borane	Alcohol	Yield (%)[a]
1		$BH_3.SMe_2$		87
2		$BH_3.SMe_2$		99

[a] Isolated yields after purification. 50g scale.

The hydroboration/oxidation of (R)-(+)-limonene **3** using diborane is known to lead to a mixture of products,[34, 35] as a result of hydroxylation reactions taking place in both double bonds. Therefore, in order to install the hydroxyl functionality in only one of the double bonds, it was necessary to use a sterically demanding borane such as 9-borabicyclo(3.3.1)nonane (also called 9-BBN) (Figure 3-8).

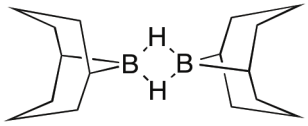


Figure 3-8. Chemical structure of 9-Borabicyclo(3.3.1)nonane.

The hydroboration mechanism in the presence of 9-BBN (Figure 3-9) is similar to the use of diborane (Figure 3-3). In the first step of the reaction 9-BBN adds to the alkene, generating an alkyl borane. The latter then reacts with H_2O_2 leading to the corresponding alkyl borate. The difference with the diborane mechanism is that, after formation of the alkyl borate, this one reacts with two more equivalents of H_2O_2, generating a dioxaborabicyclo. Subsequently the boron displaces the

alkoxide product and cyclooctane-1,5-diol is formed as byproduct. This diol, boron acid, and borane salts are the byproducts of the reaction.

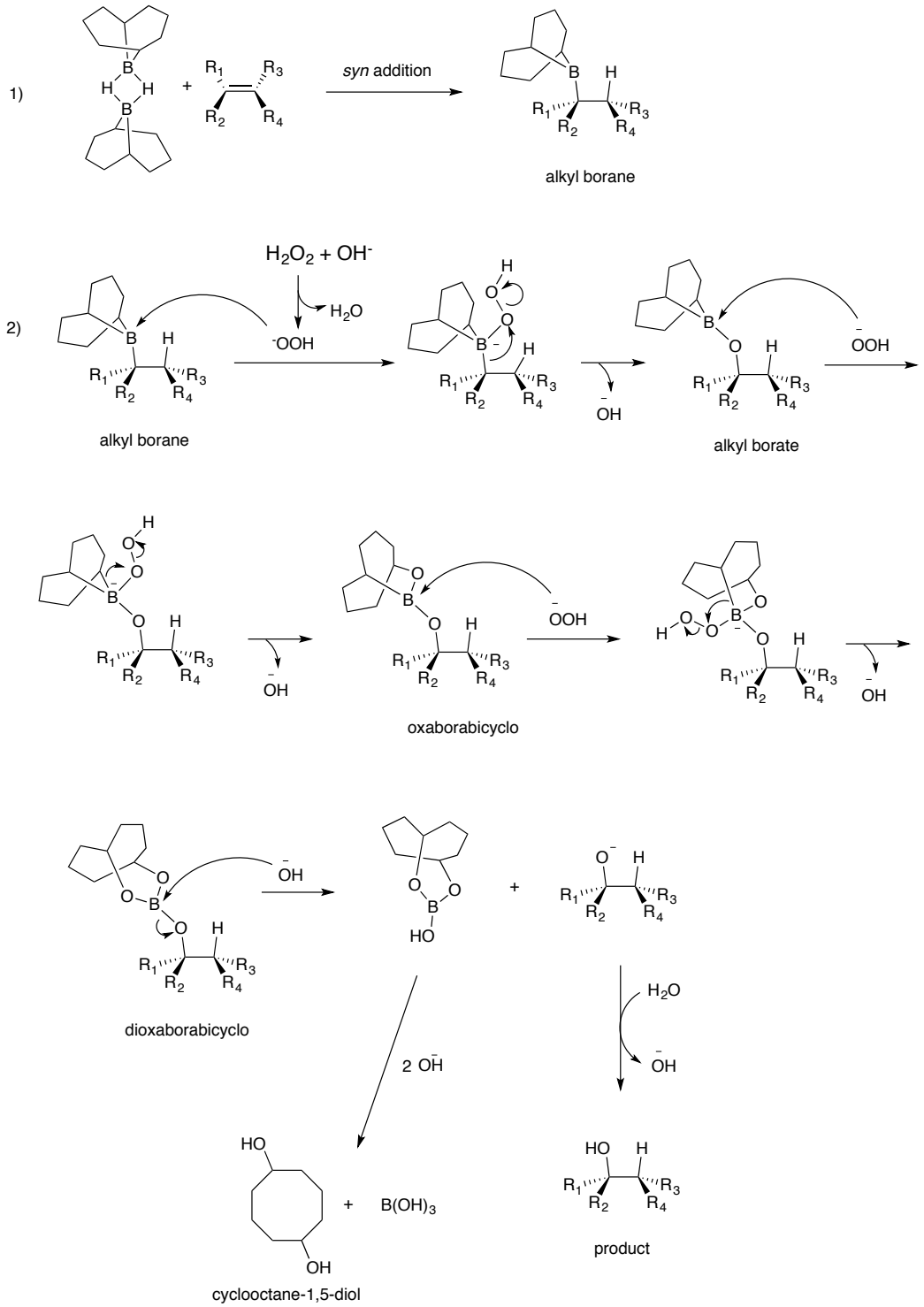
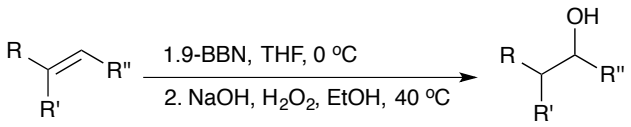
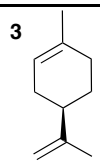
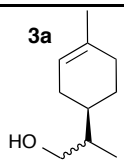


Figure 3-9. Hydroboration mechanism in the presence of 9-BBN as the boron agent.

The hydroboration of limonene in the presence of 9-BBN yielded the corresponding alcohol **3a** as a 1:1 mixture of diastereoisomers (Table 3-2). This alcohol had been previously reported by Labadie et al.[30]

Table 3-2. Hydroboration/oxidation of limonene.

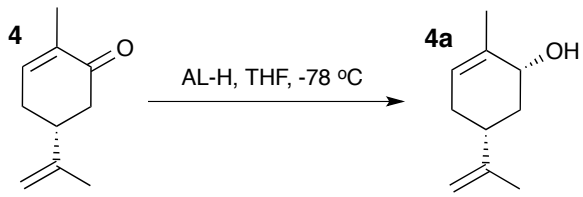


Entry	Alkene	Borane	Alcohol	Yield (%)
1		9-BBN		82 %[b]

[b] 1:1 mixture of diastereoisomers

In the case of (R)-(-)-carvone) **4**, alcohol **4a** was formed by reduction of the enone functionality *via* a hydroalumination reaction (Table 3-3).

Table 3-3. Hydroalumination of carvone.



Entry	AL-H	d.r.[a]	Yield (%)[b]
1	DIBAL [c]	5:1	99
2	$LiAlH_4$	95:5	99

[a] Diastereomeric ratio. [b] Isolated yield. 50g scale. [c] Diisobutylaluminium hydride.

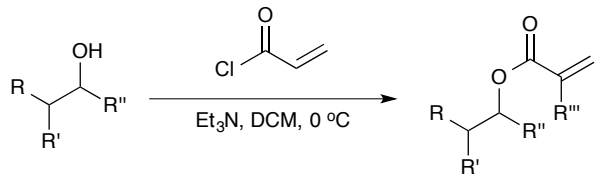
The use of diisobutylaluminium hydride (DIBAL) afforded the product in a quantitative yield with a diastereomeric ratio of 5:1. The same reaction in the presence of $LiAlH_4$ yielded **3a** with a diastereomeric ratio of 95:5 with quantitative conversion. Garver et al. had previously described this alcohol in 1976.[31]

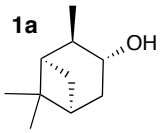
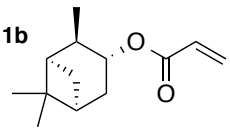
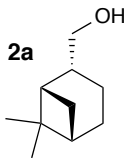
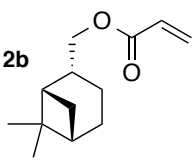
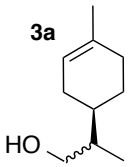
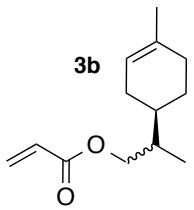
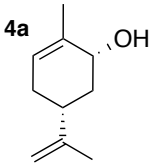
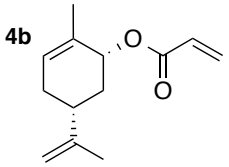
In order to work with the purest precursor the synthesis was conducted using the carvone alcohol **4a** obtained with $LiAlH_4$. Hydroboration/oxidation and hydroalumination reactions are well known procedures and generally yield the corresponding alcohols with very good yields and stereospecifically. These procedures allowed for the synthesis of the hydroxy terpenoids **1a**, **2a**, **3a** and **4a** from the most commercially available terpenes with excellent yields and with a level of purity that permitted their use in the esterification step without further purification.

3.3.1.2 Esterification of terpene-based alcohols

In order to synthesise acrylate and methacrylate derivatives, alcohols **1a**, **2a**, **3a** and **4a** were subjected to esterification reactions with acryloyl chloride (Table 3-4) and methacryloyl chloride (Table 3-5) respectively and Et_3N as a base.

*Table 3-4. Synthesis of terpene-based acrylate monomers via esterification of terpene alcohols with acryloyl chloride.**

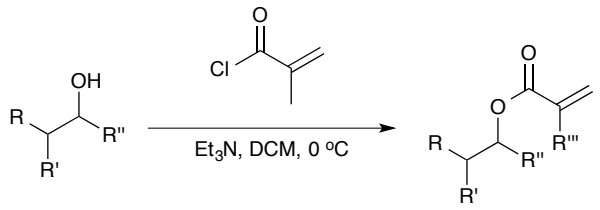


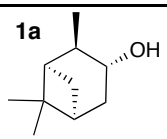
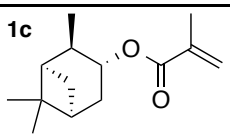
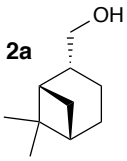
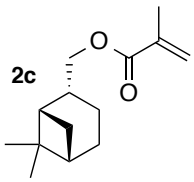
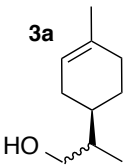
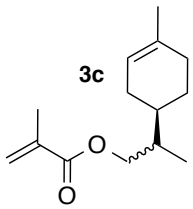
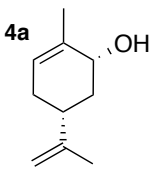
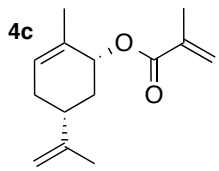
Entry	Alcohol	Acrylate	Yield (%)[a]
1			55
2			66
3			78[b]
4			91

*Reactions were conducted by dissolving the corresponding alcohol (64.8 mmol) with 500 mL of DCM, and submerging in an ice bath. Subsequently, 20 mL Et_3N (123 mmol) and acryloyl chloride (9.5 mL, 97.2 mmol) were added and the mixture was left stirring for 24 h while warming to rt. [a] Isolated yields after purification. Multigram scale. [b] 1:1 mixture of diastereomers.

For the methacrylate derivatives (Table 3-5), monomers were obtained with moderate to good yields between 47 and 78 %. However, limonene methacrylate **3c** was obtained together with an unsaturated impurity that coeluted during the purification process using a silica chromatographic column. This impurity was not identified and further research needs to be conducted in order to avoid it or to separate it from the product **3c**, since an unsaturated impurity would interfere with the monomer during the polymerisation reaction and lead to unwanted crosslinked polymers.

*Table 3-5. Synthesis of methacrylate derivatives through alcohol esterification with methacryloyl chloride.**



Entry	Alcohol	Methacrylate	Yield (%)[a]
1			47
1			64
3			73[b]
4			78

*Reactions were conducted by dissolving the corresponding alcohol (64.8 mmol) with 500 mL of DCM, and submerging in an ice bath. Subsequently, 20 mL Et_3N (123 mmol) and methacryloyl chloride (9.5 mL, 97.2 mmol) were added and the mixture was left stirring for 24 h while warming to rt. [a] Isolated yields after purification. Multigram scale. [b] 1:1 mixture of diastereomers.

3.3.1.3 Esterification in the presence of coupling agents.

When it comes to sustainability, the main issue with the synthetic strategy above is the use of the very toxic and expensive acryloyl derivatives. In order to tackle this issue, the use of acrylic and methacrylic acid was investigated. Currently, there is great industrial interest on the synthesis of acrylic and methacrylic acid from renewable resources and a number of companies have announced that they will be commercially available soon at a competitive price.[36-40] The use of

renewable (meth)acrylic acid offers several advantages over the use of acryloyl reagents since it is less hazardous, cheaper and greener.

However, esterification reactions between alcohols and carboxylic acids are known to occur very slowly and with a low conversion, since the water generated in the reaction draws the equilibrium back towards the monomers. The use of coupling agents greatly increases the reaction rate and they have become very popular in industrial processes due to their efficiency. Some of the most effective coupling agents are also very toxic such as N,N'-diisopropylcarbodiimide (DIC), N,N'-dicyclohexylcarbodiimide (DCC) or (1-[Bis(dimethylamino)methylene]-1H-1,2,3-triazolo[4,5-b]pyridinium 3-oxid hexafluorophosphate) (HATU); but there are some others that are considered green such as propane phosphonic acid anhydride (T3P®), carbonyldiimidazole (CDI) and (1-Cyano-2-ethoxy-2-oxoethylidenaminooxy)dimethylamino-morpholino-carbenium hexafluorophosphate (COMU®) (Figure 3-10).[41, 42]

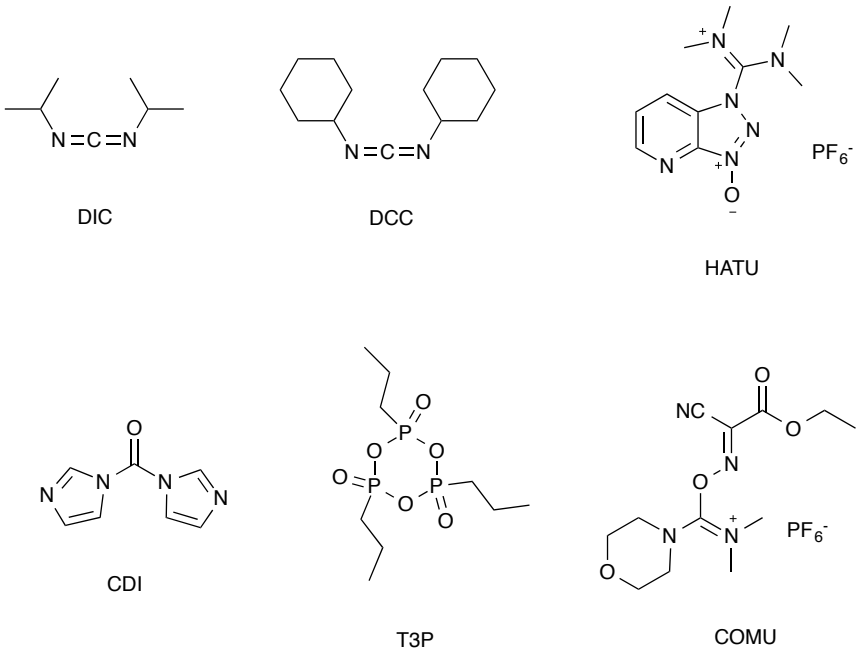


Figure 3-10. Common coupling agents used for ester and amide synthesis. Coupling agents react with carboxylic acids, activating the carbonyl group towards nucleophilic attack from the alcohol or amine.

Among the most sustainable options, COMU® has shown excellent results providing very high yields in the synthesis of esters and amides.[43, 44] However, it is a very expensive reagent and therefore it was considered not practical for the multigram synthesis of terpene methacrylate esters, since stoichiometric amounts of COMU® would be necessary to conduct the esterification.

As for CDI, it is a versatile, inexpensive and environmentally benign coupling agent that has been known for decades.[45, 46] In the first step of the mechanism (Figure 3-11), the carbonyl group in CDI is attacked by the carboxylic acid, with imidazole acting as leaving group, to form a mixed anhydride. Subsequently, the anhydride undergoes quick elimination of carbon dioxide to form a more stable acyl imidazolide. In step 2 the imidazolide experiences a nucleophilic attack from the alcohol, releasing another equivalent of imidazole and forming the ester product. However, imidazole is a poor leaving group and alcohols are relatively poor nucleophiles, which sometimes leads to long reaction times and poor yields in CDI-mediated esterification reactions.[47]

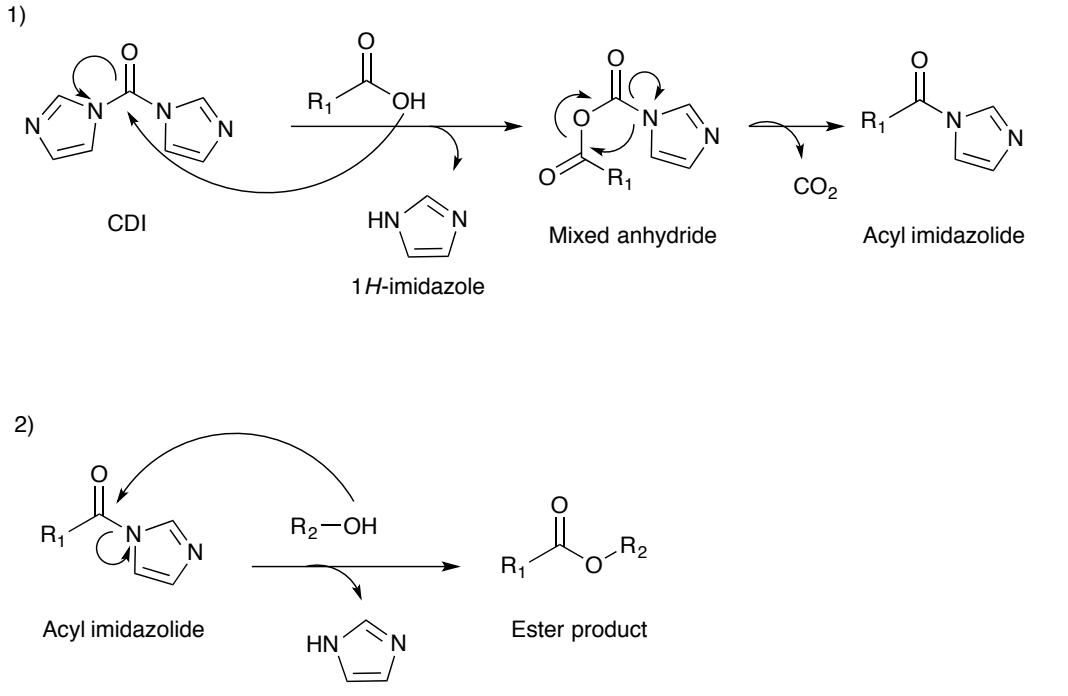
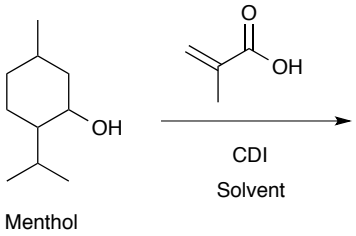


Figure 3-11. General mechanism of CDI activation of carboxylic acids during esterification reactions.

In order to test the viability of using CDI as a coupling agent in the synthesis of terpene-based (meth)acrylates, the reaction was conducted using menthol as starting material, an affordable and naturally occurring terpene (Table 3-6).

*Table 3-6. Reaction of menthol and methacrylic acid in the presence of CDI as coupling agent.**



Entry	Base	Solvent	T (^{o}C)	Methacrylate product
1	None	MeTHF	rt	NO[c]
2	None	MeTHF	50	NO[c]
3	Et_3N (3 eq.)[a]	MeTHF	rt	NO[c]
4	Et3N (3 eq.)[a]	MeTHF	50	NO[c]
5	NMI[b]	MeTHF	rt	NO[c]
6	Et3N[a]	Acetone	rt	NO[c]

*All reactions were conducted by mixing 0.06 mL of methacrylic acid (1.1 eq), 125 mg of CDI (1.1 eq.) and the corresponding base in 0.8 mL of solvent. The mix was stirred at rt for 2 h, after which 100 mg of menthol ((0.64 mmol, 1 eq.) dissolved in 0.8 mL of solvent were added. The outcome of the reactions was analysed by TLC and ^{1}H-NMR. [a] Triethylamine. [b] 1-Methyl imidazole [c] Not observed.

Reactions were conducted by mixing first CDI, the corresponding base (if any) and methacrylic acid, and stirring for 2 h. Bubbling was observed in all cases upon addition of the methacrylic acid to the reaction flask, indicating the formation of carbon dioxide as a result of imidazolide formation. Subsequently, menthol was added and the mixture was stirred at the indicated temperature (Table 3-6) for 48 h. When the reaction was conducted at room temperature (rt) and in the absence of base no menthol-derived methacrylate was detected after 48 h by TLC or ^{1}H-NMR. The reaction outcome was identified as a mixture of CDI, acrylic acid, acyl imidazolide and menthol. An increase of temperature led to

minor decomposition products which were detected by TLC but were difficult to determine by ^{1}H-NMR. The addition of triethylamine (entries 3, 4 and 6) or N-methyl imidazole (NMI) (entry 5) as base was tested to create a basic environment and facilitate nucleophilic attack by the alcohol. However, the methacrylic ester was not observed and unreacted menthol or mentholate (in the presence of base) was observed instead. Given the lack of methacrylate ester formation no further investigation was conducted using CDI as coupling agent.

An interesting alternative is T3P®. This coupling agent is widely used in industry[48] because of the high yields that it affords and its lack of toxicity. Another advantage of using T3P® is that the byproduct of the reaction (Figure 3-12) is also non-toxic and soluble in water. Therefore it is easily removed by aqueous work up.

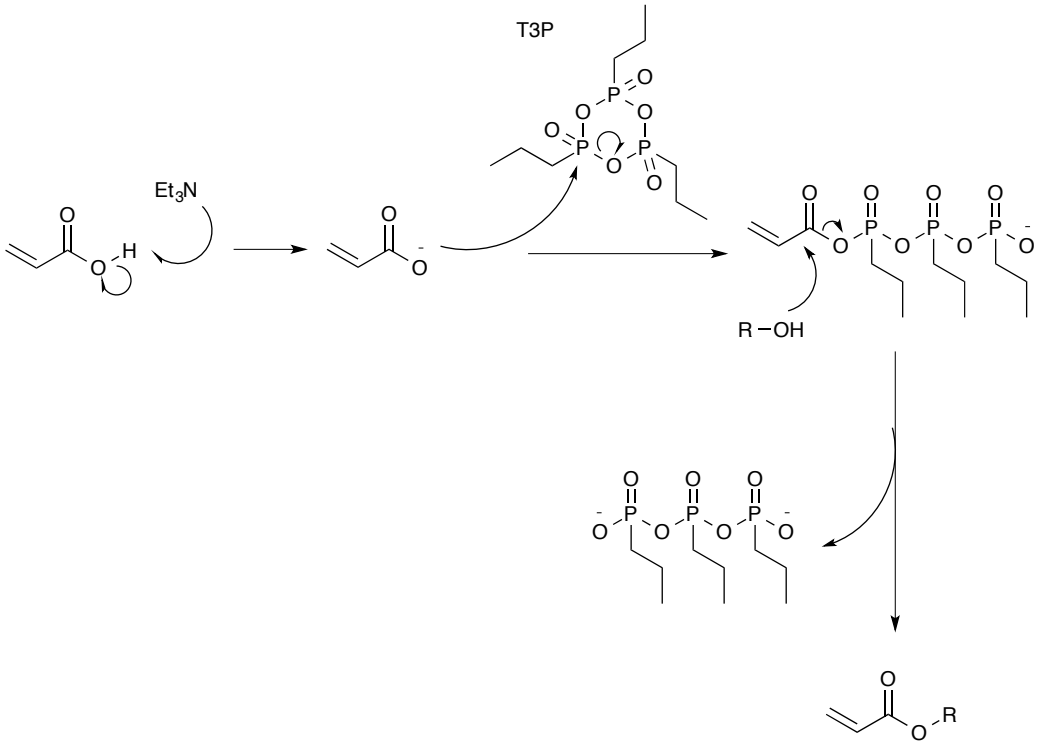
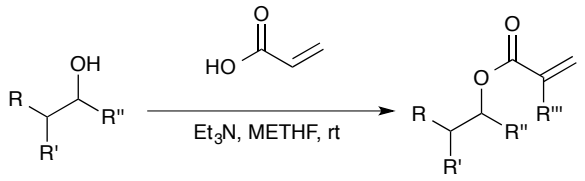
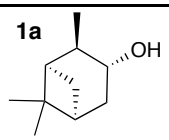
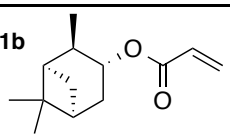
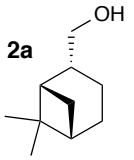
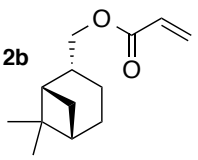
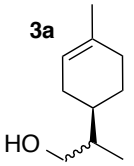
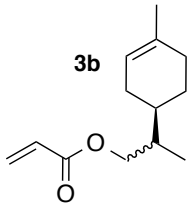
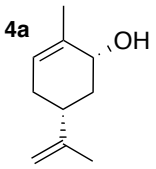
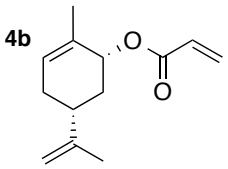


Figure 3-12. General mechanism of T3P-mediated esterification of acrylic acid. After a base deprotonates acrylic acid, the resulting acrylate attacks T3P. Subsequently, an alcohol unit attacks the activated carboxylic bond in the acrylate, forming the corresponding acrylate ester and releasing T3P® byproduct.

When T3P® was used as coupling agent in the esterification reaction between terpene alcohols **1a**, **2a**, **3a** and **4a**; and acrylic acid, the corresponding terpene acrylates **1b**, **2b**, **3b** and **4b** were obtained with quantitative yields (Table 3-7).

*Table 3-7. Esterification of terpene alcohols and acrylic acid mediated by T3P.**



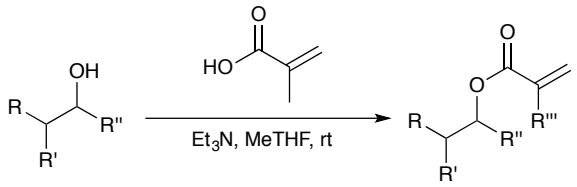
Entry	Alcohol	Acrylate	Yield (%)[a]
1			99
2			99
3			96[b]
4			99

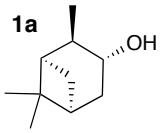
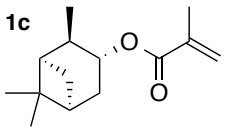
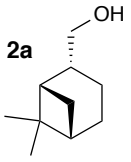
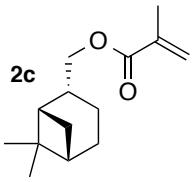
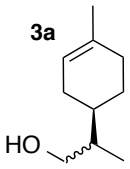
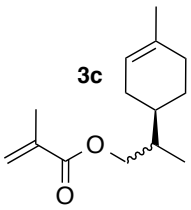
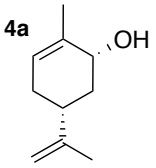
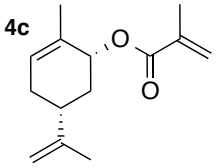
*All reactions were conducted by mixing terpene alcohol (6.48 mmol) with acrylic acid (0.6 mL, 7.13 mmol), Et3N (2.7 mL, 19.4 mmol), T3P (7.78 mmol) (50 wt% in ethyl acetate) and MeTHF (40 mL) in a 100 mL round-bottomed flask. The mixture was stirred for 48 h at rt. [a]Yields correspong to isolated products. [b] Product obtained as a 1:1 mixture of diastereoisomers.

Additionally, the use of T3P® allowed for the reactions to be conducted at rt. To make the reaction even more sustainable MeTHF was used as the solvent. MeTHF is a renewable solvent generally considered as the "green" replacement for DCM and THF.[49]

Unfortunately, when the same reactions were conducted with methacrylic acid to form the methacrylate monomers very poor yields were observed (Table 3-8).

*Table 3-8. Esterification of terpene alcohols with methacrylic acid mediated by T3P.**



Entry	Alcohol	Methacrylate	Yield (%)[a]
1			-
1			-
3			13[b,c]
4			7

*All reactions were conducted by mixing terpene alcohol (6.48 mmol) with methacrylic acid (0.6 mL, 7.13 mmol), Et3N (2.7 mL, 19.4 mmol), T3P (7.78 mmol) (50 wt% in ethyl acetate) and MeTHF (40 mL) in a 100 mL round-bottomed flask. The mixture was stirred for 48 h at rt. [a]Yields correspong to isolated products. [b] Product obtained as a 1:1 mixture of diastereoisomers. [c]Purified compound contained an identified unsaturated impurity.

The esterification reaction of α-pinene and β-pinene-derived alcohols **1a** and **2a** with methacrylic acid (entries 1 and 2) yielded no methacrylate product. Meanwhile, methacrylate derivatives **3b** and **4b** were obtained from limonene and

carvone alcohols **3a** and **4a** in a 13 % (entry 3) and 7 % (entry 4) yield respectively. It is proposed that such a dramatic difference in reactivity between acrylic and methacrylic acid must be caused by the steric hindrance around the methyl group in methacrylic acid (Figure 3-13).

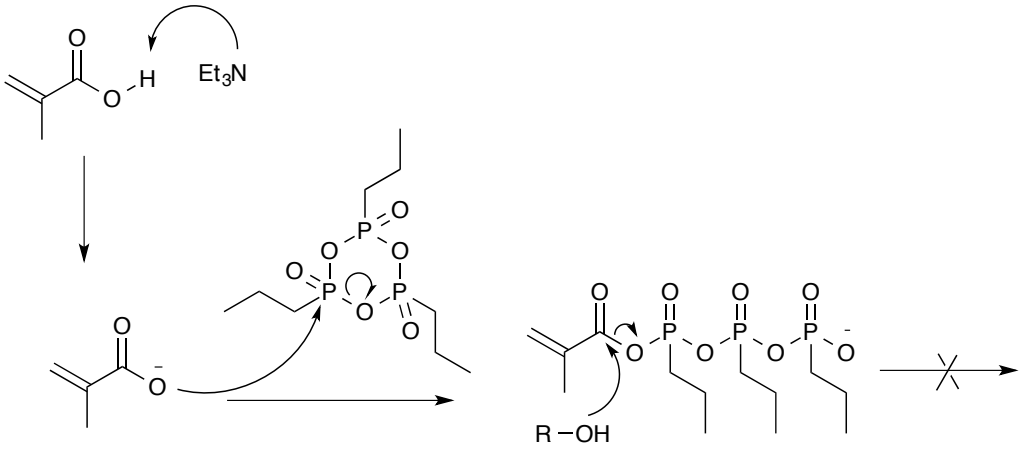


Figure 3-13. After an acrylate unit reacts with T3P, the carboxylic group in the acrylate moiety is too sterically hindered for the alcohol to attack.

The methyl group limits the free volume around the acrylate group, preventing an attack from a voluminous terpene alcohol. Therefore, further investigation needs to be conducted in order to improve the sustainability of the two-step synthesis of terpene-based methacrylates.

As discussed earlier, esterification reactions of terpene alcohols with acryloyl and methacryloyl chloride described in Table 3-4 and Table 3-5 yielded stoichiometric amounts of ammonium chloride as byproduct. When the esterification reactions were conducted using acrylic acid and T3P (Table 3-6, Table 3-7), ammonium and a propyl phosphonic derivative (Figure 3-12) were obtained as waste products. Other byproducts from the two-step procedure were the boric acid and boron salts (as a result of the hydroboration step), lithium and aluminium salts (from the reduction of carvone) and ammonium chloride that precipitates during the esterification step. Therefore, it is not a fully sustainable route.

However, this two-step procedure was only the first synthetic approach towards terpene-based (meth)acrylate monomers. They are simple but robust procedures that allowed for the synthesis (meth)acrylate monomers in such a scale that they can be polymerised (15g) (Chapter 4) and be tested as potential materials for applications such as coatings (Chapter 5).

3.3.2 1-pot synthesis of terpene-based (meth)acrylate monomers *via* a Pd(II) catalysis.

One of the disadvantages of the two-step synthesis of terpene-based (meth)acrylates described in the previous section is the large amount of waste generated. Therefore, it is not green from the atom economy point of view. In order to improve upon the two-step approach, a catalytic one-pot route was investigated.

Catalytic acetoxylation of terpenes, specifically limonene, had been previously reported in the literature by Meier *et al*.[50] In Meier's work, DMSO was used as solvent with an iron co-catalyst, and mixtures of the diastereomeric and regioisomeric products attributed to the two olefinic moieties in limonene were obtained. Additionally, Ferret[51] showed coupling of a range of several olefinic organic structures with acrylic acid and methacrylic acid. Of these, a limonene coupling showed three regioisomers in an almost 1 : 1 : 1 ratio in poor yield (40 %). An example of acetoxylation of β-pinene was reported back in 1982 by Uemura *et al*..[52] Uemura utilised tert-butyl hydroperoxide and tellurium oxide together with $PdCl_2$ to obtain a mix of regioisomers with a combined yield of 26 %.

The seminal work of White on catalytic allylic oxidation was chosen as a starting point to develop a catalytic method to incorporate acrylates at allylic positions *via* C–H activation.[16, 24] Catalytic studies were conducted using β-pinene (Table 3-9) as the substrate since it is one of the most abundant terpenes and a terminal olefin.

*Table 3-9. Optimisation of the reaction of methacrylation of β-pinene catalysed by $Pd(OAc)_2$.**

Entry	$Pd(OAc)_2$ load	BQ eq.	Atm.	t (h)	Yield (%)	Product ratio 5c/6c
1	4 mol%	1	N_2	18	12	1:10
2	4 mol%	1	O_2	16	30	1:10
3	4 mol%	0.5	O_2	18	22	1:10
4	4 mol%	0	O_2	18	No reaction	-
5	10 mol%	1	O_2	16	14	1:10
6	2 mol%	2	O_2	18	33	1:10
7	2 mol%	2	O_2	72	82	1:10
8	2 mol%	2	air	72	80	1:10
9	2 mol%	2	air	72	82[a]	1:10[a]
10	2 mol%	2	air	72	21[b]	1:10[b]

*All reactions were conducted by placing β-pinene (100 mg, 0.74 mmol), methacrylic acid (0.5 mL, 8 eq., 5.9 mmol), the corresponding amounts of BQ and $Pd(OAc)_2$ and a magnetic stirrer in a 2 mL round-bottomed flask. Reaction mixtures were then sealed and heated up and stirred for the indicated period of time, after which they were left to cool to rt and filtered through Celite. The residue was diluted with toluene and solvents were removed in vacuo. Crude products were purified by silica gel chromatographic column using petroleum ether as eluent. [a]Reaction conducted in a 2 g scale. [b]Reaction conducted in a 10 g scale.

To start with, β-pinene was made to react with 4 mol% of $Pd(OAc)_2$ as catalyst, 1 eq. benzoquinone (BQ) as catalyst ligand and oxidant and methacrylic acid (MA) as reactant and solvent under a nitrogen atmosphere at 50 ºC for 18 hr (entry 1).

The benzoquinone plays three important roles in this process, acting as oxidant and ligand for Pd as well as polymerisation inhibitor for the monomer produced. Under such conditions, 12 % of isolated reaction product was obtained, which consisted of a mixture of regioisomers **5c** and **6c** (Figure 3-14) in a 1:10 ratio (Table 3-9).

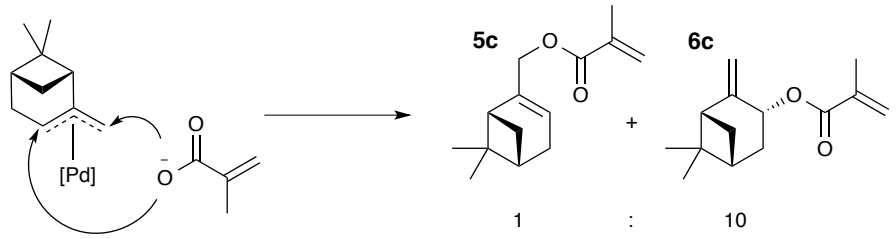


Figure 3-14. Pd-catalysed C-H activation of pinene allows nucleophilic attack from methacrylate to two different positions, leading to methacrylate derivatives 5c and 6c.

In order to help reoxidise Pd^0 to Pd^{II}, N_2 was switched to O_2. This change of atmosphere caused an increase in methacrylate yield from 12 % to 30 % (Table 3-9, entry 2). To improve the sustainability of the reaction the amount of benzoquinone was reduced from 1 eq. to 0.5 eq., which caused the yield to decrease from 30 % to 22 % (entry 3). When a blank reaction with no BQ was conducted no product was obtained (entry 4), showing that the Pd catalyst cannot be regenerated in the absence of an oxidant other than O_2. These results confirmed that at least equimolar concentrations of BQ are necessary for the reaction to reach the highest possible yield. As for the catalyst load, when it was increased from 4 mol% to 10 mol% (entry 5) the yield dropped down from 30 % to 14 %.

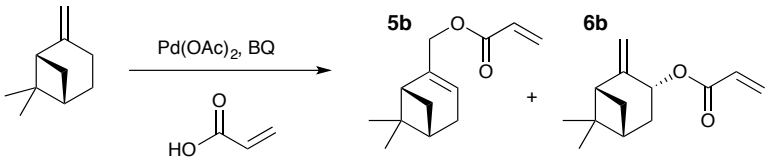
Having observed the effects of BQ and catalyst concentration, an increase in BQ to 2 eq., and a decrease of catalyst load to 2 mol% were tested, and found to lead to a 33 % yield after 18 h (entry 6). When the reaction was left to react for 72 h an 82 % of isolated product was obtained. Subsequently the same reaction was conducted in the absence of O_2, which led to a practically equivalent yield of 80 % (entry 8), showing that an O_2 atmosphere is not necessary for the success of the reaction. This simplifies significantly the protocol and facilitates the scale up.

An additional attraction of these conditions for further scaling is the use of methacrylic acid as both solvent and reactant. This catalytic protocol allowed for the synthesis of β-pinene methacrylates **5c** and **6c** on a 2 g scale with very good yields (entry 9).

Products **5c** and **6c** could not be separated by chromatographic column since they coeluted during the purification because of their structural similarities. Further scaling up to 10 g of starting material led to a considerable drop in yield to 21 % (entry 10) indicating the need to re-optimise the reaction conditions when large-scale reactions are conducted. Scaling up often requires a re-optimisation of the reaction conditions since mixing and heat transfer are normally less efficient in larger reaction volumes.[53, 54]

In order to synthesise the acrylate analogues, the same conditions were applied to β-pinene using acrylic acid (Table 3-10) instead of methacrylic acid.

*Table 3-10. Catalytic synthesis of pinene-based acrylate monomers.**



Entry	AA eq.	Yield (%)	Product ratio
			5b/6b
1	8	12[a]	1:1[a]
2	3	30[b]	1:2[b]

*Reactions were conducted by placing β-pinene, acrylic acid, BQ (2 eq.), $Pd(OAc)_2$ (2 mol%) and a magnetic stirrer in a round-bottomed flask. Reaction mixtures were then sealed, heated up to 50 °C and stirred for 72 h, after which they were left to cool to rt and filtered through Celite. The residue was diluted with toluene and solvents were removed in vacuo. Crude products were purified by silica gel chromatographic column using petroleum ether as eluent. [a]Reaction conducted in a 100 mg scale. [b]Reaction conducted in a 10 g scale.

A 45 % yield of combined products **5b** and **6b** were obtained in a 1:1 ratio (entry 1). This result suggests that further optimisation is necessary in order improve the

yields of the acrylation reaction. When the reaction was scaled up to synthesise several grams of monomer, 3 eq. of acrylic acid were added instead of 8 eq. This change was implemented in order to improve the sustainability of the reaction, which caused a decrease in yield from 45 % to 24 % (entry 2). Such a decrease could be caused by either the scaling up, as observed during the methacrylate synthesis (Table 3-10, entry 10), or by the reduction in acrylic acid concentration. Despite these drawbacks, these results were deemed very promising.

Further investigation needs to be conducted in order to improve the yields and the sustainability of the synthesis, for example by reducing further the catalyst load and substituting BQ for a more sustainable oxidant. However, the synthetic routes described in this chapter have allowed for the synthesis of β-pinene-based (meth)acrylate monomers on such a scale that the monomers could be polymerised and carefully studied.

3.4 Conclusions

A wide range of new terpene-based acrylates and methacrylates were synthesised for the first time using simple but robust protocols. A two-step methodology based on a hydroboration-oxidation protocol followed by esterification provided a wide variety of enantiomerically pure monomers with good yields. Meanwhile, Pd-catalysed allylic C-H activation of β-pinene yielded a mix of two (meth)acrylate regioisomers. This route proved to be a more promising and sustainable one towards terpene-based (meth)acrylates. Although these synthetic routes need to be further improved in order to be considered safe, green, and applicable industrially, they allowed for the synthesis of monomers in such a scale that they could be polymerised. Their polymerisation reactions were carefully studied and described in Chapter 4.

3.5 References

1. M. Winnacker and B. Rieger, *ChemSusChem*, 2015, **8**, 2455-2471.
2. K. Yao and C. Tang, *Macromolecules*, 2013, **46**, 1689-1712.
3. P. A. Wilbon, F. Chu and C. Tang, *Macromolecular Rapid Communications*, 2013, **34**, 8-37.
4. A. J. D. Silvestre and A. Gandini, in *Monomers, Polymers and Composites from Renewable Resources*, eds. M. N. Belgacem and A. Gandini, Elsevier, Oxford, 2008.
5. A. Gandini, in *Biocatalysis in Polymer Chemistry*, Wiley-VCH Verlag GmbH & Co. KGaA, 2010, pp. 1-33.
6. J. R. Lowe, M. T. Martello, W. B. Tolman and M. A. Hillmyer, *Polym. Chem.*, 2011, **2**, 702-708.
7. C. M. Byrne, S. D. Allen, E. B. Lobkovsky and G. W. Coates, *J. Am. Chem. Soc.*, 2004, **126**, 11404-11405.
8. F. Bettelheim, W. Brown and J. March, *Introduction to Organic and Biochemistry, 4th Edition*, Harcourt Brace College, 2000.
9. S. S. Stradling, *J. Chem. Educ.*, 1997, **74**, 1045-1046.
10. S. V. Ley, *Comprehensive Organic Functional Group Transformations: Volume 2: Synthesis: Carbon with One Heteroatom Attached by a Single Bond*, Pergamon, 1996.
11. T. W. Lyons and M. S. Sanford, *Chem. Rev.*, 2010, **110**, 1147-1169.
12. T. Gensch, M. N. Hopkinson, F. Glorius and J. Wencel-Delord, *Chem. Soc. Rev.*, 2016, **45**, 2900-2936.
13. J. Wencel-Delord, T. Droege, F. Liu and F. Glorius, *Chem. Soc. Rev.*, 2011, **40**, 4740-4761.
14. F. Liron, J. Oble, M. M. Lorion and G. Poli, *Eur. J. Org. Chem.*, 2014, **2014**, 5863-5883.
15. W. H. Henderson, C. T. Check, N. Proust and J. P. Stambuli, *Org. Lett.*, 2010, **12**, 824-827.
16. M. S. Chen and M. C. White, *J. Am. Chem. Soc.*, 2004, **126**, 1346-1347.
17. W. Kitching, Z. R. S. Winstein and W. G. Young, *J. Am. Chem. Soc.*, 1966, **88**, 2054-2055.
18. S. Hansson, A. Heumann, T. Rein and B. Aakermark, *J. Org. Chem.*, 1990, **55**, 975-984.
19. A. Heumann, M. Reglier and B. Waegell, *Angew. Chem. Int. Ed.*, 1982, **21**, 366-367.
20. A. Heumann and B. Åkermark, *Angew. Chem. Int. Ed.*, 1984, **23**, 453-454.
21. J. E. McMurry and P. Kocovsky, *Tetrahedron Lett.*, 1984, **25**, 4187-4190.
22. B. Aakermark, E. M. Larsson and J. D. Oslob, *J. Org. Chem.*, 1994, **59**, 5729-5733.
23. A. N. Campbell, P. B. White, I. A. Guzei and S. S. Stahl, *J. Am. Chem. Soc.*, 2010, **132**, 15116-15119.
24. M. S. Chen, N. Prabagaran, N. A. Labenz and M. C. White, *J. Am. Chem. Soc.*, 2005, **127**, 6970-6971.
25. H. Grennberg and J.-E. Backvall, *Chem. - Eur. J.*, 1998, **4**, 1083-1089.
26. S. Wolfe and P. G. C. Campbell, *J. Amer. Chem. Soc.*, 1971, **93**, 1497-1499.

27. T. W. Lyons and M. S. Sanford, *Chem. Rev. (Washington, DC, U. S.)*, 2010, **110**, 1147-1169.
28. G. Zweifel and H. C. Brown, *J. Am. Chem. Soc.*, 1964, **86**, 393-397.
29. G. Giacomelli, L. Lardicci and F. Palla, *J. Org. Chem.*, 1984, **49**, 310-313.
30. R. M. Cravero, M. Gonzalez-Sierra and G. R. Labadie, *Helv. Chim. Acta*, 2003, **86**, 2741-2753.
31. L. Garver, P. Van Eikeren and J. E. Byrd, *J. Org. Chem.*, 1976, **41**, 2773-2774.
32. V. K. Thakur and M. K. Thakur, *Handbook of Sustainable Polymers: Processing and Applications*, 2016.
33. D. L. Kaplan, *Biopolymers from Renewable Resources*, Springer Berlin Heidelberg, Berlin, Heidelberg, 1998.
34. R. Dulou and Y. Chretien-Bessiere, *Bull. Soc. Chim. Fr.*, 1959, 1362-1365.
35. A. F. Thomas and Y. Bessiere, *Nat. Prod. Rep.*, 1989, **6**, 291-309.
36. Metabolix, http://www.metabolix.com/Products/Biobased-Chemicals, (accessed 6th of June, 2016).
37. Cargill, http://www.biofuelsdigest.com/bdigest/2015/04/29/cargill-acquires-opx-biotechnologies/ https://http://www.linkedin.com/pulse/improved-bio-based-methods-acrylic-acid-transforms-strategic-kranti, (accessed 6th of June, 2016).
38. Arkema, http://www.arkema.com/en/innovation/renewable-raw-materials/bio-based-factories/, (accessed 6th of June, 2016).
39. Myriant, http://www.myriant.com/products/product-pipeline.cfm, (accessed 6th of June, 2016).
40. E. Sato, M. Yamakazi, E. Nakajima, F. Yu, T. Fujita, W. Mizunashi, *Method for manufacturing methacrylic acid and/or ester thereof with microorganisms or enzymes from biomass*, WO2014038216A1, 2014.
41. J. P. Adams, C. M. Alder, I. Andrews, A. M. Bullion, M. Campbell-Crawford, M. G. Darcy, J. D. Hayler, R. K. Henderson, C. A. Oare, I. Pendrak, A. M. Redman, L. E. Shuster, H. F. Sneddon and M. D. Walker, *Green Chem.*, 2013, **15**, 1542-1549.
42. D. S. MacMillan, J. Murray, H. F. Sneddon, C. Jamieson and A. J. B. Watson, *Green Chem.*, 2013, **15**, 596-600.
43. A. El-Faham, R. S. Funosas, R. Prohens and F. Albericio, *Chem. - Eur. J.*, 2009, **15**, 9404-9416.
44. J.-d. A. K. Twibanire and T. B. Grindley, *Org. Lett.*, 2011, **13**, 2988-2991.
45. T. Heinze, T. Liebert and A. Koschella, *Esterification of polysaccharides*, Springer, Berlin, 2006.
46. C. A. G. N. Montalbetti and V. Falque, *Tetrahedron*, 2005, **61**, 10827-10852.
47. C. Vargeese, V. Palle, *Preparation of substituted carbonyldiimidazoles as coupling activators and coupling reagents in organic synthesis*, WO9952897A1, 1999.
48. Euticals, http://www.euticals.com/attachments/article/20/EUTICALS_T3P.pdf, (accessed 7th of June, 2016).
49. F. M. Kerton, *Alternative solvents for green chemistry*, 2013.
50. M. von Czapiewski and M. A. R. Meier, *Catal. Sci. Technol.*, 2014, **4**, 2318-2325.

51. N. Ferret, L. Mussate-Mathieu, J.-P. Zahra and B. Waegell, *J. Chem. Soc., Chem. Commun.*, 1994, 2589-2590.
52. S. Uemura, S. Fukuzawa, A. Toshimitsu and M. Okano, *Tetrahedron Lett.*, 1982, **23**, 87-90.
53. C. C. Jiménez-González and D. Constable, *Green chemistry and engineering a practical design approach*, John Wiley & Sons, Hoboken, N.J., 2011.
54. M. C. Pirrung and I. Wiley, *The synthetic organic chemist's companion*, Wiley-Interscience, Hoboken, N.J., 2007.

Chapter 4 . Synthesis of terpene-based polyacrylates and polymethacrylates.

4.1 Introduction

As discussed in Chapter 1, there have been significant efforts to synthesise polymers from natural terpenes because their structures contain alkene moieties that seem to offer the opportunity for facile radical polymerisation. However, besides a few successes,[1, 2] numerous studies have shown that terpenes do not easily polymerise *via* radical methods.[3-10] Alternative strategies to polymerising terpenes involve cationic techniques,[11-14] thiol-ene chemistry[15, 16] and terpene-functionalisation previous to their polymerisation[17-23] (See Chapter 1). However, despite extensive research, the range of terpene-based polymers synthesised to date is still very limited.[8-10, 24, 25]

In Chapter 3, a wide range of new terpene-based (meth)acrylateswere synthesised for the first time using simple but robust protocols. (Meth)acrylates are a very popular family of monomers for radical polymerisation, since they generally polymerise easily and yield polymers that can be used in a number of applications such as coatings, electronics and medical applications. (Meth)acrylate monomers usually exhibit a broad range of beneficial features: stability, durability, hardness and scratch resistance among others.

In this chapter, new terpene-based meth(acrylate) monomers described in Chapter 3 are polymerised and the properties of the polymers are investigated. Studies regarding monomer reactivities are conducted using Fourier Transformed Infrared Spectroscopy (FTIR). A brief overview of FTIR spectroscopy is given below.

4.1.1 Infrared (IR) spectroscopy

The infrared spectrum is formed as a consequence of the absorption of electromagnetic radiation at frequencies that correlate to the vibration of specific sets of chemical bonds in a molecule. A molecule might absorb photons of specific energy, which results in a transfer of energy. The vibrational energy component corresponds to the absorption of energy by a molecule as its atoms vibrate about the centre of their chemical bonds. The *mid infrared*, between 4000 and 400 cm^{-1}, is the most useful region since many molecules have strong absorbances in this range. It is the region where most IR spectrometers record (Figure 4-1).

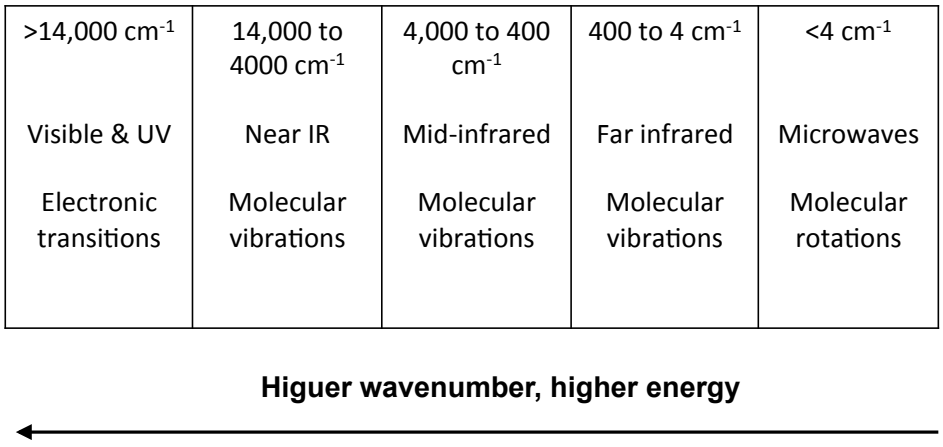


Figure 4-1. Section of the electromagnetic spectrum.

Vibrations are classified into two main categories: *stretching* and *bending (*Figure 4-2*)*. *Stretching* is the vibration mode in which the interatomic distance along the bond axis changes. Stretching vibrations can be symmetric or asymmetric. In a bending vibration mode there is a change in angle between two bonds. Bending mode includes scissoring and rocking modes, where both bonds move in the same plane, and out of plane modes, when the bonds wag or twist in different planes. Each one of these vibrations will absorb energy at a particular wavenumber depending on the atoms that are bonded, and will therefore appear in the IR spectrum at different frequencies.

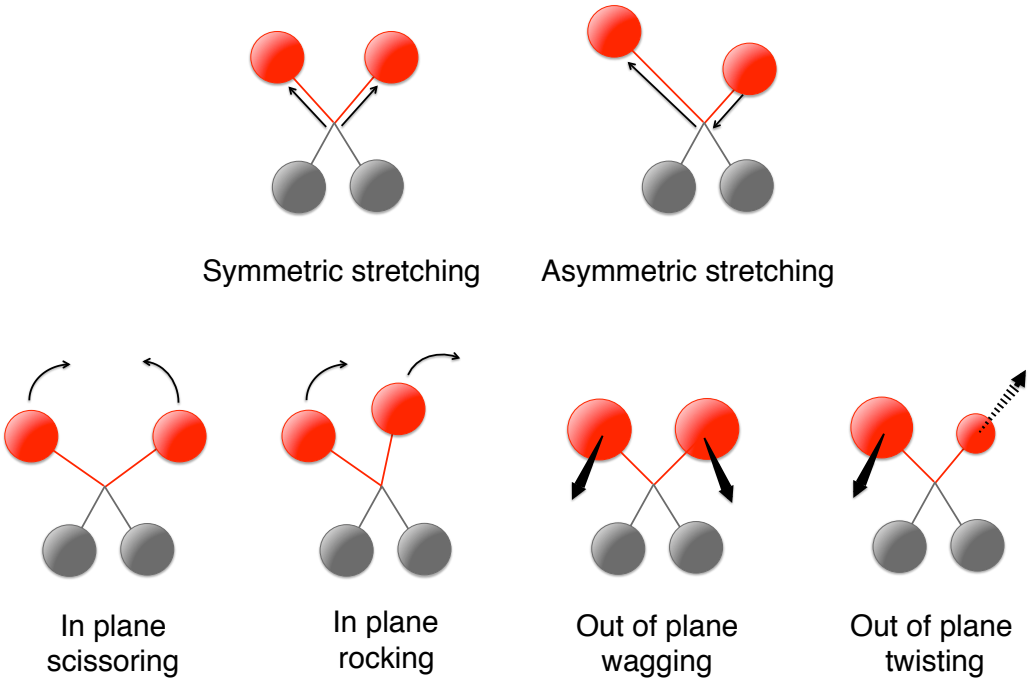


Figure 4-2. Schematic representation of the normal modes of vibration.

Two important components to the IR absorption process are the radiation frequency and the molecular dipole moment. In a spectrometer a molecule is irradiated with a whole range of frequencies but is only capable of absorbing radiation energy at certain specific frequencies that match the natural vibrational frequencies of the molecule. While the absorption frequency depends on the molecular vibrational frequency, the absorption intensity depends on the change on dipole moment in the molecule. In order for energy to be transferred from the IR photon to the molecule, the molecular vibration must cause a change in the dipole moment of the molecule.[26, 27]

4.1.1.1 Fourier transform infrared spectroscopy (FTIR)

Fourier transform infrared spectroscopy (FTIR) is a technique that is used to obtain an infrared spectrum of absorption or emission of a solid, liquid or gas. An FTIR spectrometer simultaneously collects high spectral resolution data over a wide spectral range. This presents a significant advantage over previous generations of spectrometers which measured intensity over a narrow range of wavelengths at a time. Fourier transform infrared is a method of obtaining infrared spectra by collecting an interferogram of a sample signal using an

interferometer, and then performing a Fourier Transform (FT) on the interferogram to obtain the spectrum. An interferogram is a plot of intensity versus time. Interference is the combination of two or more electromagnetic waveforms to form a resultant wave. Interferometers work by merging two or more sources of light to create an interference pattern, which can be measured and analysed. Fourier transform is a mathematical operation that can separate the individual absorption frequencies from the interferogram, producing an intensity versus frequency spectrum. A FTIR spectrometer collects and digitizes the interferogram, performs the FT function, and displays the spectrum.[28]

4.1.2 Summary and research aims

In this chapter, the polymerisability of new terpene-based monomers described in Chapter 3 is studied. A wide range of terpene-based (meth)acrylate monomers were polymerised for the first time. The aim of this work was to explore the possibilities of these new monomers and to test their ability to perform as commercial (meth)acrylates and lead to polymers with interesting properties. Monomers were polymerised using conventional free radical polymerisation (FRP) techniques and the use of conventional chain transfer agents (CTAs) was tested to control polymer molecular weight. In the case of bifunctional monomers, FTIR-monitored polymerisations were conducted in order confirm or refute the presence of branching and/or crosslinking reactions.

4.2 Experimental

4.2.1 Materials

Unless otherwise stated, reagents were purchased from commercial sources and used without further purification. 2,2-Azobis(2-methylpropionitrile) (AIBN, 98%), 1,1'-azobis(cyclohexane-1-carbonitrile) (V88), cyclohexanone (99 %), dodecylmercaptan (98 %) chloroform ($CHCl_3$, 99 %) and dichloromethane (DCM, 99.5 %) were purchased from Sigma Aldrich. Methanol (99.8 %) was provided by VWR.

4.2.2 General polymerisation method

All polymerisation reactions were carried out under O_2-free conditions. Monomer was mixed with 0.5% of the corresponding initiator, the stated amount of chain transfer agent and dissolved in the corresponding solvent. In all cases the reaction flask was degassed through 3 freeze-pump-thaw cycles and then filled with argon and sealed. After reaction completion, reaction mixtures were cooled down in an ice bath for 10 min. Samples of reaction crudes were taken for ^{1}H-NMR analysis and conversion calculations. Polymers were purified by dissolving in the minimum amount of DCM, precipitated in methanol (DCM:methanol ratio was around 1:20), filtered and dried in a vacuum oven at 50ºC. Pure polymers were analysed by ^{1}H-NMR and GPC.

A typical experiment, in which α-pinene acrylate was polymerised in the presence of 5 mol% of DDM with respect to monomer, was conducted by placing 1 g of α-pinene acrylate (4.8 mmol), 0.5 wt% of AIBN (5 mg, 0.03 mmol), 5 mol% of dodecyl mercaptan (50 mg, 60 μL, 0.24 mmol), 1.5 mL of cyclohexanone and a magnetic stirrer into a 10 mL round bottomed flask. After sealing the reaction vessel with a septum, oxygen was removed through 3 cycles of freeze-pump-thaw. Subsequently, the reaction vessel was filled with argon and submerged into a pre-heated bath at 65 ºC. The reaction was stirred at 65 ºC for 24 h, after which the reaction vessel was removed from the oil bath and submerged into an ice bath for 10 min to quench the reaction. At this point, a sample was taken from the reaction crude, dissolved in $CDCl_3$ and analysed by ^{1}H-NMR to calculate the reaction conversion (95 %). Next, 1.5 mL of DCM was added to the reaction crude, which was then dripped into 30 mL of cold methanol to precipitate the polymer. Poly(α-pinene acrylate) was obtained as a white powder that was then filtered and dried in the vacuum oven at 50 ºC for 72 h. ^{1}H-NMR analysis of the pure polymer was conducted for characterisation purposes. GPC analysis revealed an average number molecular weight (M_n) of 4,800 g mol^{-1} and a dispersity of 1.34. DSC analysis showed a glass transition temperature (T_g) of 12 ºC. TGA analysis revealed a decomposition temperature of 285 ºC (See Annex).

4.2.3 Real Time Fourier Transform Infrared spectroscopy (RT-FTIR)

Real Time Fourier Transform Infrared Spectroscopy (RT-FTIR) analysis was carried out using a Perkin-Elmer Spectrum 2000 FT-IR instrument (Norwalk, CT) equipped with a single reflection (ATR: attenuated total reflection) accessory unit (Golden Gate) from Graseby Specac LTD (Kent, England), connected *in-situ* to a heater circular plate, and a TGS detector using the Golden Gate setup. Each spectrum collected was based on 16 scans averaged at 4.0 cm^{-1} resolution range of 600-4000 cm^{-1}. Data were recorded and processed using the software Spectrum from Perkin-Elmer.

Samples for FTIR analysis were prepared by dissolving 25 mg of monomer in 5 mL of $CHCl_3$. A stock solution of AIBN was prepared by dissolving 12.5 mg of AIBN in 5 mL of $CHCl_3$. Subsequently, 50 μL of the AIBN solution was added to the monomer solution and stirred. The final mix contained 0.5 wt% of initiator with respect to monomer. Two drops of the monomer/initiator mixture (~75 μl) were then applied onto the surface of the ATR diamond probe that had been pre-heated to the corresponding experiement temperature, and the measurements were started immediately.

4.2.4 Nuclear Magnetic Resonance (NMR)

All NMR spectra were obtained in $CDCl_3$ at room temperature using Bruker® DPX300 and Bruker® AV400 spectrometers for which chemical shifts are expressed in ppm relative to the solvent.

4.2.5 Gel Permeation Chromatography (GPC)

Polymers molecular weight and dispersity were analysed by Gel Permeation Chromatography (GPC) with a differential refractive index (dRI) detector. Samples were run on a Polymer Laboratories PL GPC 50 in THF. Samples were prepared as ~15 mg ml^{-1} solutions, filtered and injected into the GPC system at a flow rate of 1 ml min^{-1} and 40 °C, where they passed through the columns (1 x PLGel 5um guard, 2 x PLGel Mixed D 5um). The dRI detectors were calibrated

with PMMA narrow standards with molecular weight from 1,010 to 955,000 g mol^{-1}.

4.2.6 Differential scanning calorimetry (DSC)

TA- Q2000 DSC (TA instruments) was employed for thermal analysis of the polymers synthesised and described in this chapter. DSC equipment was calibrated with an indium standard and a heating/cooling rate of 10 °C/min was applied for all sample runs, with a nitrogen flow rate of 50 mL/minute, and a temperature range between 0 °C and 200 °C. Aluminium sample pans were employed with a sample mass of approximately 5 mg. The T_g was determined as the midpoint of the change in heat capacity during the second run for each sample.

4.2.7 Thermo Gravimetric analysis (TGA)

TA-Q500 TGA (TA instruments) was employed for determination of decomposition temperature (T_{dec}) of the polymers synthesised and described in this chapter. Samples were placed on platinum pans and heated from room temperature up to 500 ºC, at a heating rate of 10 °C/min, with a nitrogen flow rate of 50 mL/minute.

4.3 Results and discussion

A range of new terpene-based monomers was described in Chapter 3. In this chapter, terpene-based monomers are divided into monofunctional and bifunctional monomers and their ability to form polymers and the properties of those polymers will be investigated.

4.3.1 Synthesis of polymers from monofunctional terpene-based acrylate and methacrylate monomers.

Monofunctional monomers are those containing just one polymerisable double bond in their chemical structure. Five of the terpene-based monomers described in

Chapter 3 are monofunctional: α-pinene acrylate (**1b**), α-pinene methacrylate (**1c**), β-pinene acrylate (**2b**), β-pinene methacrylate (**2c**) limonene acrylate (**3b**) and limonene methacrylate (**3c**) (Figure 4-3). Limonene derivative **3b** is included in this category despite the fact that it contains two double bonds C=C in its chemical structure, since it was experimentally observed that only one of these double bonds is susceptible to radical polymerisation. Due to time limitations, synthesis of limonene methacrylate **3c** was not scaled up before the end of this PhD work and therefore its polymerisation reactions are not included in this thesis.

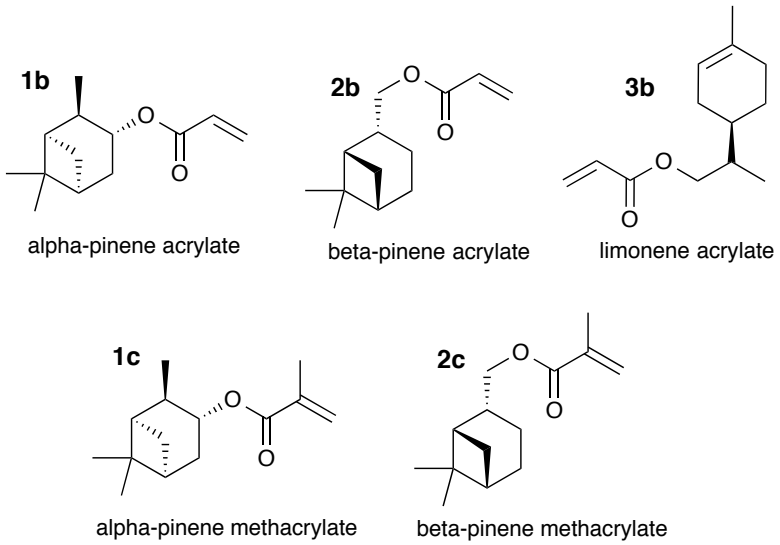


Figure 4-3. Monofunctional terpene-derived acrylate and methacrylate monomers.

In order to test the polymerisability of the terpene-derived monofunctional monomers, conventional free radical polymerisation (FRP) reactions were conducted, in the presence of 0.5 wt% of azobisisobutyronitrile (AIBN) as initiator (Table 4-1). In radical polymerisation of (meth)acrylate monomers, typical initiator concentrations range from 0.1 to 2 wt% with respect to the monomer.

*Table 4-1. FRP of terpene-based acrylate and methacrylate derivatives.**

Entry	Monomer	Conversion (%)[a]	M_n (g mol^{-1})[b]	Đ[b,c]
1	**1b**	≥95	47,200	2.3
2	**2b**	≥95	62,900	5.0
3	**3b**	≥95	19,000	4.2
4	**1c**	≥95	33,900	3,1
5	**2c**	≥95	106,500	5.8

*All reactions were carried out by mixing of 1g of monomer, 0.5 wt% of AIBN and 1.5 mL of cyclohexanone in a 10 mL round-bottomed flask. The mixture was previously degassed by freeze-pump-thaw technique and then heated up to 65 ºC for 24 h. [a]Determined by ^{1}H NMR. Values ≥95% indicate that less than 5% of monomer was detected in the NMR, being 5% the detection limit of the NMR equipment. [b]Determined by GPC-SEC in THF using PMMA standards. [c]Đ: Dispersity.

Each monomer was successfully polymerised with practically quantitative conversions. The analysis of the polymers revealed relatively high molecular weights. The dispersities observed were rather high from 2.3 to 5.8, which is characteristic of a FRP where no controlling agent is added. The minimum dispersities that can be obtained in a FRP are between 1.5 and 2. However, these are the limiting dispersity values in a system where monomer and polymer concentration remain constant, which is an incorrect assumption for batch polymerisations.[29] Therefore typical dispersities in FRP are higher than 2 and can be as high as 20.[30] These experiments (Table 4-1) confirmed the polymerisability of the new terpene-derived monomers.

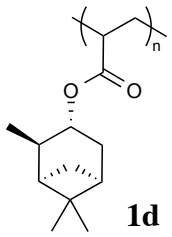
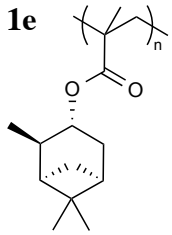
The next step consisted of polymerising these monomers using a chain transfer agent (CTA) to control the polymer molecular weight. The molecular weight of a polymer is important because it determines many physical properties such as transition temperatures, stiffness, strength and viscosity. Therefore, it is crucial to be able to control the molecular weight. Different concentrations of a conventional CTA, dodecyl mercaptan (DDM, Figure 4-4) were added to the polymerisation reactions of terpene-derived monomers. The glass transition temperatures (T_gs) of the new polymers were measured and the differences were carefully studied.



Figure 4-4. Chemical structure of dodecyl mercaptan.

Polymers with different molecular weights were successfully synthesised, with average molecular weight (M_n) decreasing with increasing amounts of CTA added, as expected (Table 4-2, Table 4-3, Table 4-4). The polymerisation reactions of the α-pinene derivatives **1b** and **1c** were carried out in the presence of 0.5%, 1% and 5% of DDM (Table 4-2).

*Table 4-2. Polymerisation of α-pinene based acrylate and methacrylate monomers.**

Entry	**Mon.**[a]	**Polymer structure**	**[DDM] mol%**	**Conversion (%)**[b]	**M_n (g mol^{-1})**[c]	**Đ**[c,d]	**T_g (°C)**
1	**1b**	 **1d**	5	≥95	4,800	1.34	12
2			1	≥95	15,100	2.04	63
3			0.5	≥95	23,600	2.20	71
4	**1c**	**1e** 	5	≥95	7,900	1.41	85
5			1	≥95	17,400	1.71	140
6			0.5	≥95	22,200	1.85	142

*All reactions were conducted by mixing of 1g of monomer, 0.5 wt% of AIBN and DDM in 1.5 mL of cyclohexanone in a 10 mL round-bottomed flask. The mixture was previously degassed by freeze-pump-thaw technique and then heated up to 65 ^{O}C for 24 h. [a]Monomer. [b]Determined by ^{1}H NMR. Values ≥95% indicate that less than 5% of monomer was detected in the NMR, being 5% the detection limit of the NMR equipment.. [c]Determined by GPC-SEC in THF using PMMA standards. [d]Dispersity.

By varying the amount of CTA added, polymers were produced with molecular weights ranging between 4,800 (Table 4-2, entry 1) and 32,600 g/mol (Table 4-2, entry 5). By controlling the molecular weight, the T_g is also controlled. It can clearly be seen that the T_g increases with molecular weight from 12 to 71 ºC for polymer **1d,** and from 85 to 142 ºC for polymer **1e**. This dependence of the T_g on the molecular weight in linear polymers is well known and was first described by the so-called Flory-Fox equation:

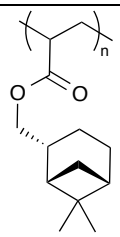
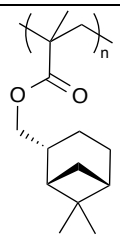
$$T_g(M)=T_g(\infty)-K/M$$

where $T_g(M)$ is the T_g of a polymer with certain molecular weight (M), $T_g(\infty)$ is the T_g of that polymer at an infinite molecular weight and K is a constant. The T_g is not just affected by the molecular weight but also by a variety of parameters such as chain stiffness, degree of crystallinity, tacticity and crosslink density.[31]

There is a considerable difference between the α-pinene based polyacrylates (**1d**) and polymethacrylates (**1e**) with T_gs in the ranges 12-71 ºC and 85-142 ºC respectively (Table 4-2). The presence of a methyl group in the chain backbone in methacrylates brings increased steric hindrance to segmental rotation, therefore increasing chain stiffness and raising the T_g value with respect to the acrylate polymers. This effect is experimentally observed in other polymers. For example, the T_g of poly(methyl methacrylate) (PMMA) is 115 ºC as opposed to 14 ºC for poly(methyl acrylate) (PMA). Another example is poly(α-methyl styrene) (PαMS) and polystyrene (PS), with T_gs of 168 ºC and 100 ºC respectively.[31]

The β-pinene based monomers **2b** and **2c** also yielded polymers with very high conversions and molecular weights as high as 31,500 g/mol for **2b** and 21,000 g mol^{-1} for **2c** (Table 4-3). The T_gs vary from -8 to 41 ºC for the acrylate polymer and from 65 to 115 ºC for the methacrylate analogue.

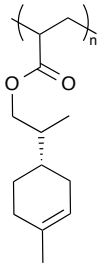
*Table 4-3. Polymerisation of β-pinene based acrylate and methacrylate monomers.**

Entry	Mon.[a]	Polymer structure	[DDM] (%mol)	Conversion (%)[b]	M_n (g mol^{-1})[c]	Đ[c,d]	T_g (°C)
1	**2b**	 **2d**	5	94%	4,200	1.31	-8
2			1	≥95	27,100	1.63	40
3			0.5	≥95	31,500	2.06	41
4	**2c**	 **2e**	5	≥95	8,000	1.34	65
5			1	≥95	14,500	1.45	101
6			0.5	≥95	21,000	1.53	115

*All reactions were coonducted by mixing of 1g of monomer, 0.5 wt% of AIBN and DDM in 1.5 mL of cyclohexanone in a 10 mL round-bottomed flask. The mixture was previously degassed by freeze-pump-thaw technique and then heated up to 65 °C for 24 h. [a]Monomer. [b]Determined by ^{1}H NMR. Values ≥95% indicate that less than 5% of monomer was detected in the NMR, being 5% the detection limit of the NMR equipment.. [c]Determined by GPC-SEC in THF using PMMA standards. [d] Dispersity.

The limonene-based monomer **3c** was also polymerised in the presence of different concentrations of DDM (Table 4-4).

*Table 4-4. Polymerisation reactions of limonene based acrylate monomer.**

Entry	Mon.[a]	Polymer structure	[DDM] %mol	Conversion (%)[b]	M_n (g mol^{-1})[c]	Đ[c,d]	Tg (°C)
1	**3b**	 **3d**	5	93	5,100	2.35	-18
2			1	90	13,000	1.87	-10
3			0.5	88	17,000	2.23	-5

*All reactions were conducted by mixing of 1g of monomer, 0.5 wt% of AIBN and DDM in 1.5 mL of cyclohexanone in a 10 mL round-bottomed flask. The mixture was previously degassed by freeze-pump-thaw technique and then heated up to 65 ^{O}C for 24 h. [a]Monomer. [b]Determined by ^{1}H NMR. Values ≥95% indicate that less than 5% of monomer was detected in the NMR, being 5% the detection limit of the NMR equipment.. [c]Determined by GPC-SEC in THF using PMMA standards. [d] Dispersity.

The absence of crosslinking suggests the lack of reactivity of the endocyclic double bond. This lack of reactivity was expected since trisubstituted double bonds do not normally polymerise through radical polymerisation due to steric hindrance.

Conversions were high and the molecular weights obtained were lower than those for monomers **1c**, **1d**, **2c** and **2d**, which suggests a lower propagation rate associated with this monomer. The T_g of a polymer is also influenced by the side groups' length and flexibility.[31] It can be seen how the T_g of the polyacrylates were affected by the terpene moiety when comparing entries 1 in Table 4-2, Table 4-3 and Table 4-4. T_g decreased in the order **1d>2d>3d** as the number of carbons with free rotation in the pendant terpene increased from 0 in **1d** to 2 in **3d**. The same effect was observed in the methacrylates, where **2e** had a lower T_g than **1e** due to a more flexible terpene moiety. In conclusion, a very wide range of T_gs has been observed. Future work will involve the synthesis of terpene-based copolymers. This flexibility should allow the synthesis of polymers with targeted physical properties.

4.3.2 Synthesis of polymers from bifunctional terpene-based acrylate and methacrylate monomers.

Terpene-derived bifunctional monomers (Figure 4-5) are discussed in this section.

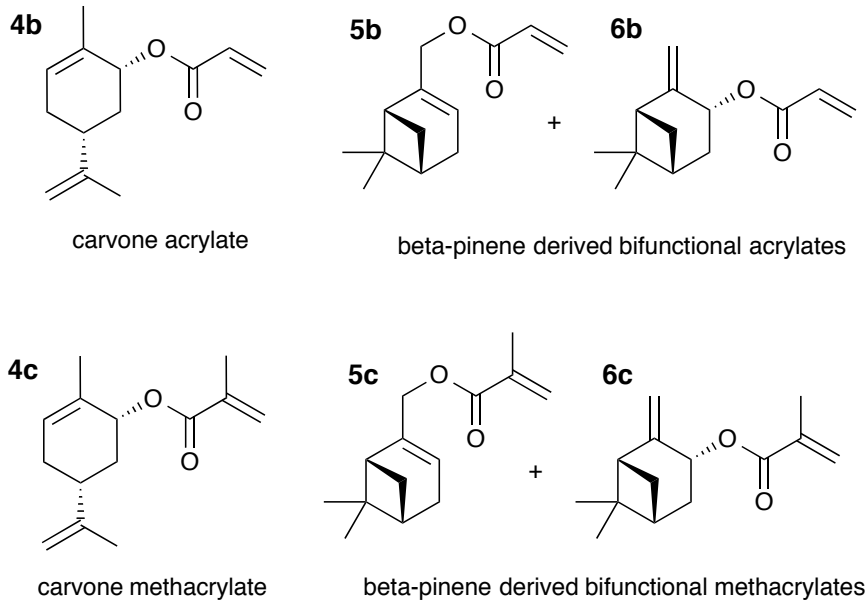


Figure 4-5. Terpene-derived new monomers with two or more unsaturated C=C bonds.

Carvone-derivatives **4b** and **4c** were obtained from esterification of carvone alcohol **4a**, as described in Chapter 3. As for monomers **5b**, **6b**, **5c** and **6c**, they were obtained from β-pinene *via* Pd catalysis. They differentiate from α- and β-pinene derived monomers **1b**, **1c**, **1b** and **2c** (Figure 4-3) in that they contain two double bonds in their chemical structure as opposed to just one. Monomers with two or more unsaturated C=C double bonds can in theory polymerise through both double bonds and therefore, they can lead to branched and crosslinked polymers, as opposed to monomers with only one C=C double bond, that can only lead to linear polymers (previous section). The differences between acrylate and methacrylate polymers were carefully studied.

4.3.2.1 Polymerisation of carvone acrylate and carvone methacrylate 4b and 4c.

order to test the susceptibility to polymerisation of the carvone-derived monomers **4b** and **4c,** conventional FRP reactions were conducted. Both

monomers were polymerised in the presence of 0.5 wt% of azobisisobutyronitrile (AIBN) as initiator at 65 ºC for 24 hr (Table 4-5).

Table 4-5. Polymerisation of carvone-derived monomers 4b and 4c in the presence of AIBN at 65 ºC.*

Entry	Monomer	T (ºC)	T (h)	Conversion (%)[a]	M_n (g mol^{-1})[b]	Đ [b,c]
1	Acrylate **4b**	65	24	5	ND[d]	ND
2	Acrylate **4b**	65	48	Crosslinked	ND	ND
3	Methacrylate **4c**	65	24	≥95	52,300	4.38

*All reactions were conducted by mixing of 1g of monomer, 0.5 wt% of AIBN and 1.5 mL of cyclohexanone in a 10 mL round-bottomed flask. The mixture was previously degassed by freeze-pump-thaw technique and then heated up to 65 ºC for 24 h. [a]Conversion of (meth)acrylic functionality determined by ^{1}H-NMR. Values ≥95% indicate that less than 5% of monomer was detected in the NMR, being 5% the detection limit of the NMR equipment.. [b]Determined by GPC-SEC in THF using PMMA standards. [c] Dispersity. [d] ND: Not determined.

Surprisingly, the polymerisation of carvone-based acrylate **4b** gave rise to a very low conversion (5%) (Table 4-5, entry 1), which suggests either low propagation rate, inefficient initiation, formation of stable (persistent) radicals and/or an unfavourable structural conformation towards polymerisation. When longer reaction times were allowed, an insoluble gel was obtained (entry 2), indicative of a crosslinked polymer.

As for the carvone-methacrylate monomer **4c,** it was succesfully polymerised to essentially quantitative conversion as expected. This was characteristic of a FRP where no controlling agent was added. ^{1}H-NMR of the precipitated polymer revealed that the methacrylate moiety was responsible for the polymerisation, with non-acrylic double bonds remaining essentially unreacted (Figure 4-6).

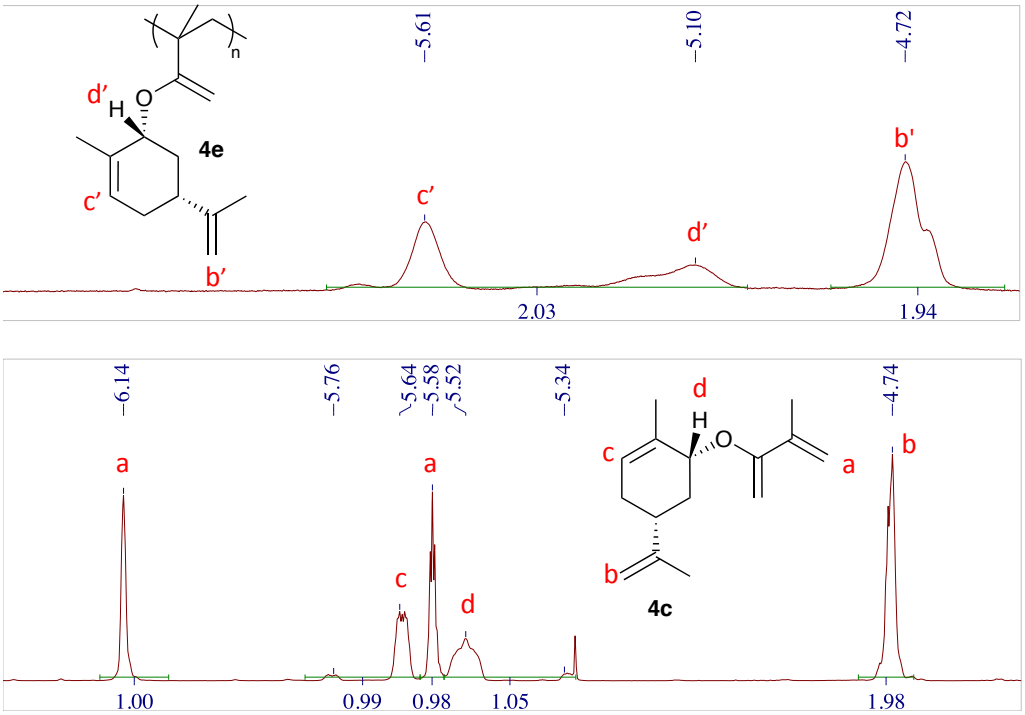


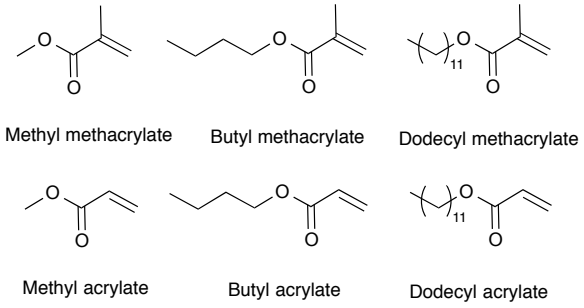
*Figure 4-6. ^{1}H-NMR of carvone-based methacrylate **4c** and poly(carvone methacrylate) **4e**. NMR spectrum of polymer product (top) shows that methacrylate signals (a) at 6.14 ppm and 5.58 ppm from the monomer spectrum (bottom) have disappeared. Meanwhile, non-acrylic olefinic hydrogens b and c remain unreacted as part of the polymer molecule, appearing at 5.61 ppm and 4.72 ppm.*

Subsequent analysis of the polymethacrylate polymer revealed a relatively high molecular weight of 52,300 g/mol and a dispersity (Đ) of 4.38, typical of a FRP (Table 4-5, entry 3).

It is striking that there is such a difference in reactivity between two monomers that only differ in one methyl group (acrylate **4b** contains a hydrogen on the α-carbon where methacrylate **4c** has a methyl group). Furthermore, acrylate monomers generally react and propagate faster than their methacrylate analogues. The reaction rate constant k is given by the Arrhenius equation $k=Ae^{(-Ea/RT)}$ where A is the Arrhenius constant, E_a is the activation energy, R is the gas constant and T is the reaction temperature. Acrylate monomers activation energies are generally lower than those of methacrylates (Table 4-6) and therefore their reaction rate constants k are higher.[32, 33]

Table 4-6. Activation energies of acrylate and methacrylate monomers.[32, 33]

Monomer	E_a (kJ mol^{-1})
Methyl methacrylate	22.4
Butyl methacrylate	22.9
Dodecyl methacrylate	21.0
Methyl acrylate	17.7
Butyl acrylate	17.4
Dodecyl acrylate	17.0



The difference between carvone-derived monomers **4b** and **4c** and conventional monofunctional (meth)acrylate monomers is that the first ones contain three double bonds in their chemical structure (labelled as **a**, **b**, **c** and **a'**, **b'**, **c'** in Figure 4-7) as opposed to just one.

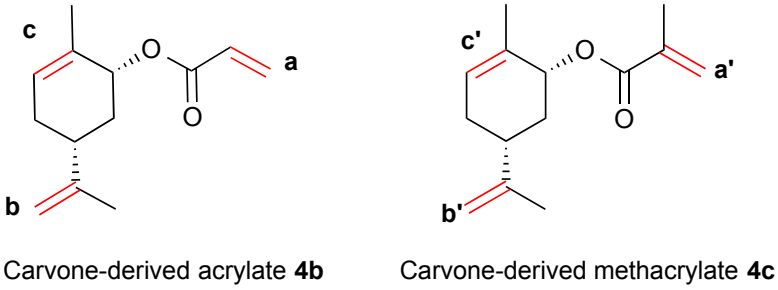


Figure 4-7. Carvone-derived monomers 4b and 4c showing double bonds highlighted in red.

This means that in addition to chain growth, both monomers can in theory branch and crosslink, forming an insoluble network as observed for carvone acrylate (Table 4-5, entry 2). However, polymethacrylate obtained from **4c** was soluble, which indicates the absence of crosslinking, and ^{1}H-NMR revealed double bond **b'** remains essentially unreacted. It is proposed that, for monomer **4c**, methacrylate double bond **a'** (Figure 4-7) was mainly responsible for the polymerisation, while secondary exocyclic double bond **b'** had a much lower reactivity at 65 ºC.

This can be explained by the lack of electron-withdrawing character and resonance stabilisation that the methacrylate group presents. It is also proposed that endocyclic double bond **c'** was too sterically hindered to participate in radical polymerisation reactions. When the possible radical attacks to a monomer unit are studied (Figure 4-8), there are two possibilities: attack to methacrylate functionality **a'** yielding a tertiary radical (**A1)**, or attack to double bond **b'** leading also to a tertiary radical (**A2)**.

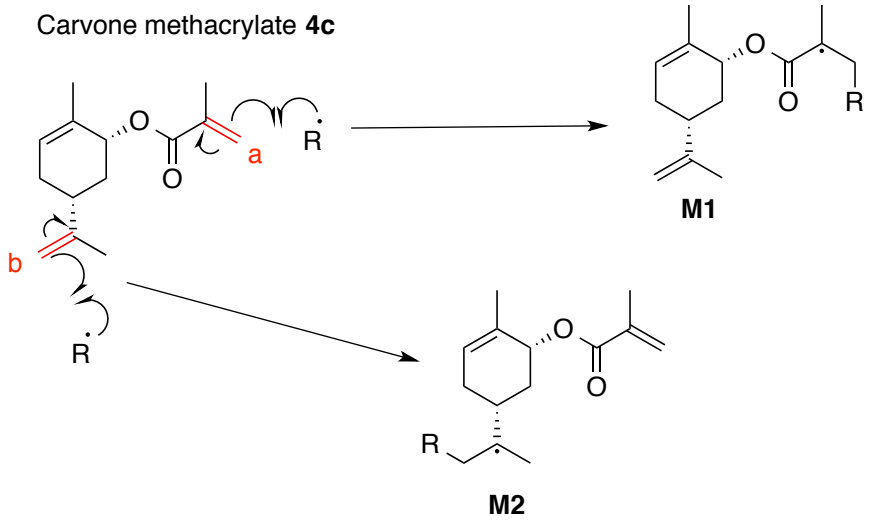


Figure 4-8. Possible radical structures formed after attack of a radical R to a carvone-based methacrylate monomer unit leads to two possible radicals M1 and M2.

However, when the same analysis is applied to the acrylate derivative (Figure 4-9), a radical attack to the acrylate moiety **a** would lead to a secondary radical **M1**, while a tertiary radical **M2** would form instead if attack takes place on the exocyclic double bond **b**.

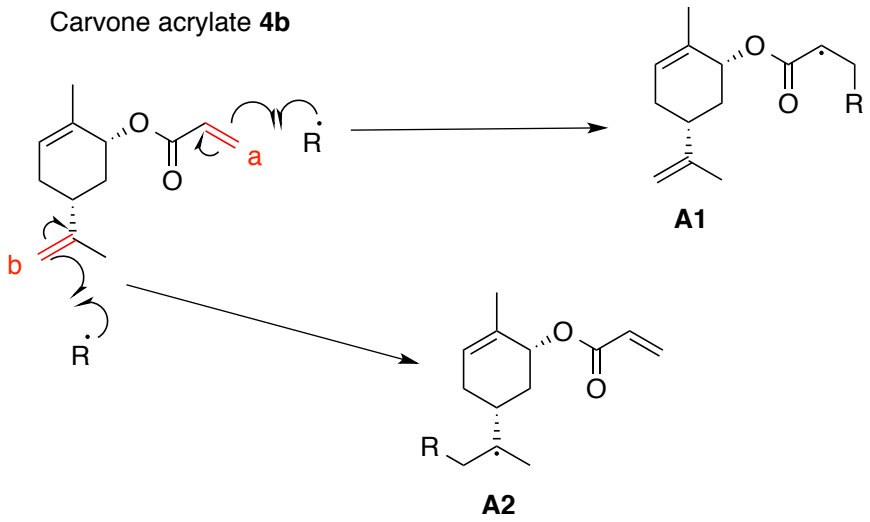


Figure 4-9. Possible radical structures A1 and A2 formed after attack of a radical R to a carvone-derived acrylate monomer.

Herein lies the explanation to the differences in reactivity between acrylate **4b** and methacrylate **4c**. As detailed above, the methacrylate functional group is mainly responsible for polymerisation in methacrylate monomer **4c**. In terms of stability both radicals **M1** and **M2** are tertiary radicals, therefore thermodynamically, one is not significantly favoured over the other one. The outcome of the reaction will then depend on the reaction rate. The electron-withdrawing character of the methacrylate functionality, that double bond **b'** lacks, activates the double bond towards polymerisation and acts as the driving force of the polymerisation reaction. However, in the case of acrylate derivative **4b**, there is a significant difference in stability between **A1**, which is secondary and very reactive, and **A2**, tertiary and therefore much more stable radical. The low acrylate **4b** conversion (Table 4-5, entry 1) suggests that the tertiary radical **A2** was preferably formed, and due to its stability and low reactivity towards polymerisation the reaction is essentially terminated. The gelling observed at long reaction times suggests that exocyclic double bond **b** did eventually react as well as the acrylic double bond **a**, leading to a crosslinked network.

If we look at the chemical structures of (meth)acrylates **4b** and **4c**, they can be partitioned into limonene plus methyl acrylate (MA) and limonene plus methyl methacrylate (MMA) respectively (Figure 4-10).

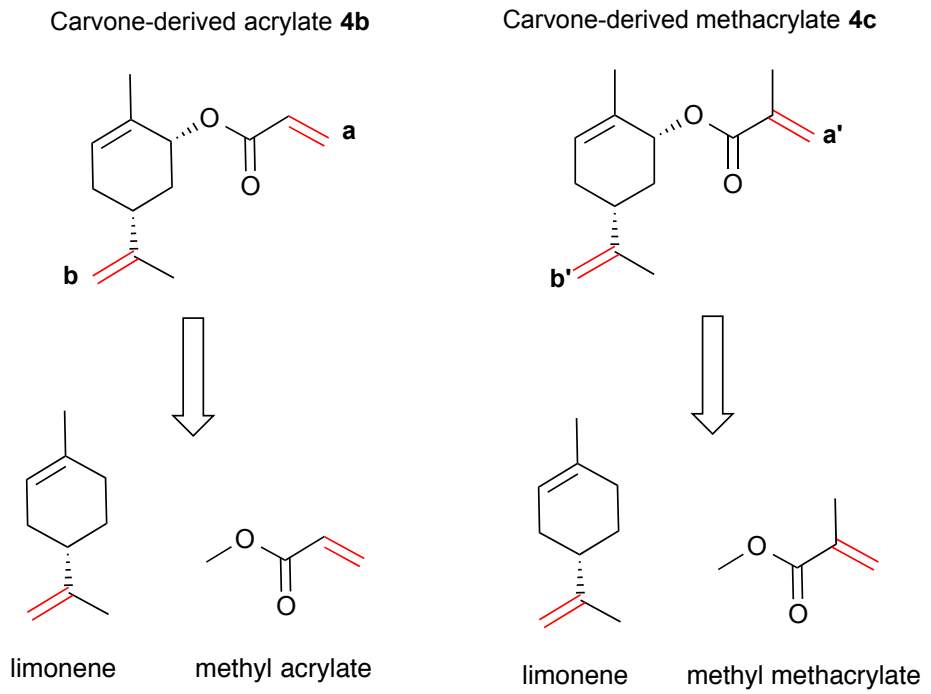


Figure 4-10. Carvone derived (meth)acrylates 4b and 4c have structures equivalent to the combination of limonene+methyl acrylate and limonene+methyl methacrylate respectively.

Therefore, it is interesting to compare the polymerisation results observed for monomers **4b** and **4c** and those of the copolymerisation reactions between limonene and methyl (meth)acrylate monomers conducted by Masuda *et al.*[34, 35] (Table 4-7).

Table 4-7. Radical polymerisation of limonene with MMA and MA reported in the literature.*

M_1 [a]	M_2 [b]	f_{limo} [c]	time (h)	% Conversion (Limo/(meth)acrylate)	M_n [d]	F_{limo} [e]
Limonene	MMA	0.5	120	≈0/98	13,800	0.01
Limonene	MA	0.5	490	18/65	9,700	0.21
Limonene	MMA	0.33	27	≈1/95	25,600	0.01
Limonene	MA	0.33	660	38/76	10,000	0.16

*Data extracted from Thesis Precision Radical Polymerisation of Plant-Derived Terpenes for Novel Bio-Based Polymers by Masaru Matsuda.[34] [a]Monomer 1. [b]Monomer 2. [c]Limonene fraction in monomer feed. [d]Average molecular weight. [e]Limonene fraction incorporated into the polymer.

It has been reported in the literature that it is difficult to copolymerise limonene with MMA, which generally leads to a fully converted poly(methyl methacrylate) (PMMA) homopolymer mixed with unreacted limonene.[34, 36] This behaviour is analogous to the one observed for methacrylate **4c** polymerisation, where the methacrylate functionality propagated while the non-acrylic double bond did not participate in the reaction. However, when limonene was reacted with MA instead, it was found that MA polymerisation was inhibited, leading to a limonene-co-methyl acrylate copolymer with low limonene incorporation (20%) and low conversions (Table 4-7). This is certainly comparable with acrylate **4b** polymerisation, since in both cases the reaction reaches only relatively low conversions, but with both acrylic and non-acrylic double bonds reacting.

A few attempts of copolymerisations between limonene and acrylate monomers have been reported before in the literature.[37, 38] The lack of publications is certainly due to the fact that it is difficult to copolymerise limonene with acrylate monomers because of the issues highlighted above. It has been proposed that this lack of polymerisability is caused by a chain transfer reaction where a growing polymer chain abstracts an allylic hydrogen from limonene, yielding a terminated polymer chain and a non-reactive allylic radical, and therefore terminating the reaction. Although it is possible that this reaction takes place during acrylate **4b** polymerisation (Figure 4-11), it does not explain the presence of crosslinking.

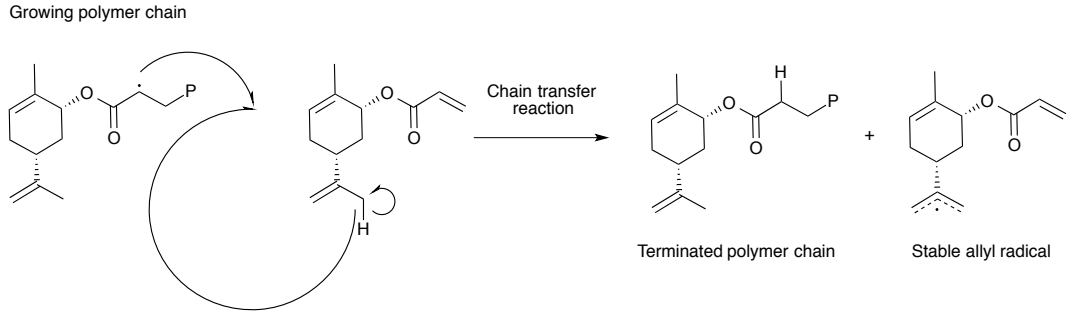


Figure 4-11. Chain transfer reaction from growing polymer chain to monomer. The acrylic radical abstracts a labile allylic hydrogen, yielding a terminated polymer chain and a stable allylic radical that is essentially unable to react.

A crosslinked network would only be generated by attack to the exoxyclic double bond, not by hydrogen abstraction.

As for the polymerisation of methacrylate monomer **4c**, it is also possible that a degradative chain transfer reaction analogous to the one shown in Figure 4-11 takes place. However, the fact that the monomer polymerised to full conversion indicates that such degradative chain transfer reaction is not inhibiting **4c** polymerisation.

In order to see if an increase in temperature would lead to a higher yield, a range of temperatures were tested between 65 ºC and 110 ºC (Table 4-8).

*Table 4-8. Polymerisation of carvone acrylate 4b in the presence of AIBN at different temperatures.**

Entry	**T (°C)**	**t (h)**	**Conv. (%)[a]**	**% branching[b]**	**M_n (g mol $^{-1}$)[d]**	**Đ[d,e]**
1	65	24	5	ND	ND	ND
2	65	48	Cross-linked			
3	80	4	21	<5[c]	ND	ND
4	80	24	29	<5[c]	18,600	1.33
5	80	48	Cross-linked			
6	90	3	30	20	27,400	14.1
7	90	4	Cross-linked			
8	110	5	38	3	4923	1.84
9	110	6	Cross-linked			

*All reactions were conducted by mixing of 1g of monomer, 0.5 wt% of AIBN and 1.5 mL of cyclohexanone a 10 mL round-bottomed flask. The mixture was previously degassed by freeze-pump-thaw technique and then heated up to the given temperatures. [a] Conversion of acrylic functionality determined by ^{1}H NMR. [b] Conversion of non-acrylic terminal double bond determined by ^{1}H NMR. [c] No decrease in integral value detected, detection limit of NMR equipment was 5%. [d]Determined by GPC-SEC in THF using PMMA standards. [e] Đ: Dispersity.

The experiments showed that increasing temperatures led to higher monomer conversions. At 80 ºC a conversion of 29 % was achieved after 24 h and a conversion of 30 % was measured after 3 h at 90 ºC. At 90 ºC a molecular weight

of 27,400 g/mol was obtained, while at 80 ºC the polymerisation yielded a polymer molecular weight of 18,600 g/mol. These results suggest that higher ratios of acrylate radical **A1** (Figure 4-9) were formed at higher temperatures. However these conversions are still rather low, even after reaction times long enough to allow the initiator to be practically consumed (AIBN half life is slightly higher than 1 h at 80 ºC and around 20 min at 90 ºC).

At longer reaction times the polymer crosslinked, yielding an insoluble gel that could not be analysed (Figure 4-8, entries 2, 5, 7 and 9). If one compares the reactions conducted at 80 ºC and 90 ºC, it can be seen that the dispersity of the polymer synthesised at 90 ºC is 14, indicative of a branched polymer, much higher than 1.33, the dispersity value obtained at 80 ºC. This implies that the reactivity of the stable tertiary radical **A2** is enhanced at higher temperatures (increase in the propagation rate would be expected at higher temperatures), therefore providing branching points and leading to branched or crosslinked polymers. ^{1}H-NMR confirmed the participation of the non-acrylic double bond in the polymerisation, with a decrease of around 20% in its integral value.

When the reaction was carried out at 110 ºC a conversion of 38 % was obtained after 5 h. In this case the dispersity was rather low (1.84) which might be due to the low molecular weight polymer synthesised. It is well known that when carrying out reactions in the presence of divinyl monomers (cross-linkers) the extent of the reaction at which gelation occurs can be increased by reducing the weight average chain length.[39] The half-life of AIBN at 110 ºC is of only a few minutes. Therefore, a high number of chains are initiated at the same time, yielding low molecular weight chains, and reducing the possibility of branching and crosslinking. ^{1}H-NMR showed a conversion of the non-acrylic double bond of around 3 %. We can conclude from the experiments where AIBN was used as initiator that higher temperatures provide higher conversions and higher degrees of branching, 38 % being the higher conversion obtained, at 110 ºC. In order to work with high temperatures to enhance monomer propagation, while keeping the concentration of radicals under control, which is to say, allowing a slower decomposition of the radical initiator, we tested 1,1'-azobis(cyclohexane-1-

carbonitrile) (V88) as initiator at 90 ºC and 110 ºC (Table 4-9). The half-life time of V88 is just under 10 h at 90 ºC, and 1h at 110 ºC.

*Table 4-9. Polymerisation of carvone-based acrylate 4b in the presence of V88 as initiator.**

Entry	T (ºC)	t (h)	Conv. (%)[a]	% branching[b]	M_n (g mol^{-1})[d]	Đ[d,f]
1	90	24	16	<5[c]	25,300	2.15
2	110	2	29	8	ND[e]	ND[e]
3	110	2.5	Cross-linked			

*All reactions were conducted by mixing of 1g of monomer, 0.5 wt% of V88 and 1.5 mL of cyclohexanone a 10 mL round-bottomed flask. The mixture was previously degassed by freeze-pump-thaw technique and then heated up to the given temperatures. [a]Conversion of acrylic functionality determined by ^{1}H NMR. [b]Conversion of non-acrylic double bond determined by ^{1}H NMR. [c]No decrease in integral value detected, detection limit of NMR equipment was 5%. [d]Determined by GPC-SEC in THF using PMMA standards. [e]Polymer blocked filter during sample preparation, which indicated a highly branched or cross-linked polymer that would block GPC equipment. [f] Đ: Dispersity.

At 90 ºC, after 2½ half-lives, conversions were very low (16%, entry 1) while molecular weight reached 25,300 g/mol. By comparing this result with that one obtained with AIBN under the same temperature (Table 4-8, entry 6, 30% conversion) we can dedude that conversion is not only dependent on the temperature, but also on the radicals concentration. Half-life at 90 ºC is around 15 min for AIBN and 10 h for V88. Therefore, at 90 ºC, the initiator decomposition rate is somewhere around 40 times higher for AIBN than that for V88. At 110 ºC in the presence of V88, acrylate and non-acrylic conversion after 2 h was 29 % and 8 % respectively. After 2.5 h, gelation was observed. When the polymerisation was undertaken at 110ºC using AIBN as initiator instead, higher conversion was achieved (38 %, Table 4-8) and gelation occurred at higher conversion. It can then be concluded that a higher concentration of radicals increased acrylate propagation. This can be explained by the fact that when a propagating radical attacks non-acrylate double bond **b** (Figure 4-9) the propagating chain gets essentially terminated due to the low reactivity of the radical formed. When the concentration of radicals is increased a greater number of chains are initiated and therefore overall conversion increases. In order to

synthesise a soluble, not-crosslinked polymer from carvone acrylate **4b**, it is necessary to suppress crosslinking by reducing average molecular weight. This can be accomplished by either generating a high concentration of initiator radicals (Table 4-8, entry 8) or by adding a chain transfer agent to the reaction. The use of a chain transfer agent in the polymerisation of carvone acrylate **4b** is discussed in the following section.

4.3.2.2 Polymerisation of carvone-derived (meth)acrylates in the presence of a chain transfer agent.

High radical concentration generated by rapid initiator decomposition had led to a low molecular weight polymer with the appearance of a viscous liquid (Table 4-8, entry 8). The alternative method to suppress crosslinking requires use of a chain transfer agent. In order to enhance monomer propagation while keeping the concentration of radicals low, V88 was chosen as initiator at 110 ºC. Dodecyl mercaptan (DDM) was added in order to increase the conversion before gelation occurs. Under these conditions, the polymer gelled after 5 h (Figure 4-10, entry 2).

*Table 4-10. Polymerisation of carvone-based acrylate 4b at 110 ºC, in the presence of V88 as initiator and 5 mol% of DDM as chain transfer agent.**

Entry	t (h)	Conversion (%)[a]	M_n (g mol^{-1})[b]	Đ[b,c]
1	4.5	60	10,600	8.34
2	5	Cross-linked	ND	ND

*All reactions were conducted by mixing of 1g of monomer, 0.5 wt% of V88, 5 mol% of DDM and 1.5 mL of cyclohexanone in a 10 mL round-bottomed flask. The mixture was previously degassed by freeze-pump-thaw technique and then heated up to the given temperatures. [a]Conversion of acrylic functionality determined by ^{1}H NMR. [b]Determined by GPC-SEC in THF using PMMA standards. [c]Đ: Dispersity

By stopping the reaction just before it crosslinked (entry 1), a branched polymer (Đ=8.34) was obtained with 60 % conversion and an average molecular weight of 10,600 g mol^{-1}. In order to gain a better understanding of the process, this polymerisation reaction was monitored by the analysis of samples taken every hour (Table 4-11).

Table 4-11. Progression of polymerisation for carvone acrylate 4b polymerisation at 110 °C, in the presence of V88 as initiator and DDM as chain transfer agent.

Entry	t (h)	Conversion (%)[a]	% Branching[b]	M_n (g mol^{-1})[d]	Đ[d,e]
1	1	35	<5[c]	4,600	1.70
2	2	44	6	6,500	2.84
3	3	52	9	8,600	4.82
4	4	60	13	10,600	8.34
5	5	Cross-linked	ND	ND	ND

*The reaction was carried out by mixing of 1g of monomer **4b**, 0.5 wt% of V88, 5 mol% of DDM and 1.5 mL of cyclohexanone in a 10 mL round-bottomed flask. The mixture was previously degassed by freeze-pump-thaw technique and then heated up to 110 °C for 4 h. [a]Conversion of acrylic functionality determined by ^{1}H-NMR. [b]Conversion of non-acrylic exoxyclic double bond determined by ^{1}H-NMR. [c] Detection limit of NMR equipment was 5%. No conversion was observed for non-acrylic double bond. [d]Determined by GPC-SEC in THF using PMMA standards. [e]Đ: Dispersity.

As conversion increased and the polymer chains grew, the level of branching also increased, leading to broader dispersities. This process of gradual branching is clearly observed in the GPC traces (Figure 4-12).

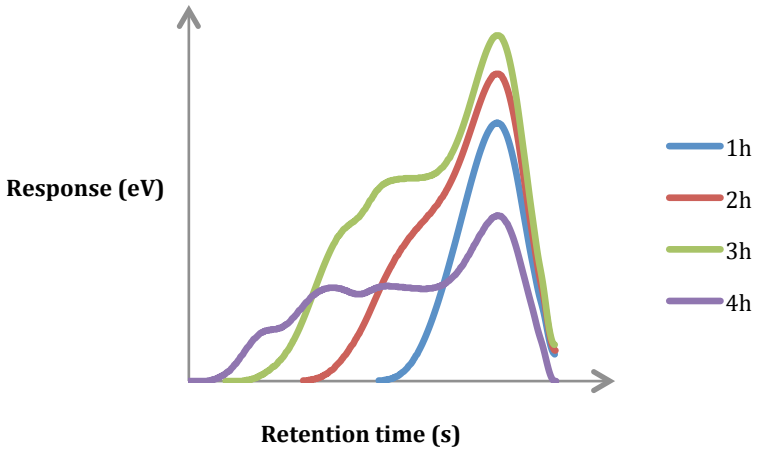


Figure 4-12. GPC traces of polymer product obtained at different reaction times during carvone-derived acrylate 4b polymerisation in the presence of DDM.

After 1 h of reaction the GPC trace showed a well-defined peak, but as the reaction proceeded, the peak got wider, showing several shoulders, characteristic of a branched polymer. ^{1}H-NMR also showed an increasing conversion of non-acrylic functionality, up to 13% after 4 h of reaction (Table 4-11, entry 4).

If these results are compared with those obtained in the absence of DDM (Table 4-9, entries 2 and 3), it can be seen that by adding a chain transfer agent, not only the extent of reaction before gelation was increased, but also the propagation of the acrylate double bond was enhanced. In the absence of DDM, after 2 h of reaction the conversion was 29 %. When 5 mol% of DDM was added to the reaction, the conversion after the same period of time, 2 h, was 44 %. The proposed chemical structure of the polymer obtained from carvone-based acrylate **4c** is shown in Figure 4-13.

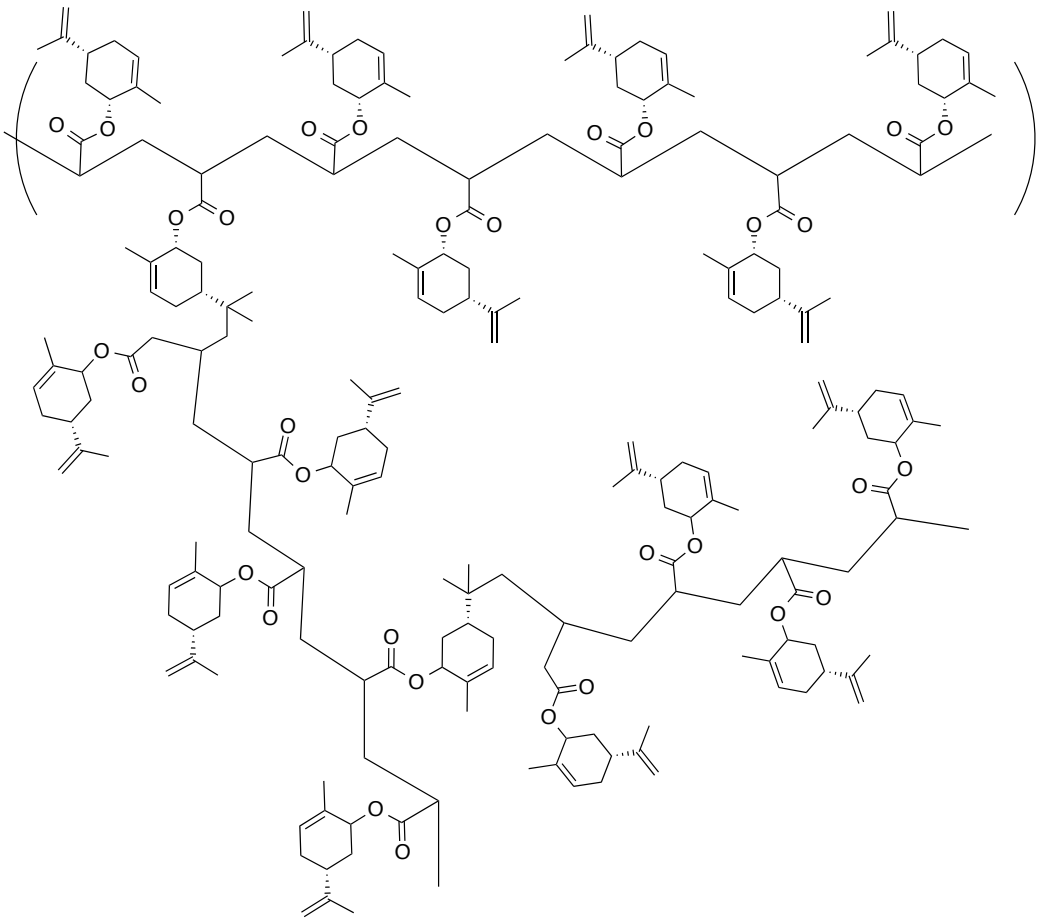
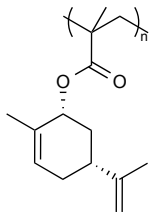


Figure 4-13. Chemical structure of the branched polymer obtained from the carvone-based acrylate 4c.

Regarding carvone methacrylate derivative **4c,** the fact that it does not crosslink during polymerisation allowed for the synthesis of linear polymers with different molecular weights. This monomer was polymerised in the presence of AIBN and different concentrations of DDM, at 65 ºC for 24 h. By adding DDM in concentrations between 0.5 % and 5 %, polymers with molecular weights ranging between 9,000 and 26,500 g mol^{-1} were obtained with dispersities between 1.59 and 2.40 (Table 4-12).

Table 4-12. Polymerisation reactions of carvone-based methacrylate monomer.

Entry	**Mon.**[a]	**Polymer structure**	**[DDM] mol%**	**Conversion (%)**[b]	**M_n (g mol^{-1})**[c]	**Đ**[c,d]	**T_g (ºC)**
1	**4c**		5	>95	9,000	1.59	90
2			1	>95	26,000	2.40	117
3			0.5	>95	26,500	2.24	117

*All reactions were carried out by mixing of 1g of monomer, 0.5 wt% of AIBN and DDM in 1.5 mL of cyclohexanone in a 10 mL round-bottomed flask. The mixture was previously degassed by freeze-pump-thaw technique and then heated up to 65 ºC for 24 h. [a]Monomer. [b]Determined by ^{1}H NMR. Values ≥95% indicate that less than 5% of monomer was detected in the NMR, being 5% the detection limit of the NMR equipment.. [c]Determined by GPC-SEC in THF using PMMA standards. [d]Đ: Dispersity

GPC analysis of the polymers obtained at 1 mol% and 0.5 mol% concentrations of DDM revealed molecular weights of 26,000 and 26,500 g mol^{-1} respectively. For any given monomer, there is a limiting molecular weight that can be achieved under a determined set of conditions. The limiting molecular weight is governed by chain transfer to monomer. All other termination steps, including chain transfer to CTAs, will only reduce further the molecular weight, below the limiting molecular weight determined by transfer to monomer.[40] It seems that, at 1 mol% of DDM the limiting molecular weight has been reached and, a decrease in the concentration in DDM did not provoke a rise in M_n or T_g.

In order to investigate further the reactivity of acrylic and non-acrylic unsaturated moieties in both acrylate **4b** and methacrylate **4c**, FTIR-monitored polymerisations were conducted, and are discussed in the following section.

4.3.2.3 FTIR-monitored polymerisation of carvone acrylate

A study of the reactivities of the different double bonds present in the chemical structure of both carvone acrylate **4b** and methacrylate **4c** was conducted *via* Fourier Transform Infrared Spectroscopy (FTIR). Reactions were conducted in the presence of 5 % of AIBN at 110 ºC in order to mimic the previous experimental conditions. Spectra of FTIR- monitored polymerisation of carvone acrylate **4b** can be seen in Figure 4-14.

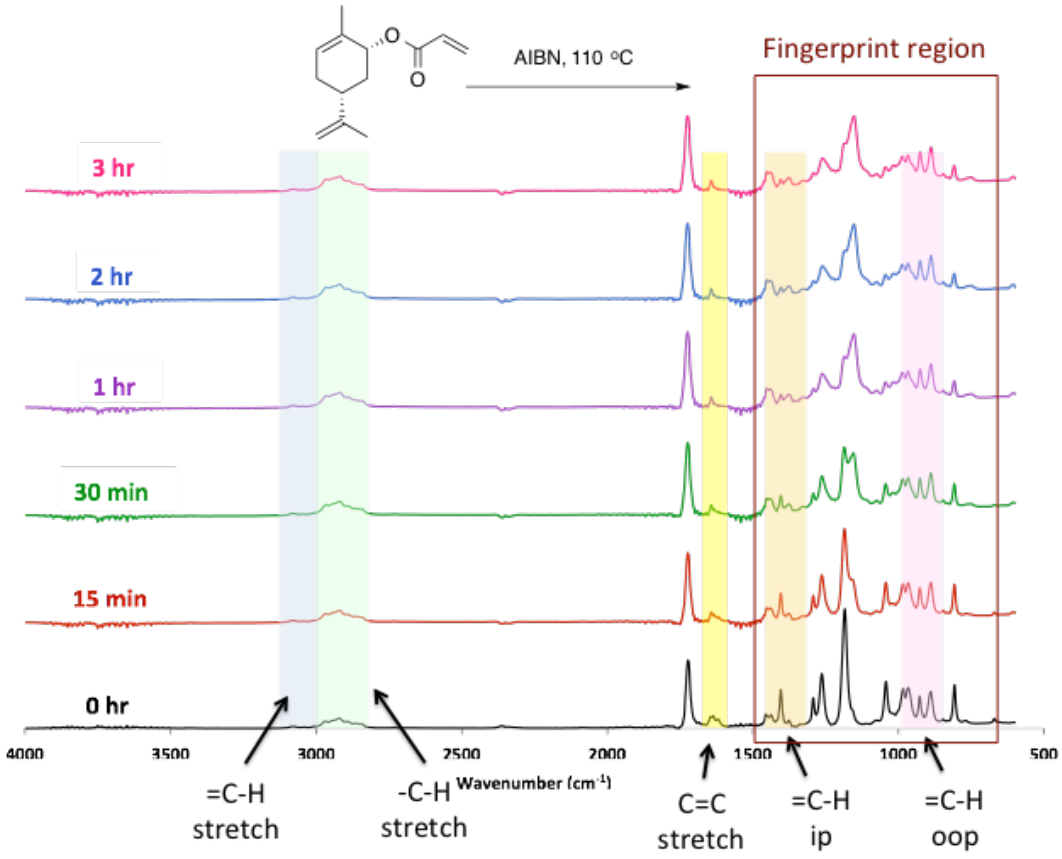


Figure 4-14. FTIR-monitored polymerisation of carvone-based acrylate monomer 4b. Coloured bands show the most representative bands in alkenes.

The bands appearing at the highest wavenumber (between 3100 and 3000 cm^{-1}) in the IR spectra correspond to =C-H stretch vibrations. However, these bands

overlap with each other and with other -C-H stretch bands from the molecule, becoming undistinguishable from each other and therefore not useful when monitoring the reaction. Additional bands (Figure 4-15) corresponding to alkene functionality are the C=C stretch vibrations, between 1660 and 1600 cm^{-1}, =C-H in plane bend (ip), normally between 1420 and 1290 cm^{-1}, and =C-H out of plane bend (oop), generally between 995 and 700 cm^{-1}.[41]

The region of the infrared spectrum below 1500 cm^{-1} is referred to as the "fingerprint region". This region is notable for the large number of infrared bands that are found here and it is often the most complex and confusing region to interpret. Most bending and skeletal vibrations absorb between 1500 cm^{-1} and 650 cm^{-1}. For these absorptions, small steric or electronic effects in the molecule lead to large shifts in the wavenumber at which bands appear in the IR spectrum. Therefore quite similar molecules give different absorption patterns at these frequencies, which makes it difficult to interpret.[42] For this reason, skeletal and bending vibrations are left unassigned in this work.

Other bands that can be observed in the spectra are the corresponding to the carbonyl group C=O stretch, appearing at 1723 cm^{-1} and the C-O stretch band that appears at 1184 cm^{-1} (Figure 4-15). C-O stretch bands characteristically exhibit high intensities because of the high dipole moment of the C-O bond.

These two bands shift slightly as the polymerisation proceeds due to a change in the chemical environment around the ester group, as it changes from monomer to polymer. The C=O stretch shift is practically undetectable visually. However the peak peaking revealed a very slight change in wavenumber from 1723 cm^{-1} (grey dotted line in Figure 4-15) to 1725 cm^{-1} (orange dotted line) A new C-O stretch band corresponding to polymerised acrylate appears at 1153 cm^{-1} and increases gradually in intensity over time, while the monomeric C-O stretch band at 1184 cm^{-1} decreases as the reaction proceeds.

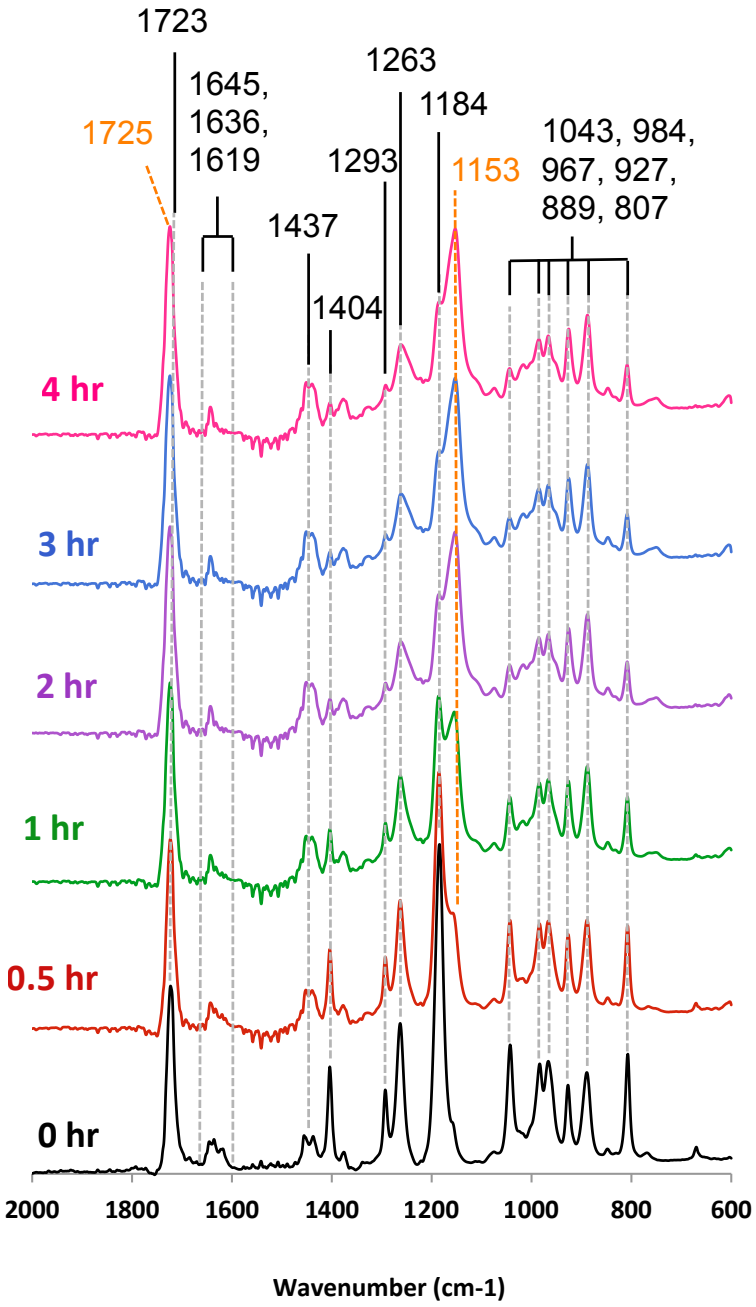


Figure 4-15. FTIR-monitoring of carvone-based acrylate monomer 4b – Zoom region between 600 and 2000 cm^{-1}. Peak wavenumbers in black correspond to peaks common to both monomer and reaction product. Those in orange correspond to new peaks that appeared as a consequence of polymer formation.

The most useful region in this study is that one between 1660 and 1600 cm^{-1}, where the C=C stretch bands appear (Figure 4-16).

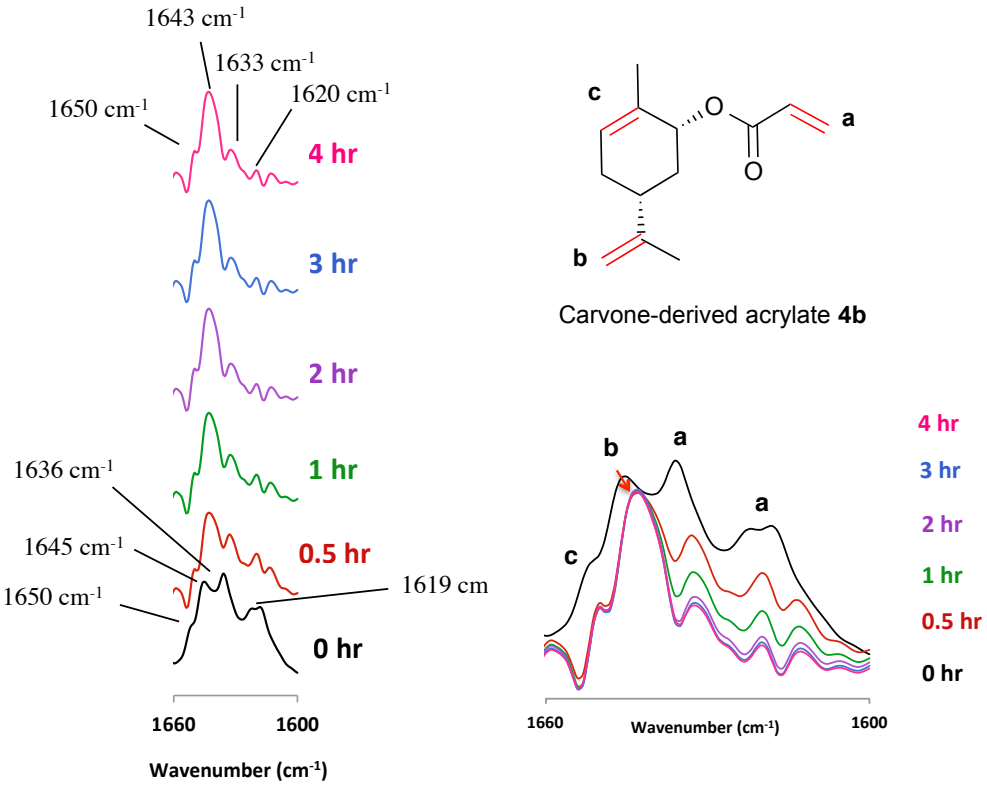


Figure 4-16. FTIR-monitored polymerisation of carvone acrylate 4b – Zoom region between 1660 and 1660 cm^{-1}(left). Carvone-derived acrylate monomer with double bonds highlighted in red and labelled as a, b and c (top right). Assignments are shown in overlapped spectra (bottom right), where red arrow points at peak wavenumber shift due to a decrease in double bond b population.

In the IR spectrum of the monomer (Figure 4-16, 0 h), three partially overlapped bands can be identified at 1645, 1636 and 1619 cm^{-1} and a small shoulder is observed at 1650 cm^{-1}. It is well known that conjugation with the carbonyl group leads to lower wavenumber as the double bond character decreases, while a higher level of substitution increases the wavenumber as a consequence of a stronger C=C bond.[43] Therefore it is expected that the the three double bonds appear in the order endocylic > exocyclic (non-acrylic) > acrylate. Tri-substituted double bonds generally absorb with low intensities because of the low dipolar moment as a consequence of substitution. Thus, the intensity of this band should be lower than the intensity of the bands associated with terminal double bonds.

Additionally, acrylate functionality can adopt an s-*cis* or s-*trans* configuration due to conformational isomerism, which leads to a doublet in the IR spectrum[44] (Figure 4-17). Hence, four peaks are observed.

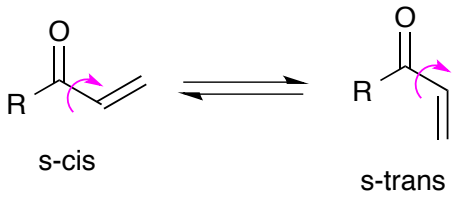


Figure 4-17. Conformational s-cis and s-trans isomerism in acrylates. Due to free rotation around the single double bond the carbonyl and C=C double bond can adopt an s-cis or s-trans conformation. Each conformation gives rise to a vibrational mode, hence leading to a doublet in the IR spectrum.

When the C=C stretch region in the IR spectra of limonene and methyl acrylate is examined, it can be observed that the peaks of these two compounds combined, which led to a spectrum equivalent to carvone acrylate **4b** spectrum (Figure 4-18).

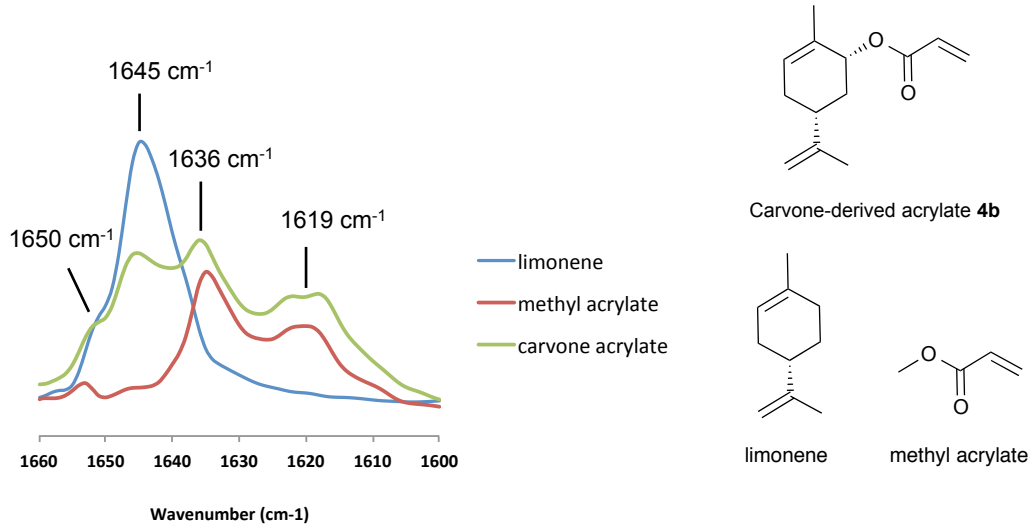


Figure 4-18. Overlapped IR spectra of limonene, methyl acrylate and carvone acrylate 4b (left), showing C=C stretch bands in the region between 1660 and 1600 cm-1. Chemical structures of carvone acrylate 4b, limonene and methyl acrylate are shown at the right.

It is therefore proposed that peaks at 1619 cm^{-1} and 1636 cm^{-1} are the doublet corresponding to the acrylate group, while the peak at 1645 cm^{-1} corresponds to the non-acrylic exocyclic double bond and the shoulder at 1650 cm^{-1} corresponds to the endocyclic double bond.

In the FTIR spectra taken at different reaction times between 0 h and 4h (Figure 4-16), it is clear that acrylate peaks at 1636 cm^{-1} and 1619 cm^{-1} decrease dramatically in intensity, indicative of a consumption of acrylate functional groups due to polymerisation. As for the peak at 1645 cm^{-1} and the shoulder observed at 1650 cm^{-1}, they both decrease in intensity. It can also be observed that the peak at 1645 cm^{-1} shifted towards a lower wavenumber, at 1643 cm^{-1} and that the shoulder corresponding to internal double bond **c,** at 1650 cm^{-1} became more pronounced.

When two bands are closely overlapped, the apparent peak position shifts because of a change in the chemical species population. The individual frequencies of both bands remain essentially unchanged, but peak maxima shift due to the variation in the relative intensity contributions of the overlapped bands.[45] In this case, the peak shifting towards a lower wavenumber can only be explained as a consequence of exocyclic double bond **b** consumption; since it is assumed that internal double bond **c** does not participate in the reaction, as confirmed by ^{1}H-NMR. A decrease in population of exocyclic double bond **b**, has a direct effect on its peak positions, and a decrease in intensity of peaks corresponding to double bonds **b** and **c**.

It is therefore clear from the IR spectra that both terminal bonds, acrylic **a** and non acrylic **b**, take part in the polymerisation reaction. Quantitave calculations of the reactivity ratios cannot be obtained since the three peaks corresponding to the three double bonds overlap. However, it is clear that the peak corresponding to the acrylate functionality decreases dramatically in intensity while the drop in intensity of the non-acrylic double bond is much less pronounced (Figure 4-16). Qualitative relative propagation constants can be proposed for carvone acrylate **4b** polymerisation at 110 ºC. The possible radical additions during the

polymerisation of carvone-based acrylate monomer **4b** are shown below in Figure 4-19 and Figure 4-20.

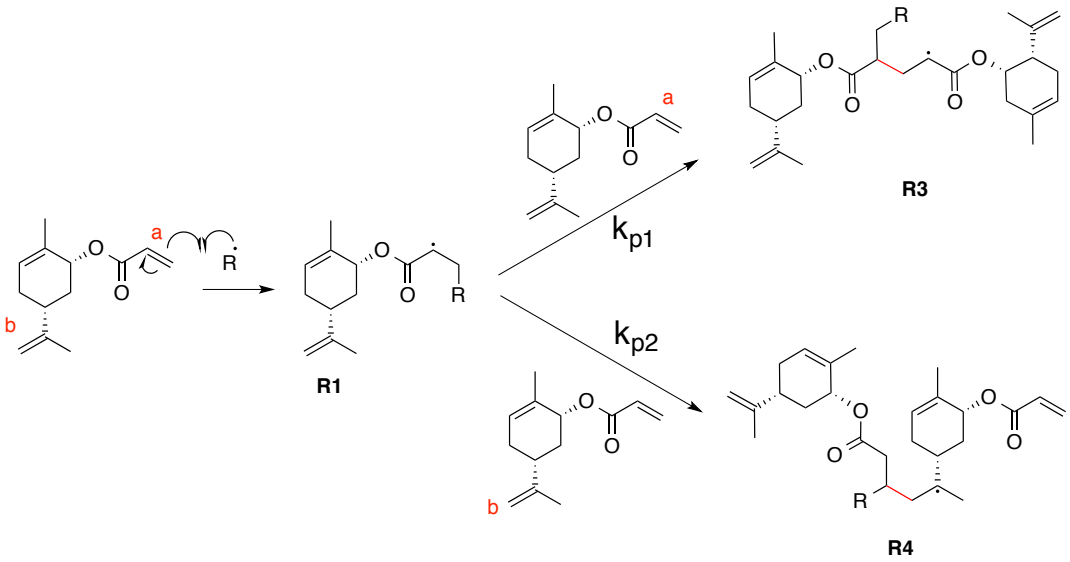


Figure 4-19. Representation of the two possible radical additions of acrylate radical R1 to a carvone-based acrylate monomer unit.

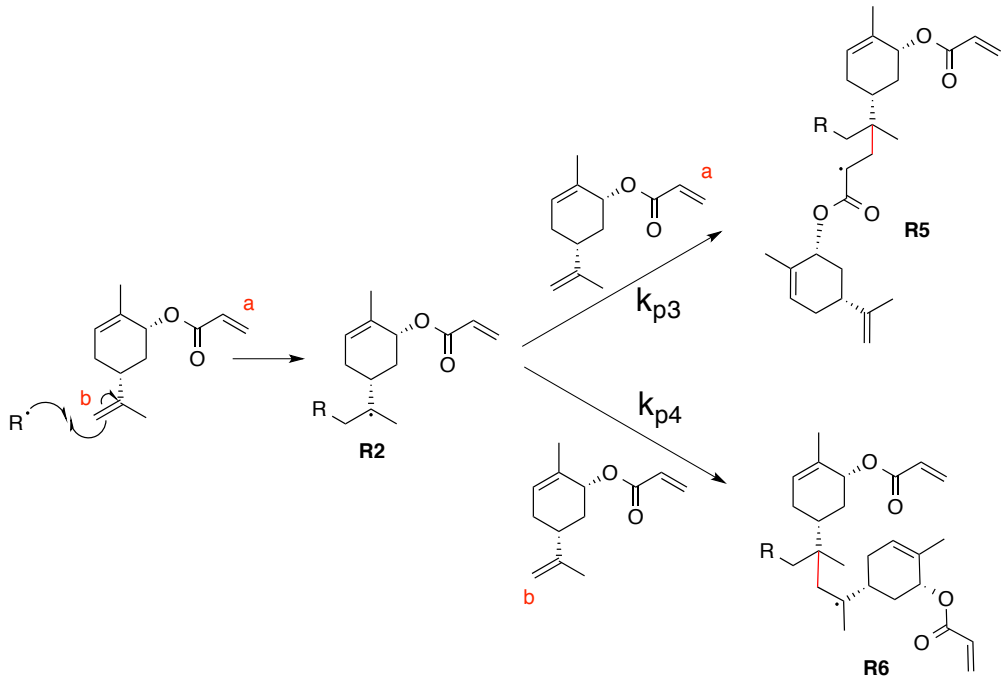


Figure 4-20. Representation of the two possible radical additions of acrylate radical R2 to a carvone-based acrylate monomer unit.

It is proposed that the propagation step in which acrylate radical **R1** reacts with the acrylate double bond **a** of a monomeric unit has a higher propagation constant

(k_{p1}) than the reaction between radical **R1** and the exocyclic double bond **b** (k_{p2}), since double bond **b** lacks the electron-withdrawing character of the acrylate group (Figure 4-19). Regarding the reactivity of radical **R2** (Figure 4-20), it is logical to assume for the same reason that the propagating reaction (k_{p3}) is noticeably faster than the reaction between **R2** and the exocyclic double bond **b** from the monomeric unit (k_{p4}).

When comparing k_{p1} and k_{p3}, the results observed in **4b** polymerisation reactions show that the acrylate double bond **a** is much more reactive than **b** (section 4.3.2.1), with the acrylic moiety **a** being mainly responsible for the polymerisation at 110 ºC. Therefore the propagation constants for the four possible radical additions showed in Figure 4-19 and Figure 4-20 can be related as follows: $k_{p1}>k_{p2}>k_{p3}>k_{p4}$

4.3.2.4 FTIR-monitored polymerisation of carvone methacrylate

FTIR-spectra of carvone methacrylate polymerisation at different reaction times are shown in Figure 4-21.

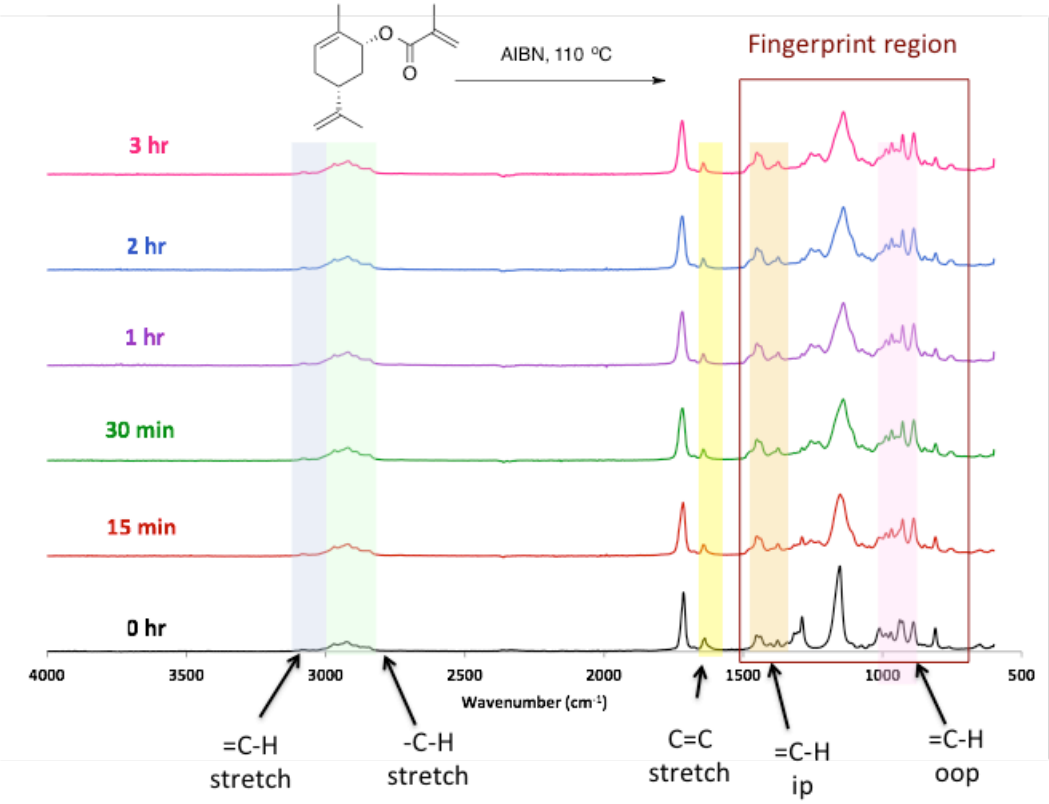


Figure 4-21. FTIR-monitored polymerisation of carvone-derived methacrylate monomer 4c.

Similar to the carvone-based acrylate spectra (Figure 4-14), the =C-H stretch region between 3100 and 3000 cm^{-1} does not provide much information about the reaction because these bands overlap each other and other C-H stretch absorptions. Other bands are easily identified such as the C=C stretch between 1660 cm^{-1} and 1600 cm^{-1}; the C=O stretch absorbing at 1715 cm^{-1} in the monomer and at around 1720 cm^{-1} in the polymer; and the C-O stretch that shifts from 1154 cm^{-1} to 1117 cm^{-1} during the polymerisation reaction (Figure 4-22). The rest of the bands observed in the spectra correspond to =C-H in plane and out of plane bending, and skeletal vibrations. These bands appear in the fingerprint region and are not easily identifiable.

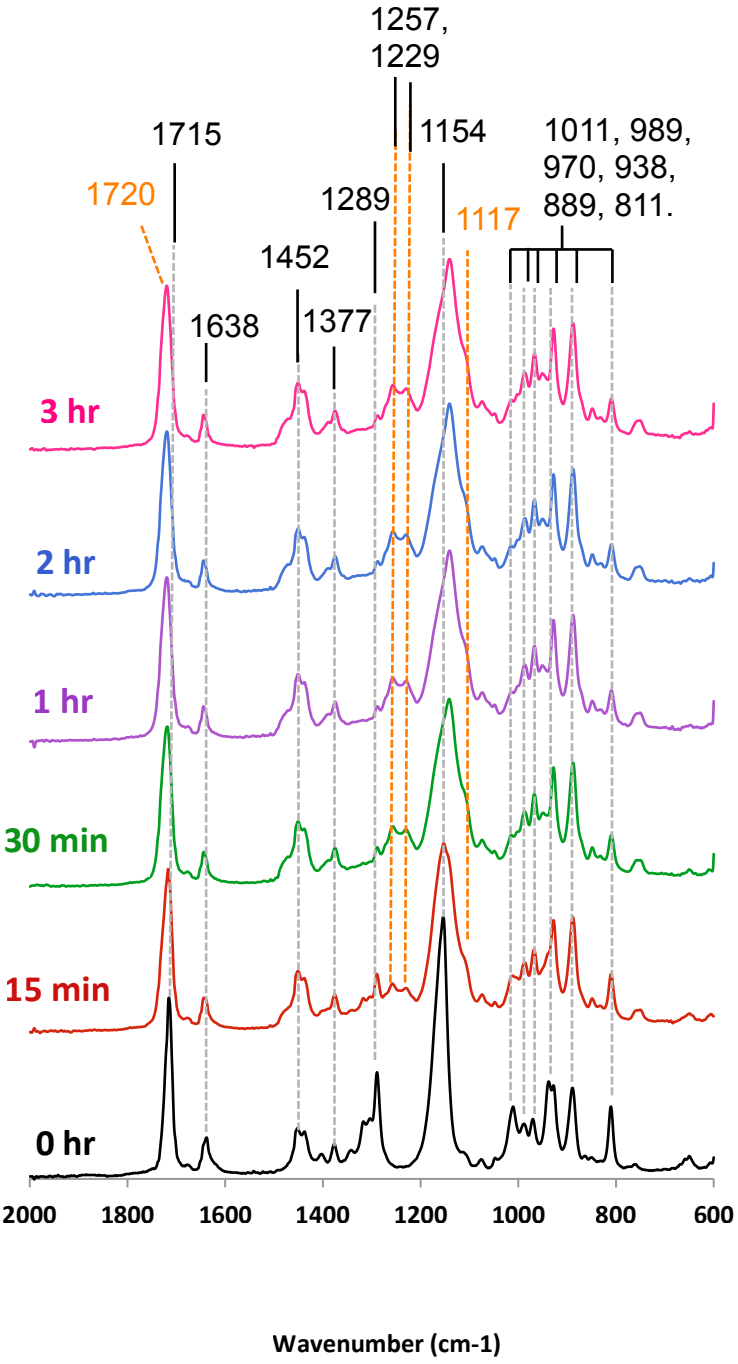


Figure 4-22. FTIR-monitored polymerisation of carvone-derived methacrylate monomer 4c - Zoom region between 600 and 2000 cm-1. Peak wavenumbers in black correspond to peaks common to both monomer and reaction product. Peak wavenumbers in orange correspond to new peaks that appeared as a consequence of polymer formation.

However, a comparison of the reactivity between the different double bonds in the structure of carvone methacrylate **4c** can be made by studying the region between 1660 cm^{-1} and 1600 cm^{-1} (Figure 4-23).

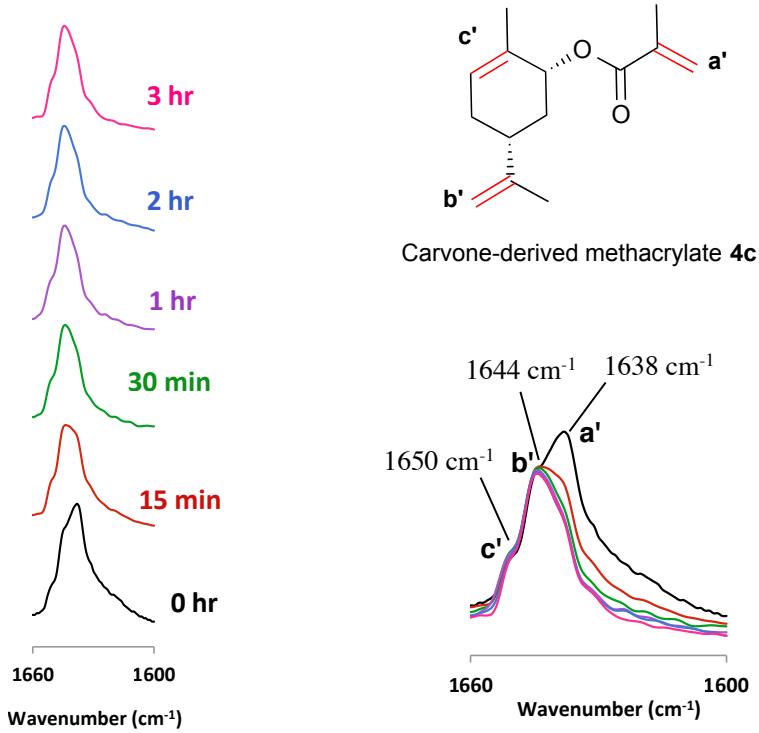


Figure 4-23. FTIR-monitored polymerisation of carvone methacrylate 4c – Zoom region between 1660 and 1660 cm^{-1} (left). Carvone-derived methacrylate monomer with double bonds highlighted in red and labeled as a', b' and c' (top right). Assignments are shown in overlapped spectra (bottom right).

At 0 h (monomer), one peak with three shoulders at 1650, 1644 and 1638 cm^{-1} can be observed. Considering the effects of conjugation and substitution on absorption wavenumber as explained in the previous section, it is proposed that the peak maximum at 1638 cm^{-1} corresponds to the acrylate C=C stretching vibration, while peaks at 1644 cm^{-1} and 1650 cm^{-1} correspond to double bonds **b'** and **c'** respectively.

A comparison with limonene and methyl methacrylate IR spectra supports these assignments (Figure 4-24). Methyl methacrylate shows a C=C stretching band at 1638 cm^{-1}, while the limonene spectrum presents a band with a peak maximum at

1644 cm^{-1} and a shoulder at 1650 cm^{-1}, corresponding to exocyclic and endocyclic double bonds respectively. These peaks in limonene and methyl methacrylate appear in the IR spectrum at the same wavenumbers as those observed in carvone methacrylate **4c** spectrum (Figure 4-23). In the overlapped spectra (Figure 4-23), it is clearly seen that as the reaction proceeds, the acrylate peak maximum at 1638 cm^{-1} considerably diminishes while the other two peaks remain practically invariable. These data confirm that carvone methacrylate reacts only through its methacrylate functionality, yielding linear polymers.

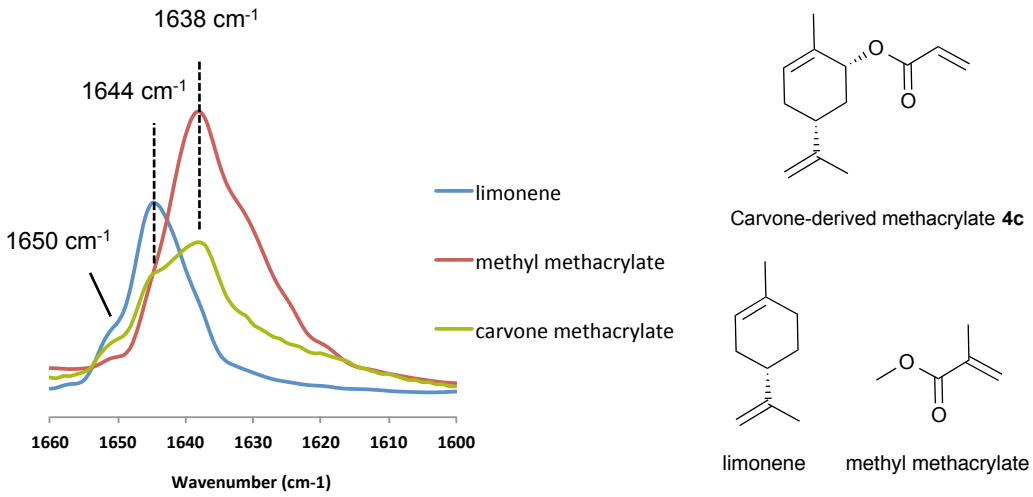


Figure 4-24. Overlapped IR spectra of limonene, methyl methacrylate and carvone methacrylate 4c (left), showing C=C stretch bands in the region between 1660 and 1600 cm^{-1}. Chemical structures of carvone methacrylate 4c, limonene and methyl acrylate are shown at the right.

4.3.2.5 Polymerisation of bifunctional β-pinene (meth)acrylate derivatives.

Polymerisation reactions of monomers **5b**+**6b** and **5c**+**6c** (Figure 4-25), which were obtained *via* catalysis (Chapter 3), are described in this section. These monomers were obtained as a mix of regioisomers which were difficult to separate and were therefore polymerised as a mixture.

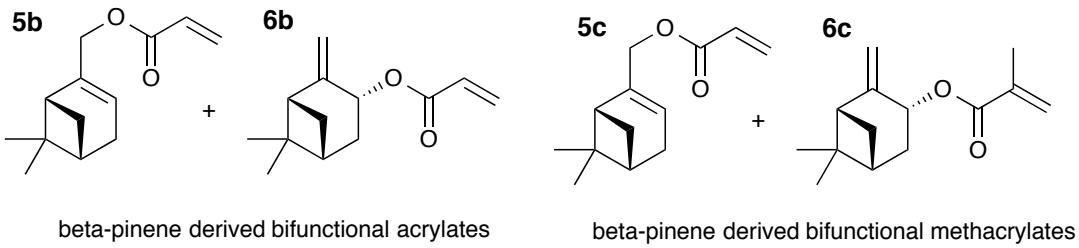
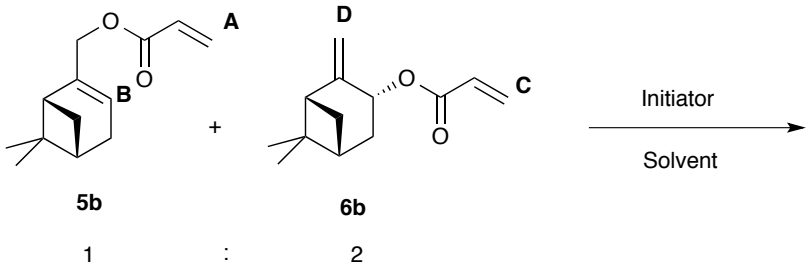


Figure 4-25. Chemical structure of β-pinene derived acrylates 5b and 6b, and methacrylates 5c and 6c.

To start with, a monomer mix containing β-pinene derived acrylates **5b** and **6b** in a 1:2 ratio was mixed with 5 % of AIBN as initiator and 1.5 mL of cyclohexanone as solvent (Table 4-13, entry 1).

Table 4-13. Polymerisation reactions of β-pinene derived acrylates 5b and 6b.



Entry	I[a]	T (ºC)	t (h)	Conversion (%)[b]		Mn (g mol^{-1})[c]	Đ[c,d]
				A+C	D		
1	AIBN	65	24	22	4.5	21,000	3.1
2	AIBN	90	3	25	8.5	20,300	2.7
3	V88	110	3	42	10	13,000	1.9

*All reactions carried out by mixing of 1g of monomer mix, 0.5 wt%. of initiator and 1.5 mL of cyclohexanone in a 10 mL round-bottomed flask. The mixture was previously degassed by freeze-pump-thaw technique and then heated up to the corresponding temperature. [a] Initiator. [b] Conversion determined by ^{1}H-NMR. [c] Determined by GPC-SEC in THF using PMMA standards. [d]Đ: Dispersity

The mix was stirred at 65 ºC for 24 h (around 2.5 half-lives), after which the reaction was quenched and the product was analysed by ^{1}H-NMR and GPC. ^{1}H-NMR analysis of the crude revealed that total acrylate conversion was only 22%, while 4.5% of non-acrylic double bond in **6b** reacted (Figure 4-26).

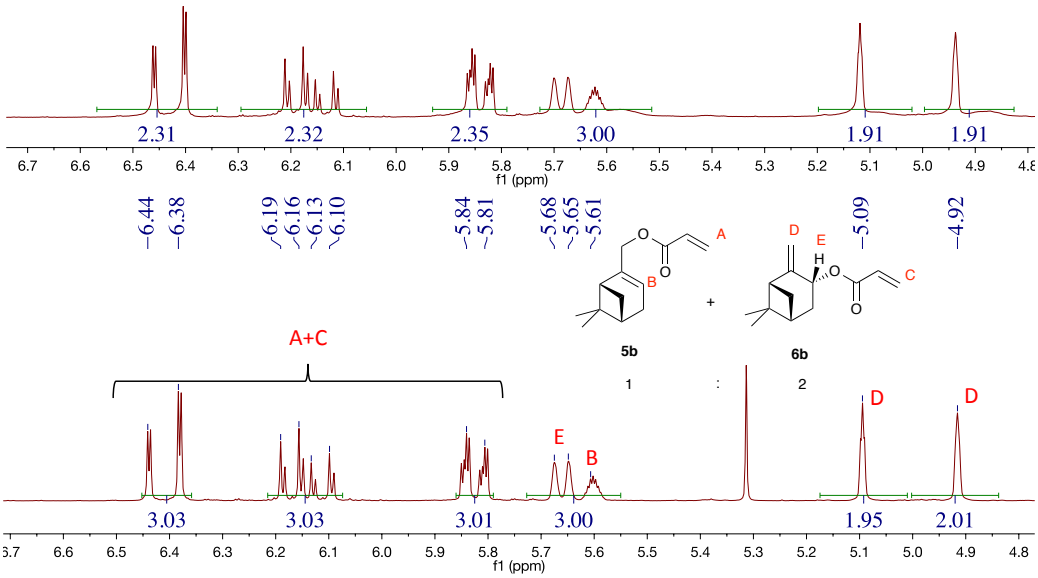


Figure 4-26. ^{1}H-NMR spectra of pinene-based acrylates 5b and 6b before (bottom) and after polymerisation at 65 °C (top). A decrease in integrals value of acrylate and non-acrylic double bonds indicates that both functionalities reacted.

The signal corresponding to the hydrogen in the internal double bond in **5b** showed that this functionality remained unreacted, as expected from a sterically hindered tri-substituted double bond. GPC analysis of the polymer showed a relatively high molecular weight of 21,000 g/mol and a dispersity of 3.1. This dispersity value is typical of a FRP and does not indicate a high level of branching. Hyperbranched polymers typically exhibit dispersity values between 5 and 25.[46, 47]

In order to increase conversion, a higher temperature of 90 ºC was tested (Table 4-13, entry 2). AIBN half-life at 90 ºC is of 20 min. Therefore after 3 h esentially all initiator radicals have been consumed. However, at this temperature, a very slight increase in acrylate conversion was observed from 22 % to 25 %, while 8.5 % of the non-acrylic functionality reacted. GPC analysis of the product revealed similar molecular weight and dispersity with values of 20,300 g mol^{-1} and 2.7 respectively. In order to test the effect of a further increase in temperature while

keeping the same radical concentration, V88 was used as initiator at 110 ºC (entry 3). This increase in temperature caused a rise in conversion from 25 % at 90 ºC to 42 % at 110 ºC. Acording to ^{1}H-NMR integrals, 10 % of non-acrylic double bond **D** reacted. A new signal (F) integrating for around 10 % is also observed in the spectrum (Figure 4-27).

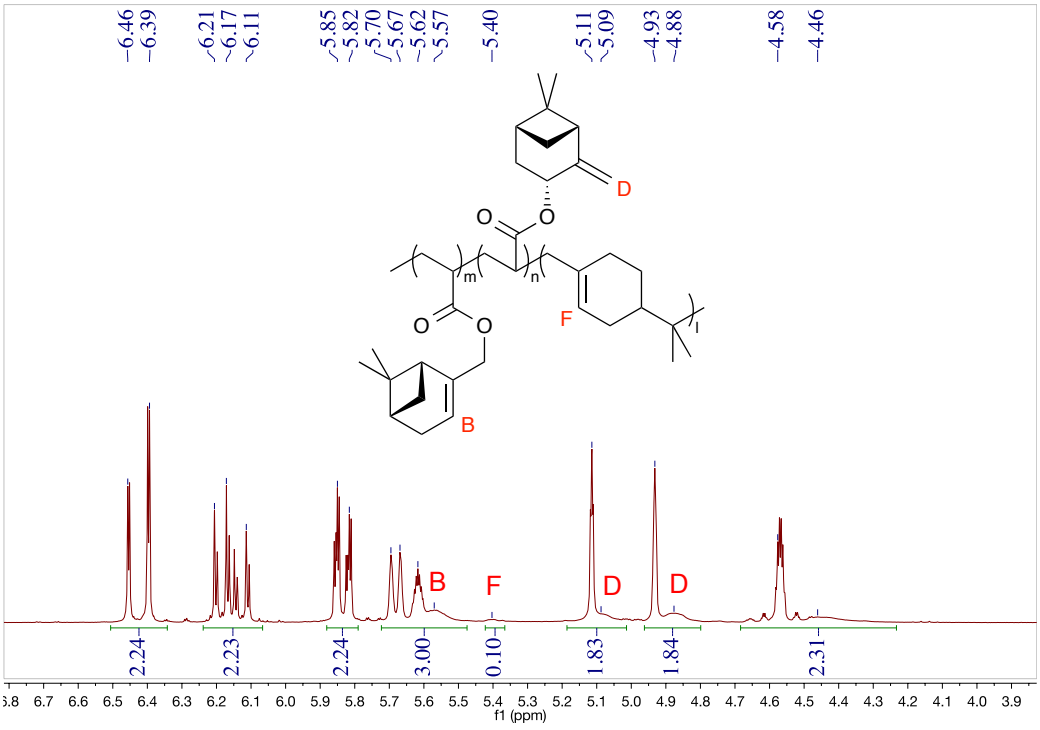


Figure 4-27. ^{1}H-NMR spectrum of reaction crude of 5b+6b polymerisation. Unsaturations in the polymer structure are labelled as B, D and F.

This signal corresponds to isomerised monomer **6b** units (Figure 4-28).

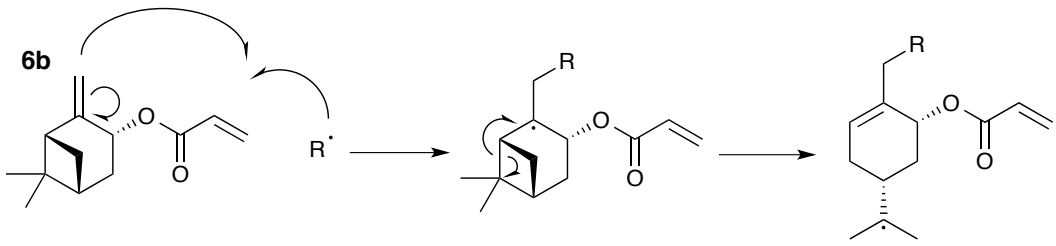


Figure 4-28. Isomerisation of monomer 6b during radical polymerisation. After radical attack on the non-acrylic functionality, the new radical rearranges via ring opening to form a more stable chemical structure.

After radical attack, the unstable cyclobutene cycle in **6b** ring-opens leading to a new structure with an endocyclic double bond. Endo-olefinic hydrogen appears at 5.40 ppm in the NMR spectrum.

This isomerisation had been previously reported in the literature for β-pinene radical copolymerisation, with the endo-olefinic hydrogen appearing between 5.35 and 5.58 ppm in ^{1}H-NMR spectrum.[6] In the same work, Lu *et al*. copolymerised β-pinene with methyl acrylate (MA), obtaining a copolymer with MA blocks and isolated isomerised β-pinene units, with an overall conversion of 10 %.

Those experiments can be compared with copolymerisation of monomers **5b** and **6b**. Compound **6b** is a bifunctional monomer whose chemical structure can be split into β-pinene and MA. Monomer **5b** acts as a monofunctional monomer, and only its acrylate functionality is involved in the polymerisation reaction. In both cases, copolymerisation of β-pinene with MA and copolymerisation of **5b** with **6b**, the non-acrylic functionality in β-pinene and β-pinene moiety in **6b** acted as retarder of acrylate polymerisation, since propagation through acrylate functionality is competing with the formation of a tertiary radical, which is thermodynamically more stable than the secondary acrylate radical (Figure 4-29).

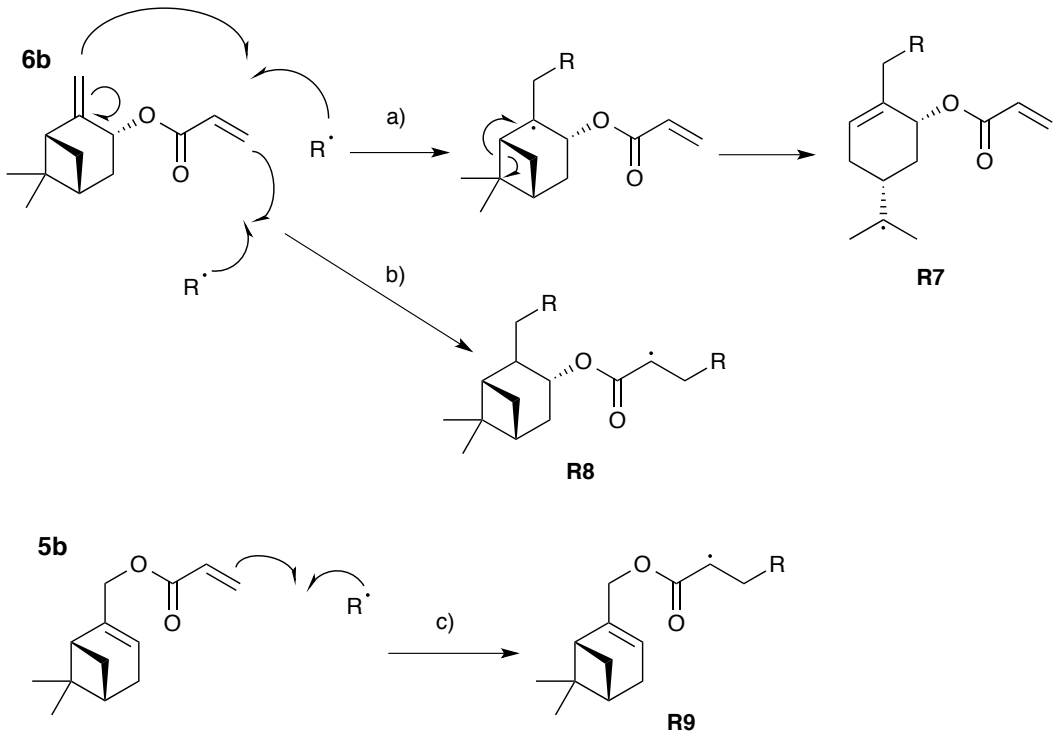
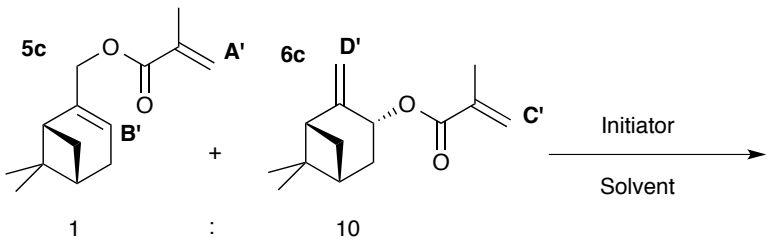


Figure 4-29. Possible radical attacks to monomers 5b and 6b. Attack to acrylate groups via routes b) and c) leads to secondary radicals R8 and R9. Attack on β-pinene moiety in 6b via route a yields a more stable tertiary radical R7.

This is a similar scenario to the one observed in carvone acrylate **4b** polymerisation (Figure 4-9), where acrylate conversion was relatively low as a consequence of this competition between secondary and tertiary radical formation. The main difference between **5b**+**6b** polymerisation and **4b** polymerisation is the absence of crosslinking in **5b**+**6b** reaction, which suggests that reactivity towards polymerisation of the non-acrylic functionality at 110 ºC is somewhat lower in β-pinene derivate **6b** than it was in carvone derivative **4b**.

As for β-pinene methacrylate derivatives **5c** and **6c**, they were copolymerised in a 1:10 ratio in the presence of AIBN at 65 ºC (Table 4-14).

*Table 4-14. Polymerisation of β-pinene derived methacrylates 5c and 6c at 65 °C.**



Entry	I[a]	T (°C)	t (h)	Conversion (%)[b]		Mn (g mol^{-1})[c]	Đ[c,d]
				A'+C'	D'		
1	AIBN	65	24	Crosslinked			

*Reaction was carried out by mixing of 1g of monomer mix, 0.5 wt%. of AIBN and 1.5 mL of cyclohexanone in a 10 mL round-bottomed flask. The mixture was previously degassed by freeze-pump-thaw technique and then heated up to the corresponding temperature. [a] Initiator. [b] Conversion by ^{1}H-NMR. [c] Determined by GPC-SEC in THF using PMMA standards. [d]Đ: Dispersity

After 24 h of reaction, an insoluble gel was obtained, denoting a crosslinked polymer. Deuterated chloroform was added to the mixture, which was then stirred for 24 h. The soluble fraction was analysed by ^{1}H-NMR and no monomer was detected, indicating full monomer conversion. The presence of crosslinking evidences the reactivity of both acrylic (**A'** and **C'**) and non-acrylic (**D'**) functionalities. It can be assumed that endocyclic double bond **B'** did not participate in the reaction due to steric impediments. This lack of reactivity in the tri-substituted double bond had been confirmed by NMR for the acrylate analogue **5b** (Figure 4-26).

This reaction can be compared to the polymerisation of carvone-based methacrylate **4c**, where the presence of a terminal non-acrylic double bond was not an impediment for methacrylate propagation (Table 4-5). In section 4.3.2.1 it was proposed that this lack of polymerisation inhibition, that had been observed for the acrylate analogue **4b**, was due to the fact that both functionalities led to tertiary radicals when attacked by a radical (Figure 4-8), and therefore one was not thermodynamically favoured over the other one.

The electron-withdrawing character of the methacrylate functionality was responsible for the polymerisation. The same hypothesis is proposed for β-pinene derived methacrylate **6c**. It does not apply to methacrylate **5c** since it is assumed that internal double bond is not polymerisable. However, the difference with carvone methacrylate **4c** is that in the case of **6c**, the non-acrylic functionality seems to be participating in the polymerisation, either because higher ratios of non-acrylic functionality in **6b** are being attacked or because the resulting radical **R10** (Figure 4-30) is slightly more reactive towards polymerisation, therefore leading to a crosslinked polymer.

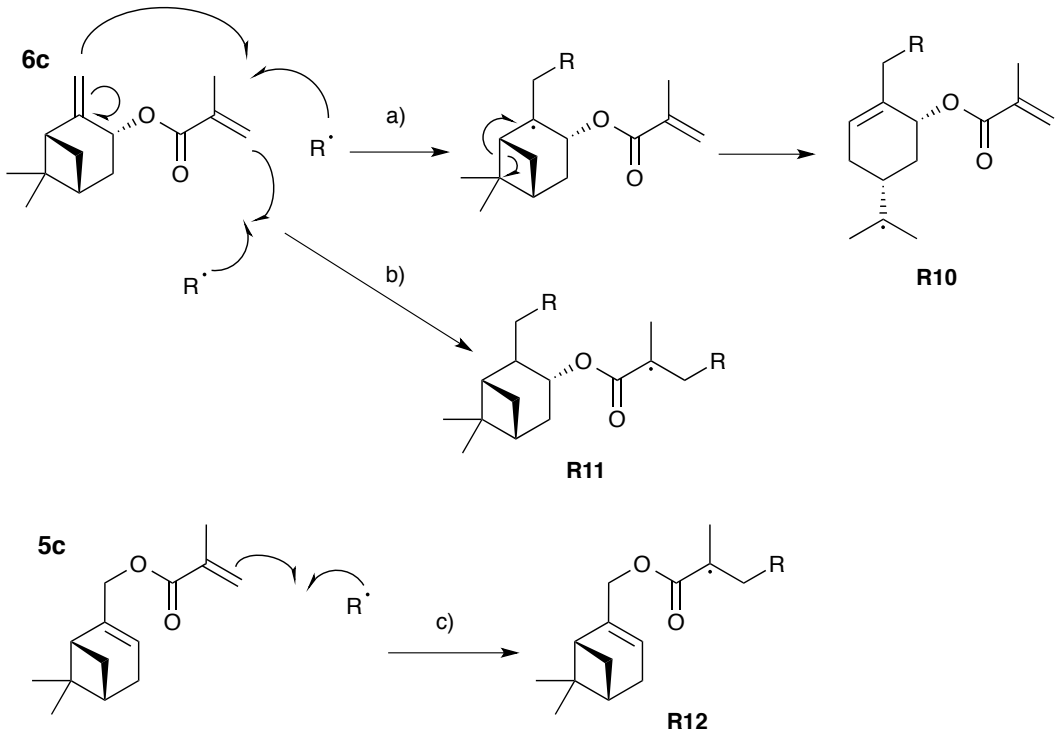


Figure 4-30. Schematic representation of the possible radical attacks to monomers 5c and 6c. It is proposed that attack to the non-acrylic functionality in 6c causes a rearrangement in the chemical structure via ring-opening isomerisation that leads to radical R10 (a). Attack to any acrylic (b,c) or non-acrylic (a) functionalities leads to tertiary radicals in all cases R10, R11 and R12.

If we compare **5c**+**6c** copolymerisation with β-pinene or α-pinene and methyl methacrylate (MMA) copolymerisations reported previously in the literature,[3] it can be concluded that results are very similar. When β-pinene was made to

copolymerise with MMA, monomer conversion was 12 % for β-pinene and 80 % for MMA. During α-pinene and MMA copolymerisation, MMA polymerised to full conversion, while only 15% of α-pinene reacted. Therefore, in both MMA copolymerisations with α-pinene and β-pinene most of the MMA was consumed, and 12 to 15 % of pinene reacted.[3] During β-pinene derived **5c** and **6c** copolymerisation, this reactivity of the β-pinene moiety in **6c** towards polymerisation translates into branching and crosslinking, and an insoluble gel is formed. However, the internal double bond in **5c** is unlikely to react since it is highly substituted, and no reactivity was detected in its acrylate analogue **5b**.

4.3.2.6 FTIR-monitored polymerisation of bifunctional β-pinene (meth)acrylate derivatives.

In order to gather more information about the reactivity of the different double bonds present in the chemical structures of β-pinene based (meth)acrylates **5b**, **6b**, **5c** and **6c**, FTIR-monitored polymerisations were conducted. A monomer mix containing β-pinene based acrylates **5b** and **6b** in a 1:2 ratio was made to polymerise in the presence of 0.5 wt% of AIBN. The reaction mixture was placed in between two quartz crystals and was heated at 110 ºC for 3 h, so as to mimic the experimental conditions at which maximum conversion had been previously obtained (Table 4-13, entry 3).

In order to assign the IR bands to the different double bonds present in **5b** and **6b** chemical structure, the IR spectrum of the monomer mix was compared to the IR spectra of α-pinene, β-pinene and MA (Figure 4-31).

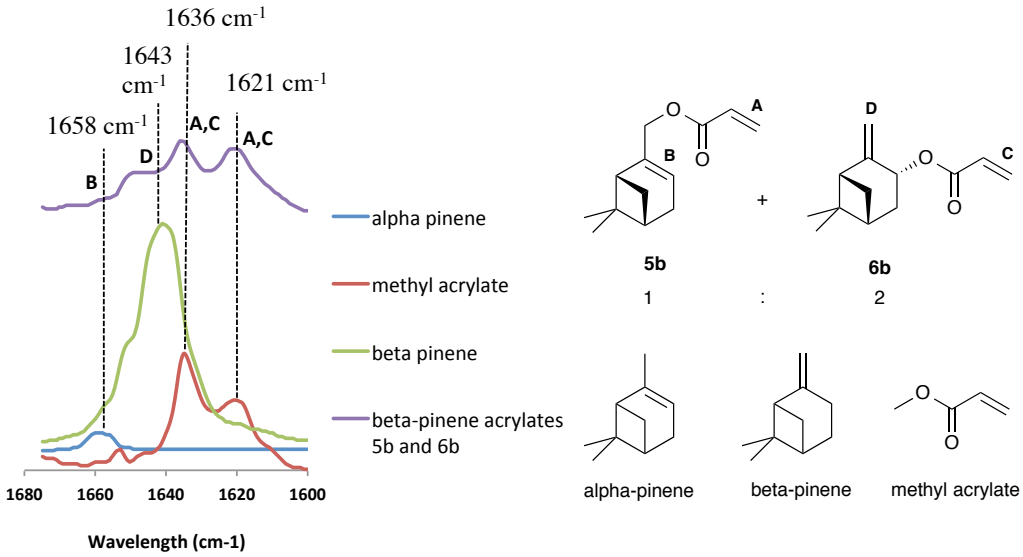


Figure 4-31. Section of IR spectra netween 1680 and 1600 cm-1 of α-pinene, β-pinene, methyl acrylate and 5b+6b monomer mix (left). Chemical structures of the corresponding compounds are shown in the right hand side. Proposed assignments are indicated in the IR spectrum.

It is clear that the signals appearing at 1621 cm^{-1} and 1636 cm^{-1} in the IR spectrum of **5b** and **6b** mixture correspond to the doublet generated by the acrylate groups (See Figure 4-17). A shoulder at around 1642 cm^{-1} is also observed and most likely corresponds to the non-acrylic double bond in the β-pinene moiety in **6b**. As for the internal double bond in **5b**, it is expected to absorb with low intensity due to substitution effects, especially in this case where **5b** represents a third of the monomer mix. There is also a very small signal at around 1658 cm^{-1}, which matches the α-pinene vibration frequency and could therefore correspond to internal double bond in **5b**.

During the polymerisation reaction (Figure 4-32), acrylate features gradually decrease. The partial overlapping between acrylate groups **A** and **C** and non-acrylic double bond **D** observed at 0 min becomes less evident as the reaction proceeds and acrylate groups are consumed.

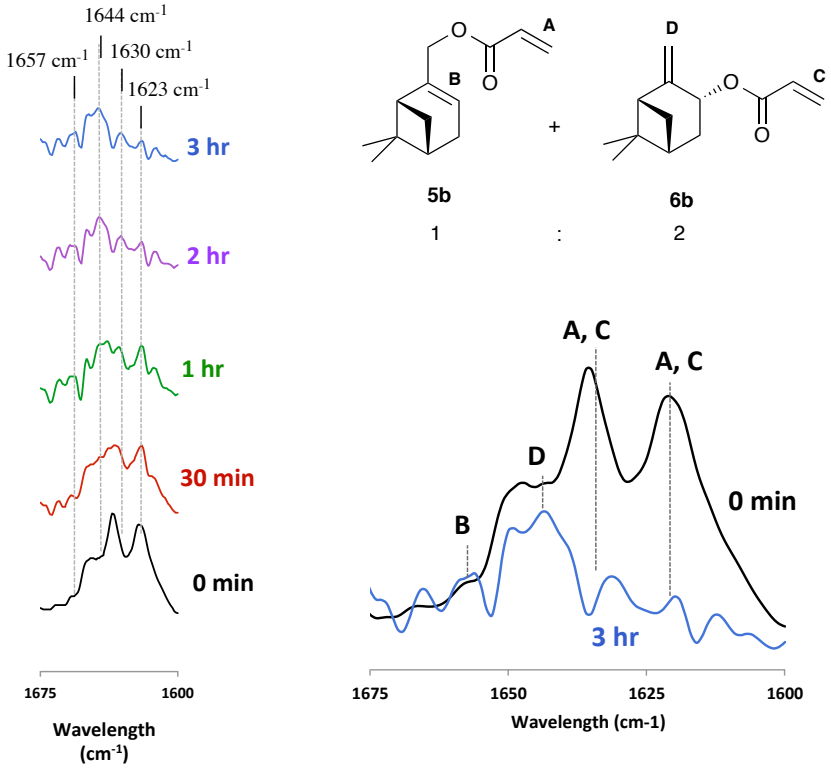


Figure 4-32. FTIR-monitored polymerisation of β-pinene derivatives 5b and 6b between 0 min and 3 h. Figure shows section of IR spectra between 1675 and 1600 cm^{-1}.

After 3 h of reaction, what had been a shoulder becomes a peak maximum at 1644 cm^{-1}, most likely generated by internal double bond **D**. The low-intensity signal observed at 0 min at 1657 cm^{-1} and assigned to **B** becomes a low-intensity well-defined peak, as a consequence of intensity loss in contiguous bands. By looking at Figure 4-32, it can be concluded that all terminal double bonds, acrylic and non-acrylic, participated in the reaction, given the decrease in intensities for **A**+**C** and **B** bands. Unfortunately, it is not possible to make quantitative calculations of consumption of each double bond due to the overlapping of the bands.

Additionally, β-pinene methacrylate derivatives **5c** and **6c** were polymerised in a 1:10 ratio, as they had been obtained. IR spectrum of the monomer mixture is shown in Figure 4-33.

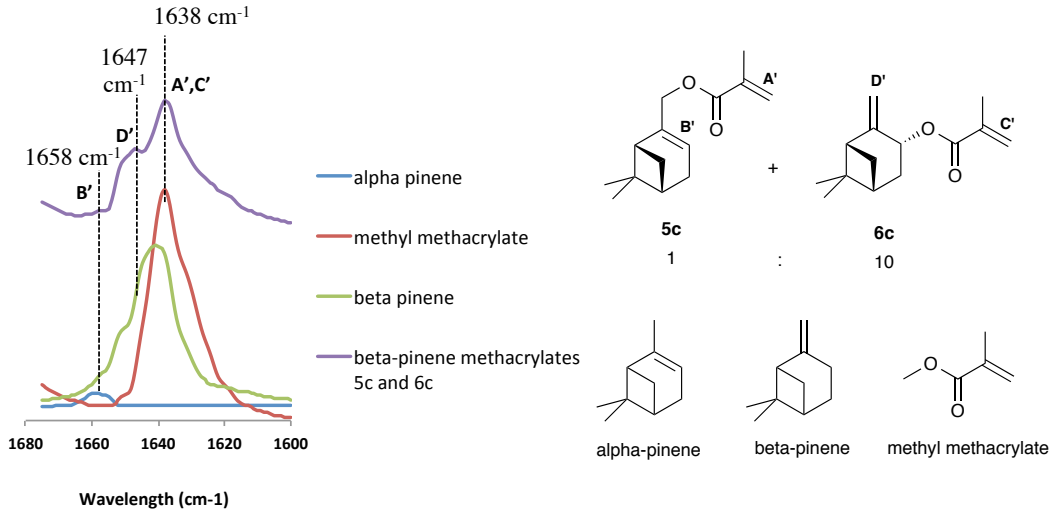


Figure 4-33. Section of IR spectra in between 1680 and 1600 cm^{-1} of α-pinene, β-pinene, methyl methacrylate and 5c+6c monomer mix (left). Chemical structures of the corresponding compounds are shown in the right hand side. Proposed assignments are indicated in IR spectrum.

In this case one band with two peak maximums is observed. Peak maximums appear at 1647 cm^{-1} and 1638 cm^{-1} and are proposed to correlate to terminal double bond **D'** and acrylates **A'** plus **C'** respectively. These peaks maximums are very close to those of β-pinene and methyl methacrylate (Figure 4-33), which confirms the assignments. As for internal double bond **B'**, it is expected to absorb with a low intensity due to the low degree of bond polarisability and the high substitution.

Besides, it is present in the mixture in a low concentration of 9 %. α-Pinene C=C stretch vibration absorbs at 1658 cm^{-1} in the IR, and a negligible peak appears at the same frequency in the monomer mix spectrum. FTIR spectra taken during polymerisation of **5c** and **6c** (Figure 4-34) show a dramatic decrease in acrylates **A** and **C** features over time.

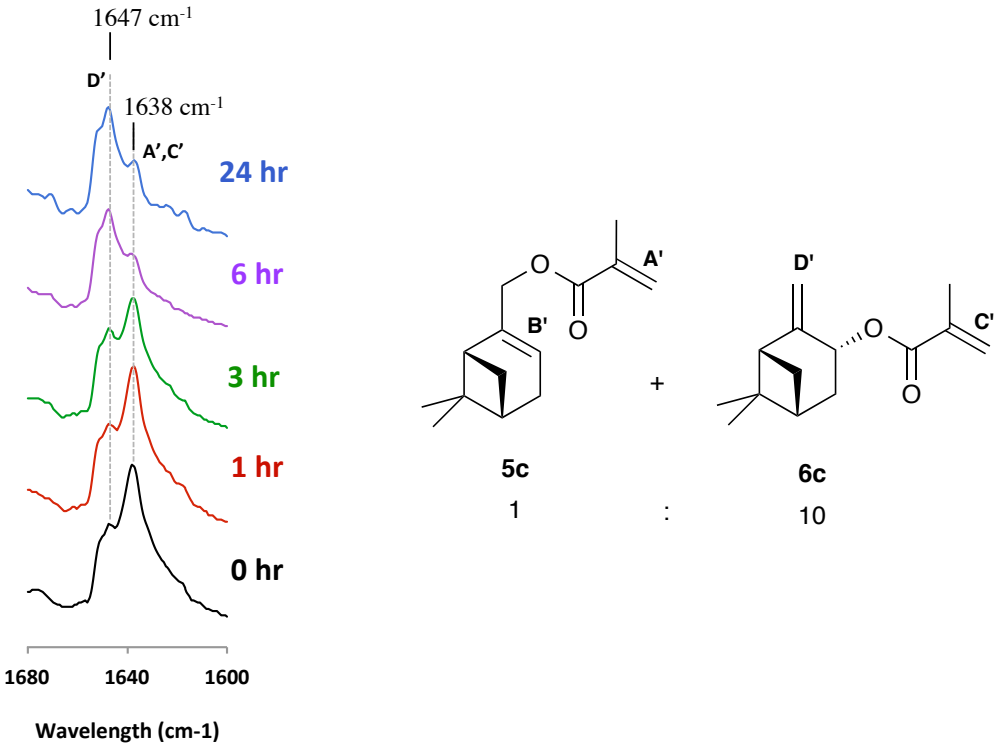


Figure 4-34. FTIR-monitored polymerisation of β-pinene methacrylate derivatives 5c and 6c between 0 min and 3 h. Figure shows section of IR spectra between 1675 and 1600 cm^{-1}. Assignments for all terminal double bonds are shown in the IR spectra.

However, there is not a clear change in intensity in signal at 1647 cm^{-1} and unfortunately not much more information can be obtained from the spectra since all bands are almost completely overlapped. Not only the monomer signals overlap, but also the new signals corresponding to the C=C double bonds in the polymer. This means that IR is not a practical tool to estimate the degree of crosslinking in the case of methacrylate derivatives **5c** and **6c**.

As for **5c** and **6c** polymerisation reaction, different reaction conditions should be tested in order to gather more information about the reactivity of the monomers. Further investigation needs to be conducted to synthesised soluble, non crosslinked polymers under control, and measure their mechanical properties.

4.4 Conclusions

In this chapter, polymerisation reactions of a wide variety of terpene-based monomers have been described. All terpene-based meth(acrylate) monomers described in this chapter proved to be readily polymerisable using conventional FRP techniques. Terpene-based monofunctional (meth)acrylates gave rise to linear polymers with relatively high molecular weight. Different molecular weight polymers have been synthesised in each case by using different concentrations of a conventional CTA, dodecyl mercaptan. These data showed how the ability to control molecular weight allows for the synthesis of polymers with target T_gs. Terpene-based bifunctional methacrylates have been studied. In some cases, bifunctional monomers gave rise to linear monomers, while some others reacted through both of their polymerisable moieties, leading to branched and crosslinked polymers. The reactivity of the different functionalities have been studied by ^{1}H-NMR and FTIR, showing significative differences in crosslinking between bifunctional acrylate and methacrylate monomers. The data obtained during polymerisation studies of terpene-based (meth)acrylates revealed a promising future for these monomers, since there is a wide scope of polymers that can be synthesised simply by changing the starting terpene.

4.5 References

1. A. J. Johanson, F. L. McKennon and L. A. Goldblatt, *J. Ind. Eng. Chem.*, 1948, **40**, 500-502.
2. A. Singh and M. Kamal, *J. Appl. Polym. Sci.*, 2012, **125**, 1456-1459.
3. A. M. Ramos, L. S. Lobo and J. M. Bordado, *Macromol. Symp.*, 1998, **127**, 43-50.
4. A.-L. Li, Y. Wang, H. Liang and J. Lu, *J. Polym. Sci., Part A: Polym. Chem.*, 2006, **44**, 2376-2387.
5. A.-L. Li, X.-Y. Wang, H. Liang and J. Lu, *React. Funct. Polym.*, 2007, **67**, 481-488.
6. Y. Wang, A.-L. Li, H. Liang and J. Lu, *Eur. Polym. J.*, 2006, **42**, 2695-2702.
7. K. Satoh, M. Matsuda, K. Nagai and M. Kamigaito, *J. Am. Chem. Soc.*, 2010, **132**, 10003-10005.
8. A. J. D. Silvestre and A. Gandini, in *Monomers, Polymers and Composites from Renewable Resources*, eds. M. N. Belgacem and A. Gandini, Elsevier, Oxford, 2008.

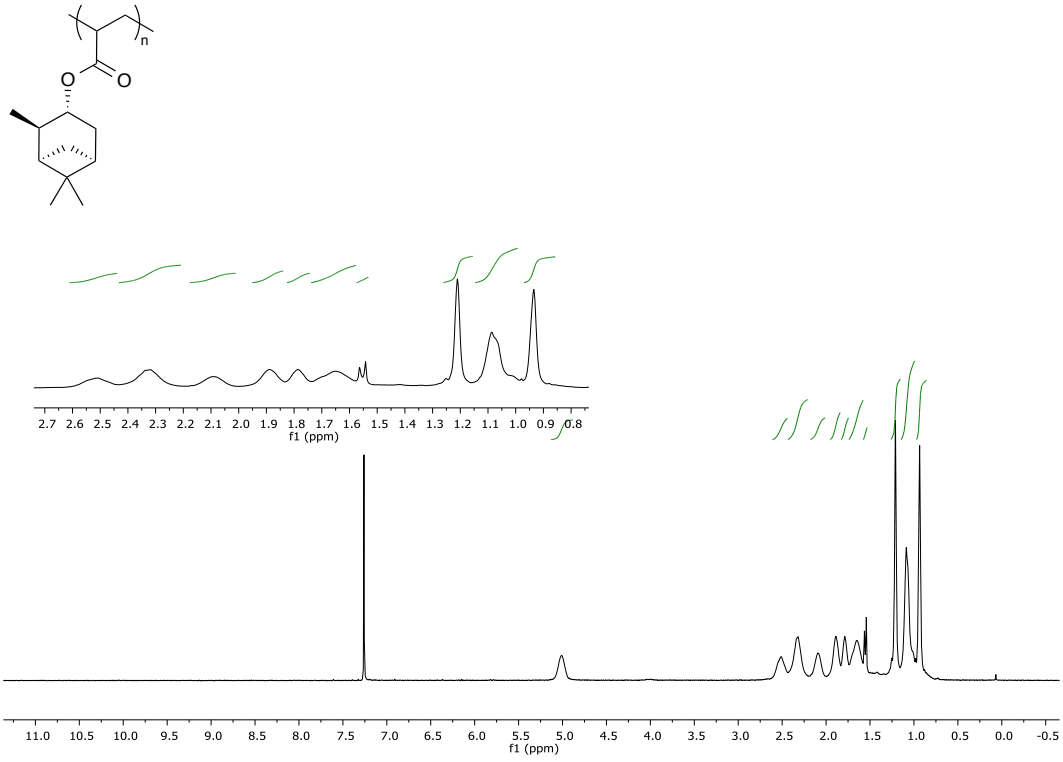
9. A. Gandini, *Macromolecules*, 2008, **41**, 9491-9504.
10. A. Gandini, in *Biocatalysis in Polymer Chemistry*, Wiley-VCH Verlag GmbH & Co. KGaA, 2010, pp. 1-33.
11. J. Lu, M. Kamigaito, M. Sawamoto and T. Higashimura, *Macromolecules*, 1997, **30**, 27-31.
12. K. Satoh, H. Sugiyama and M. Kamigaito, *Green Chem.*, 2006, **8**, 878-882.
13. N. A. Kukhta, I. V. Vasilenko and S. V. Kostjuk, *Green Chem.*, 2011, **13**, 2362-2364.
14. P. Yu, A.-L. Li, H. Liang and J. Lu, *J. Polym. Sci., Part A: Polym. Chem.*, 2007, **45**, 3739-3746.
15. M. Firdaus, L. Montero de Espinosa and M. A. R. Meier, *Macromolecules*, 2011, **44**, 7253-7262.
16. M. Firdaus and M. A. R. Meier, *Green Chem.*, 2013, **15**, 370-380.
17. D. J. Darensbourg, *Chem. Rev.*, 2007, **107**, 2388-2410.
18. L. Pena Carrodeguas, J. Gonzalez-Fabra, F. Castro-Gomez, C. Bo and A. W. Kleij, *Chem. - Eur. J.*, 2015, **21**, 6115-6122.
19. L. Maisonneuve, O. Lamarzelle, E. Rix, E. Grau and H. Cramail, *Chem. Rev.* , 2015, **115**, 12407-12439.
20. J. R. Lowe, M. T. Martello, W. B. Tolman and M. A. Hillmyer, *Polym. Chem.*, 2011, **2**, 702-708.
21. O. Hauenstein, M. Reiter, S. Agarwal, B. Rieger and A. Greiner, *Green Chem.*, 2016, **18**, 760-770.
22. M. Baehr, A. Bitto and R. Muelhaupt, *Green Chem.*, 2012, **14**, 1447-1454.
23. D. Zhang, M. A. Hillmyer and W. B. Tolman, *Biomacromolecules*, 2005, **6**, 2091-2095.
24. K. Yao and C. Tang, *Macromolecules*, 2013, **46**, 1689-1712.
25. P. A. Wilbon, F. Chu and C. Tang, *Macromolecular Rapid Communications*, 2013, **34**, 8-37.
26. N. Colthup, *Introduction to Infrared and Raman Spectroscopy*, Elsevier Science, 2012.
27. P. Larkin, *Infrared and Raman Spectroscopy; Principles and Spectral Interpretation*, Elsevier Science, 2011.
28. D. L. Pavia, G. M. Lampman, G. S. Kriz and J. A. Vyvyan, *Introduction to Spectroscopy*, Cengage Learning, 2014.
29. C. McGreavy, *Polymer Reactor Engineering*, Springer Netherlands, 2012.
30. G. Akovalı, *Polymers in Construction*, Rapra Technology, 2005.
31. J. E. Mark, *Physical Properties of Polymers Handbook*, AIP, 1996.
32. J. Brandrup, E. H. Immergut and E. A. Grulke, *Polymer Handbook*, Wiley, 1999.
33. T. Meyer and J. Keurentjes, *Handbook of Polymer Reaction Engineering*, Wiley, 2005.
34. M. Matsuda, Precision Radical Polymerisation of Plant-Derived Terpenes fro Novel Bio-Based Polymers, Thesis dissertation, 2013, Department of Applied Chemistry of Nagoya University, http://ir.nul.nagoya-u.ac.jp/jspui/bitstream/2237/17975/1/k10143.pdf, (accessed 19th of February, 2016).
35. M. Matsuda, K. Satoh and M. Kamigaito, *KGK, Kautsch. Gummi Kunstst.*, 2013, **66**, 51-56.

36. E. Norstrom, Terpenes as renewable monomers from biobased materials, Master of Science Thesis, 2011, KTH, School of Chemical Science and Engineering (CHE), http://urn.kb.se/resolve?urn=urn:nbn:se:kth:diva-49875, (accessed 19th of February, 2016).
37. S. Ren, E. Trevino and M. A. Dube, *Macromol. React. Eng.*, 2015, **9**, 339-349.
38. Y. Zhang and M. A. Dube, *Polym.-Plast. Technol. Eng.*, 2015, **54**, 499-505.
39. M. Chanda, *Introduction to Polymer Science and Chemistry: A Problem-Solving Approach, Second Edition*, Taylor & Francis, 2013.
40. D. Kukulj, T. P. Davis and R. G. Gilbert, *Macromolecules*, 1998, **31**, 994-999.
41. J. Coates, in *Encyclopedia of Analytical Chemistry*, John Wiley & Sons, Ltd, 2006.
42. B. H. Stuart and D. J. Ando, *Biological Applications of Infrared Spectroscopy*, Wiley, 1997.
43. B. C. Smith, *Infrared Spectral Interpretation: A Systematic Approach*, Taylor & Francis, 1998.
44. M. Orgill, B. L. Baker and N. L. Owen, *Spectrochim. Acta, Part A*, 1999, **55A**, 1021-1024.
45. S. R. Ryu, I. Noda and Y. M. Jung, *Am. Lab.*, 2011, **43**, 40-43.
46. I. A. Barker, J. El Harfi, K. Adlington, S. M. Howdle and D. J. Irvine, *Macromolecules*, 2012, **45**, 9258-9266.
47. W. Wang, Y. Zheng, E. Roberts, C. J. Duxbury, L. Ding, D. J. Irvine and S. M. Howdle, *Macromolecules*, 2007, **40**, 7184-7194.

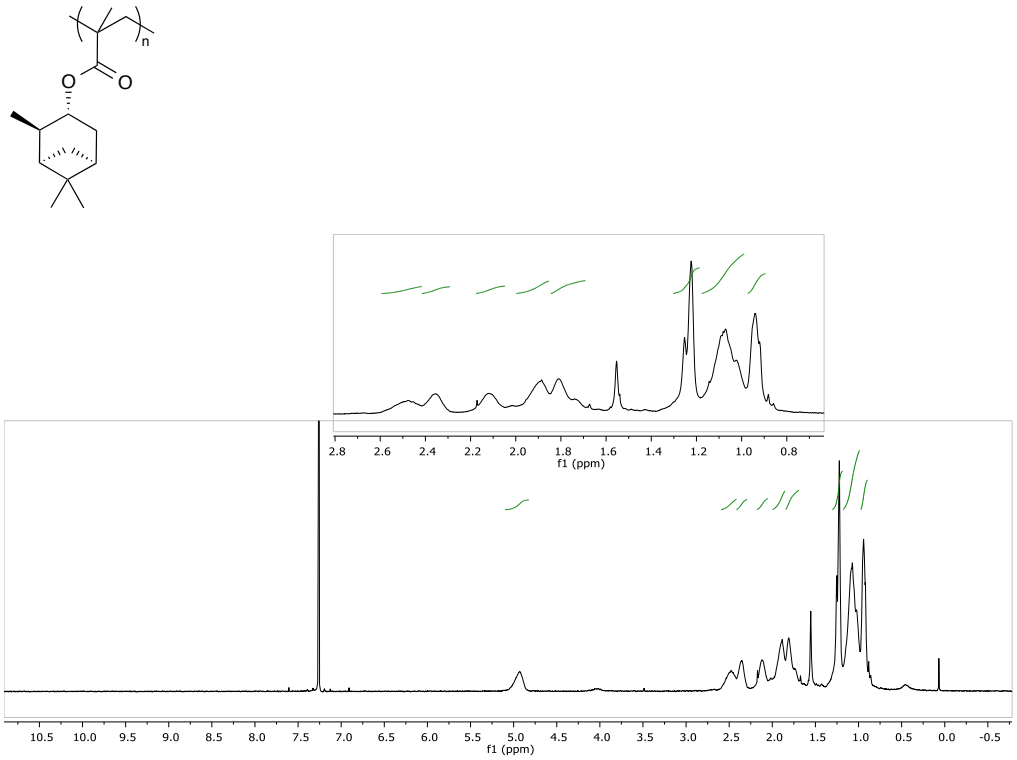
4.6 Appendix: ^{1}H-NMR and TGA spectra

4.6.1 ^{1}H-NMR spectra (300 MHz, $CDCl_3$)

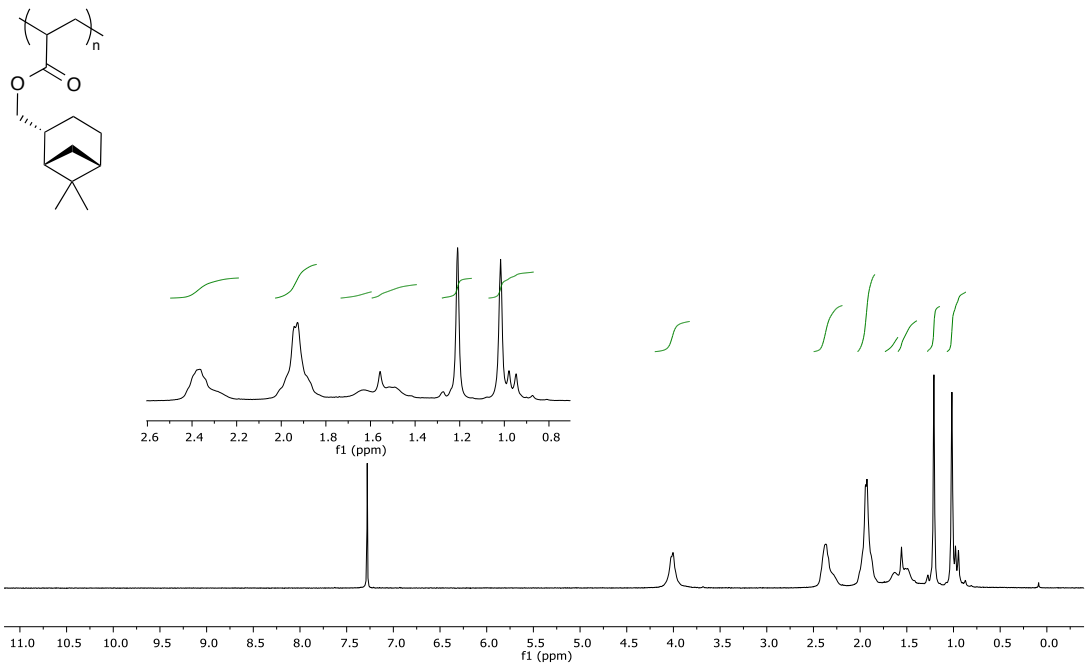
*Poly(α-pinene acrylate) (**1d**)*



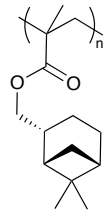
*Poly(α-pinene methacrylate) (**1e**)*

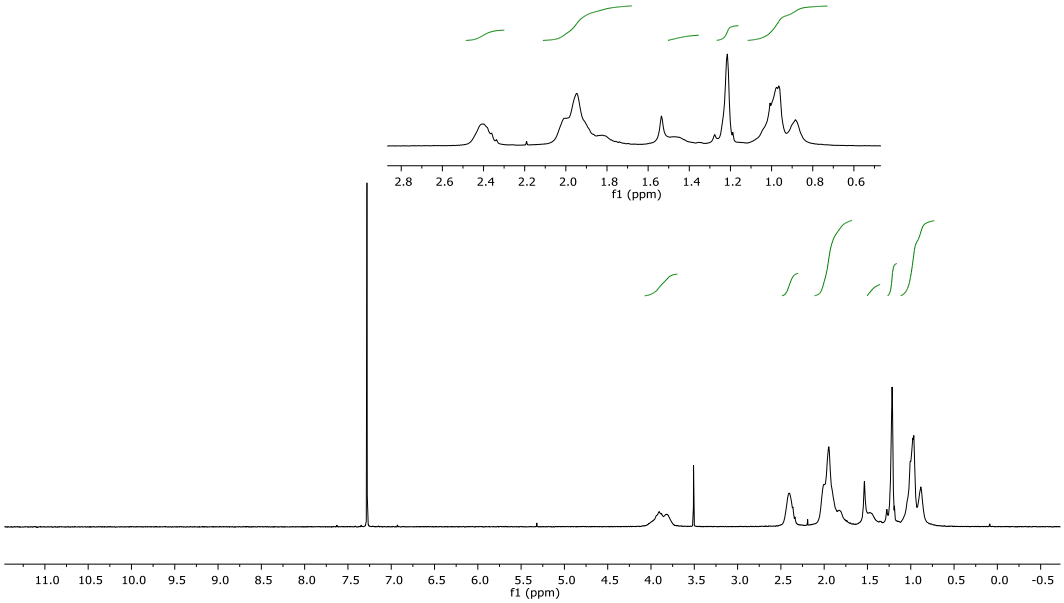


*Poly(β-pinene acrylate) (**2d**)*

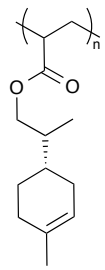


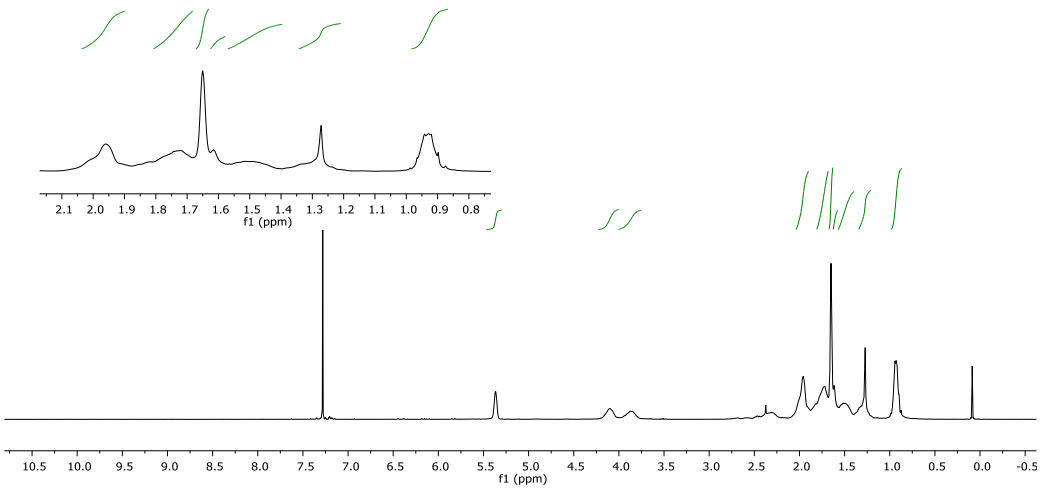
*Poly(β-pinene methacrylate) (**2e**)*



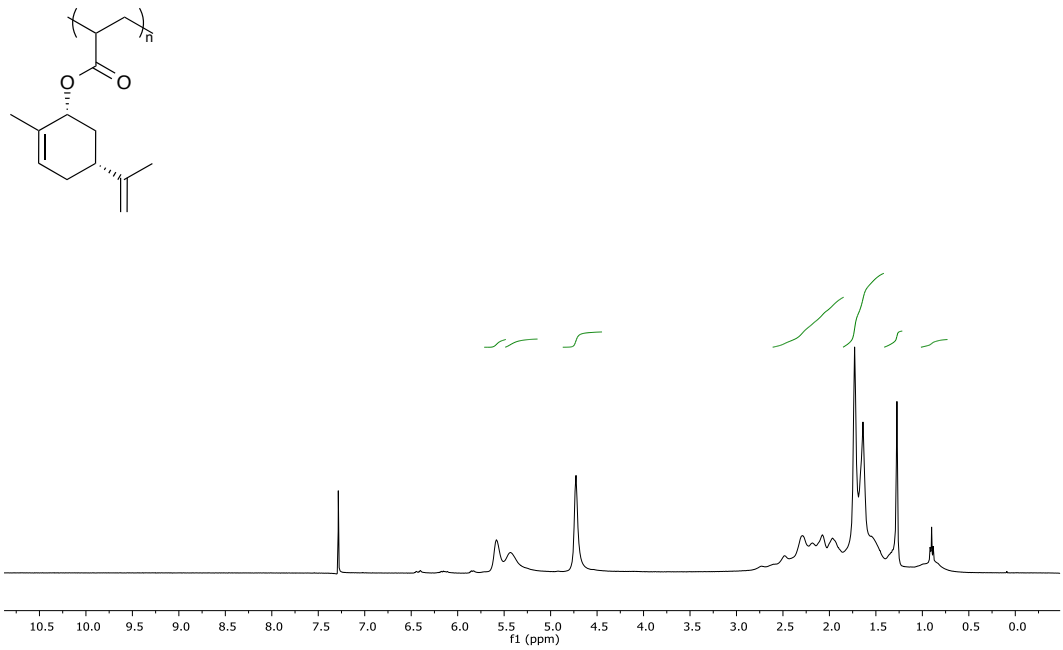


*Poly(limonene acrylate) (**3d**)*

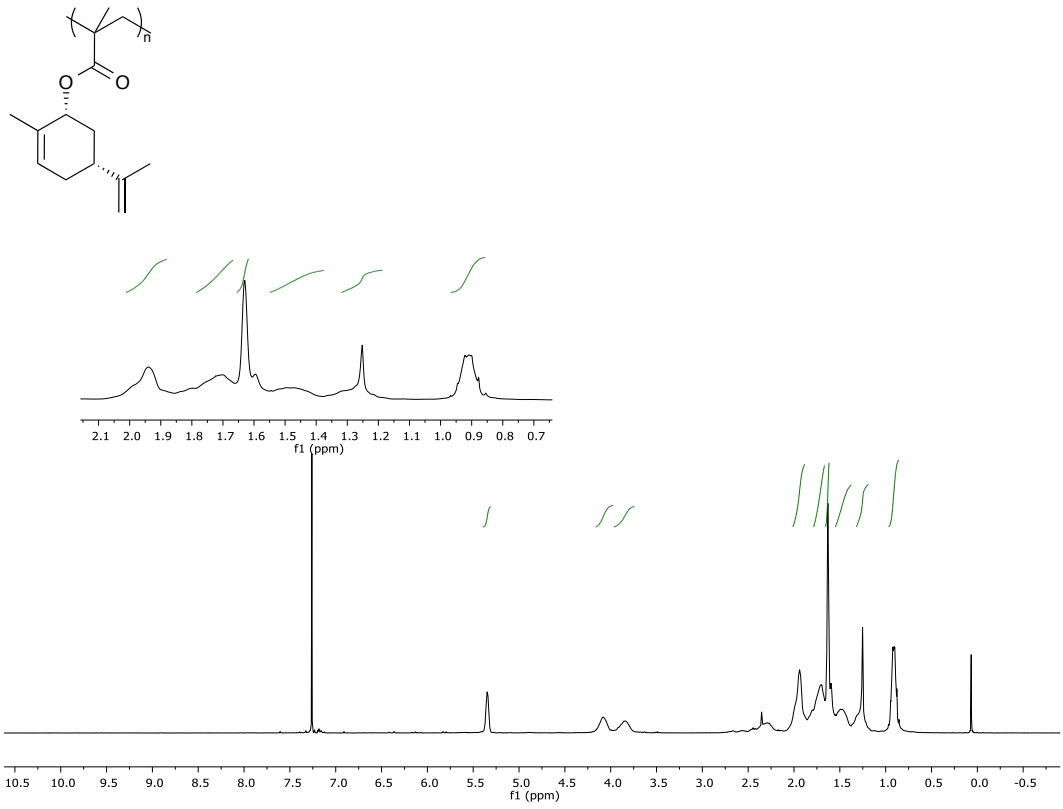




*Poly(carvone acrylate) (**4d**)*

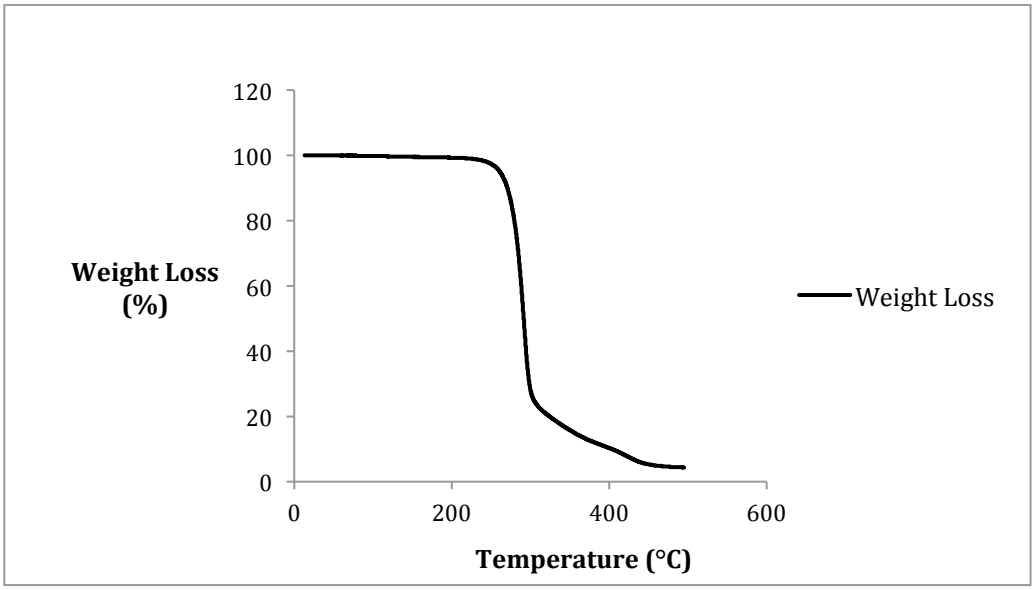


*Poly(carvone methacrylate) (**4e**)*

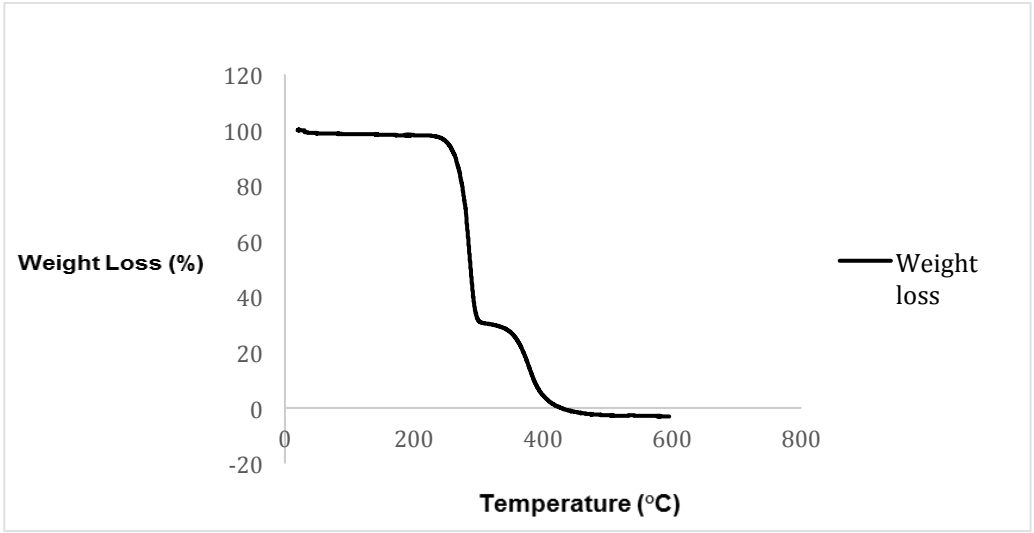


4.6.2 TGA spectra

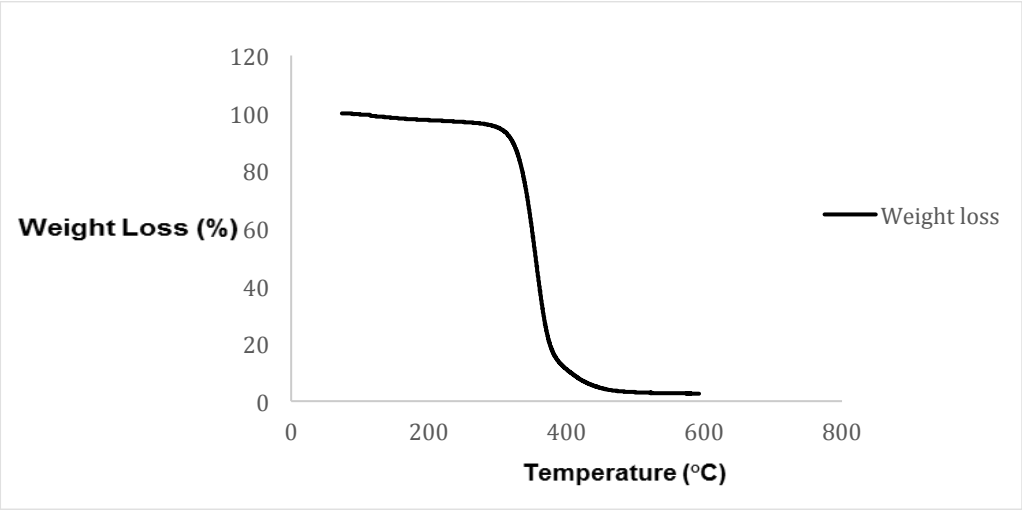
*Poly(α-pinene acrylate) (**1d**)*



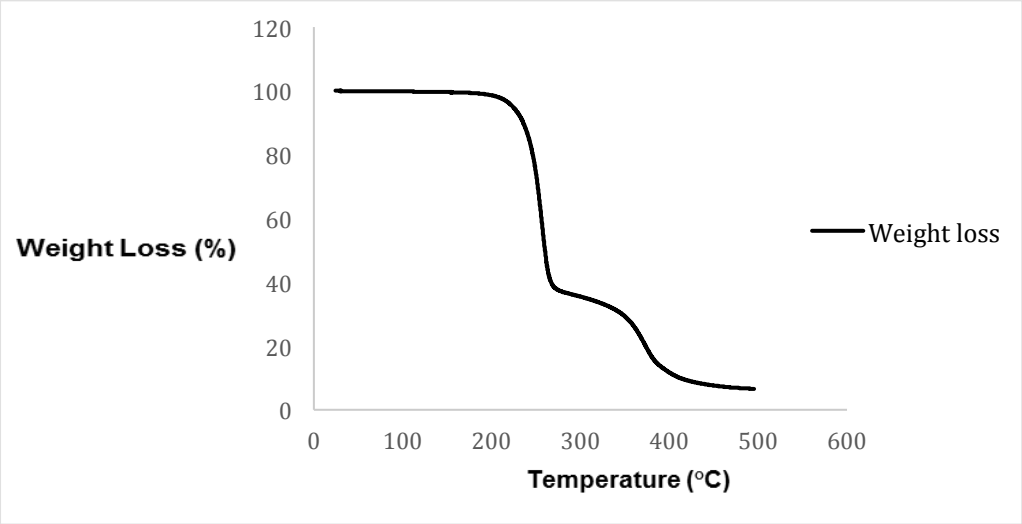
*Poly(α-pinene methacrylate) (**1e**)*



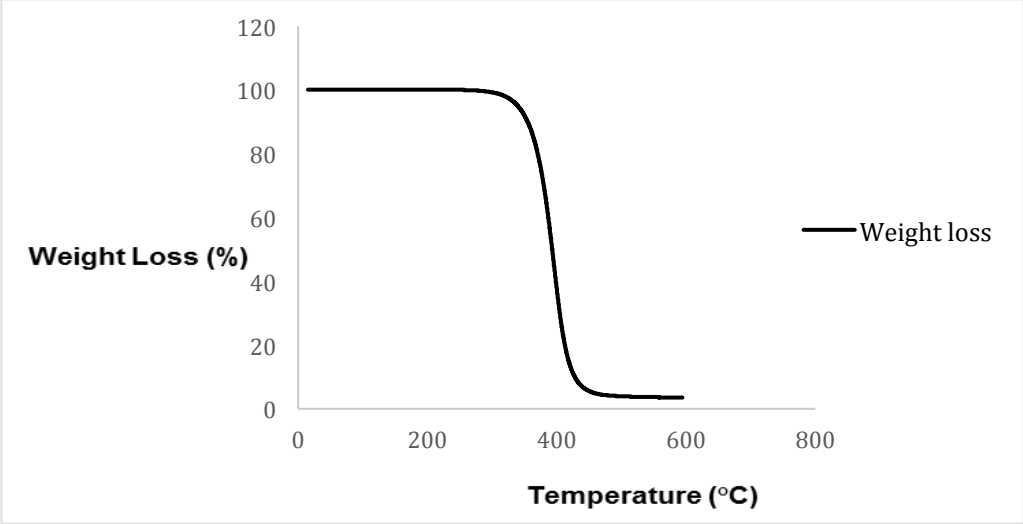
*Poly(β-pinene acrylate) (**2d**)*



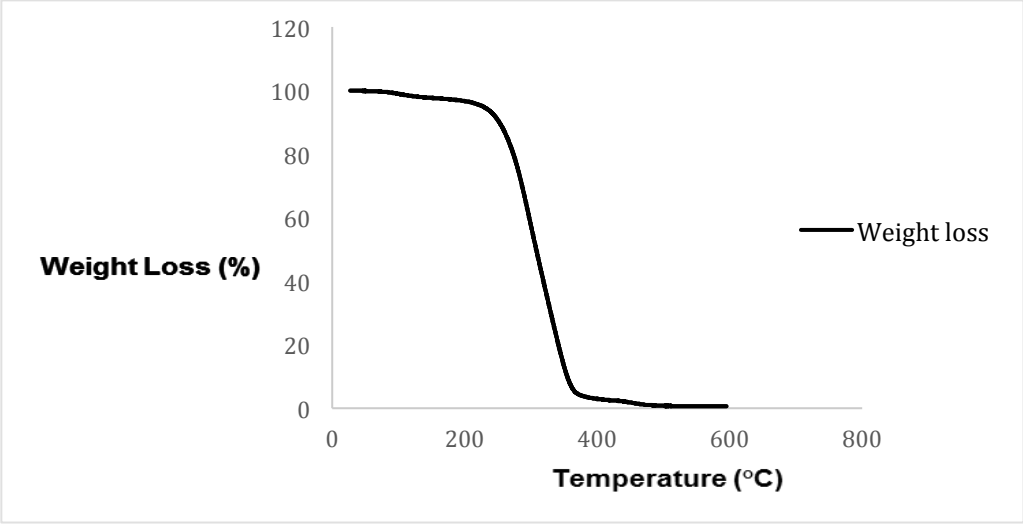
*Poly(β-pinene methacrylate) (**2e**)*



*Poly(limonene acrylate) (**3d**)*



*Poly(carvone methacrylate) (**4e**)*



Chapter 5: Application testing: Carvone-based poly(meth)acrylate coatings

5.1 Introduction

A coating is a covering that is applied to the surface of a substrate for functional or decorative purposes. Functional coatings may be applied to change the surface properties of the substrate, such as adhesion, wettability, corrosion resistance, or wear resistance. Surface coatings include paints, drying oils and varnishes, and other products whose primary function is to protect the surface of an object from the environment. Surface coatings can also be formed from polymeric precursors upon crosslinking reactions that lead to insoluble three-dimensional networks. Polymeric coatings are usually applied to provide superior adherence and protection from corrosion. They can be applied to metals, ceramics, wood as well as synthetic materials. Examples of polymeric coatings include natural and synthetic rubber, polyurethane, acrylics, nylon, polyvinyl chloride and phenolic resins.

In particular, acrylics can be used in a wide range of applications. The term "acrylics" is used to designate coatings that are based on acrylic and/or methacrylic polymers or copolymers. The advantageous features of acrylic coatings are their inertness and excellent colour retention when exposed to outdoor conditions. According to an HIS report on surface coatings,[1] acrylics are used on the three coating market categories: architectural coatings, for indoor and outdoor surfaces in building and construction applications; as product finishes for original equipment manufacture (OEM); and in special-purpose coatings. Special-purpose coatings are required to protect surfaces that are exposed to abnormal environment effects such as radiators, laundries, swimming pools, piping and so on.

Acrylic surface coatings are the leading finishes used in the paint and coatings

industry, having surpassed alkyd finishes over the past few years. Currently, they are one of the fastest-growing sectors in the coatings industry and they account for about 25 % of all coatings in the market.[1]

5.1.1 Curing process: crosslinking

Some of the highest-performance coatings films are based totally on the reaction of polymer precursors to build up a three-dimensionally crosslinked network (Figure 5-1).

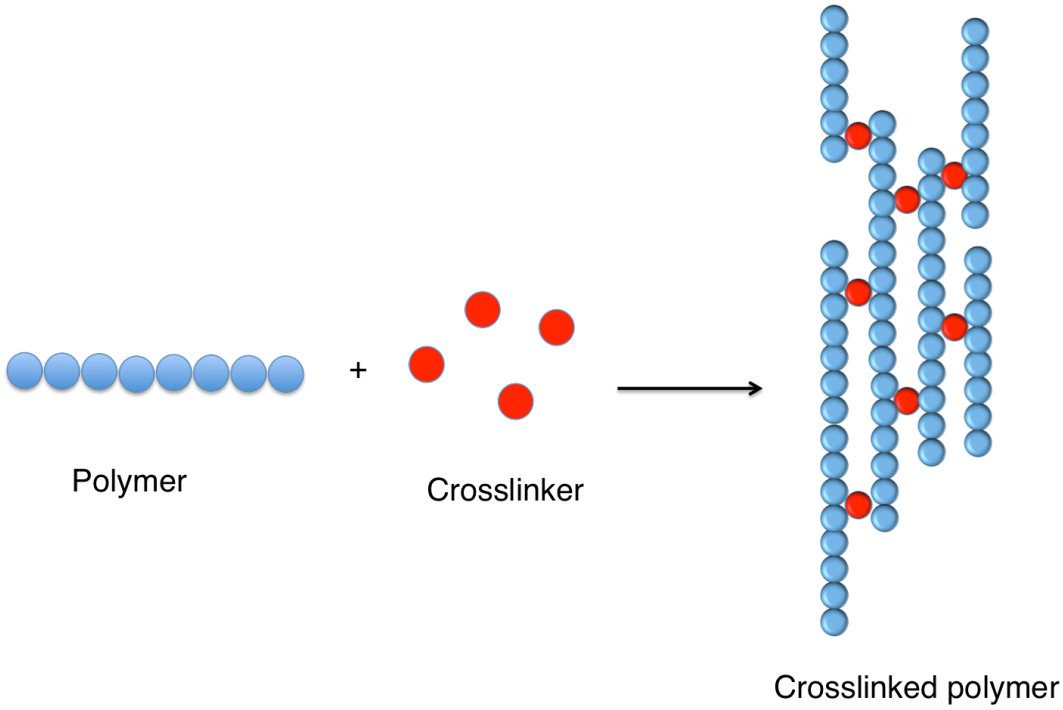


Figure 5-1. Schematic representation of a crosslinking reaction. The structure and crosslinked density of the film determines the properties and applications of the coating.

The formation of films upon crosslinking reactions is a very old technology. Back in the Middle Ages drying oils were used to formulate a paint that formed films totally by oxidative cross-linking. Drying oils are natural products, such as linseed oil or tung oil, that contain at least 50 percent unsaturated fatty acid triglycerides. When they react with oxygen in the air, these oils crosslink to form network polymers. Drying oils modified with soluble natural resins, such as tree gum and rosin and naturally derived solvents such as turpentine, are known as varnishes. When cast and allowed to dry on a substrate, varnishes form films by

evaporation of the solvent and by the crosslinking reactions of the unsaturated fatty acids in the oils. The cross-linking reactions are quite complex (Figure 5-2), but they essentially involve the addition of atmospheric oxygen to the fatty acids, leading to the formation of hydroperoxide derivatives of the fatty acids.

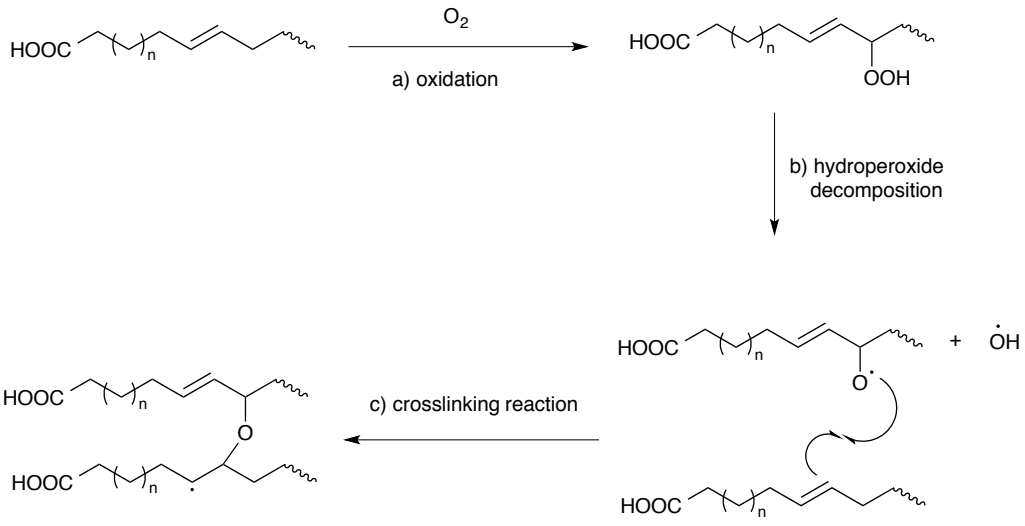


Figure 5-2. Oxygen reacts slowly with double bonds in fatty acids to produce small amounts of organic hydroperoxides (a). Subsequent hydroperoxide decomposition (b) generates a radical species that reacts with another fatty acid chain (c), crosslinking the chains.

Subsequently, these hydroperoxides decompose, especially in the presence of driers such as white lead or cobalt naphthenate, to form free radicals, which then cross-link with the remaining unsaturated fatty acid.

New crosslinking technologies are normally based on two-component systems that are mixed prior to or during application and form the final polymer coating by rapid crosslinking. In many cases, solvents are used to control viscosity, which can increase considerably as rapid polymerisation proceeds.[2]

Curing refers to the toughening of a polymeric material by the crosslinking of polymer chains. Crosslinking can be a condensation, cationic or radical reaction. Crosslinking reactions in curing processes are typically induced by heating (thermal curing), UV light (photo-curing), electron-beam irradiation (EB curing),

or by mixing with a chemical curing agent. Acrylic coatings are typically cured by radical crosslinking.[3-7] In free radical crosslinking an initiator is required for monomer combination or addition to take place and for polymerisation to occur. The type of initiator differs depending on the cure method. Two processes can initiate the cure mechanism: the action of heat and the action of UV-light.

The use of heat has traditionally been the more popular process. Benefits of heat curing include greater bond strength, hardness, rigidity, toughness and impact resistance. Chemical resistance, thermal resistance and electrical insulation performance can also improve with heat. On the other hand, flexibility, elongation and crack resistance may be reduced as a result of heat exposure.[8] Epoxies and urethanes are the most common components used in heat-cure applications.[9, 10]

Ultraviolet curing (commonly known as UV curing) is a photochemical process in which high-intensity ultraviolet light is used to initiate the radical reaction. UV curing offers many advantages over traditional heat curing methods. UV curing has been shown to increase production speed, reduce energy consumption, improve scratch and solvent resistance, and facilitate superior bonding. Since it was originally introduced in the 1960s, UV curing has been widely adopted in many industries including automotive, telecommunications, electronics, graphic arts, converting and metal, glass and plastic decorating coatings.[11, 12]

Surface coatings can also be classified into solvent cast and powder coatings. Solvent casting is the oldest technology in plastic films manufacturing. The continuous solvent cast process was developed more than hundred years ago driven by the needs of the emerging photographic industry. Nowadays, the solvent cast technology is becoming increasingly attractive for the production of films with extremely high quality requirements. The advantages of this technology include uniform thickness distribution, maximum optical purity and extremely low haze. For the raw materials of the solvent casting process there are some prerequisites: a) the polymer must be soluble in a volatile solvent or water; b) stable solution with a reasonable minimum solid content and viscosity should be formed; c) formation of a homogeneous film and release from the casting

support must be possible.[13] Upon application by spraying, brushing, or various industrial processes, surface coatings undergo what is known as film formation.[14] However, 40 to 70 % of toxic volatile organic solvents are normally required for solvent casting formulations. This presents some key disadvantages such as: flammability hazard, health hazards for operators, high energy consumption to evaporate solvents, hazardous waste generated that requires expensive disposal, air pollution and low self-life of solvent casting formulations (low storage stability).[15]

Powder coating is a type of coating that is applied as a dry powder. The coating is typically applied electrostatically and is then cured under heat to allow it to flow and form a film. It is usually used to create a hard finish that is tougher than solvent cast films.[16] Powder coating is mainly used for coating of metals, such as household appliances, aluminium extrusions, and cars and bicycle parts. A combination of technological, environmental and economic benefits when compared to solvent casting has caused a rapid growth in the use of powder coatings over past decades. The main advantages are: a) fire risk is reduced; b) more environmentally friendly due to lack of solvent wastage; c) air pollution is reduced, any over sprayed powder is recoverable and no powder need escape into the atmosphere; d) health hazard to operators is reduced; e) reduced energy requirements as there are no solvents to evaporate; f) 95 % of powder utilisation, any powder overspray can be recovered and material loss can be kept to less than 5 %; g) a powder application plant is less costly since it is extremely simple to operate and less costly than a liquid electro-deposition system.[11, 17]

5.1.2 Thiol-ene curing

The term thiol-ene chemistry is generally used to describe the reaction of thiols with a wide range of unsaturated functional groups such as maleimides, acrylates, and norbornenes, in addition to unactivated carbon–carbon double bonds.[18] The reactions of sulfur containing compounds with alkenes is not a recent discovery. The thermal crosslinking of natural rubber, poly(cis-isoprene), with elemental sulfur was discovered in 1839 by Charles Goodyear (Figure 5-3). This process is

referred to as “vulcanisation”, and is still extensively used by the tyre industry nowadays.[18, 19]

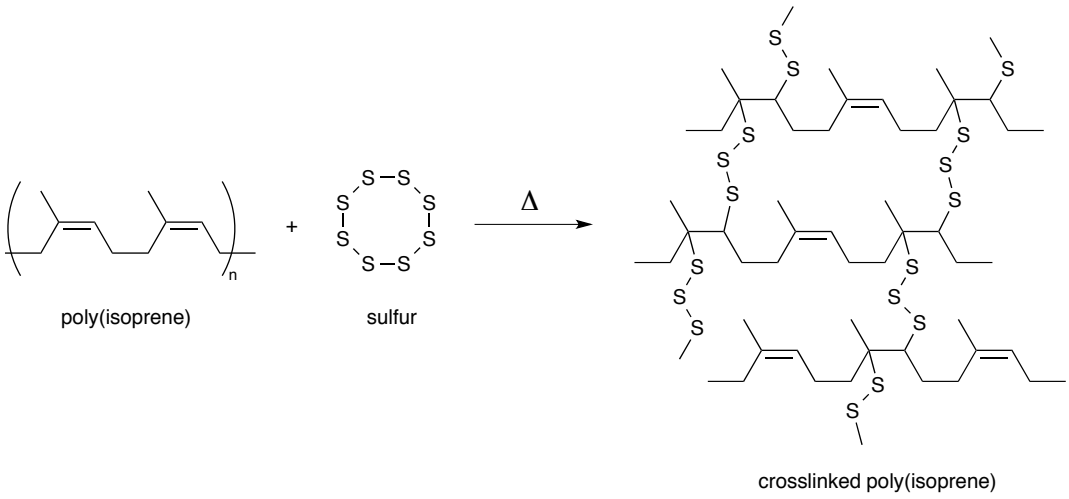


Figure 5-3. Vulcanisation of natural rubber. Discovered in 1836 by Charles Goodyear, vulcanisation is a chemical process in which natural rubber reacts with elemental sulfur under heat to lead to a covalently crosslinked polymer network.

In thiol-ene chemistry, molecules with double bond functionalities are denominated “enes”. The reaction between thiols and enes was first shown by Posner in 1905,[20] but it was not until 1926 that it was presented as a polymer forming reaction.[21] In thiol-ene systems, the reaction is initiated by initiator decomposition and radical attack to a thiol R-SH, generating a thyil radical R-S• (Figure 5-4). Subsequently, propagation occurs by a free-radical chain mechanism involving two steps: an initial addition of the thiyl radical to the carbon of an ene functionality and a subsequent hydrogen abstraction of a thiol group by a carbon-centered radical to generate a thiyl radical. This results in the addition of a thiol group across an ene double bond.[22] The use of diene and dithiol monomers results in linear polymers, whereas the use of tri- or tetra-substituted enes and thiols leads to crosslinked polymers.[19, 22]

Crosslinked networks might be synthesised *via* thiol-ene polymerisation or *via* thiol-ene curing of a polymer containing alkene functional groups. Typical multifunctional thiols employed on thiol-ene curing are depicted in Figure 5-5.

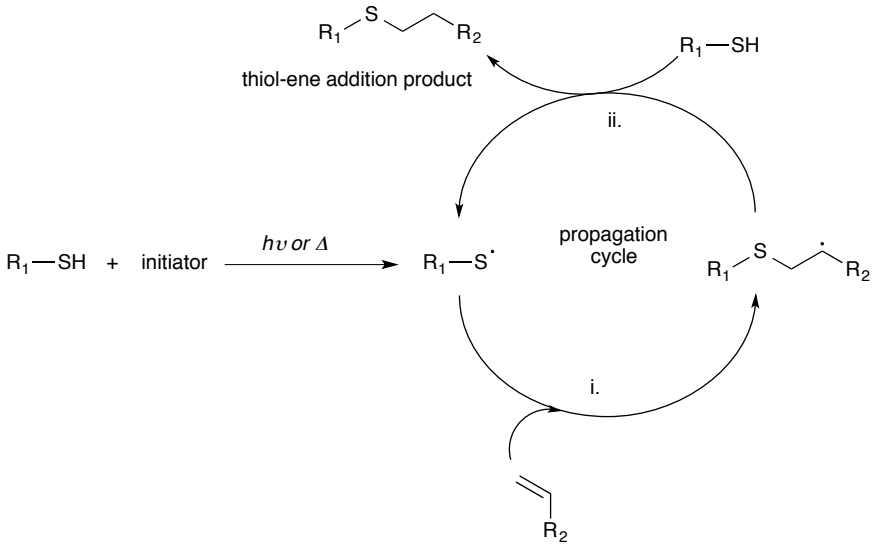


Figure 5-4. Mechanism of free-radical thiol-ene coupling. The thiol–ene propagating cycle revolves around the alternation between radical addition of thiol to alkene (i) and the chain-transfer reaction between a thiol and a carbon-centered radical (ii).[23]

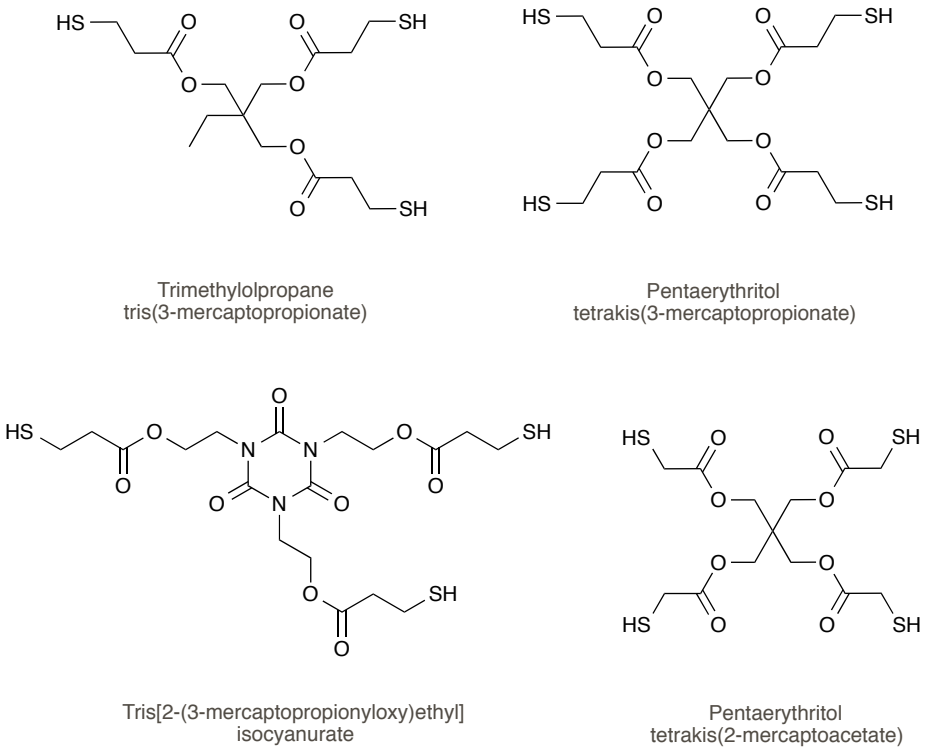


Figure 5-5. Typical multifunctional thiols used in thiol-ene curing systems.[22] *Multifunctional thiols react via a free-radical reaction with enes or polymers with multiple ene functions to form crosslinked networks.*

During the middle part of the 20th century thiol-ene chemistry was used extensively as a method for making crosslinked networks for applications such as relief printing plates (also known as the Letterflex process), wear layers for floor tiles (based on UV-curable resins) and coatings for electronics. However, for a wide variety of economic and technical reasons, thiol-ene photocuring was progressively abandoned in favour of acrylate-based photocurable systems. Objections at the time to thiol-ene-based ultraviolet-curable resins included odour, as well as the incorrect perception that all thiol-ene coatings were subject to rapid yellowing and discoloration upon weathering. The actual reason for discoloration was that benzophenone (BP) was used in large quantities in these systems as a photoinitiator, giving rise to significant light stability problems of the cured networks. As a consequence, coloured byproducts were formed upon exposure to interior and exterior light. As new low-cost acrylate multifunctional monomers and oligomers of high purity became available at prices that allowed for widespread applications, the use of thiol-ene chemistry was severely diminished.[22]

Resurgence over the past decades has occurred in response to the benefits that thiol-ene coupling presents for polymer synthesis: tolerance to many different reaction conditions/solvents, clearly defined reaction pathways/products, and facile synthetic strategies from a range of easily obtained starting materials. However, the two most remarkable properties of thiol-ene curing are the lack of oxygen sensitivity and the homogeneity of the films formed. Hoyle and coworkers have published a considerable body of work regarding the use of thiol-ene chemistry to prepare crosslinked networks with improved physical and mechanical properties.[18] These data have consistently shown that networks formed by thiol-ene chemistry have more regular structures than those formed by standard free-radical polymerisation of diacrylates. These qualities have led to thiol-ene chemistry being used increasingly in polymer functionalisation and macromolecular synthesis, as well as more traditional applications ranging from crosslinked networks to functionalised biomaterials.[22-25]

5.1.3 Summary and research aims

Carvone-based polyacrylate **4d** and polymethacrylate **4e** described in Chapter 4 contain a high density of double bonds in their chemical structrure, which makes them promising candidates for crosslinking reactions, or curing, to form coating films. In this Chapter, carvone-based polymers are cured *via* thiol-ene chemistry under a range of different conditions: heat and UV induced curing, solvent casting and powder coating. The properties of the films are carefully studied and the films are evaluated as potential acrylic coatings.

5.2 Experimental

5.2.1 Materials

All materials were used as received unless otherwise stated. Poly(carvone acrylate) and poly(carvone methacrylate) were prepared following the synthetic procedures described in Chapter 4. Trimethylolpropane tris(3-mercapto-propionate (TMP-SH) was obtained from Bruno Bock Chemie. 2,2′-Azobis(2-methylpropionitrile) (AIBN) was bought from Merck. DCM was purchased from Sigma Aldrich. Bis(2,4,6-trimethylbenzoyl)-phenylphosphineoxide (Irgacure 819) was obtained from Ciba Specialty Chemicals. The flow control agent Resiflow PV5 was provided by Worlée Chemie GmbH.

5.2.2 Solvent casting

200 mg of carvone-based polymer and the curing agent trimethylolpropane tris(3-mercaptopropionate) (TMP-SH) (ene/SH molar ratio of 1:1 or 1:1.5) were dissolved in the minimum amount of DCM (around 0.3 mL to dissolve acrylate and 0.5 mL to dissolve methacrylate) in the presence of 2 mol% of AIBN or Irgacure 819 as thermal- and photoinitiators respectively. A wet film with a thickness of around 120 μm was applied onto a chromated aluminum panel (ALQ-46) plate using a doctor blade. The film was left to dry at room temperature in a well ventilated fumehood and subsequently cured. The thermal curing took place under nitrogen in an oven at 160 ºC for 45 min. The UV curing was conducted in a custom built heating device with a quartz lid at the top under a

nitrogen flow at 150 ºC and were subjected to UV irradiation (3x200s) for 15 minutes.

5.2.3 Powder coating preparation and curing

30 g of poly(carvone methacrylate) was mixed in a laboratory blender with 4.5 g of TMP-SH (ene/SH molar ratio was 4:1), 0.54 g of the flow agent Resiflow PV5, 0.27 g of the degassing agent benzoin and 0.71 g of the UV initiator Irgacure 819. The mixture was subsequently fed to a home-built co-rotating twin-screw DSM Micro-Extruder®. Extrusion and melt-mixing occurred smoothly at 120 ºC using a screw speed of 200 rpm and was performed using a back-mixing by-pass device. The resulting strand was turned into chips which were milled to a fine powder in a Retsch ZM100 machine with a 0.5 mm ring sieve at 18,000 rpm and then sieved (sieve fraction with particle size below 90 μm was used) and subsequently deposited on 0.8 mm thick chromate aluminium Q-panels (type ALQ-46) using an electrostatic spraying gun. The plate with the deposited polymethacrylate powder was then heated for 2 min at 120 ºC in an IR oven to force flow and film formation and subsequently irradiated two times in a home-designed UV curing chamber using a H-bulb lamp to cure the film. The total UV dosing, measured by a UV Power Puck PP200 was 6000 mJ cm^{-2}.

5.2.4 Measurement of coatings properties

Coating thicknesses were determined with a PosiTector 6000 coating thickness gauge from DeFelsko Corporation. The impact properties of the solvent-cast poly(meth)acrylate coatings were evaluated with a reverse falling dart impact test. Tests were performed with a 20 mm diameter and 1 kg weight ball dropped from a height of 1 m (ASTM D2794). For the polymethacrylate powder coatings the reverse impact resistance was tested according to ASTM D2794, with a 5/8″ ball. The solvent resistance was considered as being satisfactory if 75 double-rubs (DR) with a tissue soaked in acetone did not show any visual damage of the coating. A metal adhesion test (Gitterschnitt) was performed according to ASTM D 3359. The smoothness of the powder coatings obtained upon full cure of the corresponding thermosetting powder compositions on ALQ-46 panels was

determined by comparing the smoothness of the coatings with PCI Powder Coating Smoothness Panels (ACT Test Panels Inc., APR22163 (A) Batch: 50708816). The rating of smoothness ranges from 1 to 10, with 1 representing the roughest coating and 10 the smoothest coating. Pencil hardness was tested with a set of pencils with varying hardnesses, ranging from 1H to 9H.

5.3 Results and discussion

5.3.1 Solvent casting and curing of carvone-based poly(meth)acrylates using thiol-ene chemistry.

In order to conduct the thermal curing of linear poly(carvone methacrylate) (Figure 5-6) and branched poly(carvone acrylate) (Figure 5-7), the polymers were mixed with trimethylolpropane tris(3-mercaptopropionate) (TMP-SH, Figure 5-8) as crosslinker and AIBN as initiator and then dissolved in DCM.

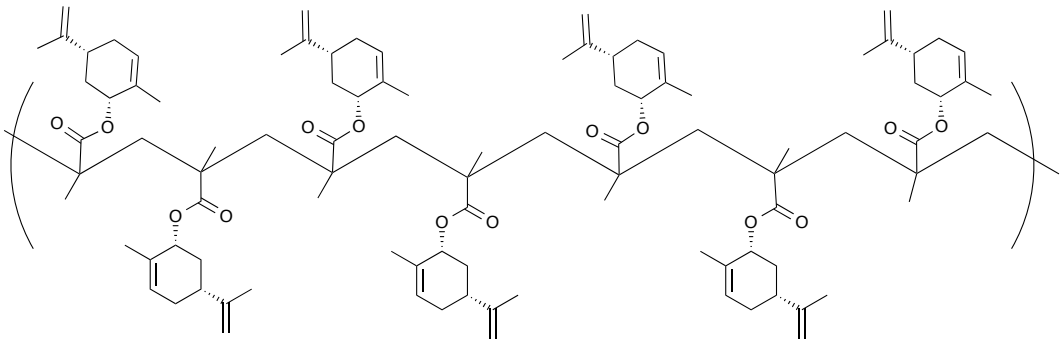


Figure 5-6. Chemical structure of linear poly(carvone methacrylate) showing one unreacted double bond per monomer unit. The high density of double bonds in the polymer structure makes it an ideal candidate for crosslinking reactions.

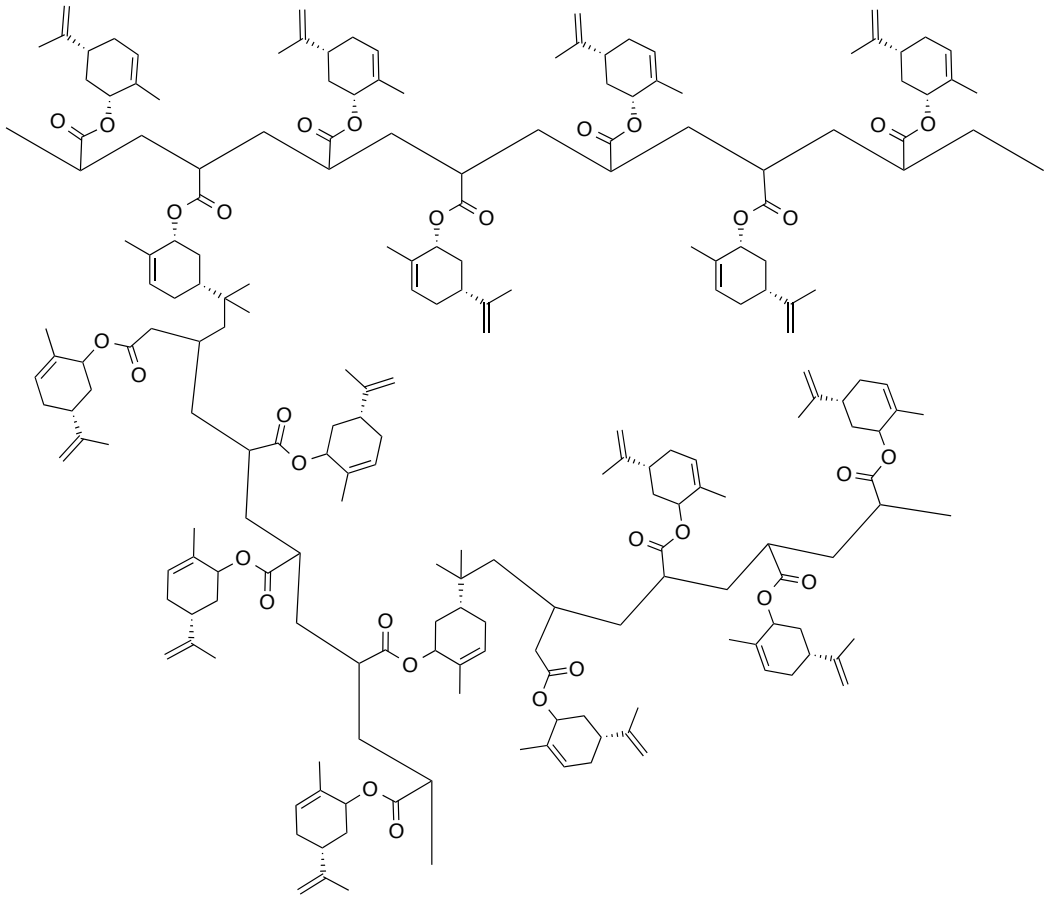


Figure 5-7. Chemical structure of branched poly(carvone acrylate) showing ready availability of pendant olefinic moieties that could be exploited to create crosslinked networks.

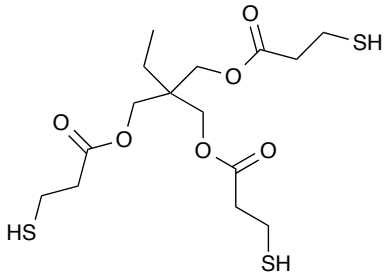


Figure 5-8. Chemical structure of tri-thiol crosslinker TMP-SH. This trifunctional thiol can react with three double bonds from different polymer chains, forming a crosslinked structure.

When solvents other than DCM (such as THF and $CHCl_3$) were tested, a higher volume of solvent was necessary to fully dissolve the polymer. DCM was chosen as the solvent because of the lower volume required and the high volatility. The

mix was spread into an aluminium panel using a doctor blade and after solvent evaporation at room temperature the aluminium plate was placed into an oven at 160 ºC for 45 minutes. It was necessary to set up the oven temperature above the glass transition temperature (T_g) of the polymer to ensure a homogeneous flow of the polymer.

The glass transition temperatures of poly(carvone acrylate) and poly(carvone methacrylate) are 45 ºC and 117 ºC respectively. At 160 ºC a full consumption of radicals (AIBN half-life is of only a few seconds at 160 ºC), good flow of the polymer and evaporation of solvent traces were ensured. After 45 min the coatings were taken out of the oven and visually analysed. A transparent film would be indicative of full curing and homogeneous coating. The coatings obtained from poly(carvone acrylate) and poly(carvone methacrylate) (Table 5-1) showed powdery (non-transparent) regions evidencing under-curing. They also showed visible defects such as craters (Figure 5-9) and cracks (Figure 5-11).

Generally, ene:thiol ratios are required to be between 8:1 and 1:1 in order to obtain a fully crosslinked polymer. To start with, an ene:thiol ([ene]:[SH]) ratio of 1:1 was tested. Under these conditions, a film with a white, powdery surface was obtained in both cases, indicating under-curing. When the crosslinker ratio was increased to 1:1.5, some under-cured regions were detected in the film (See Figure 5-9). In order to obtain a fully-cured transparent film, the crosslinker concentration was increased to 1:2.

Table 5-1. Thermal curing of carvone-based polyacrylate and polymethacrylate.

Polymer	**[SH]:[=]**	**Appearance**
Poly (carvone acrylate)	1:1	Under-cured, cratering
Poly (carvone acrylate)	1:1.5	Under-cured, cratering
Poly (carvone methacrylate)	1:1	Under-cured, cratering, cracking
Poly (carvone methacrylate)	1:1.5	Under-cured, cratering

However, the latter solution was too viscous and difficult to apply homogeneously and therefore these films were discarded. It is striking that such a high concentration of crosslinker was necessary in order to obtain a fully cured film, since the polymers contain one double bond per monomer unit (slightly lower density of double bonds on the branched poly (carvone acrylate)). This might be a sign of a non-homogeneous solution previous to the curing, with an uneven distribution of the crosslinker. It could also be due to the fact that as soon as the aluminium pan was placed in the oven, the crosslinking process starts, not allowing enough time for the deposited polymer mix to flow and mix effectively, leading toa non-uniform coating.

Aside from the incomplete curing, some defects such as cratering and cracking were observed in the films. Cratering (Figure 5-9) is characterised by the formation of small bowl shaped depressions in the film.

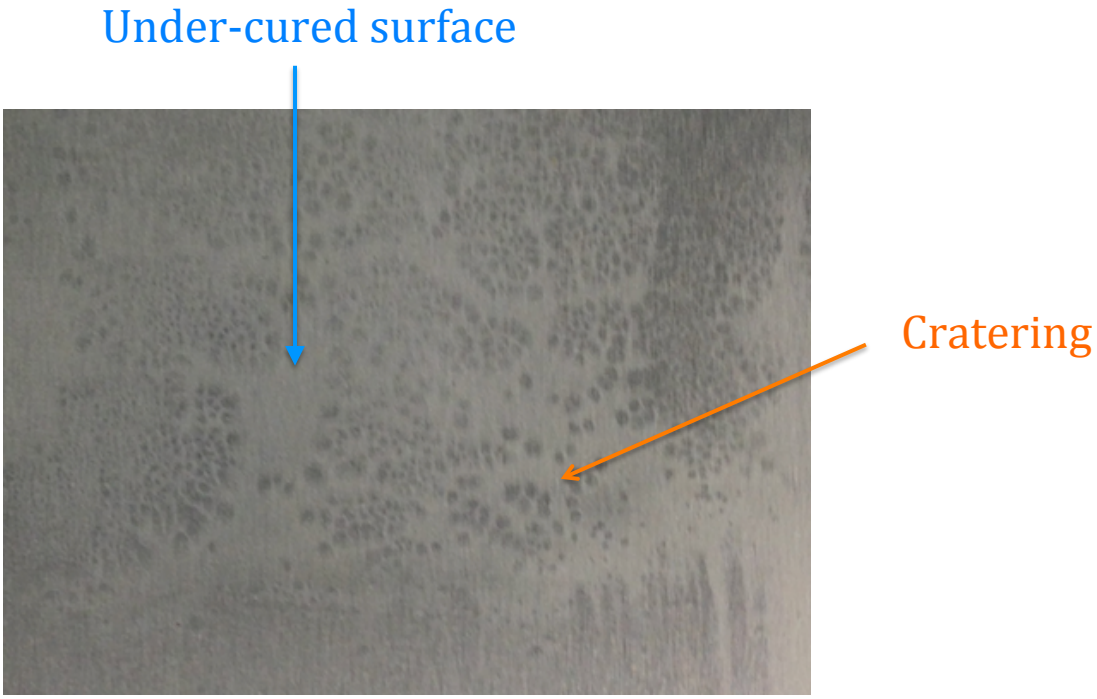


Figure 5-9. Poly(carvone acrylate) coating showing under-cured regions and cratering deffects.

This defect is normally caused by trapped air or solvent bubbles which burst to leave small craters. In the carvone-based coatings, these bubbles could come from residual solvent from the bottom of the polymer film, from the initiator (N_2 is released when AIBN decomposes, Figure 5-10) or from low-molecular weight polymer chains with a boiling point under 160 ºC.

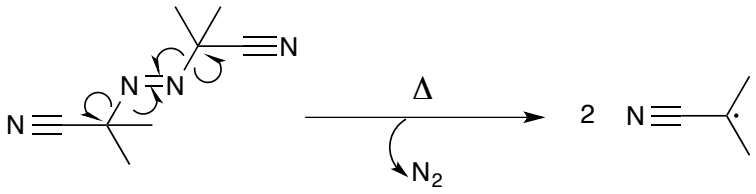


Figure 5-10. Decomposition reaction of radical initiator AIBN.

Since the crosslinking process occurs very quickly at 160 ºC (AIBN half-life is less than a minute), there was insufficient time for the polymer mix to flow and release these bubbles and form a flat homogeneous film. The other defect observed is cracking (Figure 5-11) and is generally caused by mechanical stress in the coating.

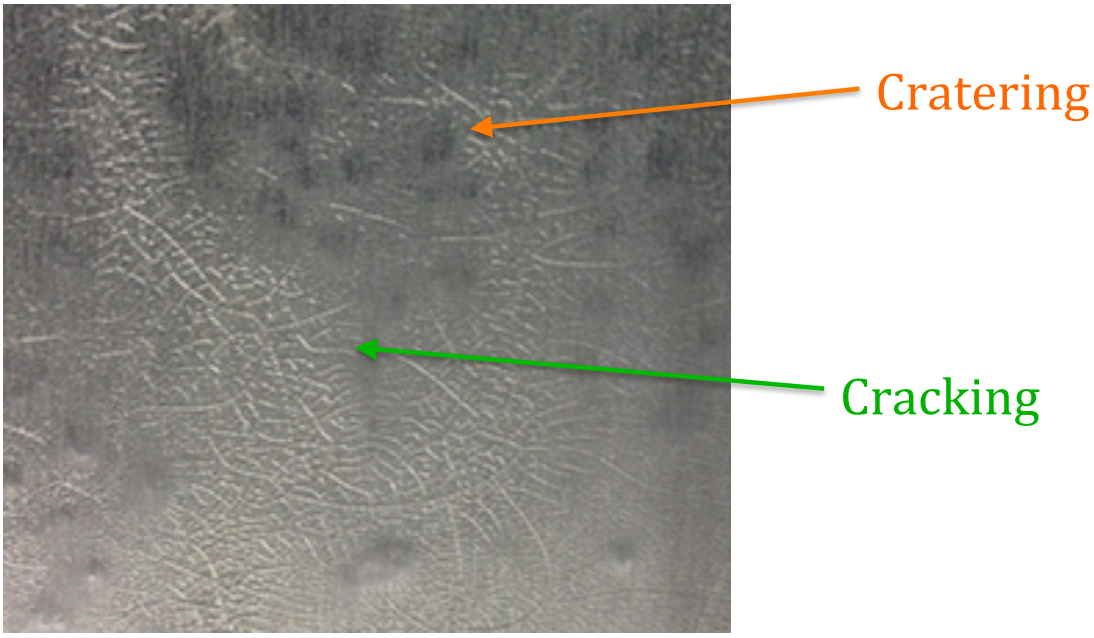


Figure 5-11. Poly(carvone methacrylate) coating showing cratering and cracking defects.

In order to avoid the problems resulting from a rapid crosslinking reaction that does not allow time for the polymer to get homogeneous, we decided to try a different curing system: UV curing was attempted. In this process, the crosslinking begins when the UV is applied and not when the coating mix is heated up, so the polymer can be heated above its T_g before the crosslinking starts. As the polymer is above its T_g, it flows, allowing any bubbles to be released. Then UV is applied to cure the polymer.

The polymer solutions for the UV-curing were prepared by dissolving the corresponding polymer, bis(2,4,6-trimethylbenzoyl) phenylphosphineoxide (Irgacure 819, Figure 5-12) as the photoinitiator (2 mol%) and TMP-SH as the crosslinker in DCM.

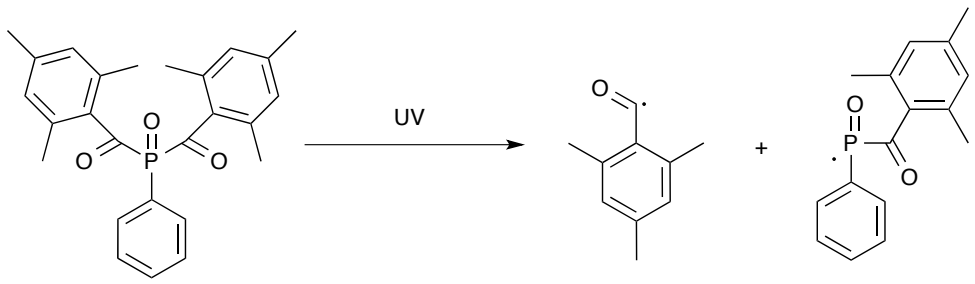


Figure 5-12. Decomposition reaction of photoinitiator Irgacure 819 under UV light.

These solutions were then spread into an aluminium pan. After solvent evaporation at room temperature they were placed into the UV oven at 150 ºC for 15 min to ensure the capability to flow and then irradiated with UV light for 15 minutes. The UV curing of poly(carvone acrylate) and poly(carvone methacrylate) (Table 5-2) yielded transparent (fully cured) films (Figure 5-13) when the ratio [ene]:[SH] was 1:1.5. Under-cured films were obtained instead when lower concentrations of crosslinker were added.

Table 5-2. UV curing of carvone-based polyacrylate and polymethacrylate.

Polymer	[SH]:[=]	Appearance
Poly (carvone acrylate)	1:1	Under-cured
Poly (carvone acrylate)	1:1.5	Transparent, uniform
Poly (carvone methacrylate)	1:1	Under-cured
Poly (carvone methacrylate)	1:1.5	Transparent, uniform

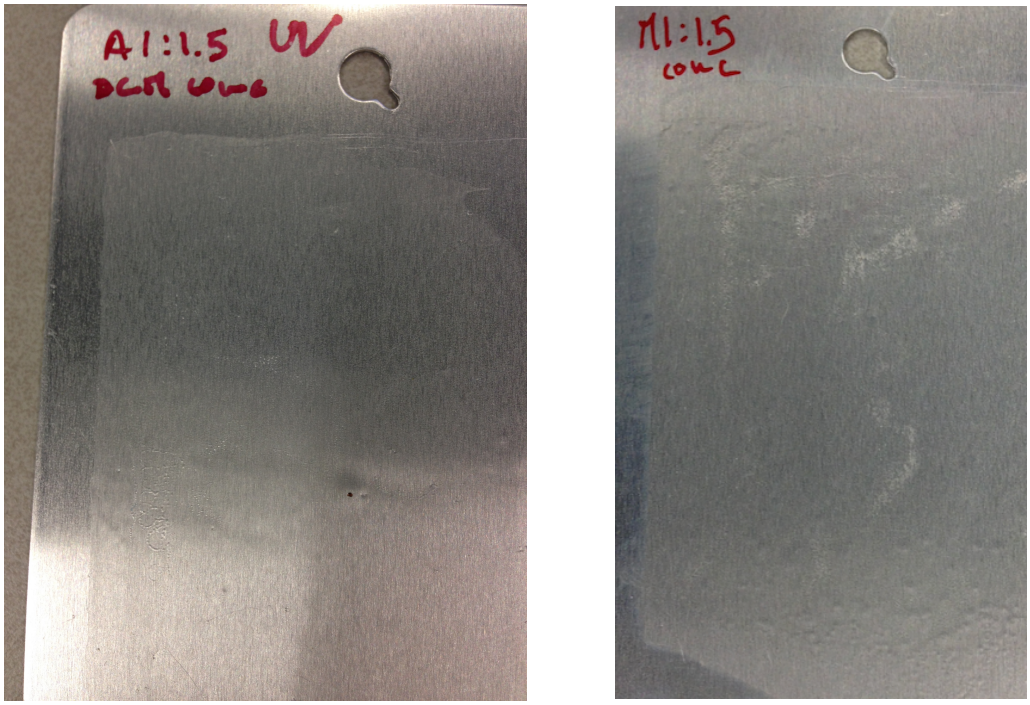


Figure 5-13. Transparent poly(carvone acrylate) (left) and poly (carvone methacrylate) (right) coatings prepared via UV curing.

The fact that a [ene]:[thiol] molar ratio as high as 1:1.5 was necessary for a complete curing suggests that there was not effective mixing of the coating components previous to the curing process (as seen above for thermally cured films). It could also be due to liquid-liquid phase separation of polymer and crosslinker during solvent evaporation. This would lead to a heterogeneous distribution of crosslinker and therefore to an uneven crosslinking density, where some regions would be highly crosslinked and other regions would contain free, non-cured polymer chains. However, other defects such as cratering and cracking

were not observed after UV curing, which suggests that the latter allows for a more uniform crosslinking process than thermal curing. This could be explained by the fact that the coating mix was heated above the T_g previous to curing, allowing the mix to flow and form a uniform film.

5.3.2 Powder coating and UV curing of poly (carvone methacrylate)

After solvent casting evaluation of the carvone-based new polymers, powder coating was attempted. Powder coating is a widely used, more sustainable and generally preferred coating method. Powder coating differs from solvent casting in that there is no solvent used to dissolve the coating components. Instead, the powder mix containing polymer, crosslinker and other components, such as initiator and degassing agent, is extruded at a temperature above the T_g of the mixture to ensure good mixing. The resulting strand is turned into a powder by grinding and is subsequently sprayed over the substrate using an electrostatic air gun. Powder coating techniques are very popular nowadays because of their sustainability and superior mechanical properties when compared to solvent coating. Use of powder coatings is growing rapidly. However, surface defects such as orange peel and pinholing prevent the expansion of powder coatings into some markets. In order to prevent such defects, degassing and flow agents are generally used in powder coating formulations.

A flow agent is a surface-tension modifier. Flow-control additives reduce the surface tension of the particles as they melt and flow both at the coating/substrate and at the coating/air surface.[26] Part of the molecule is soluble in the resin, and another portion is insoluble and orients itself at the resin/substrate or resin/air interface. This molecular orientation promotes a uniform surface tension across the surface of the molten coating, eliminating regions of low surface tension, which can result in defects such as craters.[27]

Another common defect in powder coating is the appearance of pinholes due to degassing during the curing. In order to prevent this defect, benzoin (Figure 5-14) has been used as a degassing agent in powder coating for more than 20 years.

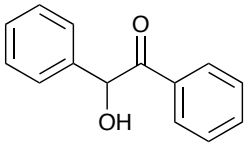


Figure 5-14. Benzoin is a degassing agent that reduces surface tension in a melted film, enabling entrapped air bubbles to scape.

The mechanism through which benzoin enhances the removal of other gases from the coating is not fully understood. One possible explanation for benzoin's effectiveness is its volatility, i.e. it rapidly migrates to the surface of the coating and vaporizes carrying along other volatiles with it.[28]

In order to powder-coat a polymer, it must have a T_g above 50ºC after mixing with the rest of the coating components. Therefore, poly(carvone methacrylate) (T_g=117ºC) was tested while poly(carvone acrylate) (T_g=45ºC) was discarded from powder coating because of its low T_g. Poly (carvone methacrylate) was mixed with TMP-SH ([ene]:[thiol] molar ratio was 4:1), Resiflow PV5 as flow agent, benzoin as degassing agent and photoinitiator Irgacure 819 (2 mol%). The powder mix had a T_g=81 ºC, and was subsequently extruded at 120 ºC, then ground and deposited on a metal plate using an electrostatic spray gun. The aluminium plate was heated to 120 ºC to enhance flow and irradiated with UV light for 15 minutes to cure the film. A glossy, transparent film was obtained (Figure 5-15).

The reason for an [ene]:[thiol] ratio of 4:1 was to ensure a high T_g. A high concentration of crosslinker would have produced a dramatic decrease on the T_g of the coating mix, preventing its use as powder coating. Even with this low concentration of crosslinker, the curing process yielded a fully cured, transparent film, proving that the chosen ratio of crosslinker was sufficient. This supports the hypothesis that undercuring in solvent casting was due to heterogeneities in the coating mix and not to an insufficient load of crosslinker. Flow-control additives and degassing agents were used to ensure a homogeneous film in powder coating, as opposed to solvent-casted films.



Figure 5-15. Poly (carvone methacrylate) coating prepared via powder coating and UV curing.

5.3.3 Evaluation of coatings properties

From the coatings described previously, only those with uniform, transparent appearance were picked for further evaluation (Table 5-3). Under-cured, defective coatings would show poor, uneven mechanical properties. The smoothness of the coating surface was visually evaluated by comparing with Powder Coating Visual Smoothness Standards (PCI).

The carvone-based (meth)acrylate coatings were highly glossy and showed PCI smoothness values of 2-3 on a scale of 1 to 10 (10 being the smoothest). The average film thickness of solvent-cast coatings was 42 μm and 9 μm for poly(carvone acrylate) and poly(carvone methacrylate) respectively. A higher volume (0.5 mL as opposed to 0.3 mL) of solvent added to the polymethacrylate coating formulation explains this difference in thickness between the two coatings. Powder-coated poly(carvone methacrylate) showed a slightly higher

polymer thickness. Powder coatings characteristically lead to thicker films than those obtained *via* solvent casting. In powder coating a solvent is not required to apply the polymer film to a substrate, therefore the polymer mix is much more viscous and consequently a thicker polymer film can be deposited on to the substrate. Additionally, there is no shrinkage due to solvent evaporation, which leads to a cured film with a thickness equal to the initial film application (as opposed to solvent casting, where the thickness of the film decreases considerably).

Table 5-3. Properties evaluation of carvone-based (meth)acrylic coatings.

Polymer	PCA[a]	PCM[b]	PCM[b]
Coating preparation method	Solvent casting	Solvent casting	Powder coating
Ene:thiol ratio	1:1.5	1:1.5	4:1
Appearance	Transparent	Transparent	Transparent
PCI powder smoothing rating (1-10)	2	2	2-3
Average film thickness	42 μm	9 μm	64 μm
Acetone resistance (ASTM D4752)	+	+	+
Falling dart impact (ASTM D2794)	-	-	-
Pencil hardness (ASTM D3363)	2H	3H	2B
Adhesion to metal (ASTM D3359)	5	0	5

[a] Poly(carvone acrylate) [b] Poly(carvone methacrylate)

The acetone-rub test consists on rubbing a cloth impregnated with acetone against the coating 100 times. This test showed a fully cross-linked coating that was not removed (did not dissolve) in all three coatings. The falling dart impact test indicated a brittle coating in all cases (Figure 5-16, films broke due to the dart impact), all of which are as expected for an acrylic based material.

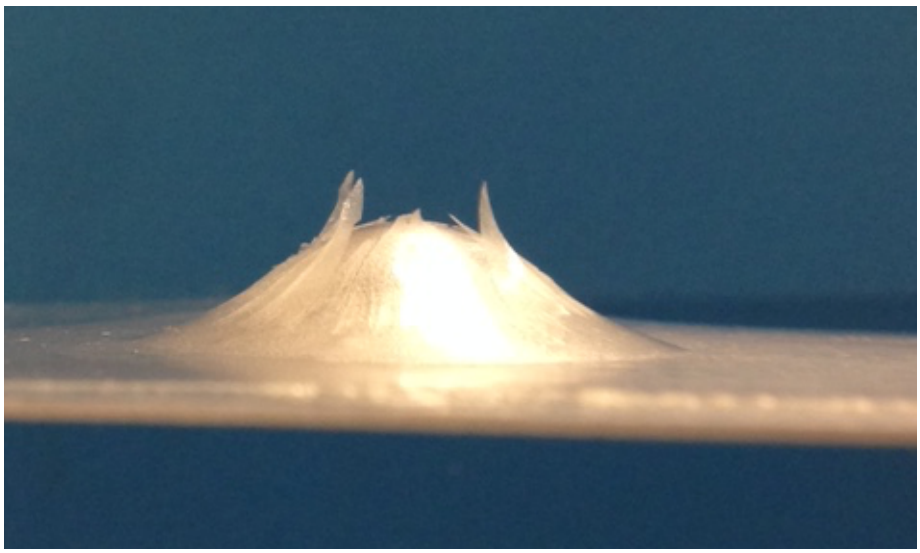


Figure 5-16. Broken poly(carvone methacrylate) coating after falling dart impact test.

The industry standard pencil hardness test consists of scratching the surface of the coating with pencils of increasing hardness. The value of the hardest pencil that does not scratch the coating corresponds to the pencil hardness value. This test yielded a value of 2H for poly(carvone acrylate) and 3H in the case of poly(carvone methacrylate). These values indicate relatively hard polymers (Figure 5-17). Methacrylate polymers are generally harder than the corresponding acrylates. The presence of a methyl group in the methacrylate backbone, compared with a hydrogen in the acrylate, limits the free rotation around the carbon chain, therefore limiting the free volume. This causes a higher T_g and a harder polymer. The polymethacrylate coating obtained through powder coating showed a much softer coating than the solvent-casted films, with 2B pencil hardness (Figure 5-17).

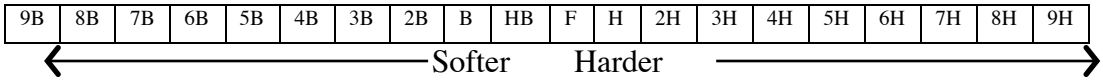


Figure 5-17. Pencil hardness scale ranges from 9B (softest) to 9H (hardest).

A much lower density of crosslinking might explain this fact. The flexibility of the polymer decreases with increasing crosslinking density since the polymer chains cannot move freely in a crosslinked network, therefore the film hardness increases. The ene:thiol ratio in the coating formulation was 4:1 in powder coating as opposed to 1:1.5 in solvent coatings. This considerable difference in crosslinker concentration explains the difference in hardness between the methacrylate coatings obtained by the two different methods.

In order to test the adhesion of the coatings to the aluminium substrate, they were analysed using a *gitterschnitt* (a lattice cutter, Figure 5-18).

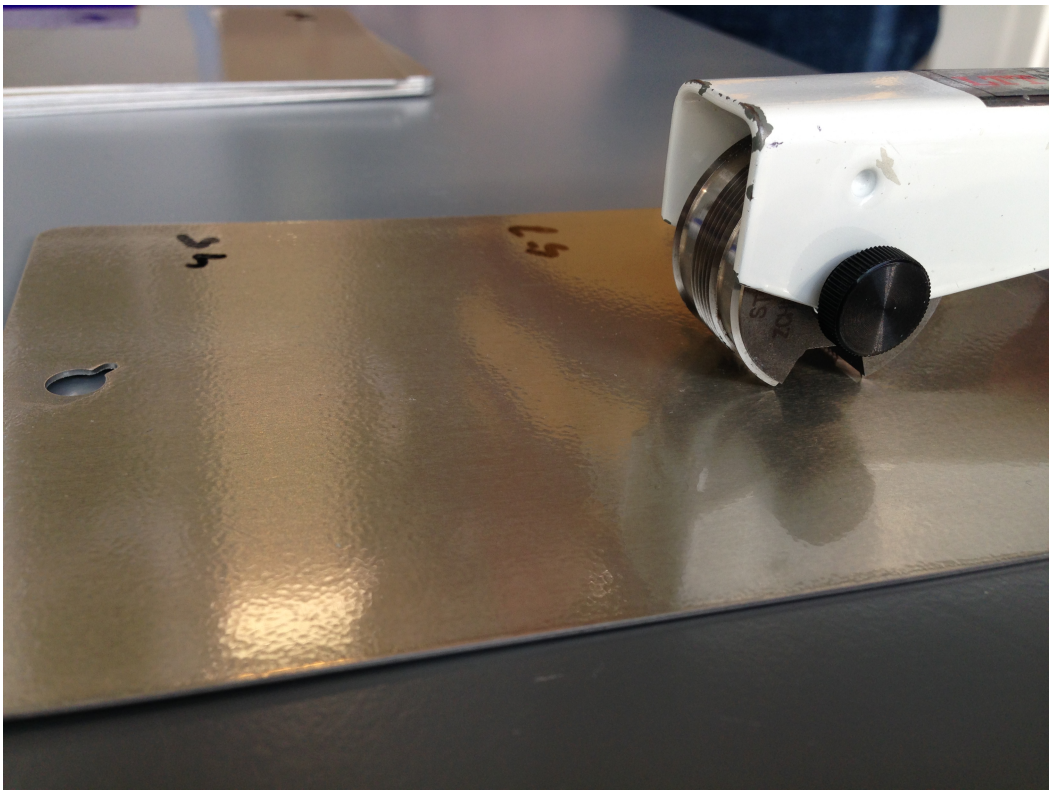


Figure 5-18. Picture of gitterschnitt scratching the surface of poly(carvone methacrylate) coating.

This test consists of conducting intersecting cuts, forming a lattice pattern. The degree of coating removal is visually analysed and a value between 0 and 5 is given and used as a measure of coating adhesion. A 0 value corresponds to 0 % of coating removal and a value of 5 is given when at least 65 % of the coating has detached from the substrate. This means that the closer the value is to 0, the better the adhesion. The comparison between the two methacrylate coatings obtained by solvent-casting (0 value) and powder coating (5 value) (Figure 5-19) reveals that the first one showed an enhanced adhesion, probably due to a higher concentration of polar thiol groups in its chemical structure (ene:thiol ratio was 1:1.5 as opposed to 4:1).

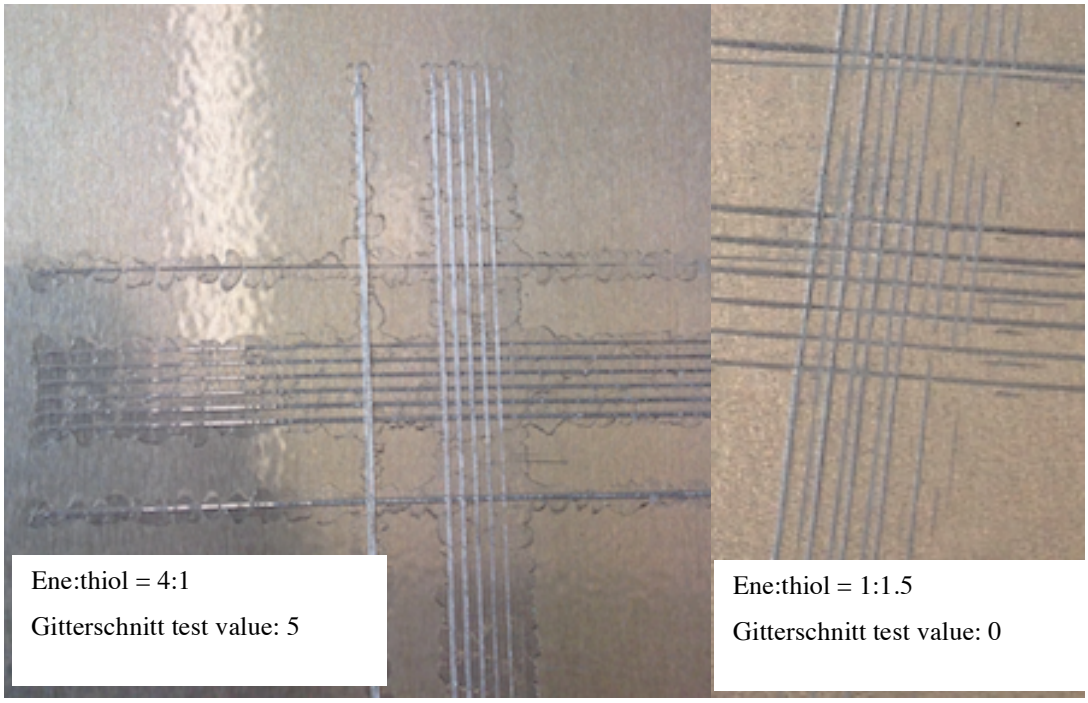


Figure 5-19. Poly(carvone methacrylate) coatings containing ene:thiol ratios of 4:1 (left) and 1:1.5 (right) after adhesion testing.

Chromated aluminium panels used for this work had been treated with a chromate coating that improves paint adhesion and resistance to underfilm corrosion. The chromate coating contains Cr(VI) or Cr(III) oxide compounds (non-specified by the manufacturer). Adhesion strongly depends on the bonding in the interfacial region between the surfaces of the coating and the aluminium substrate. A higher

concentration of tri-thiol crosslinker in the solvent-cast coating increases the number of polar-interactions with the chromated pan, such as hydrogen bonding and dipole-dipole interactions, with respect to the powder coating, which leads to a higher adhesion to the chromated aluminium pan.

With respect to the carvone-based acrylate coating, poor adhesion was observed (Gitterschnitt test value of 5, Table 5-3), in spite of the high concentration of crosslinker used in the coating formulation (ene:thiol = 1:4). Adhesion failing is caused not only on the bonding interactions between coating and substrate but also by the coating film intrinsic stresses and the fracture mechanisms. Therefore, the mechanical properties of the carvone-based coatings have played a major role in the coatings adhesion. Further research needs to be conducted in order to elucidate the cause of the significant difference in adhesion between carvone-based acrylate and methacrylate coatings.

Therefore, thiol-ene curing of carvone-based polyacrylate and polymethacrylate led to films with properties characteristic of acrylic coatings. The films were transparent and highly glossy, which is considered the major advantage of acrylics, together with their excellent chemical resistance. It is well known that blending of acrylic polymers or formation of copolymers can be utilised to introduce other properties by forming *via* hybrid acrylic coatings. Therefore, further research needs to be conducted in order to improve the brittleness and adhesion *via* a hybrid coating formulation.

5.4 Conclusions

Carvone-based branched and linear (meth)acrylate polymers were successfully cured *via* thiol-ene crosslinking reaction, leading to fully cured, insoluble films. Carvone-based coatings showed properties characteristic of acrylic coatings such as high gloss and transparency, medium-high hardness, brittleness and poor adhesion. These are promising results, meaning that carvone-based coatings perform equal to most acrylic coatings. Acrylic coatings properties are normally enhanced by blending with other polymers and tuning the final properties in the film (hybrid acrylics). Further research needs to be conducted to study blends of

carvone-based polyacrylate and polymethacrylate with other materials in order to improve the impact resistance and adhesion.

5.5 References

1. E. Linak and A. Kishi, HIS CEH Marketing Report: Acrylic Surface Coatings, https://http://www.ihs.com/products/acrylic-surface-chemical-economics-handbook.html, (accessed 4th of February, 2016).
2. G. P. Bierwagen, Surface coating, http://www.britannica.com/technology/surface-coating, (accessed 4th of February, 2016).
3. M. Zhao, D. R. Hughes, M. V. Bhadimipati, *Low odor reactive methacrylate composition for fast room temperature-curing floor coatings*, US20150191622A1, 2015.
4. R. S. Chandran, S. M. Shah, P. B. Foreman, *Radiation curable free radically polymerized star-branched polymers*, US6165563A, 2000.
5. Z. Shi, D. Jin, R. Petcavich, X. Zhang, *Scratch-resistant coating composition for touch sensor*, WO2016007239A1, 2016.
6. X. Xie, A. Schneider, *Heat- and moisture-resistant acrylic adhesive composition*, US20150361313A1, 2015.
7. N. D. Carbone, M. Ene, J. R. Lancaster and J. T. Koberstein, *Macromolecules*, 2013, **46**, 5434-5444.
8. A. Weber, *Journal*, 2015, **May 2015**.
9. L. Byczynski, M. Dutkiewicz and H. Maciejewski, *Polym. Bull.*, 2015, Ahead of Print.
10. F.-L. Jin, H.-C. Liu, B. Yang and S.-J. Park, *J. Ind. Eng. Chem.*, 2015, **24**, 20-23.
11. A. Tiwari and A. Polykarpov, *Photocured materials*, Royal Society of Chemistry, Cambridge, 2015.
12. R. Schwalm, 2007.
13. U. Siemann, *Prog. Colloid Polym. Sci.*, 2005, **130**, 1-14.
14. E. Lokensgard, *Industrial plastics : theory and applications*, Delmar Cengage Learning, 2014.
15. R. Schwarb, M. Knoblauch and J. Cox, *CoatingsTech*, 2010, **7**, 44-49.
16. M. Manea, *High solid binders*, Vincentz Network, Hannover, 2008.
17. N. Liberto, 2003.
18. M. J. Kade, D. J. Burke and C. J. Hawker, *J. Polym. Sci., Part A: Polym. Chem.*, 2010, **48**, 743-750.
19. M. Kryger, 2008.
20. T. Posner, *Ber. Dtsch. Chem. Ges.*, 1905, **38**, 646-657.
21. J. v. Braun and R. Murjahn, *Ber. Dtsch. Chem. Ges. B*, 1926, **59B**, 1202-1209.
22. C. E. Hoyle, T. Y. Lee and T. Roper, *J. Polym. Sci., Part A: Polym. Chem.*, 2004, **42**, 5301-5338.

23. C. E. Hoyle and C. N. Bowman, *Angew. Chem., Int. Ed.*, 2010, **49**, 1540-1573.
24. A. Dondoni, *Angew Chem Int Ed Engl*, 2008, **47**, 8995-8997.
25. C. R. Becer, R. Hoogenboom and U. S. Schubert, *Angew Chem Int Ed Engl*, 2009, **48**, 4900-4908.
26. S. A. Stachowiak, *Org. Coat.*, 1983, **5**, 67-89.
27. M. A. Grolitzer and D. E. Erickson, *Proc. Waterborne, High-Solids, Powder Coat. Symp.*, 1994, **21st**, 128-143.
28. B. E. Maxwell, R. C. Wilson, H. A. Taylor, D. E. Williams, W. Farnham and J. Tria, *Prog. Org. Coat.*, 2001, **43**, 158-166.

Chapter: 6 Conclusions and Future work

In this PhD thesis naturally abundant terpenes were investigated as a sustainable alternative to synthetic monomers and controlling agents that are commonly used in radical polymerisation. In this chapter, conclusions regarding the results of this PhD research are drawn and future work for the further development of terpene-based monomers and polymers is proposed.

6.1 Conclusions

In Chapter 2, the effectiveness of renewable terpenes as controlling agents in radical polymerisation was studied. Terpinolene and γ-terpinene were revealed to be the most effective CTAs among the range of terpenes tested at controlling the bulk polymerisation of MMA. This enhanced effectiveness was proposed to be caused by the presence of bisallylic hydrogens. Mechanistic studies were conducted for the first time and confirmed that both terpenes controlled radical polymerisation through a chain transfer mechanism *via* radical abstraction of bisallylic hydrogens. Terpinolene and γ-terpinene proved to be efficient at controlling molecular weight and dispersity as well as preventing the Trommsdorff effect for a range of commercial monomers such as MMA, MA, VAc and Sty. This work represents the first systematic study of terpenes as controlling agents in radical polymerisation to date. The relevance of this study resides on the significant advantages that terpinolene and γ-terpinene offer over the use of other common controlling agents because they are renewable, cheap, colourless and non-hazardous.

In Chapter 3, the use of terpenes as monomers in radical polymerisation was investigated. As discussed in Chapter 1, natural terpenes do not easily undergo radical polymerisation. The introduction of (meth)acrylates as polymerisable moieties in the structure of terpenes was explored in this chapter. The application of simple but robust protocols based on hydroboration followed by esterification reactions led to the synthesis of a wide range of new terpene-based acrylate and

methacrylate monomers. Alternatively, a catalytic route was investigated. Pd-catalysed allylic C-H activation of β-pinene provided new (meth)acrylate monomers and proved to be a more promising and sustainable route towards terpene-based (meth)acrylates.

The synthetic methodologies developed in Chapter 3 allowed for the synthesis of monomers on such a scale that they could be polymerised. Their polymerisation reactions were carefully studied and described in Chapter 4. The application of conventional FRP techniques led to a variety of new terpene-based polymers that exhibited diverse structures from linear to branched and crosslinked materials. The formation of branched and crosslinked networks was monitored by FTIR and the differences between the different functional groups were carefully analysed and discussed, revealing significant differences in reactivity between acrylate and methacrylate monomers. The data obtained during polymerisation studies of terpene-based (meth)acrylates revealed a promising future for these monomers, since there is a wide scope of polymers with different structures and mechanical properties that can be synthesised simply by changing the starting terpene.

Finally, in Chapter 5, application testing for some of the new terpene-based polymers was conducted. The linear poly(carvone methacrylate) and branched poly(carvone acrylate) described in Chapter 4 were tested as coating materials. Carvone-based polymers offer opportunity for crosslinking and film formation because of the high density of unsaturated moieties that they present in their chemical structure. These carvone-based polymers were successfully cured *via* thiol-ene crosslinking reactions and fully cured, transparent films were obtained. Analysis of the films showed that these terpene-based coatings exhibited properties characteristic of commercial acrylic coatings, revealing a promising future for the new renewable, carvone-based polymers.

6.2 Future work

The synthetic procedures described in Chapter 3 for the formation of terpene-based (meth)acrylate monomers needs further investigation in order to improve their sustainability. First of all, the hydroboration-oxidation protocol generates a considerable amount of waste. This procedure was chosen because it yields enantiopure monomers, which generally lead to polymeric materials with crystalline structures. By contrast, polymers synthesised from mixtures of enantiomers normally show amorphous structures and exhibit very different mechanical properties than those with crystalline structures. Considering that the terpene-based polymers described in this thesis were amorphous, despite being synthesised from enantiopure monomers, it would be interesting the utilisation of more rudimentary protocols such as the acid catalysed addition of water. This would lead to terpene-based alcohols as mixtures of enantiomers but would bring a considerable reduction of waste. It would also be interesting to use naturally occurring terpene alcohols, thus eliminating one synthetic step.

The development of a new esterification route for the synthesis of terpene-based (meth)acrylates is also necessary, since methacryloyl chloride is an expensive and toxic reagent, and the T3P protocol was not effective in catalysing the esterification reaction of methacrylic acid and terpene-based alcohols. Other sustainable esterification catalysts such as enzymes or montmorillonite clays could be investigated.[1, 2] As for the catalytic route, the employment of the carcinogenic benzoquinone in high concentrations represents a hazard and therefore investigation using other palladium oxidants in catalytic amounts such 4,5-diazafluorenone[3] should be conducted.

Other terpene functionalisations would be very interesting, such as the synthesis of terpene-based vinyl acetates. Alternatively, terpenes containing more than one double bond could be transformed into bifunctional monomers that could be used as cross-linkers. The synthesis of terpene-based dialcohols and diamines would open opportunities for polycondensation reactions to form biodegradable polyesters and polyamides respectively.

Additionally, there is plenty of scope for research regarding the polymerisation of terpene-based monomers described in Chapter 4. Analysis of the mechanical properties of these polymers such as strength, toughness and ductility needs to be conducted, since they will dictate the applications that these polymers can be used for. Furthermore, the utilisation of modern polymerisation techniques such as RAFT could be utilised for the synthesis of block copolymers with targeted molecular weights and mechanical properties. Polymerisation techniques such as emulsion polymerisation are known to lead to polymers with higher molecular weight than those obtained by bulk FRP.[4] Therefore, it would be useful to synthesise terpene-based polymers with high molecular weights of a few hundred thousand, which widens the scope of potential applications for these new polymers.

6.3 References

1. J. P. Adams, C. M. Alder, I. Andrews, A. M. Bullion, M. Campbell-Crawford, M. G. Darcy, J. D. Hayler, R. K. Henderson, C. A. Oare, I. Pendrak, A. M. Redman, L. E. Shuster, H. F. Sneddon and M. D. Walker, *Green Chem.*, 2013, **15**, 1542-1549.
2. S. B. Neji, M. Trabelsi and M. H. Frikha, *Energies (Basel, Switz.)*, 2009, **2**, 1107-1117.
3. A. N. Campbell, P. B. White, I. A. Guzei and S. S. Stahl, *J. Am. Chem. Soc.*, 2010, **132**, 15116-15119.
4. C. S. Chern, *Prog. Polym. Sci.*, 2006, **31**, 443-486.